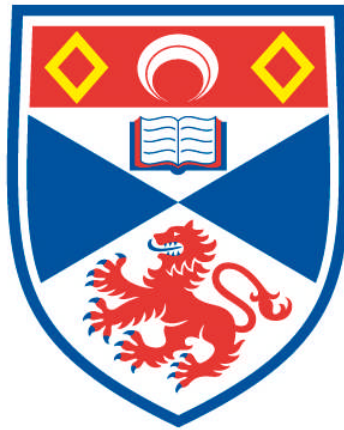


A STUDY OF EARLY-TYPE CLOSE BINARIES

Steven A. Bell

**A Thesis Submitted for the Degree of PhD
at the
University of St Andrews**



1987

**Full metadata for this item is available in
Research@StAndrews:FullText
at:**

<http://research-repository.st-andrews.ac.uk/>

Please use this identifier to cite or link to this item:

<http://hdl.handle.net/10023/3702>

This item is protected by original copyright

**This item is licensed under a
Creative Commons License**

6.10.1987/10.1

A STUDY OF EARLY-TYPE CLOSE BINARIES

by

STEVEN A. BELL

A thesis submitted to the University of St. Andrews in application
for the degree of Doctor of Philosophy.

St. Andrews

27th February, 1987



Declaration

=====

The research detailed in this thesis and the composition are my own work except where reference is made to the work of others. No part of this work has been previously submitted for another degree at this or any other University. I was admitted to the Faculty of Science of the University of St. Andrews as a research student on 1st. October, 1983, under Ordinance General No. 12. I was accepted as a candidate for the degree of Ph.D. on the 1st. October, 1984, under Resolution of the University Court, 1967, No.1.

27th February, 1987

Steven A. Bell

Certificate

=====

I certify that Steven A. Bell has spent nine terms in research work at the University Observatory, St. Andrews, that he has fulfilled the conditions of the Ordinance General No. 12 and the Senate Regulations under Resolution of the Court, 1967, No. 1, and that he is qualified to submit the accompanying thesis in application for the degree of Ph.D.

27th February, 1987

R. W. Hilditch

I acknowledge that in submitting this thesis to the University of St. Andrews I am giving permission for it to be made available for use in accordance with the regulations of the University library for the time being in force, subject to any copyright vested in the work not being affected thereby. I also understand that the title and abstract will be published, and that a copy of the work may be made and supplied to any bona fide research worker.

Acknowledgements

I am especially indebted to my supervisor, Dr. R.W. Hilditch, for his patient guidance, help and encouragement throughout the course of this study. It is also a great pleasure to thank Drs. Andy Adamson, Dave Kilkenny, Gordon Malcolm and, of course, Ron Hilditch, who have collaborated with me in one form or another to acquire the data for the seven papers presented in this thesis.

I would like to express my gratitude to the staffs of the University Observatory, the Observatorio del Roque de los Muchachos, the Instituto de Astrofisica de Andalucia, the South African Astronomical Observatory and the Institute of Astronomy of the University of the Orange Free State for their assistance during the observing runs, especially Dr. Victor Costa for his hospitality, Prof. A.H. Jarrett for his help in obtaining a Visiting Fellowship to work at Boyden for three months and Cindy for giving her name to the photometric package written during that time.

My thanks also go to the members of the "Night Shift", both past and present, who have helped make the not inconsiderable task of data reduction somewhat more tolerable on countless all-night sessions. In particular I would like to thank Dr. Tam McFarlane for many helpful discussions and for showing me the finer points of the "Glaswegian approach" to research and Dr. Ian Skillen for many useful discussions on the vagaries and pitfalls of LIGHT and for his prodigious tea-making during the photometric observations of AH Cephei at the Observatorio del Sierra Nevada. I am also grateful to Dr. John Worrell for his assistance in coming to grips with the subject of stellar modelling.

It is also a pleasure to thank Prof. D.W.N. Stibbs for the use of the facilities of the University Observatory and for his useful comments on the grammatical quality of the papers and Dr. Johannes Andersen for his constructive criticism in the form of referee's reports and advice. I am also indebted to Dr. Graham Hill for the use of his spectroscopic and photometric analysis software without which the analyses for this thesis would have been severely limited.

I would like to thank the Science & Engineering Research Council for financial support in the form of a postgraduate studentship and PATT for the generous allocation of telescope time. The use of the computing facilities of the University of St. Andrews as well as those of STARLINK are gratefully acknowledged. My thanks also go to the University Photographic Unit for their assistance in the preparation of the diagrams in this thesis.

Last, but certainly not least, I am extremely grateful to my parents for their encouragement and support, both financial and moral, without which this thesis would not have seen the light of day.

For my Parents

Abstract

It has become increasingly clear that many binary systems will pass through a common envelope stage at some point during their evolution. For short period systems composed of main-sequence O and early B stars this stage will probably occur for the first time towards the end of hydrogen-core burning in the primary component (case A evolution) rather than during the transition to the giant stage (case B evolution).

If masses, radii, luminosities, temperatures and orbital parameters were well determined for a good sample of those systems, it could be established whether the individual components were so close that case A evolution was inevitable or whether the primary component had enough room to complete its main-sequence phase before reaching its Roche limit and hence case B evolution. The latter mode has been studied extensively (both conservatively and non-conservatively) whereas the reception of matter by the secondary component in the rapid mass-transfer phase of case A evolution has only very recently been investigated. It is still one of the principal problems impeding further progress on this scenario.

To resolve this situation and provide observational material with which to compare these theoretical models, an observing program was established to study systems of spectral type earlier than B5 and of orbital period of less than 1.8^d in both the Northern and Southern Hemispheres. Light curves were obtained at St. Andrews using the newly-refurbished Twin Photometric Telescope and analysed using software developed specifically for this instrument. Further spectroscopic and photometric data were obtained at La Palma, SAAO,

Sierra Nevada and Boyden. Analyses of these spectroscopic and photometric observations have provided the necessary physical parameters to determine the evolutionary status of these systems. The systems observed were AH Cephei and V1182 Aquilae which are shown to be detached systems, TT Aurigae, SX Aurigae and AI Crucis which are all semi-detached systems and V701 Scorpii and RZ Pyxidis which are contact systems.

Accurately-determined parameters of 14 stars have been found, including four O stars in detached systems. Therefore the number of stars with well-determined masses of greater than $30M_{\odot}$ has been increased by 25%! It is clear from this study that case A mass transfer will play and has played an important role in the evolution of five out of the seven systems. It is debatable whether or not the contact systems have passed through a mass transfer phase, particularly RZ Pyx. The evolutionary history of this system is of particular interest, especially if this binary was in a marginal contact configuration when it arrived on the main sequence.

Attempts have been made to look for intrinsic variability in these systems but no periodic variation has been found in any of them. If such a phenomenon exists in one of the components of the binaries in the sample then it must have an amplitude of less than 0.01^m .

The comparison of the physical parameters of 67 stars compiled by the author from this work and from published data with theoretical zero-age and terminal-age main sequences shows that traditional modelling of semi-convection without mass loss is not adequate. Convective overshooting and mass loss play a very important role in the evolution of massive close binary systems of

short period.

Table of Contents

Chapter 1 : Introduction.

1)	Preamble	1
2)	The evolution of an intermediate-mass star	2
3)	Mass loss	4
4)	Modelling of single stars	6
5)	Modelling of case A evolution	10
6)	Project outline	17
	References	20

Chapter 2 : Methods of Observation, Reduction and Analysis.

1)	Introduction	
1.1)	Spectroscopy	24
1.2)	Photometry	25
1.3)	Observational preparation	27
2)	Observations	
2.1)	Spectroscopy	
2.1.1)	The Isaac Newton Telescope	
2.1.1.1)	Instrumentation	29
2.1.1.2)	Observations	31
2.1.2)	The SAAO 1.9m telescope	
2.1.2.1)	Instrumentation	32
2.1.2.2)	Observations	34
2.2)	Photometry	
2.2.1)	Twin Photometric Telescope	35
2.2.2)	Steavenson 0.75m telescope	39
2.2.3)	SAAO 0.5m telescope	40
2.2.4)	Boyden 0.41m telescope	41

3)	Reductions	
3.1)	Spectroscopy	
3.1.1)	Preliminary reductions with SPICA and FIGARO	44
3.1.1.1)	IPCS data	44
3.1.1.2)	RPCS data	45
3.1.2)	DAO-based software	45
3.2)	Photometry	
3.2.1)	Simultaneous two-star photometry	49
3.2.2)	All-sky photometry	54
4)	Analysis	
4.1)	Spectroscopy	67
4.2)	Photometry	
4.2.1)	LIGHT	68
4.2.2)	WUMA5	70
	Appendix A	72
	References	74

Chapter 3 : Simultaneous differential photometry with
the St. Andrews Twin Photometric Telescope;
I. - The eclipsing binary TT Aurigae.

	Summary	78
1)	Introduction	79
2)	Observing technique	80
3)	Observational data	81
4)	Analysis of the light curve	83
5)	Conclusions	85
	Acknowledgements	86
	References	87
	Figure captions	89

Chapter 4 : A photometric and spectroscopic study of the
early-type binary AH Cephei.

	Summary	106
1)	Introduction	107
2)	Spectroscopy	
2.1)	Observations	108
2.2)	Reduction and Analysis	109
3)	Photometry	
3.1)	Observations	111
3.2)	Reductions	112
3.3)	Ephemeris	113
3.4)	Colour indices	115
3.5)	Analysis	115
4)	Discussion	
4.1)	Spectroscopy and Photometry	118
4.2)	Evolutionary state	119
5)	Conclusion	122
	Acknowledgements	123
	References	124
	Figure captions	127

Chapter 5 : Simultaneous differential photometry with
the St. Andrews Twin Photometric Telescope;
II. - The eclipsing binaries SX Aurigae & TT Aurigae.

	Summary	162
1)	Introduction	163
2)	Spectroscopy	
2.1)	Observations	164
2.2)	Reduction and Analysis	164

2.2.1)	SX Aurigae	165
2.2.2)	TT Aurigae	167
3)	Photometry	
3.1)	Observations	167
3.2)	Ephemeris	168
3.3)	Analysis	169
4)	Discussion	
4.1)	Spectroscopy and Photometry	172
4.2)	Evolutionary state	
4.2.1)	SX Aurigae	173
4.2.2)	TT Aurigae	175
5)	Conclusion	176
	Acknowledgements	176
	References	178
	Figure captions	181

Chapter 6 : A photometric and spectroscopic study of the
early-type binary V1182 Aquilae.

	Summary	207
1)	Introduction	208
2)	Spectroscopy	
2.1)	Observations	209
2.2)	Reduction and Analysis	211
3)	Photometry	
3.1)	Observations	214
3.2)	Reductions	215
3.3)	Ephemeris	216
3.4)	Colour indices	217
3.5)	Analysis	217

4)	Discussion	
4.1)	Spectroscopy and Photometry	219
4.2)	Evolutionary state	221
5)	Conclusion	223
	Acknowledgements	223
	References	224
	Figure captions	227
	Appendix A	229

Chapter 7 : A photometric and spectroscopic study of the
early-type binary AI Crucis.

	Summary	257
1)	Introduction	258
2)	Spectroscopy	
2.1)	Observations	259
2.2)	Reduction and Analysis	260
3)	Photometry	
3.1)	Observations	264
3.2)	Reductions	265
3.3)	Ephemeris	266
3.4)	Colour indices	267
3.5)	Analysis	268
4)	Discussion	
4.1)	Spectroscopy and Photometry	270
4.2)	Membership of NGC 4103	271
4.3)	Evolutionary state	272
5)	Conclusion	275
	Acknowledgements	276
	References	277

Figure captions	280
-----------------------	-----

Chapter 8 : A photometric and spectroscopic study of the
early-type binary V701 Scorpii.

Summary	302
1) Introduction	303
2) Spectroscopy	
2.1) Observations	304
2.2) Reduction and Analysis	305
3) Photometry	
3.1) Observations	308
3.2) Reductions	309
3.3) Ephemeris	309
3.4) Colour indices	311
3.5) Analysis	312
4) Discussion	
4.1) Spectroscopy and Photometry	315
4.2) Membership of NGC 6383	316
4.3) Evolutionary state	317
5) Conclusion	318
Acknowledgements	319
References	320
Figure captions	323

Chapter 9 : RZ Pyxidis : An early-type marginal contact binary.

Summary	344
1) Introduction	345
2) Spectroscopy	
2.1) Observations	346

2.2)	Reduction and Analysis	346
3)	Photometry	
3.1)	Observations	349
3.2)	Reductions	351
3.3)	Ephemeris	351
3.4)	Colour indices	352
3.5)	Analysis	354
4)	Discussion	
4.1)	Spectroscopy and Photometry	358
4.2)	Evolutionary state	360
4.3)	Kinematics	362
5)	Conclusion	362
	Acknowledgements	363
	References	364
	Figure captions	367

Chapter 10 : Conclusion.

1)	Resume of analyses	
1.1)	Detached systems	388
1.2)	Semi-detached systems	390
1.3)	Contact systems	391
2)	Comparison with evolutionary models	392
3)	Summary	394
	References	411

CHAPTER 1

Introduction

1) Preamble

The evolution of binary stars is dominated principally by the changes in radius of the two individual stars and the upper limit imposed upon these changes by the presence of the respective Roche lobes around each component. Three phases of stellar evolution, each involving substantial increases in radius, are most important: (a) the gradual increase in the radius through the main-sequence phase; (b) the rapid increase in the radius when a star evolves to the red-giant stage, and (c) the further increase in radius beyond the core-helium burning-phase. If one component of a binary system should reach its respective Roche limit during one of the above phases of expansion, then mass transfer to the other component and/or mass loss from the system may occur. Kippenhahn and Weigert (1966) first introduced the nomenclature of cases A, B and C evolution for (a), (b) and (c) above. Such terminology is now standard within the subject.

In the past 25 years, most of the theoretical studies into mass transfer in close binary systems have centred on case B evolution not only because it appeared to be the most frequently-observed mode of mass transfer, but also because of the relative ease with which this type of mass transfer could be modelled. Case A evolution has

not been studied in the same depth as case B because the accretion of mass on to the secondary component led to complex evolutionary consequences. In order to be able to identify observed systems which are likely to pass through case A evolution detailed understanding of the evolutionary increase in the radius of an intermediate mass star during hydrogen-core burning is necessary.

The modelling of single stars with and without mass loss and including such refinements as semi-convection and convective overshooting enables predictions to be made as to whether the primary component will fill its critical Roche lobe during the course of its main-sequence evolution. Comparisons can also be made between these theoretical models and accurately-determined absolute dimensions of detached systems to show the validity of the physical approximations that have been used. In those cases where modelling of both components during case A evolution is available, comparisons can be made between observed systems and the predictions made by the theoretical studies.

2) The evolution of an intermediate-mass star

A typical upper main-sequence star of approximately five solar masses or greater, has a high-enough central temperature to permit the carbon-nitrogen cycle to be the dominant source of energy. The energy generation by this mechanism is strongly temperature dependent and therefore is concentrated in the innermost core of the star. In order to transport the energy flux efficiently, the star has a convective core surrounded by a radiative envelope.

For the purposes of this discussion, it will be assumed that the star has contracted on to the zero-age main sequence and that hydrogen-core burning has started. Convective motions in the core ensure that the chemical composition is homogeneous and that hydrogen becomes depleted throughout the core. During the main-sequence lifetime of the star, the core contracts and the central temperature of the star increases in such a manner that the luminosity increases by more than 50% and the star expands. The overall effect on the star is a decrease in the effective temperature and a movement upwards and to the right in the HR diagram. The hydrogen-core burning stage of a star represents the major part of the lifetime of a star up to the beginning of the red giant phase.

As the hydrogen abundance in the core falls, the energy-production rate is maintained by a contraction of the core causing a rise in the central temperature. This procedure accelerates as the core becomes more depleted of hydrogen and the whole star contracts raising the central temperature further. The star now moves upwards and to the left in the HR diagram. The increase in luminosity is primarily due to the conversion of gravitational potential energy to heat and thence to radiation.

Once the hydrogen in the core is consumed, the contraction phase ceases. The source of energy generation shifts to a hydrogen rich shell surrounding the hot helium core. The ignition of the hydrogen drawn towards the core is mildly explosive and the stellar envelope expands. The energy used in expanding the envelope accounts for the initial drop in the luminosity of the star. The hydrogen-burning shell moves progressively out from the centre and the rate of energy production increases. At the same time the core

grows hotter and continues to contract.

Energy production in the shell again becomes mildly explosive and the stellar envelope expands rapidly. The width of the hydrogen-burning shell decreases and the rate of energy generation falls. The luminosity of the star decreases and the effective temperature also decreases making the star move downwards and to the right in the HR diagram. Convection becomes the dominant mode of energy transport in the envelope as the radiative opacity increases in the cooling and expanding envelope. At this point, opacity changes in the remaining radiative envelope favour a larger energy flow and the luminosity increases. By this stage, the star has reached the foot of the red-giant branch, well beyond the evolutionary phases reached by the stars discussed in this thesis.

3) Mass loss by stellar wind

A brief review of the observational and theoretical aspects of mass loss is given here. A complete study of the causes of mass loss is beyond the scope of this thesis. However, the effect of mass loss on the evolution of close binary systems is extremely relevant to this work. A discussion of these effects in the context of single stars is given in Section 4.

The first explanation for stars showing P Cygni profiles was made by Beals (1929). These profiles consist of an emission component and a violet-shifted absorption component. The outflow from the star inferred from this absorption feature constitutes the stellar wind which leads to the concept of mass loss. Snow and Morton (1979) made a study of early-type stars using UV data from the Copernicus satellite and found that all the stars brighter than

$M_{\text{bol}} \sim -6.0^{\text{m}}$ (i.e. all O-type stars) in their sample were losing mass via stellar winds. Further analyses show that these stars are losing mass at rates as high as $10^{-5} M_{\odot} \text{yr}^{-1}$.

Observational evidence for mass loss via stellar winds can be found at radio, infrared, optical and UV wavelengths. Excess free-free emission at $10 \mu\text{m}$ was used by Barlow and Cohen (1977), to make determinations of mass loss for a sample of OBA supergiants and Of stars. Of stars also show emission in the $\lambda 4686$ HeII feature, a situation which can only be found in the stellar envelope, inferring the presence of a stellar wind. A similar situation exists for the $H\alpha$ feature for most Of stars and OB supergiants. The clearest evidence for mass loss comes from UV spectra showing P Cygni profiles in resonance lines such as NV, SiIV and CIV. Wind velocities of up to 3000kms^{-1} are observed which are sufficiently larger than the escape velocity of the star to confirm that material was leaving the star. Optical observations of P Cygni profiles also provide estimates of the outflow velocities, but are not as reliable as the UV-derived estimates.

Most of the work done on mass loss has been directed towards OBA supergiants, Of stars and WR stars. Comparatively little work has been done on main-sequence O and B stars. Further details of the observational evidence for mass loss in early-type stars have been reviewed by Conti (1978, 1981), Cassinelli (1979), Barlow (1982), de Loore (1984) and references therein.

Lucy and Solomon (1970) suggested that material is driven outwards by radiation pressure acting on the resonance lines of dominant elements. An expanded radiative-pressure model (Castor et al., 1975) proved consistent with many of the observed features of

the expanding envelopes of early-type stars. These models showed that mass loss of $10^{-5} M_{\odot} \text{yr}^{-1}$ could be predicted as well as the linear relation between mass loss and stellar luminosity found by Barlow and Cohen (1977).

Observations of highly-ionised species such as NV and OVI imply the dissipation of non-thermal energy. Cassinelli and Olson (1979) suggested a hybrid version of the radiation-pressure model in which a thin corona provides X-rays to ionise the stellar wind. Other theories have been proposed by Lamers and Rogerson (1978) and Cannon and Thomas (1977) along similar lines, although adopting different wind temperatures. However, all these modifications cannot give simple predictions of the mass-loss rate.

The radiation-pressure model cannot predict the variation in mass-loss rates from stars of similar luminosity (Lamers et al, 1980, Conti and Garmany, 1980) and also the observed variability in the mass loss. A different approach was suggested by Andriesse (1980) involving thermodynamic fluctuations in the star itself to provide a source of energy to the envelope to drive a stellar wind.

The current relationship between mass-loss rate and stellar luminosity for stars of known effective temperature is given in Figure 2 of Chiosi and Maeder (1986). The slope of this relationship is approximately 1.7 which is in reasonable agreement with the revised radiation pressure model by Abbott (1985). The spread in mass-loss rate with stellar luminosity is still unexplained. An overview of the current formulations for mass loss, both theoretical and empirical, is given in Table 2 of Chiosi and Maeder. The theoretical aspects of mass loss has been discussed by Hearn (1981), and Abbott (1985). The parameters for the various

theoretical formulations for mass loss must be selected to fit the observations. No self-consistent model of mass loss has yet been found to explain all the observed phenomena.

4) Modelling of single stars

A number of studies have been made in the evolution of intermediate- and high-mass stars. The following discussion is not exhaustive, but serves to show the improvement in theoretical modelling of these stars over the past 20 years.

Stothers (1972) provided a range of models from 5 to $120M_{\odot}$ with three different chemical compositions. The study demonstrated how increasing the mass fraction of hydrogen (X) or that of the metals (Z) reduces the luminosity and effective temperature of a star of fixed mass and also prolongs its main-sequence lifetime. References to earlier work on the subject can be found in that paper. Comparisons with systems whose absolute dimensions were considered to be well-determined showed that a composition of (X = 0.70, Z = 0.03) was in good agreement with the observed data. Mass loss was also thought to be small for normal main-sequence systems. Further modelling by Stothers (1974) using the opacities of Carson (Jeffery, 1982) provided the theoretical comparison for 96 components of binary systems compiled by Lacy (1978). The zero-age and terminal-age main sequences showed good agreement with the observed data.

Hejlesen (1980a,b) produced 11 calibrations between 0.6 and $12.6M_{\odot}$ for 10 chemical compositions using two different mixing lengths in the treatment of convection. From these data, evolutionary tracks, isochrones and calibrations in terms of age and

mass for the main-sequence band were provided. This presentation lends itself particularly well to comparison with the observed parameters of the components of binary systems. These models can be compared with the work of Becker (1981) over a comparable range.

The inclusion of mass loss in the evolution of these stars has been considered by a number of authors whose work is discussed by Chiosi and Meader (1986) and references therein. Maeder (1981a,b) provided evolutionary tracks for stars in the range $9-60M_{\odot}$ both with and without mass loss. The parameterisation of the mass loss follows that used by Barlow and Cohen for two possible constants of proportionality. This representation of mass loss is similar to that used by de Loore et al. (1978) in their study of the evolution of O stars with respect to the origin of Wolf-Rayet stars.

Chiosi et al. (1978) used the theoretical formulation of Castor et al. (1975) for their study of $20-100M_{\odot}$ stars. These models showed reasonable agreement with work by de Loore et al. (1977). In these models, mass loss causes a less rapid increase in the central temperature than for conservative evolution and results in a smaller convective core. The luminosity of the star is lower than that of a star of constant mass and the main-sequence lifetime is increased by mass loss. For moderate mass loss, a slight widening of the main-sequence is found whilst a narrowing of the main sequence is found for more extreme mass loss.

Doom (1982a,b) explored the combined effect of mass loss and convective overshooting on stars of $10-100M_{\odot}$. He used the empirical mass-loss relation derived by Lamers (1981) and varied the amount of overshooting in terms of the mixing length. The topic of convective overshooting had been revived by Bressan et al. (1981), who

produced a restricted number of evolutionary sequences including mass loss based on their own treatment of overshooting. A more complete set of evolutionary tracks without mass loss has been presented by Bertelli et al. (1986) for stars of intermediate mass which can be contrasted with the conservative models presented by Hejlesen (1980b).

An alternative model for convection was employed by Doom (1985) based on the theory of convection by Roxburgh (1978). Convective overshooting is an integral part of this model which leads to the formation of a substantially larger convective core. The models produced with this theory evolve towards higher luminosities and smaller effective temperatures than those models produced with normal mixing-length theory. Doom calculated evolutionary tracks up to the exhaustion of hydrogen in the core for stars of masses $1.2-120M_{\odot}$ and suggested that better agreement with observations can be obtained thereby.

Xiong (1986) has produced models for massive main-sequence stars without mass loss using a non-local theory of convection. This method alleviates the necessity for semi-convection required to overcome problems with the local treatment of convection. The amount of convective overshooting is somewhat greater than previous theories have adopted and results in evolutionary tracks that run at higher luminosities than those produced by traditional methods and also a wider main-sequence band which is in agreement with observations of massive stars by Humphreys (1978).

5) Modelling of case A evolution

Crawford (1955) made the suggestion that mass transfer in a binary system commences when one of the components fills its Roche lobe. Kippenhahn and Weigert (1966) and Lauterborn (1969) defined three possible cases of mass transfer from the initially more massive primary component to the secondary component. Case A mass transfer starts during core-hydrogen burning whilst case B starts just after core-hydrogen exhaustion when the outer layers of the primary component are expanding rapidly. Case C mass transfer starts after core-helium exhaustion when the outer envelope of the star again expands rapidly.

Plavec (1968) defined three critical periods in low- and intermediate-mass binaries corresponding to extreme values of the primary-component radius (i.e. the radii at the zero-age main sequence, the end of core-hydrogen burning and the most luminous tip of the red-giant phase). For a mass ratio of 0.5 and primary component of mass $9M_{\odot}$ with no mass loss, case A evolution would be expected in a system of initial period P such that $0.65^d < P < 1.9^d$, case B for $1.9^d < P < 394^d$ and case C for $394^d < P < 533^d$. These calculations were shown to have little dependence on the mass ratio chosen.

Ziolkowski (1970) introduced case AB mass transfer for systems where mass transfer starts in the same way as case A but proceeds up to the shell-hydrogen burning phase in a continuous process. The review by Paczynski (1971) details the modelling undertaken before 1970 by various authors in all three phases of mass transfer and the assumptions made in their analyses.

The scenario for case A evolution at that time was considered to proceed in the same manner for binaries of all masses. When the primary component fills its Roche Lobe, a phase of rapid mass transfer occurs which more than reverses the mass ratio of the system. The original primary component departs from its previous thermal equilibrium state and the subsequent evolution proceeds on a slow, nuclear time scale and the configuration of the binary becomes semi-detached. The primary component, now the less massive star burns hydrogen and fills its Roche lobe as an over-luminous sub-giant. This phase of evolution is roughly as long as the main-sequence lifetime of the original primary component.

Despite the considerable theoretical effort on mass transfer in close binary systems, little work had been done on the mass-accreting component of these systems. Benson (1970) investigated this aspect of mass transfer in low- and intermediate-mass systems and concluded that the radius of the secondary component expanded rapidly during the accretion phase after relatively small amounts of mass had been transferred resulting in the formation of a contact system. Further work on the role of the secondary component during the mass transfer phase has been carried out by Yungel'son (1973), Ulrich and Berger (1976), Neo et al. (1977), Flannery and Ulrich (1977), Kippenhahn and Mayer-Hofmeister (1977), Packet and de Greve (1979) and Hellings (1983) confirming the work of Benson. Once again, most of these studies have concentrated on case B evolution.

More recent studies of case A evolution including convective overshooting have been made by Doom (1984) who showed that a binary with an initial primary mass of $33M_{\odot}$ can only evolve through case A mass transfer or undergo no mass exchange with the secondary

component. Doom also showed that binaries with initial masses of $20 + 10M_{\odot}$ and periods of 4 and 6 days evolved through case A evolution followed by case B evolution whereas a system with a period of 2 days would probably form a contact binary. However, these models did not take into account the behaviour of the secondary component. He also found that 28% of systems should evolve through case A evolution as opposed to 5% which had been determined by Vansina and de Grève (1982).

Sybesma (1985) performed similar evolutionary calculations to Doom (1984) making simultaneous calculations of both the primary and secondary components. He studied a $20 + 10M_{\odot}$ system with periods of between 10 and 1.5 days. For systems with periods of between 3 and 10 days, case A evolution with a peak mass transfer rate of around $10^{-4} M_{\odot} \text{yr}^{-1}$ occurs followed by a slow phase of mass transfer at a rate substantially less than that of the stellar wind. The secondary expands and becomes overluminous but eventually relaxes back to the main sequence as the mass transfer rate drops. Mass transfer ceases when the original primary component starts to contract or if the stellar wind is large enough to keep the star within its critical Roche lobe and the system takes on a detached configuration. Case B mass transfer starts when the primary component expands at core-hydrogen exhaustion. The secondary component again becomes overluminous receiving nuclear-processed material from the primary resulting in the star relaxing to a position just below the main sequence. The evolution of a system with a period of 10 days is shown in Figure 1. The resulting system is a Wolf-Rayet star and an O-type companion with a depressed hydrogen abundance.

For periods less than 3 days, the mass transfer phases differ considerably from those discussed above (see Figure 2). Case A evolution takes place with a similar mass transfer rate and the secondary component expands. A contact system is formed without mass loss from the system. When the primary component reaches minimum luminosity, it contracts and the mass loss rate drops. The secondary component contracts and the contact phase is broken. The stellar wind is sufficient to keep the primary within its critical Roche surface and the system takes on a detached configuration.

A second case A mass-transfer phase occurs when the primary again fills its Roche lobe and the secondary expands. However, a mass loss rate of $10^{-7} M_{\odot} \text{yr}^{-1}$ is sufficient to keep the primary component within its Roche lobe and as it contracts once more, the secondary component relaxes back to the zero-age main sequence. A second phase of contact does not occur as the secondary component does not expand sufficiently. When core-hydrogen exhaustion occurs in the primary, case B mass transfer starts which results once again in a system containing a Wolf-Rayet star and an O-type star. In all cases convective overshooting enlarges the stellar cores of both stars increasing the central hydrogen abundance and removing the possibility of semi-convection regions. Core-hydrogen burning phases are longer than would otherwise be the case. The shorter-period systems spend a very large proportion of their time in semi-detached configurations. However the contact phase can be lengthened with shorter periods and larger mass ratios.

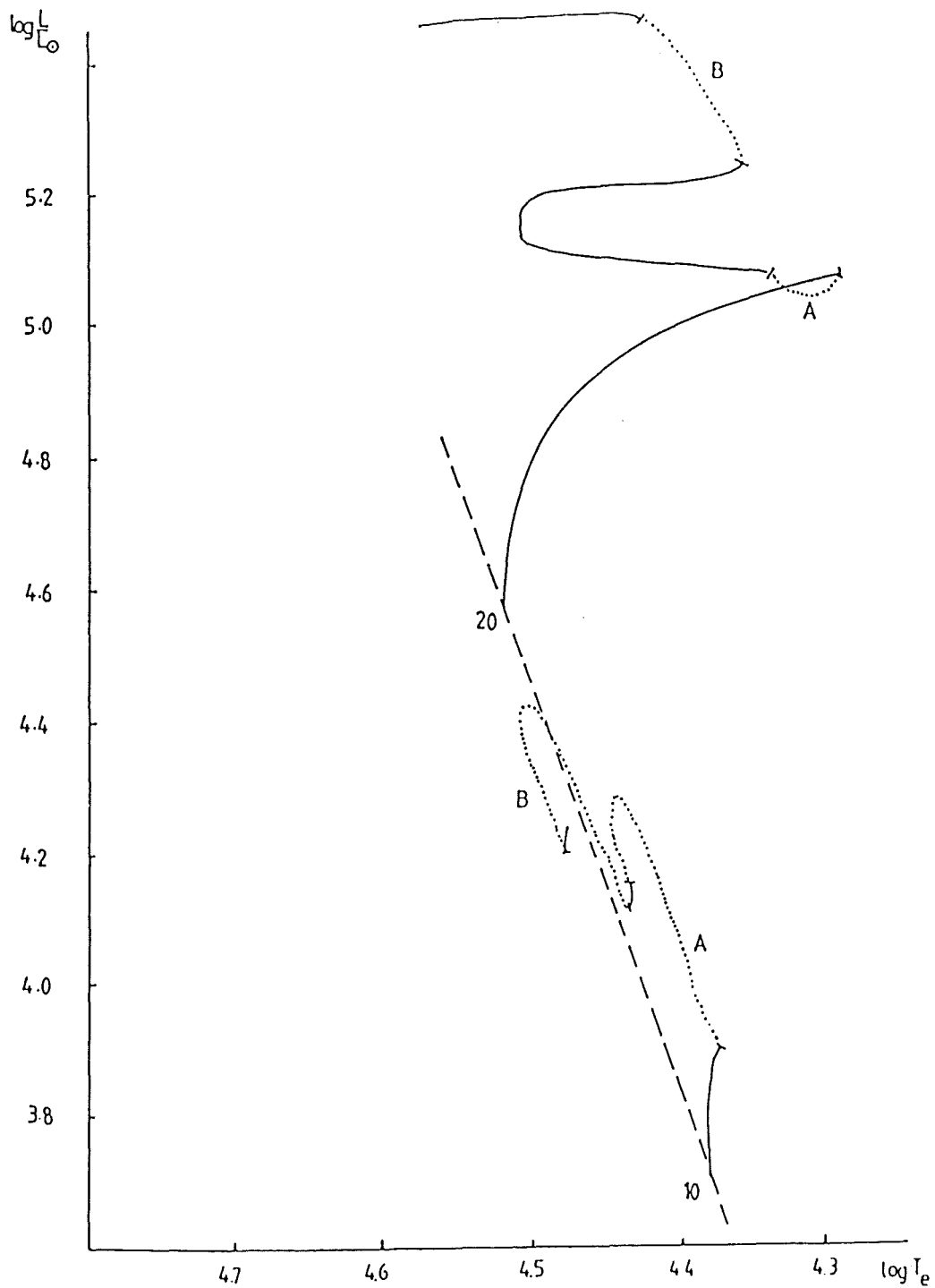


Figure 1: Evolution in the HR diagram of a $20 + 10M_{\odot}$ binary with an initial period of 10 days. The dotted lines correspond to the mass-transfer stages, the zero-age main sequence by a dashed line. This diagram is taken from Sybesma (1985, Figure 1).

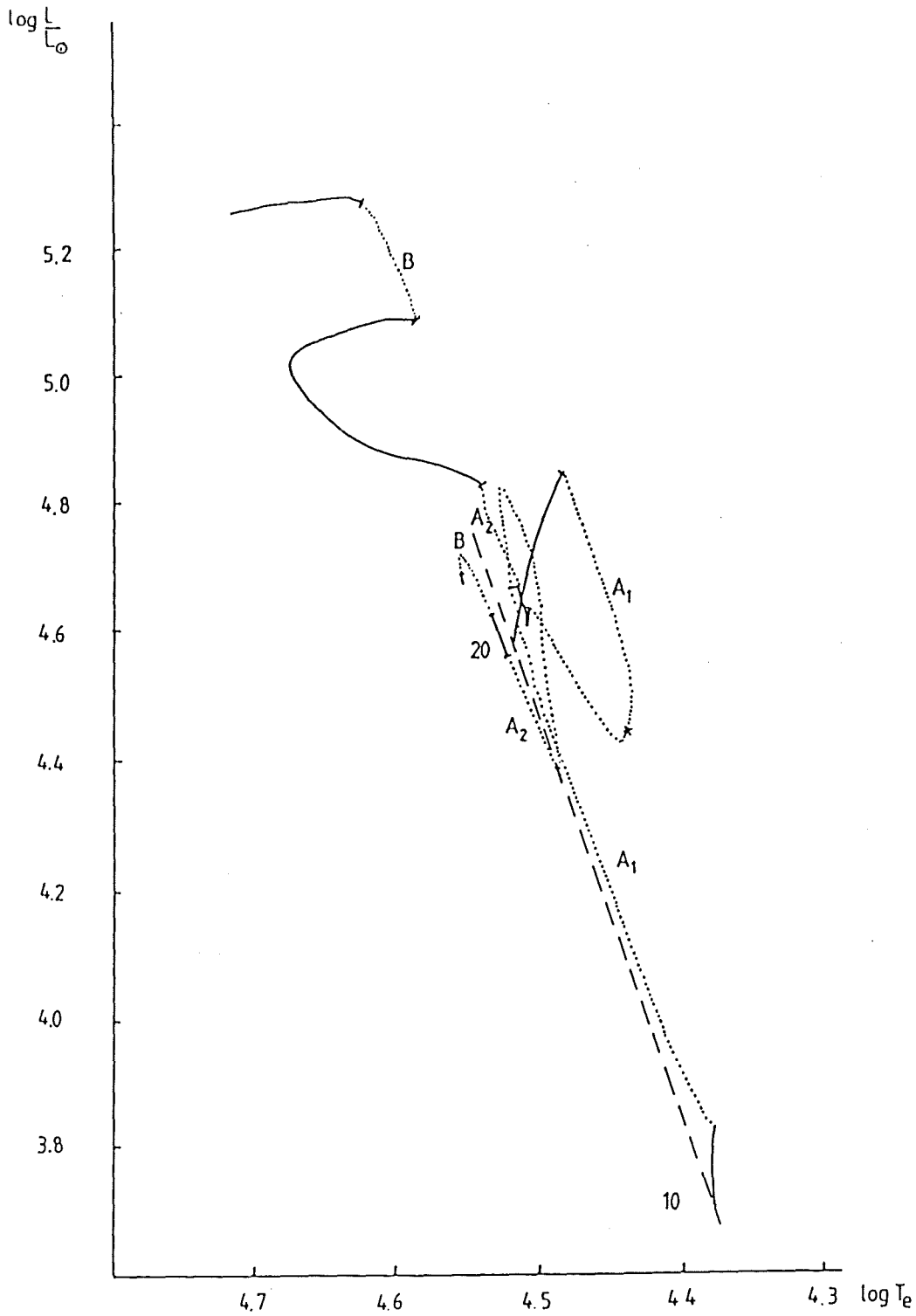


Figure 2: As Figure 1 with an initial period of 2 days. The point of contact is denoted by an asterisk. A_1 and A_2 correspond to the two phases of case A mass transfer. This diagram is taken from Sybesma (1985, Figure 7).

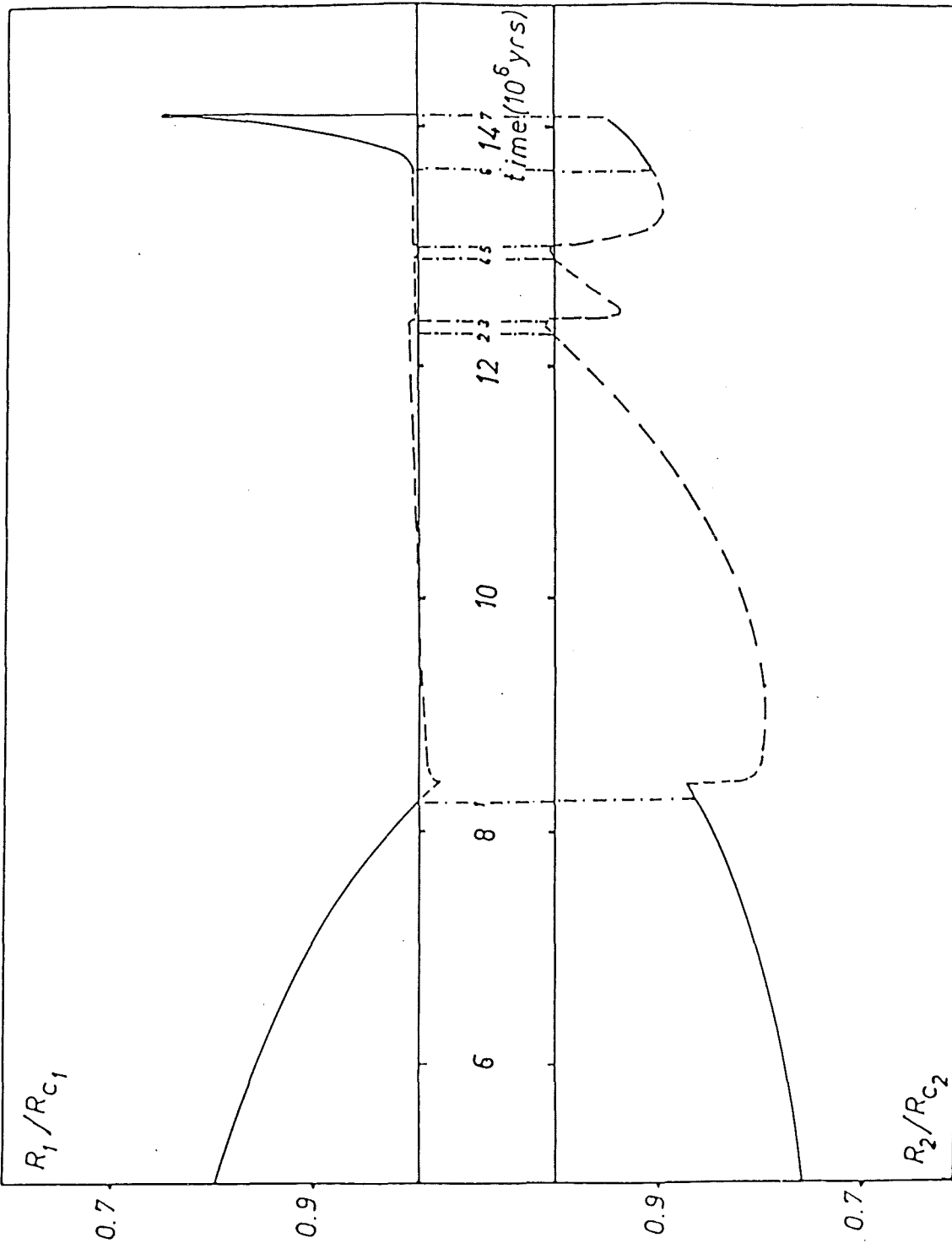


Figure 3: The radius of the two components in terms of the radius of the critical Roche lobe as a function of time of a $20 + 16M_{\odot}$ binary with a period of 2 days. The dashed lines show where mass transfer takes place. The dash-dotted lines connect the radii at several important points: 1) the onset of case A mass transfer, 2-5) successive phases of mass transfer reversal, 6) the end of case A mass transfer and 7) the onset of case B mass transfer and the formation of a contact system. This diagram is taken from Sybesma (1986, Figure 9).

Further work on case A mass transfer has been made by Sybesma (1986) on systems with a $20M_{\odot}$ primary component and mass ratios of 0.6 and 0.8 with periods between 10 and 1.5 days. Those systems with period of larger than 3 days evolve in a similar manner to those systems with comparable periods discussed above. The secondary components appear to be somewhat more evolved because of the similarity of the evolutionary timescales of the two components. and their ability to absorb transferred matter without large radius increases. For the shorter period systems, case A mass transfer is continuous but with a reduced mass transfer rate compared to those systems with more extreme mass ratios. The evolution of the secondary component will force its radius past its critical surface and reverse the mass transfer so it loses mass. The secondary component will become detached from its Roche lobe and once again will become the accreting star (see Figure 3). At no point can the system form a stable contact configuration. For the higher mass ratios, several reversals can take place. The situation can arise where both stars want to lose mass and the formation of a long-lived common envelope appears likely with mass loss through the outer Lagrangian point as a result of their evolution. Case B evolution may also bring about a short-lived contact phase unless the secondary component radius passes the outer Lagrangian point.

6) Project outline

It has become increasingly clear that many binary systems will pass through a common envelope stage at some point during their evolution (van den Heuvel, 1982). For short period systems composed of main-sequence O and early B stars this stage will probably occur for the first time towards the end of hydrogen-core burning in the

primary component (case A evolution) rather than during the transition to the giant stage (case B evolution). Extensive angular momentum losses and some mass losses from the system are likely to result as has been put forward by several authors (e.g. Ziolkowski, 1979). A classical example of this scenario is SV Cen in which stellar winds and some Roche lobe overflow have been suggested in the explanation of the observations already obtained (Dreschel et al., 1982).

If masses, radii, luminosities, temperatures and orbital parameters were well determined for a good sample of those systems, it could be established whether the individual components were so close that case A evolution was inevitable or whether the primary component had enough room to complete its main-sequence phase before reaching its Roche limit and hence case B evolution. The latter mode has been studied extensively (both conservatively and non-conservatively) whereas the reception of matter by the secondary component in the rapid mass-transfer phase of case A evolution has only very recently been investigated. It is still one of the principal problems impeding further progress on this scenario.

To resolve this situation and provide observational material with which to compare these theoretical models, an observing program was established to study a number of systems of spectral type earlier than B5 and of orbital period of less than 1.8^d in both the Northern and Southern Hemispheres. Analyses of these spectroscopic and photometric observations should provide the necessary physical parameters to facilitate the evaluation of the evolutionary status of these systems. The observations made for this study are outlined in Table 1.

Table 1: Observations made for this study.

	Spectroscopy	Photometry
<u>Northern Hemisphere</u>		
TT Aur *	INT/SAB/AJA	TPT/SAB
SX Aur *	INT/SAB/AJA	TPT/SAB
BF Aur	INT/SAB/AJA	TPT/SAB
AH Cep *	INT/SAB/AJA	STV/SAB
	DAO/RWH	
V1182 Aql *	INT/SAB/AJA	STV/SAB/AJA
	DAO/RWH	
BE Dra	INT/SAB/AJA	JKT/SAB
	DAO/RWH	
ZZ Cas	INT/SAB/AJA	JKT/SAB
<u>Southern Hemisphere</u>		
AI Cru *	RDC/SAB/DK	REP/SAB
V701 Sco *	RDC/SAB	BDN/SAB/GJM
RZ Pyx *	RDC/SAB	BDN/SAB/GJM
V758 Cen	RDC/SAB	BDN/SAB/GJM
V883 Sco	RDC/SAB	BDN/SAB/GJM

* denotes a complete analysis presented in this thesis.

Key:

Observers	SAB - the author.
	RWH - Dr. Ronald Hilditch.
	AJA - Dr. Andrew Adamson.
	GJM - Dr. Gordon Malcolm.
	DK - Dr. David Kilkeny.
Instruments	TPT - Twin Photometric Telescope, St. Andrews.
	STV - Steavenson telescope, Sierra Nevada, Spain.
	JKT - Jacobus Kapteyn telescope, La Palma.
	INT - Isaac Newton Telescope, La Palma.
	RDC - 1.9m telescope, SAAO, South Africa.
	REP - 0.5m telescope, SAAO, South Africa.
	BDN - 0.41m telescope, Boyden, South Africa.
	DAO - 1.8m telescope, DAO, Canada.

References

- Abbott, D.C., 1985. In "O, Of and WR Stars", ed. Conti, P.S. & Underhill, A.B., NASA/CNRS Monogr. Ser., In press.
- Andriessse, C.D., 1980. Mon. Not. R. astr. Soc., 192, 95.
- Barlow, M.J., 1982. In "Wolf Rayet Stars: Observations, Physics, Evolution", ed. de Loore, C. & Willis, A.J., Reidel, Dordrecht, 149.
- Barlow, M.J. & Cohen, M., 1977. Astrophys. J., 213, 737.
- Beals, C.S., 1929. Mon. Not. R. astr. Soc., 90, 202.
- Becker, S.A., 1981. Astrophys. J. Suppl. Ser., 45, 475.
- Benson, R.S., 1970. Ph.D. thesis, University of California, Berkeley.
- Bertelli, G., Bressan, A., Chiosi, C. & Angerer, K., Astron. Astrophys. Suppl. Ser., 66, 191.
- Bressan, A., Bertelli, G. & Chiosi, C., 1981. Astron. Astrophys., 102, 25.
- Cannon, C.J. & Thomas, R.N., 1977. Astrophys. J., 211, 910.
- Castor, J.I., Abbott, D.C. & Klein, R.I., 1975. Astrophys. J., 195, 157.
- Cassinelli, J.P., 1979. Ann. Rev. Astron. Astrophys., 17, 275.
- Cassinelli, J.P. & Olson, G.L., 1979. Astrophys. J., 229, 304.
- Chiosi, C., Nasi, E. & Sreenivasan, S.R., 1978. Astron. Astrophys., 63, 103.

- Chiosi, C. & Maeder, A., 1986. *Ann. Rev. Astron. Astrophys.*, 24, 329.
- Conti, P.S., 1978. *Ann. Rev. Astron. Astrophys.*, 16, 371.
- Conti, P.S., 1981. In "Effects of Mass Loss on Stellar Evolution", ed. Chiosi, C. & Stalio, R., Reidel, Dordrecht, 1.
- Conti, P.S. & Garmany, C.D., 1980. *Astrophys. J.*, 238, 190.
- Crawford, J.A., 1955. *Astrophys. J.*, 121, 71.
- Doom, C., 1982a. *Astron. Astrophys.*, 116, 303.
- Doom, C., 1982b. *Astron. Astrophys.*, 116, 308.
- Doom, C., 1984. *Astron. Astrophys.*, 138, 101.
- Doom, C., 1985. *Astron. Astrophys.*, 142, 143.
- Dreschel, H., Rahe, J. & Wargau, W., 1982. *I.A.U. Coll.*, 69, 205.
- Flannery, B.P. & Ulrich, R.K., 1977. *Astrophys. J.*, 212, 533.
- Hearn, A.G., 1981. In "Effects of Mass Loss on Stellar Evolution", ed. Chiosi, C. & Stalio, R., Reidel, Dordrecht, 125.
- Hejlesen, P.M., 1980a. *Astron. Astrophys.*, 84, 135.
- Hejlesen, P.M., 1980b. *Astron. Astrophys. Suppl. Ser.*, 39, 347.
- Hellings, P., 1983. *Astrophys. Space. Sci.*, 96, 37.
- van den Heuvel, E.P.J., 1982. *I.A.U. Commission 42 Report*.
- Humphreys, R.M., 1978. *Astrophys. J. Suppl. Ser.*, 38, 309.
- Jeffery, C.S., 1982. Ph.D. thesis, University of St. Andrews.

- Kippenhahn, R., & Weigert, A., 1966. *Mitt. Astron. Ges.*, 21, 106.
- Kippenhahn, R., & Mayer-Hofmeister, E., 1977. *Astron. Astrophys.*, 54, 539.
- Lacy, C.H., 1978. *Astrophys. J.*, 228, 817.
- Lamers, H.J.G.L.M., 1981. *Astrophys. J.*, 245, 593.
- Lamers, H.J.G.L.M. & Rogerson, J.B., 1978. *Astron. Astrophys.*, 66, 417.
- Lamers, H.J.G.L.M., Paerels, F. & de Loore, C., 1980. *Astron. Astrophys.*, 87, 68.
- Lauterborn, D., 1969. In "Mass Loss from Stars", ed. Hack, M., Reidel, Dordrecht, 262.
- de Loore, C., 1984. *Phys. Scr.* T7, 25.
- de Loore, C., de Grève, J.P. & Vanbeveran, D., 1978. *Astron. Astrophys.*, 67, 373.
- de Loore, C., de Grève, J.P. & Lamers, H.J.G.L.M., 1977. *Astron. Astrophys.*, 61, 251.
- Lucy, L.B. & Solomon, P.M., 1970. *Astrophys. J.*, 159, 879.
- Maeder, A., 1981a. *Astron. Astrophys.*, 99, 97.
- Maeder, A., 1981b. *Astron. Astrophys.*, 102, 401.
- Neo, S., Miyagi, S., Nomoto, K. & Sugimoto, D., 1977. *Publ. Astron. Soc. Japan*, 29, 249.
- Packet, W. & de Grève, J.P., 1979. *Astron. Astrophys.*, 75, 255.

- Paczynski, B., 1971. Ann. Rev. Astron. Astrophys., 9, 183.
- Plavec, M., 1968. Adv. Astron. Astrophys., 6, 202.
- Roxburgh, I.W., 1978. Astron. Astrophys., 65, 281.
- Snow, T.P. & Morton, D.C., 1979. Astrophys. J. Suppl. Ser., 32, 429.
- Stothers, R., 1972. Astrophys. J., 175, 431.
- Stothers, R., 1974. Astrophys. J., 194, 651.
- Sybesma, C.H.B., 1985. Astron. Astrophys., 142, 171.
- Sybesma, C.H.B., 1986. Astron. Astrophys., 159, 108.
- Ulrich, R.K. & Burger, H.L., 1976. Astrophys. J., 206, 509.
- Vansina, F. & de Grève, J.P., 1982. Astrophys. Space Sci., 87, 377.
- Xiong, D.R., 1986. Astron. Astrophys., 167, 239.
- Yungel'son, R.L., 1973. Nauchn. Inf. Astron. Akad. Nauka., USSR, 27, 93.
- Ziolkowski, J., 1970. Acta Astr., 20, 213.
- Ziolkowski, J., 1979. I.A.U. Symp. 83, 385.

CHAPTER 2

Methods of Observation. Reduction and Analysis

1) Introduction

1.1) Spectroscopy

In order to provide reliable absolute dimensions for the binary systems observed in this study, systematic and random errors in the radial-velocity determinations due to the effects of blending of spectral lines broadened by rapid rotation and by collisional damping must be minimised. Such observations must therefore be made at sufficiently high resolution and signal-to-noise to provide good measurements of radial-velocity. Well-defined radial-velocity curves will then provide good estimates of the mass ratio for these systems as well as minimum masses and separations for their components. A good quality spectrum can also be used to determine the luminosity ratio and projected rotational velocities of the primary and secondary components of a system from the equivalent widths and full-width half maxima of suitably-resolved features. This information can be used to discriminate between light-curve solutions of comparable quality.

The two combinations of telescope and instrument used for these observations cannot be described as ideal for this purpose. They represent a compromise between the need for high quality

spectroscopic observations and the availability of observing time on large telescopes and their ancillary instrumentation. Both the IPCS and RPCS are linear devices provided that count-rate limitations of 1 and 5 counts pixel⁻¹s⁻¹ respectively are observed. To maintain this linearity, neutral-density filters were necessary in all but the poorest weather. The length of the wavelength region observable at any one time is restricted by the size of the detector; in the case of the IDS/IPCS data, only 480Å could be observed at one time, making a small grating rotation necessary to observe the relevant helium lines in the spectra of the programme stars. The ITS/RPCS combination did not suffer from this problem to the same degree but at the cost of a lower dispersion. However, the data from both instruments have the advantage of being in digital form and consequently ready for immediate analysis. A photographic plate as a detector would have given much larger regions of the spectrum per exposure but the problems of low quantum efficiency, non-linear response and the need to scan and calibrate the plate to convert the spectrum to a digital form would make the orbital phase resolution inadequate and the reduction procedure more arduous. It was therefore decided to use these digital detectors and observe those wavelength ranges offering the most readily measurable features.

1.2) Photometry

The quality of a light-curve solution is largely dependent on the quality and definition of the light curve itself. It is therefore desirable to obtain complete light curves with a precision of better than 0.01^m. Assuming that a comparison star of constant brightness can be found within one degree of the eclipsing binary system, differential photometry can yield magnitude differences with

a precision of nearer 0.005^m in favourable circumstances. Furthermore, if each section of the light curve is observed on at least two different nights, the detection of intrinsic variability in the system becomes very much easier at this level of precision.

In ideal circumstances, the light curves of any binary system should be obtained in two or more colours in a well-defined and well-calibrated photometric system. Intermediate- and narrow-band systems are better suited to the observations of early-type systems; wide-band systems suffer from bandwidth effects in the determination of extinction corrections and the transformations to the relevant standard system. However, careful reduction procedures can minimise these problems although some difficulties can be encountered with light-curve simulation programs using wide-band data as the models themselves are essentially monochromatic. Photometric indices on a system which provides quantitative and sensitive reddening-free parameters related to effective temperature and gravity are also desirable to confirm the validity of photometric solutions. The Strömgren uvby system is the most suitable photometric system for observations of these systems although the Johnson system has been used where the former was not available at the time the observations were made (i.e. at St. Andrews and Boyden).

In the course of the photometric observations for this study, several different approaches have been made to the problem of acquiring high-precision light curves. Four different instrumental combinations have been used, ranging from single-band simultaneous two-star photometry to multi-channel single-star photometry. Each telescope and photometer combination is described in more detail in Section 2.2. These facilities are not necessarily ideal and, once again, represent a compromise between observational requirements and

the availability of suitable instrumentation and telescope time.

To complement the high-precision observations, methods are required to analyse the resulting light curves which mimic the flux distribution and shapes of the components in the most realistic manner possible. Most modern techniques of light-curve analysis rely upon the creation of theoretical light curves generated from a variety of models employing different geometrical approximations and integration schemes. Two codes were used to analyse the photometric data obtained for this study; the computer program LIGHT was employed for detached, semi-detached and contact systems whereas the program WUMA5 was used to analyse the over-contact systems since LIGHT is not well suited to the analysis of this particular configuration. A brief description of the two codes is given in Section 2.2 although more detailed descriptions of their use are given in Chapters 3-9.

1.3) Observational preparation

The observation of an eclipsing binary system in a restricted period of time requires some planning in order to give the observer the maximum opportunity of observing the whole light curve. The situation is more acute for spectroscopic observations where spectra near both quadratures offer the best chance or in some cases, the only chance, to acquire radial-velocity measurements for both components of the binary. A program which provides information on the position of the star in the sky and its orbital phase would clearly be of use.

With this aim in mind, a program was written by the author to provide the observer with data pertinent to the night of observation for a given star. The times of sunrise and sunset, the beginning and end of civil, nautical and astronomical twilights and the position and orbital phase of a eclipsing binary can be provided by a computer program PREDICT. This program will also provide information on the position and age of the moon and its proximity to the programme star. The program can be run for a number of stars on consecutive nights.

The program uses the same master files for stellar and observatory data as SIMPHOT (see Section 3.2.1) and the all-sky photometry program (see Section 3.2.2). The output is specifically designed for printing on 132 character wide printer and tabulates the local mean time, Greenwich mean time, local sidereal time, right ascension, declination, azimuth, altitude, phase and age of the moon. Similarly quantities for the programme star are tabulated every 15 minutes with the exception of right ascension, declination and age. These quantities are replaced by heliocentric Julian date, airmass and angular separation from the moon. If a minimum occurs during the night, the time at which it takes place is given separately. The precessed right ascension and declination are given along with the adopted ephemeris for the star. Warnings are provided for the proximity of the moon within a preset limit and for airmasses higher than two for the programme star. A diagram displaying the phase availability for each star is given at the end of each night. These diagrams are summarised at the end of a run to assist the observer with planning his observations.

2) Observations

2.1) Spectroscopy

2.1.1) The Isaac Newton Telescope

2.1.1.1) Instrumentation

An allocation of six nights was made for this project during 1985 August to obtain spectroscopic observations of several northern-hemisphere binary systems with the 2.5m Isaac Newton Telescope (INT) at the Observatorio del Roque de los Muchachos on La Palma. The data were obtained with the Intermediate Dispersion Spectrograph (IDS) and the Image Photon Counting System (IPCS).

The IDS is a medium-dispersion spectrograph sharing a common structure with the Faint Object Spectrograph situated at the f/15 Cassegrain focus of the INT. Two cameras of a folded short-Schmidt design, with focal lengths of 235mm (Camera 1) and 500mm (Camera 2) may be used to focus the 85mm diameter beam produced by one of three interchangeable collimators. The maximum slit length is 44mm corresponding to 4' on the sky. The slit width is variable from 40 μm to 2mm in steps of 5 μm . A selection of six gratings specially fabricated for the IDS provides a wide range of possible dispersions in conjunction with the two cameras. The spectrograph is attached to the Acquisition and Guiding Unit (AGU) which houses the calibration and comparison-source lamps, the above-slit neutral-density and colour filters and an integrating TV camera system to view the field and slit regions. The slit assembly, dekker plates and a second set of filters positioned below the slit are located within the IDS itself.

The AGU, IDS and relevant detector are computer-controlled via a user-friendly software environment known as ADAM (Astronomical Data Acquisition Monitor) running on a Perkin-Elmer 3220 instrument computer. However, changes of grating, collimator, filter and dekker slides are made manually at the telescope. The current status of the AGU and IDS is monitored by ADAM to produce a schematic display of the important elements of the system. ADAM also allows procedures to be constructed to control the setting-up and use of the IDS and IPCS as well as real-time viewing of the data and some preliminary data analysis.

Two detectors are available for use with the IDS, a red-sensitive CCD system and an IPCS whose blue sensitivity is best-suited to these observations. The IPCS detects individual photon events by using a four-stage, high gain, magnetically-focused EMI intensifier with an S-20 photocathode. The intensifier is lens-coupled to a continuously scanning, lead-oxide vidicon television camera. Once individual photon events have been detected and event-centred by the scanning electronics, the encoded positions of these events are passed to an external digital memory store every 50ms. At the end of each exposure, the contents of the memory store are transferred via CAMAC to disk and magnetic tape units attached to the instrument computer.

The usable area of the intensifier photocathode is about 30mm in diameter and the typical mode of operation for the IPCS gives a 15 μ m pixel size in the dispersion direction when scanned with the maximum 2048 scan lines. The number of pixels in the direction perpendicular to the dispersion direction can be selected by the observer within the range 18 to 514. Since the IPCS is a two-dimensional device, a single exposure of a programme star

contains the stellar spectrum and the sky background adjacent to the object being observed.

2.1.1.2) Observations

Before starting the observations for each night, the IDS was focused using a Hartmann test; the instrument is said to be in focus when a null shift is found from the cross-correlation of arc exposures made by closing the left and right Hartmann shutters respectively. Procedures within ADAM were then used to adjust the orientation of the television camera head so that the scan lines of the camera were perpendicular to the dispersion direction and to ensure the optical axis of the IPCS was normal to the focal plane of the camera. The S-distortion induced by the image-tube was removed as far as possible by applying correction signals to the scanning electronics. Finally, a flat-field integration was made using a tungsten comparison lamp with an exposure time of 10000s. A second flat-field exposure was obtained at the end of the night whenever possible.

The Jobin-Yvon 1200 grating was used for these observations with a slit width of 100 μm . Both the wide-band and UV collimators were employed in order to eliminate a focus problem in the spectrograph. By means of Camera 2 of the IDS, spectra were obtained at a dispersion of $16.7\text{\AA}\text{mm}^{-1}$. A small grating rotation was used to obtain exposures of adjacent regions of the spectrum of the object centred on 4040\AA and 4400\AA , each region being 480\AA wide. Typical stellar exposures were of the order of 600s and were coupled with a Cu/Ar comparison source exposure of 150s relevant to the wavelength region being observed. The format chosen for the IPCS

was 2048 by 66 pixels giving the smallest pixel size in the dispersion direction and a large area of sky background. A data area of 2048 by 50 pixels was actually written to tape since the first 13 cross-sections of the IPCS are unusable. To ensure that the saturation limit of the IPCS was not exceeded, above slit neutral-density filters were used at all times.

Several observations of radial-velocity standard stars were obtained at regular intervals throughout each night to ensure that there were no systematic departures from the standard system. The programme stars were observed at a wide range of phases with particular emphasis being given to those systems passing through quadratures. One B-type secondary radial-velocity standard was also observed on several occasions to allow cross-correlation analyses to be made with the programme stars at a later stage.

2.1.2) The SAAO 1.9m telescope

2.1.2.1) Instrumentation

An allocation of one week was made in 1986 February to obtain spectroscopic observations of the southern-hemisphere members of the sample. The 1.9m Radcliffe Telescope at SAAO, Sutherland was used to obtain these data in conjunction with the Image-Tube Spectrograph (ITS) and the Reticon Photon Counting System (RPCS). The telescope is mounted on a 2-pier asymmetrical mounting and is operated almost exclusively on the eastern side of the mounting which, under certain circumstances, reduced the amount of observing time available to obtain spectra of those systems rising later in the night. In certain cases, the phase coverage of some objects was restricted by the proximity of the position of the telescope to areas of the sky

where flexure of the spectrograph is known to be prohibitive.

The ITS is a medium-dispersion spectrograph of modular construction which is located at the f/18 Cassegrain focus of the 1.9m telescope. A Cassegrain collimator produces a 10cm diameter beam which is brought to a focus using a Maksutov-Cassegrain camera working at f/1.4. Slit widths in the range 100 to 300 μm are normally used, with the field and slit area being viewed by an integrating TV system. Six different diffraction gratings are available with a selection of neutral-density and colour filters. Most spectrograph functions can be operated remotely as well as at the telescope with the exception of adjustments to the grating angle, slit width, spectrograph focus and comparison lamp filters. A Cu/Ar lamp is normally used to provide comparison-source exposures whilst a tungsten lamp is used for flat-fielding the RPCS.

Spectrograms obtained with the ITS are converted to a digital form by the RPCS. An EMI9914(I) 3-stage image intensifier with an S-20 response photocathode detects photon events which are then amplified by a chain of three VARO intensifiers. The resultant signal is then fed via a fibre-optic coupling to a twin 936 element Reticon detector. Scanning electronics read the detector arrays every 3ms, and recorded events are event centred to half a diode before being added to an external memory. The size of the diodes in the direction perpendicular to the dispersion direction is such that dekkers are normally used to define star and sky "holes" for the two arrays of the detector.

The RPCS is controlled by a NOVA 3/12 minicomputer via a CAMAC interface by means of the program RENATA. The software provides a real-time display of the incoming data in each array and some crude

processing of the data. This includes flat-fielding of the spectrum and sky subtraction assuming that the programme star is being observed in one array and the sky in the other. RENATA also provides cross-correlation routines to facilitate the focusing of the spectrograph. This function can also be used for cross-correlating program stars to assess relative velocity changes between the two spectra. At the end of each integration the data are written to disk.

2.1.2.2) Observations

Before each observing run, the spectrograph was focused in a similar manner to the IDS by means of a Hartmann test. Flat-field integrations were made at the beginning and end of each night in order to make corrections for the pixel-to-pixel noise of each array of the Reticon. The typical integration time for a flat-field exposure was of the order of 12000s.

The observations themselves were made using the second-order spectrum of Grating 3 together with a slit width of $100\ \mu\text{m}$ corresponding to $0.9''$ on the sky orientated east-west. Spectra at a dispersion of $30\ \text{\AA mm}^{-1}$ were obtained with a range of just over $500\ \text{\AA}$ centred on $4200\ \text{\AA}$. Dekker 3 was used to provide two $6''$ wide sections of the slit $29''$ apart to provide a star "hole" for array A and a sky "hole" for array B. The integration times for stellar exposures were 600s whereas comparison-source exposures were made over 150s. All stellar integrations were alternated with comparison source exposures from the Cu/Ar lamp to monitor any flexure in the ITS. A copper-sulphate filter was used to remove any first-order long-wavelength contamination and neutral-density filters were used

for all stellar observations.

The observing procedure used for these observations was very similar to that described for the INT data. Three early-type stars were also observed on several occasions whose radial velocities had been determined with good precision. These stars were to be used for cross-correlation analyses with the programme stars.

2.2) Photometry

2.2.1) Twin Photometric Telescope

The re-siting and complete refurbishment of the Twin Photometric Telescope (hereafter TPT) presented an excellent opportunity to obtain high-precision light curves in a single passband of two of the northern hemisphere systems. A full description of the telescope and its operation is provided in Chapter 3 (hereafter TPT I).

Since the publication of TPT I, some alterations have been made to the telescope and the data acquisition system. The auto-guider on the reference telescope was removed as the need for very accurate guiding over extended periods was deemed to be unnecessary. The PDP-11/23 minicomputer was replaced by a BBC microcomputer employing a FORTH ROM to control the data acquisition from both photometers with the advantage of making the TPT independent of external computer facilities. Previously, both the TPT photometry and Leslie Rose telescope spectroscopy packages were run simultaneously on the PDP-11/23 making the system prone to frequent "observer-induced" crashes resulting in the loss of some or all of the photometric data for that night.

A new data acquisition program based on the original software for the PDP-11/23 was written by Mr. J.R. Stapleton incorporating the most useful aspects of programs used by the author at other observatories. It has been designed around a menu-driven system making the acquisition of data a very straightforward process to reduce observer error. The observer simply has to position a sprite next to the operation he wishes to perform or the type of observation format required. The data are stored on floppy disk and a paper copy of the observations is also made. Interaction with the keyboard directly has been limited to entering the date during the loading of the program and providing a disk file name to store the data for that night and the titles of the observing modes during the setting-up procedure. Four modes are available, labelled 0,1,2 and 3, which can be allocated to suit the needs of the observations being made. The types of observation required for the simultaneous monitoring of variable and comparison stars and the modes used are summarised below.

Mode	Observation/Title
0	Sky background measurements in both telescopes.
1	Comparison star measurements in both telescopes giving zero-point differences between the two channels.
2	Comparison star measurements in the reference telescope and check star measurements in the offset telescope to monitor the constancy of the comparison star.
3	Comparison star measurements in the reference telescope and variable star measurements in the offset telescope.

Observations can be made using both the B and V filters providing

the same modes are used for each filter. For this study, emphasis was placed on obtaining well-defined B curves.

The main menu consists of four primary functions SETUP, GO, DISPLAY and FINISH. SETUP generates a second menu to enable the observer to define the types of observation he wishes to make. This menu consists of the following seven options :-

- 1) FILE NAME .. The name of the data file is selected. This option disappears after the file name has been set.
- 2) REC/IG A choice can be made between recording the data on disk and ignoring it. The selection is made by pressing one of two buttons on the sprite handset.
- 3) TITLE The title for the chosen observing mode is defined with this option. This title appears in the data file and also on the paper listing.
- 4) NO. OF INTS The number of integrations to be made in a single observation are selected via the sprite. The default number is 3 and increments of ± 1 , ± 2 , ± 5 and ± 10 can be added to the default to give the required number of integrations.
- 5) INTEG.TIME . The integration time is selected via the sprite. Integration times in the range of 5 to 60s in steps of 5s are available.
- 6) FILTER The program is notified of a change of filter with this option; however, the filter change is manual. The selection is made by pressing one of the two buttons on the sprite handset.

7) MODE One of the four observing modes is selected via the sprite. The parameter must be defined before the other options.

Returning to the main menu, the GO option starts the chosen observing sequence. During the sequence a graphical display of each integration in each channel is plotted. The five observations before the current one are also displayed on the screen with a ratio of the counts in the sense channel 1 divided by channel 2. This ratio provides a crude approximation to a differential magnitude. The sequence may also be aborted at any time without storing the current integration by pressing any key on the BBC keyboard. The DISPLAY option provides two diagrams plotting data for the current mode and filter; one depicts the counts in both channels, the other the ratio of the two counts. FINISH stops the program and closes the data file. The program can be restarted if necessary, by typing RESTART as the data for the night also reside on the program disk.

The data file produced on the floppy disk is in ASCII format allowing a simple file transfer to be made to the VAX computers of the University Computing Laboratory for subsequent reduction. Each record of the data file contains the label for the observation, the filter and mode, the time of the end of the integration in seconds since the previous midnight, a truncated Julian date for the start of observations, the integration time and the counts from each photometer. The reduction of these data is described in Section 3.2.1.

2.2.2) Steavenson 0.75m telescope

Simultaneous Strömgren photometry of two systems was obtained on this telescope which is located in the Sierra Nevada mountains near Granada. The observations were made with a Danish 6-channel uvby- β photometer which has been described in detail by Florentin Neilsen (1983). The main advantage of this photometer is the ability to observe all four Strömgren passbands simultaneously while maintaining a sufficiently high signal-to-noise for all the passbands. The simultaneity of these multi-channel observations results in more accurate colour indices being obtained as well as more observations per unit phase interval.

The photometer was controlled by a Hewlett Packard model 9816 microcomputer running menu-driven control software. This system controlled the photometer hardware, the data acquisition and the movement of the telescope around a small area of sky containing the objects in the monitoring sequence. The count rate per second for the chosen passband was displayed graphically during the integration to warn the observer of the onset of cloud or poor positioning of the stellar image in the diaphragm. Other options included the setting of integration times, the recall of data for programme stars stored on disk and the graphical display of all data acquired during the night. The program also provided information on the quality of the observations by comparing the actual signal-to-noise with expected Poisson noise. Further software was provided for the analysis of data for each night and the transmission of the data to the VAX computer of the Instituto de Astrofísica de Andalucía (IAA) in Granada.

The observational procedure involved measuring the colours of a total of up to 25 standard stars at the beginning, middle and end of each night as well as hourly observations of a local standard star. Sky background observations were made every 15 minutes during the monitoring sequence, more frequently during moon-rise and moon-set. Comparison star observations were made every 5-10 minutes. The second successful observing run at the Sierra Nevada was affected by dust and all sky photometry was not possible. The observing procedure under these circumstances was modified in the manner described in Chapter 6.

2.2.3) SAAO 0.5m telescope

Observations in the Strömberg system were obtained at SAAO, Sutherland during 1985 February on one of the southern hemisphere eclipsing binaries. The single channel Modular photometer was used in conjunction with a cooled EMI 6256QA tube. The observing technique used for these observations followed the pattern described in Section 2.2.2. Since integrations in each filter are made sequentially with this photometer, the filter sequence used for these observations was ybvuvby. This minimises the effect of any irregularities that may exist in the atmospheric extinction which are most pronounced in the u passband.

The photometer is controlled by a NOVA 1220 minicomputer using the software package WALTER. This program controls filter changes and integration times according to pre-programmed instructions. An entire observing sequence can therefore be specified in terms of a filter number, an integration time and a star/sky identifier. During the course of each integration, the incoming data can be

sampled and displayed on an oscilloscope screen to give the observer some warning of non-photometric conditions. At the end of the sequence, the integrations can be reduced to either instrumental or standard-system magnitudes and colours with their corresponding errors.

2.2.4) Boyden 0.41m telescope

UBV observations were obtained at the Boyden Observatory of the University of the Orange Free State at Mazelspoort during 1985 and 1986. A 0.41m Cassegrain telescope was used in conjunction with an uncooled Hamamatsu R585 photomultiplier tube with a bi-alkali photocathode which offered a good blue response and a very low dark count (less than 5 counts s^{-1}). The output pulses from the post-processing unit of the photomultiplier tube were counted by a Thorn-EMI Starlight-1 counter which could be interrogated by computer using a BCD interface. A more complete description of the photometer and ancillary equipment has been presented elsewhere (Malcolm and Bell, 1986).

As part of the modernisation of the photometric facilities at Boyden, it was decided that these observations should be made under the control of a Hewlett-Packard model 85 microcomputer. The data could then be stored on floppy disk in a form suitable for subsequent analysis and also on paper. Computer control also has the advantage of allowing the observer to make on-line reductions of his observations which can be of great assistance in identifying faint programme stars.

During 1985, May and June, the data acquisition and reduction software was developed to drive the system. The main program, CINDY, provides the observer with overall control of the photometer and a number of additional utilities by means of a menu-driven system. After prompting the observer for the current date and SAST of the start of the observing run, the program then keeps track of the sidereal time, SAST and universal time. An observer may load the names, positions and epochs of up to 1000 objects into a file stored on floppy disk and access these data via CINDY at any time during the night; new objects may also be loaded or existing co-ordinates precessed to the night in question at any time during the night. The E and F region standards (Cousins, 1983), with their standard magnitudes and colours, are stored in separate files and may be accessed in an exactly analogous fashion. Once the data for the object have been accessed by CINDY the co-ordinates and current hour angle are continuously available to an observer to aid its location.

Once the desired object is located and centred for observation, the observer can then define the sequence of filters and integrations times for any set of observations at any time during the observing run. Each set of observations is then automatically controlled by the computer and the data acquired are then output to the printer and stored on floppy disk, although the observer may interrupt the sequence at any time to repeat an integration or abort the sequence. The only remaining manual task is the filter change itself, for which the observer is prompted at appropriate moments. The implementation of an automatic filter change could not be made because of the shortage of suitable hardware. Once an observing sequence has been acquired, the observer has the option of on-line

reduction of the data which includes :-

- 1) The instrumental magnitudes and their statistical errors,
- 2) The mid-point time of the observing sequence and fractional Julian Date,
- 3) The airmass at the mid-point of the observing sequence,
- 4) The standard magnitudes and colours with their statistical errors.

The on-line reduction defaults to the standard system as defined by the Cousins E-Region UBVRI system, although this could easily be modified for use with the Stromgren system. The default zero-points of the system may be updated at any time during the night by observing an E or F region standard and using the zero-point facility of CINDY. After viewing the on-line reductions, or at some other suitable moment, the observer may enter whatever comments may be deemed appropriate for output to the printer and the data file on the floppy disk. The observer may also define very long sequences of repetitive integrations for programs which require single-colour monitoring with a minimum time resolution of one second.

Once the observing run is complete a number of additional programs are available to process the stored data. A data file may be listed directly to the printer, simple editing to correct entries in the data file may be made and data files can be compressed into a more compact form for longer-term storage on archive floppy disks.

The observing technique used for these observations followed the same pattern as that described in Section 2.2.2. The sequence of filters used was VBUUBV for all observations for the reasons

outlined in Section 2.2.3.

3) Reductions

3.1) Spectroscopy

3.1.1) Preliminary reductions with SPICA and FIGARO

The data obtained with the RPCS were copied from disk and written to magnetic tape in FITS format (Wells et al. 1981) at SAAO, Cape Town. The IPCS data was written in a similar format at the INT. The STARLINK software packages SPICA and FIGARO were used to flat-field the data and perform sky subtractions for the IPCS and RPCS observations respectively.

3.1.1.1) IPCS data

The two-dimensional IPCS data were flat-fielded to remove the non-uniform detector response from all the data by means of the mean flat-field for each night. The stellar spectra covered a maximum of 6 cross-sections of the 50 stored on tape. The data in the 6 cross-sections of each scan line were then summed to produce a one-dimensional data array representing the stellar spectrum. Although all the observations were made in the presence of a nearly full moon, the neutral-density filters required for the stellar observations resulted in a very small sky background count. Two strips, 6 cross-sections wide, and 15 cross-sections away from the central cross-section of the stellar data were then averaged and subtracted from the stellar data using a procedure incorporating standard SPICA functions. The data for each night were then written to a SPICA 1-D memory file in arc and stellar pairs.

3.1.1.2) RPCS data

The reduction procedure for the RPCS observations were initiated by dividing the flat fields by a heavily-smoothed version of the flat fields to produce two files containing the pixel noise data for both arrays. Subsequent arc, stellar and sky exposures were then divided by the pixel-to-pixel noise file corresponding to the array in which the data had been taken. As the detector is composed of two arrays, the possibility exists that shifts may occur between the two arrays. Under such circumstances, the presence of night sky lines would not be satisfactorily subtracted out from the stellar data. The arc exposures recorded in arrays A and B were cross-correlated against each other to reveal any systematic shift. A constant shift of 1.8 pixels was measured but the sky background signal in array B was found to be indistinguishable from the inherent cross-talk in the system produced by the spectrum in array A of 2.5%. The sky subtraction was made by scaling the sky background data in array B by the ratio of the smoothed flat fields of array A to array B and then subtracting the result from the stellar data in array A. Once again the data was written to a SPICA 1-D memory file in a similar manner to that used for the IPCS data.

3.1.2) DAO-based software

At this stage of the reduction procedure the SPICA 1-D memory files must be converted to FITS format to be compatible with REDUCE, which was originally designed for use with photographic spectra scanned on a PDS machine. The arc and stellar data for each observation is converted to a pair of FITS files using SPICON. This program requests the pixel size of the detector and then displays

the arc spectrum from which an easily-recognisable feature close to the centre of the spectrum is identified. This feature is then the reference point from which the rest of the arc spectrum is measured. S and F FITS files are then produced containing the stellar and arc data respectively. This procedure is repeated for each arc/stellar pair in the 1-D memory file for each night.

REDUCE (Hill et al., 1982a) is an interactive spectrophotometric reduction program designed to process PDS scans of photographic plates or RPCS/IPCS-type observations. Its main functions are to measure arc spectra, make a density to intensity conversion if required, linearise the stellar spectra in wavelength, rectify the spectra and finally log-linearise the spectra for cross-correlation analysis. All of these functions are called by means of a menu system which ensures that large numbers of spectra can be analysed in a homogenous manner. Two routines provide the basis of REDUCE; VELMEAS, which determines the position of a line and calculates radial velocities, and VLINE which enables measurements of the equivalent widths and full width half maxima of spectral lines and projected rotational velocities and radial velocities of stars.

VELMEAS (Hill et al., 1982b) is used to identify and measure the positions of lines in a spectrum. It uses a "standard plate", a technique described by Aitken (1935), which predicts the positions of lines in a spectrum based on known spectrograph constants such as grating equations and Hartmann constants. The positions of the lines are measured by fitting parabolae to the peak or trough of each profile. The standard-plate coefficients can be generated by preliminary identification and measurement of a relatively small number of widely-distributed features on an arc spectrum with the program STDPLATE (Hill and Fisher, 1982).

The calibration of the spectra is made by measuring positions of selected arc lines in a F file and comparing them with the predicted positions with the standard plate. If a list of wavelengths for specific lines is provided by the user, the position of any feature can be derived from the standard-plate coefficients and measured either by means of cursor placements or by VELMEAS automatically. A polynomial is fitted through the residuals of the observed positions of the arc lines from those predicted by the standard plate after the removal of mis-identified lines either by eye or by pre-selecting a rejection limit. This polynomial serves as a correction to the original standard plate. The resulting arc calibration for each F file is stored on disk to be used in the linearisation of the corresponding S file.

VLIN (Hill et al., 1982c) provides a means of fitting a combination of Gaussian, Lorentzian or rotational profiles and a linear continuum to a spectral feature to determine not only the radial velocity but the equivalent width and full-width half maximum. The heart of the subroutine is the curve-fitting routine CURFIT (Bevington, 1969) which requires some starting values to make a preliminary estimate of the shape of the feature to be fitted. This technique lends itself well to the analysis of clean blended features of spectroscopic binaries by fitting an analytic function to the specified feature. The use of this technique has been limited to those features unaffected by noise spikes despite being a more reliable method of determining radial velocities which is less affected by the blending of the lines of the individual components.

VCROSS (Hill, 1982) is a separate program which primarily uses rectified log-wavelength-linearised spectra to measure radial velocity differences between two stars by cross-correlation of regions of one spectrum with the same regions of another. The fourier transform of the template spectrum is multiplied by the conjugate transform of the programme spectrum. The inverse fourier transform of this product, suitably normalised, yields the desired cross-correlation function (CCF). The position of the peak corresponds to the relative radial-velocity between the two stars.

To be successful, this technique requires the stars to be of similar spectral type to ensure sharp CCF peaks. However, this method has been found to be unsuitable for the data obtained on the IPCS and RPCS because of the inherent noise in the data. Cross-correlating the rotationally-blended HeI features of spectroscopic binaries with the sharper features of B star standards can preclude the measurement of the weaker secondary component peak in the CCF to the point where it cannot be identified. Fourier filtering techniques cannot readily filter out these noise spikes. A technique to determine the velocity semi-amplitudes of a spectroscopic binary assuming spectra have been taken at both quadratures is described in Appendix A of Chapter 6. The mis-matching problem has been largely eliminated by cross-correlating the two quadrature spectra. Using this method, cross-correlation has been found to be successful.

ASH/FTSPLOTT is based on existing DAO software but written in St. Andrews by Dr. Andrew Adamson. This program provides a number of different routines for manipulating spectra including plotting, smoothing, rectifying and performing simple spectral arithmetic. The program is menu-driven in a similar manner to REDUCE and

incorporates the master file option common to most of Dr. Graham Hill's software. Each master file consists of a list of FITS files which are to be processed in a similar manner. The primary uses of the program were to display the spectrum, to smooth the spectrum by running-mean smoothing, to rectify the spectrum by division of a heavily-smoothed version of itself and to output the resulting data. The rectification and smoothing of all spectra for this study were made using this software in preference to the more time consuming methods used by REDUCE which were found to produce very similar results.

Further details of all of these programs are given in the references cited and a more complete description of their facilities and use can be found in the relevant user-guides.

3.2) Photometry

3.2.1) Simultaneous two-star photometry

The first stage of the data reduction procedure is to edit the output file produced by the TPT data-acquisition program to correct observer-related errors such as incorrect identification of the observing mode and to remove data that have been badly affected by cloud. The next stage of the reduction procedure is to evaluate the extinction coefficient(s) and zero-point difference(s) between the two channels for the night. Two computer programs, SIMPHOT and SIMPLOT, written by the author, are used to perform these determinations and to produce the final instrumental differential light curve for the variable star. Both of these programs make full use of graphical displays to ensure the observer has confidence in the reductions being made.

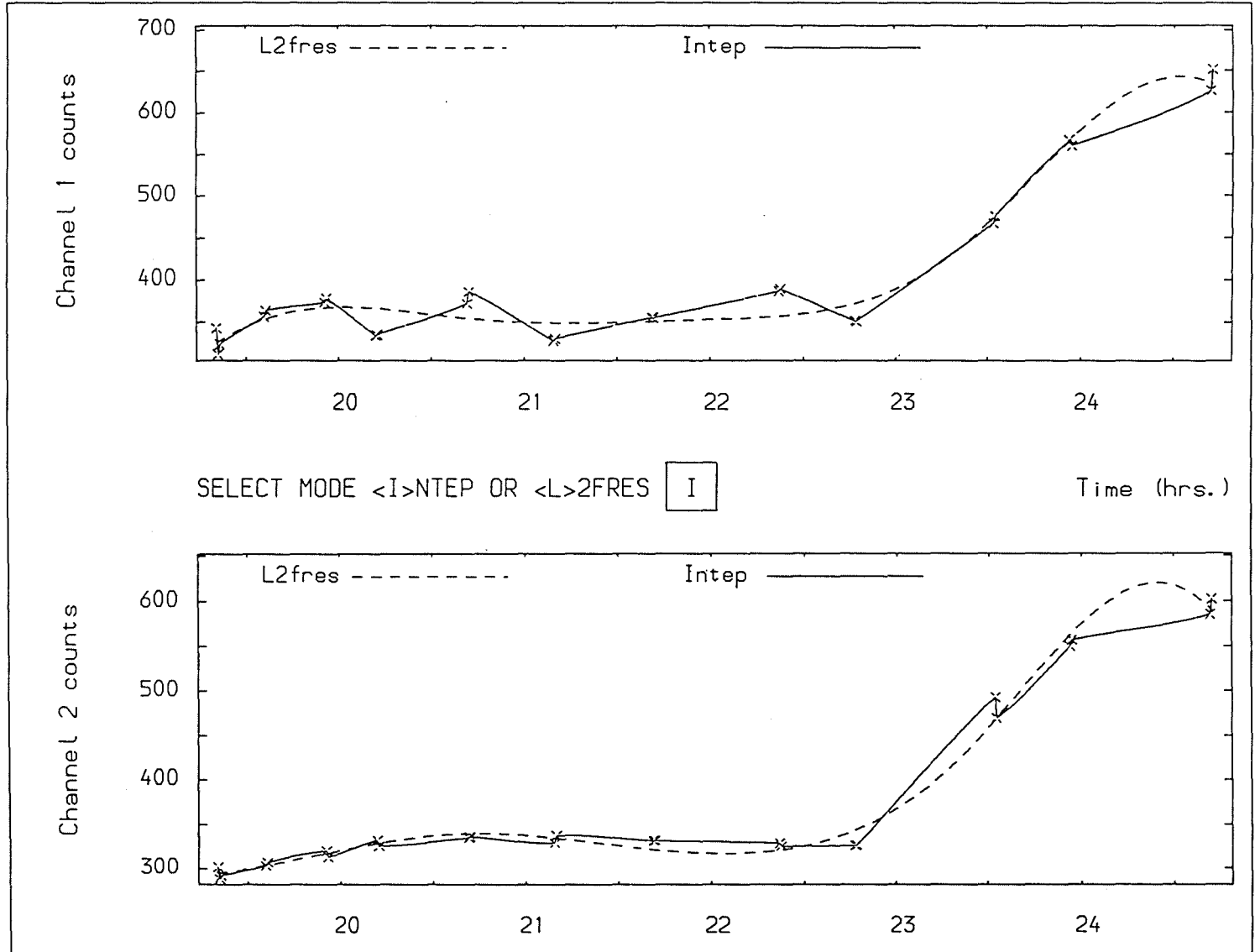
SIMPHOT is designed to cope with observations of a variable, comparison and check star in either or both of the B and V filters and is normally run twice during the reduction procedure. For the purposes of this discussion, the assumption has been made that single filter observations have been made. On the first run the extinction and zero-point difference are set to zero. During each run the program reads in the TPT data, corrects the counts for dead-time effects and performs sky background subtractions using one of two methods described below. Corrections are then made for extinction in both channels and a differential magnitude is formed from the two channels providing variable minus comparison (V-C), check minus comparison (K-C) and comparison [channel 1] minus comparison [channel 2] (C_1-C_2) observations. The extinction can then be evaluated after the first SIMPHOT run with SIMPLOT by determining the slope of the (comparison magnitude, airmass) diagram. The zero-point difference can be found from the mean (C_1-C_2) observation.

The positions of the variable, comparison and check stars at a given epoch are stored in a master data file which also contains the most modern ephemeris for the variable star. SIMPHOT simply prompts the observer for the names of the stars observed and extracts the relevant information from this master file. If a star is not found then the master file can be updated from within SIMPHOT. Further prompts are made for the dead times of the photomultiplier electronics in both channels, the mode number of the type of observation and the channel in which the variable or check star was observed. The program then prompts for the relevant extinction coefficient and zero-point difference.

A choice of two methods of sky subtraction is available; L2FRES (Powell, 1967), a least-squares cubic-spline-fitting routine and INTEP (Hill, 1982), a hermite-polynomial interpolation routine. L2FRES is used to fit the sky background counts and evaluate the resulting spline at the times of the stellar observations and has the advantage of providing a smoothing action on the background data. INTEP, however performs an interpolation based on the four counts adjacent to the time of observation. This routine follows the fluctuations of the sky background more rigorously representing the subjective curve one might draw through the data points. L2FRES can provide unrealistic fits where large numbers of sky background measurements were made in discrete groups. Since the number of knots is proportional to the number of points, the spline has greater freedom to follow small trends in the sky background data (see Figure 1). The observer can then select the most plausible fit to the data and the sky-background count evaluated at the time of the stellar observation is subtracted from the stellar count.

The resulting sky-subtracted data is converted to an instrumental magnitude in the usual manner and further corrected for extinction. The differential magnitude between the two channels is then generated by simple subtraction taking into account the zero-point difference. At this point three output files are created for V-C, K-C and C_1-C_2 observations. These files contain a heliocentric Julian date, a phase (set to zero for K-C and C_1-C_2 data), channel 1 magnitude and airmass and channel 2 magnitude and airmass. These files can be read by SIMPLOT to allow further graphical manipulation of the data they contain.

Figure 1: Sky-background subtraction using the INTEP and L2FRES options within SIMPHOT.



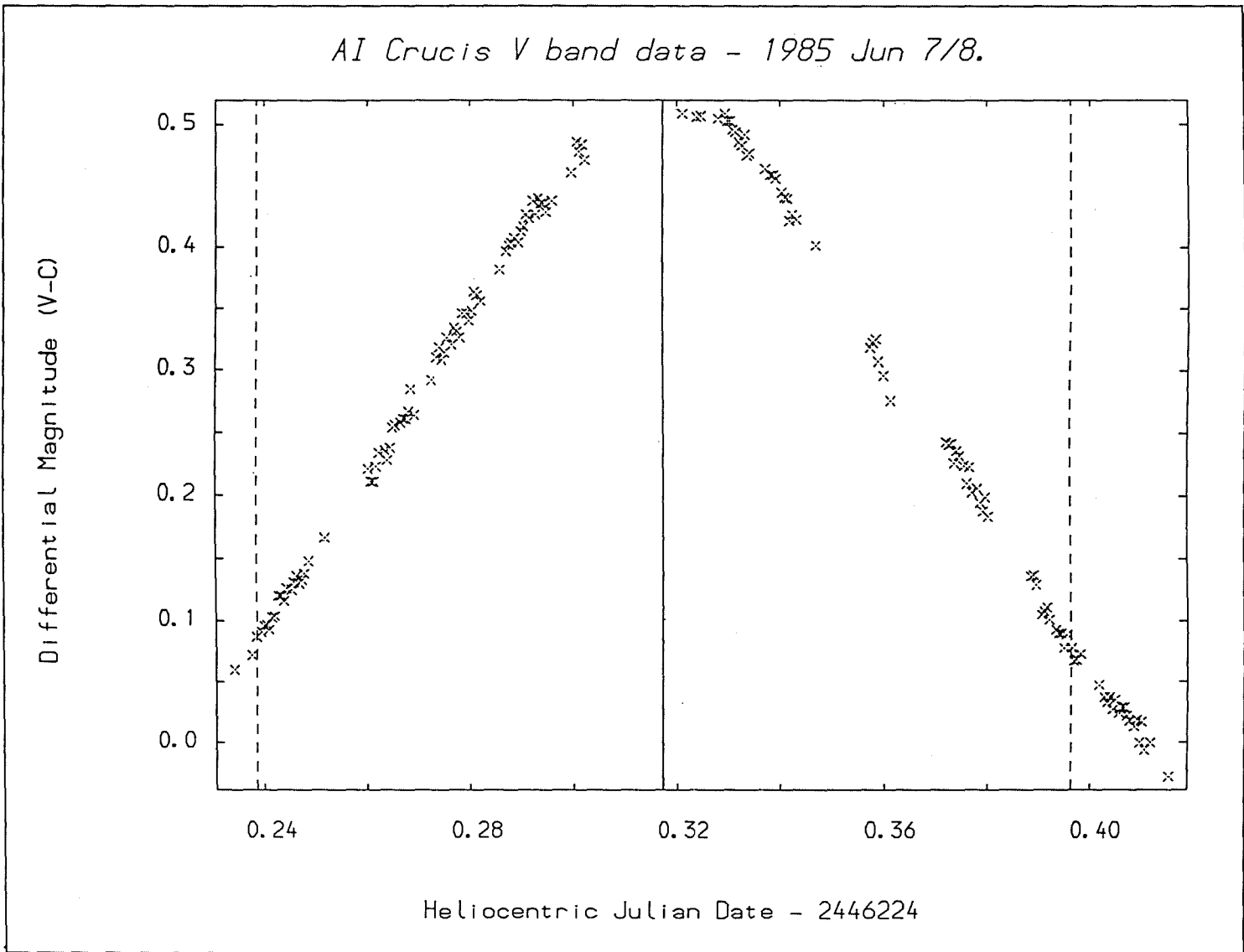


Figure 2: Determination of the time of minimum of an eclipsing binary using the method outlined in the text within SIMPLOT.

SIMPLOT reads the output files produced by SIMPHOT and allows the observer to plot out either the differential magnitude or the individual channel magnitudes against time, phase or airmass. Having selected the data to be plotted, some measure of graphical editing can be done. This involves the removal of individual points or groups of points. Parts of the plot can be examined more closely by "windowing" on the area of interest. The data can be fitted using splines and polynomials of up to order 9 and also provide summaries of those fits. Determinations of times of minima can also be calculated by means of the method of Kwee and van Woerden (1956) and displayed on the relevant plot (see Figure 2). Determinations of the extinction coefficient can be made simply using the polynomial-fitting routines on comparison magnitude against airmass plots. This piece of software is designed to run on Tektronix 4010 compatible terminals and the resulting graphical output can be stored in disk files for subsequent hard-copy output.

3.2.2) All-sky photometry

A suite of programs was written by the author to reduce photometric data obtained on both single- and multi-channel instruments in a consistent, thorough manner, emphasising the use of graphical displays of the data at all stages of the reduction procedure. The software was designed to cope with a particular style of observing which involved the monitoring of a variable star over a substantial part of the night and the measurements of standard stars to evaluate the transformations to the relevant standard system.

To facilitate the reduction procedure, a standard file format was adopted involving information on the stars observed being stored in the first section of the data file. The first stage of the analysis was to create this standard file from the data storage method used by such observatories as the SAAO, IAA and Boyden. This conversion provided the opportunity to include a preliminary editing routine to correct for errors made at the time the observations were made involving object names, filters and star/sky identifiers. All the data are corrected for dead-time effects at this stage.

The relevant data for all the programme stars and a substantial number of standard stars are kept in separate master files which can be accessed by the conversion program as required. Data for the observatory itself is stored in another master file and can be accessed in a similar manner. If the data requested does not exist in the file, the file can be updated from within the conversion program. The information stored in the file header can be summarised as follows:

First line : DATE, SITE, SYSTEM AVAILABLE, SYSTEM USED, MODE, FILE I.D., NVAR, NCMP, NCHK, NSTD, NOBS.

NVAR lines : VARIABLE NO., VARIABLE NAME, R.A., DEC., PERIOD, TIME OF MINIMUM.

NCMP lines : COMPARISON NO., COMPARISON NAME, R.A., DEC.

NCHK lines : CHECK NO., CHECK NAME, R.A., DEC.

NSTD lines : STANDARD NO., STANDARD NAME, R.A., DEC., COLOUR1, COLOUR2, COLOUR3, COLOUR4, COLOUR5, COLOUR6.

NOBS lines : OBJECT NO., OBJECT NAME, TIME, COUNT1, COUNT2, COUNT3,

COUNT4, COUNT5, COUNT6.

DATE is date in terms of the day, month and year of the beginning of the night's observation. SITE is the observatory name, SYSTEM AVAILABLE is the full photometric system offered by the observatory. SYSTEM USED refers to the subset of the available photometric system used. MODE refers to the nature of the observations i.e. simultaneous observations in n colours or single band observations. FILE I.D. is a counter to indicate how far the user has progressed through the reduction procedure. NVAR, NCMP, NCHK and NSTD are the number of variable, comparison, check and standard stars measured during the night. NOBS is the total number of observations made during the night. COLOUR1-5 refer to the filters in use (e.g. U,B,V,R,I), however COLOUR6 always refers to $H\beta$. COUNTS1-6 represent the counts in the corresponding filters. The remaining entries above are self-explanatory. For single-band observations unused filters are simply assigned zero counts. A distinction is made between sky background measurements relating to the monitoring sequence and those pertaining to standard star observations with the object name i.e. SKYM for the monitoring sequence and SKYS for the standard star measurements.

In common with SIMPHOT (see Section 3.2.1) two different methods can be used for sky background subtraction. These routines have been described in detail in Section 3.2.1 and operate only on those sky measurements which have been identified as being part of the monitoring sequence. The standard star-sky background subtraction can be effected in one of three ways. The sky observation immediately before, immediately after or simply closest in time to the standard star observation can be used. In most cases the sky background is measured immediately after the standard star

but this is not always the case. The original file header and the resulting sky-background-subtracted counts are stored in a new data file. The new output file contains stellar observations only and a simple program is used to convert the counts to magnitudes to produce another output file.

The next stage of the reduction procedure is to evaluate the extinction coefficient for each passband. Several different methods of fitting extinction curves are available using functions of airmass, and where necessary, azimuth and time. The normal first-order least-squares fit using the airmass and magnitude of the comparison star observations can be used in the majority of cases. In those cases where significant trends from the straightforward fit can be seen in both the comparison and check star magnitude versus airmass diagrams, polynomials can be fitted to the residuals of the first-order determination to assess the need for azimuthal terms and time drifts in the behaviour of the extinction. The resulting polynomial can then be used to represent accurately the extinction variations through the night and subsequently to transform the instrumental magnitudes to extra-atmospheric magnitudes. The differences between the normal linear relation between instrumental magnitude and airmass and the refinements for azimuthal and time dependencies are presented in Figures 3a, b and c. The data presented in all these diagrams was obtained during the observations of AH Cephei at the Observatorio del Sierra Nevada where Sahara dust can affect the behaviour of the extinction during the night. It is quite apparent that the simple linear model is not adequate to provide the necessary extinction corrections for that night and recourse must be made to azimuthal and time dependencies.

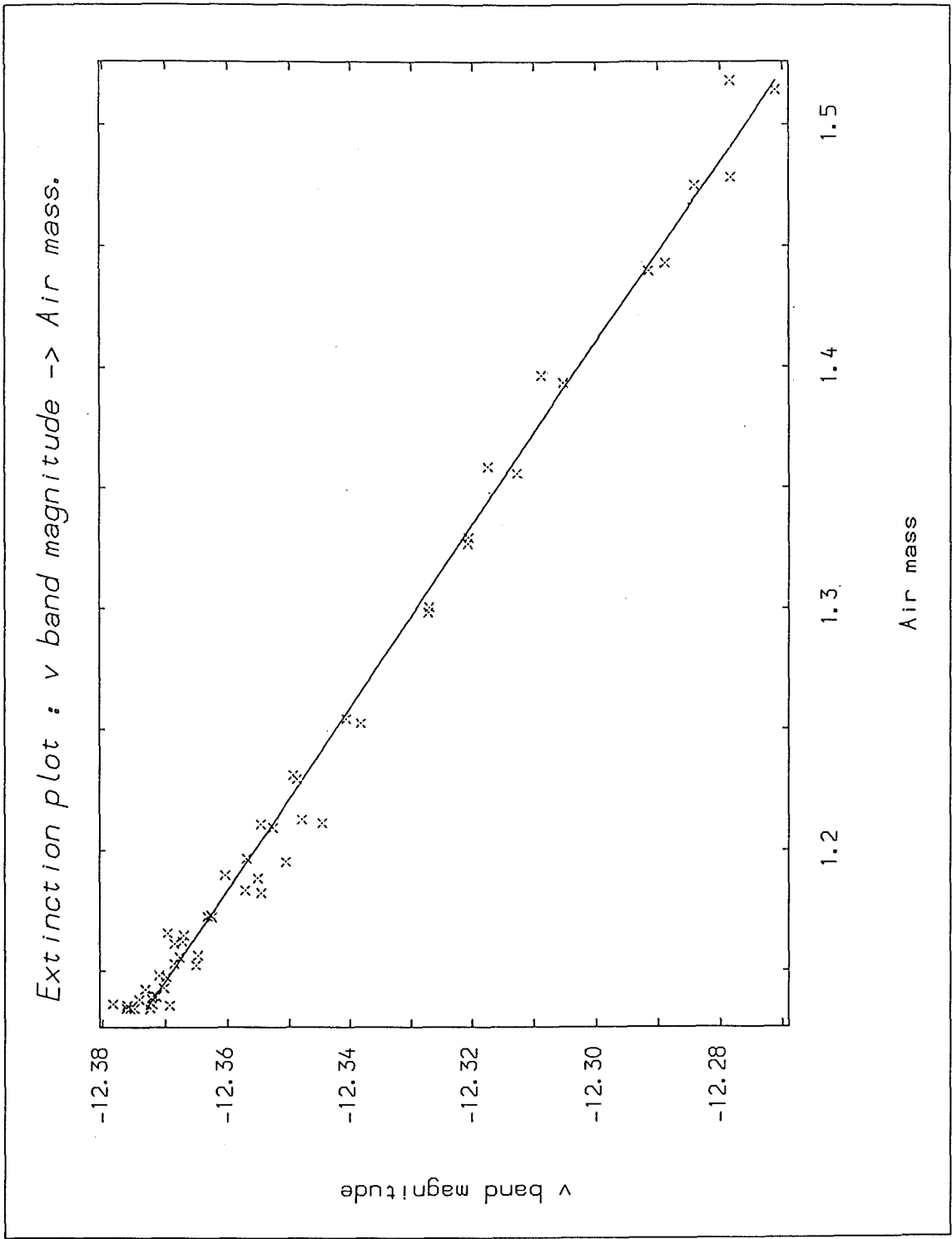


Figure 3a: Extinction curve using the linear relation between instrumental magnitude and airmass.

Differential magnitudes can then be evaluated in the sense variable minus comparison and check minus comparison via either INTEP or L2FRES in a manner similar to that used for the sky background subtraction. At this point in the reduction, the possibility of any variability in either the comparison or check stars must be evaluated. This can be achieved by several means including visual inspection, the application of a variety of statistical tests such as the Durbin-Watson test and Fourier analysis.

The final stage of the reduction procedure involves the determination of the transformation equations from the observations of the standard stars and the conversion of the instrumental magnitudes and colours to those of the standard system. A file is generated containing the instrumental and standard magnitudes and colours of the observed standard stars, their times of observation, and airmasses. Transformation equations are then determined from these data by the method of least-squares. The software used for this study is designed primarily to deal with Strömngren photometry but a similar procedure can be followed for UBV photometry with the exception of the treatment of extinction. This modification will be discussed later in this section.

Assuming n standard stars in the Strömngren system have been observed, then the necessary transformation equations are of the form:

$$C_{\text{std}} = \text{Zero point} + C_{\text{ext}} \cdot \text{Scale factor} + \text{Colour term} \cdot (b-y)_{\text{std}}$$

and,

$$C_{\text{ext}} = C_{\text{inst}} - \text{extinction coefficient} \cdot \text{airmass},$$

where C_{inst} , C_{ext} and C_{std} refer to the instrumental, extinction corrected and standard colours respectively. Knowing C_{std} , C_{inst} and the airmass, n equations of condition in four unknowns (i.e. the zero point, scale factor, colour term and extinction coefficient) can be formed. A least squares solution may then be made to obtain the best estimates of the four unknowns.

The usual procedure is to evaluate the zero point, scale factor and extinction coefficient for each night. The colour term is usually very small and is set to zero for the preliminary analysis. If the extinction has been determined reliably using the comparison star observations in the different passbands then the extinction coefficients obtained by the different methods can be checked against each other. However, the extinction coefficient determined from the comparison star observations is usually adopted.

Assuming the observations are carried out on consecutive nights on the same combination of telescope, photometer and filter set, the scale factors and colour terms should not vary appreciably during the observing run and the mean values of these terms can be adopted. The solutions can be re-run to determine the zero points and colour terms for each night fixing the scale factor to the mean value and the extinction to that determined from comparison star observations. Finally the solution should be re-run once more to evaluate the zero-point alone, fixing scale factors and colour terms to mean values and the extinction coefficient to the relevant value for that night.

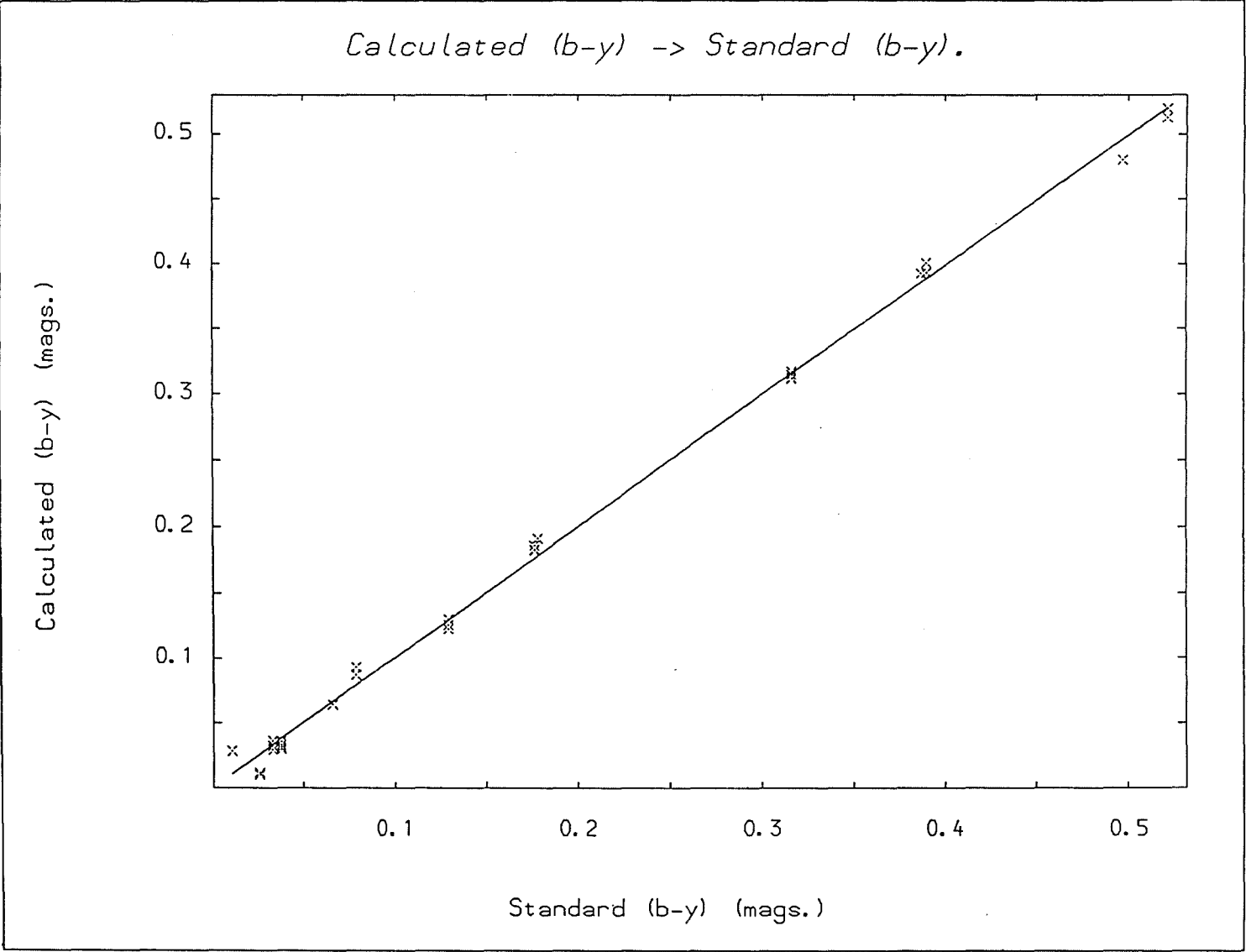


Figure 4a: Calculated (b-y) colour against standard (b-y) colour.
The line represents a linear relation between the two quantities.

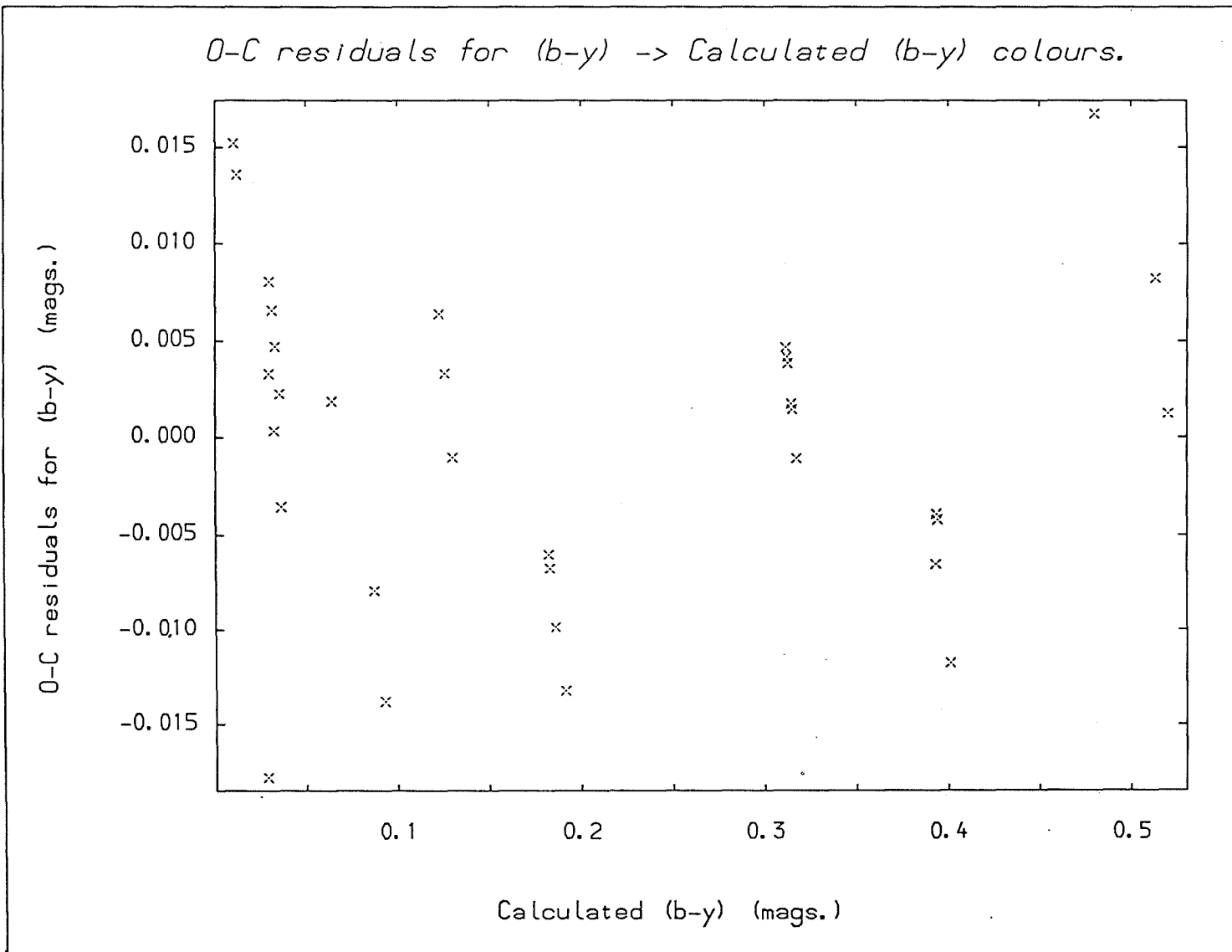


Figure 4b: (b-y) residuals against the calculated (b-y) colour.
 Any trends in colour can be seen at this stage.

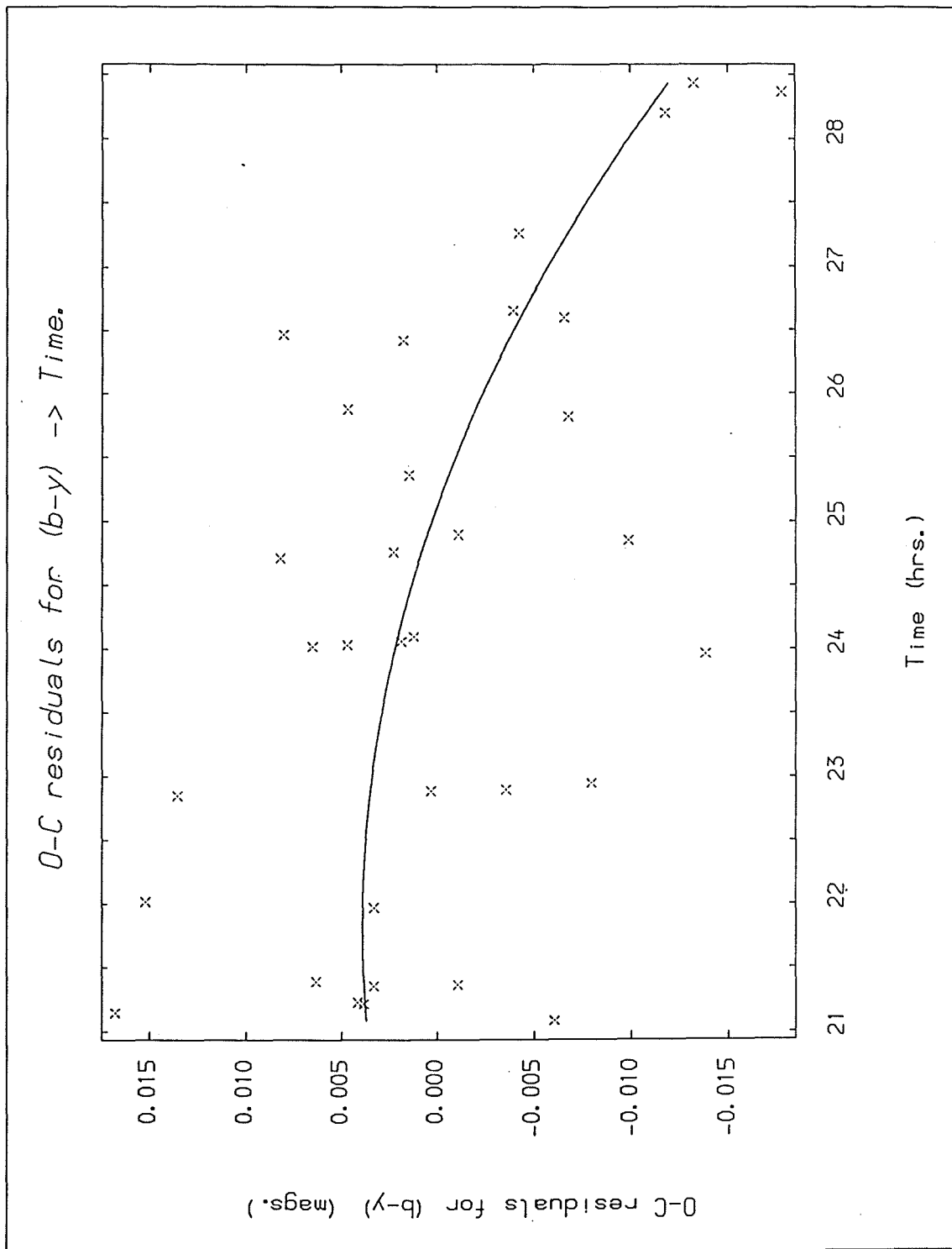


Figure 4c: (b-y) residuals against time. A second-order polynomial to represent a possible time drift has been plotted as an example.

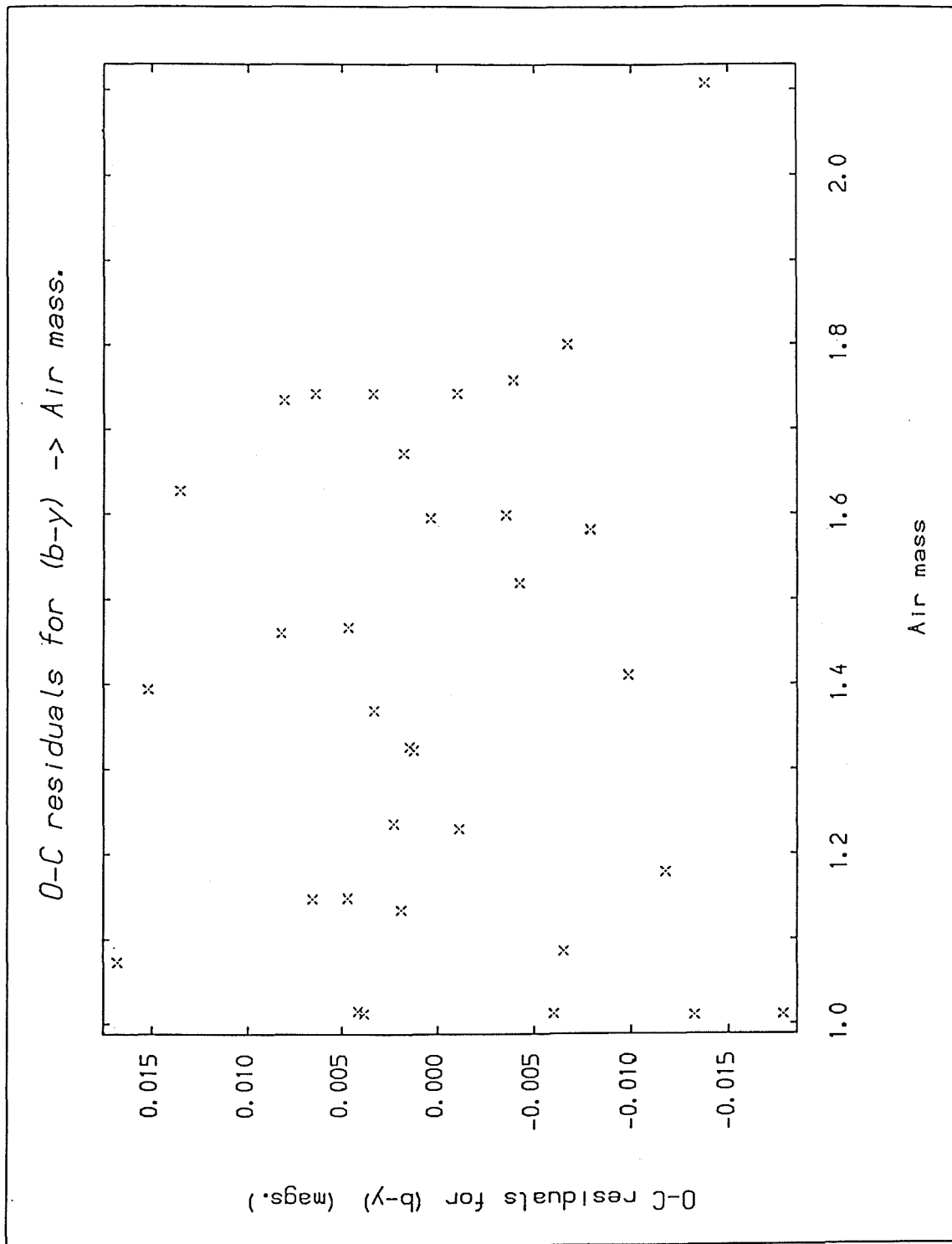


Figure 4d: (b-y) residuals against airmass. Any peculiarities relating to extinction can be identified at this stage.

After each solution, the calculated colour is plotted against the standard colour and the residuals of the observed colours from the calculated colours are plotted against the calculated colour, time and airmass to assess any trends in the data (see Figures 4a, b, c and d). At this point, the observations may be graphically edited to remove poor observations and incorrectly identified standard stars. The procedure outlined above can be repeated until the user is satisfied with the transformations derived. The main advantage of this technique is that all the data are used rather than using special groups of standards in certain parts of the sky specifically to evaluate extinction coefficients or colour terms only.

The modification for Johnson photometry requires some determination of first and second order extinction coefficients by hand. Extinction pairs of standard stars were observed at Boyden specifically to evaluate the troublesome second-order effects. The input data file can be modified to contain extinction-corrected magnitudes and the option for extinction determination in the least-squares analysis removed.

4) Analysis

4.1) Spectroscopy

The determination of the orbital elements of a spectroscopic binary system can be made in several ways. The most popular methods are those of Irwin (1973), Sterne (1941) and Lehmann-Filhes (1894). The method of Lehmann-Filhes is best-suited to orbits with eccentricities in excess of 0.1, while Sterne's method is available in two forms, a rigorous method for orbits of any eccentricity and a

simplified method for orbits of low eccentricity (< 0.03). Irwin's method is applicable to those systems with circular orbits in which pairs of radial velocities for each component can be measured. Its main use lies in the determination of the mass ratio and the systemic velocity of the system.

No evidence has been found for eccentric orbits in any of the systems studied and the recommendations of Popper (1974) have been adopted for the analysis of the radial-velocity curves. Separate least-squares solutions have been made for the velocity semi-amplitudes and systemic velocity of both components. In the case of those secondary components which are substantially less luminous than the primary, the quoted systemic velocity is that determined from the analysis of the primary radial velocity curve. The computation of the projected semi-major axes and minimum masses of both components and their standard errors is given in Appendix A.

4.2) Photometry

4.2.1) LIGHT

The majority of the photometric data gathered for this study has been analysed with LIGHT (Hill. 1979). Employing Roche geometry, it has been designed to solve a wide variety of light curves with the exception of over-contact systems for which only crude approximations can be made.

Synthetic light curves can be generated from a relatively small number of physical parameters, namely the radii and temperatures of the two components, the mass ratio and the inclination of the orbit of the system. However, LIGHT can also treat heating and scattering

effects in a realistic manner and also offers choices of either theoretical or observational limb-darkening coefficients and either black-body or model atmospheres. Light curves can be generated for up to 90 wavelengths.

The light curve is solved by means of CURFIT (Bevington, 1969) using a differential-corrections procedure, providing a reliable method of solution for up to 15 parameters. A more realistic limit of 5-6 parameters may be solved for at any one time using up to five light curves simultaneously. However, in this study, each light curve is analysed separately because LIGHT is limited to a total of 1200 data points, irrespective of the number of light curves involved in the solution.

LIGHT can also treat systems with eccentric orbits and take into account the presence of a third body which can be described in terms of its radius and temperature. Components exhibiting non-synchronous rotation may also be modelled by modifying the potential generated by the Roche geometry. A more complete description of this program can be found in the paper by Hill (1979) and the relevant user guide.

For all the subsequent work, the mass ratio in the photometric solutions was fixed at the spectroscopically-derived value and the primary-component temperature chosen by reference to a suitable empirical [photometric colour index, temperature] relation. Solutions were made for the secondary temperature, the polar radii of both components and the inclination of the orbit. A full description of the use of the program is given in the analysis of the photometric data for each system.

4.2.2) WUMA5

The surface of the common envelope of an over-contact system may be assumed to follow an equipotential surface lying between the inner and outer critical surfaces. Rucinski (1973) defined a fill-out factor which measures the degree of contact of the two components of the system. It is defined in such a way that the fill-out factor is unity when the surface of the binary is coincident with the inner critical surface and takes a value of zero when coincidence occurs with the outer critical surface. The surface of the common envelope can then be defined by two parameters, the mass ratio and the fill-out factor.

The code, written and discussed by Rucinski (1973a,b: 1976a,b,c), generates a light curve based on the parameters described above, the inclination of the orbit, and the relative increase of the local temperature of the less massive component. Five fluxes and limb-darkening coefficients are specified for the desired central wavelength at around the primary (reference) temperature. The emergent flux from the visible portions of the common envelope is evaluated taking into account the effects of limb-darkening and gravity darkening. The reflection effect is negligible for these systems where the temperature difference between the two components is small.

The use of this program as part of the analysis procedure employed for V701 Sco and RZ Pyx is described in Chapter 8. Spectroscopically derived values were again used to fix the mass ratio while solutions were made for the fill-out factor, the inclination of the orbit and the relative temperature difference. The mean radii of the components can then be evaluated from the mass

ratio and fill-out factor by means of the tabulations presented by Mochnacki (1984).

Appendix A

The semi-major axes and minimum masses are derived from Kepler's second and third laws and only the results are quoted here. The error analysis follows the methods described by Barford (1967) for linear combinations and general products of quantities. σ_x refers to the uncertainty in the determination of the quantity x . For the purposes of this study, the primary is referred to by a subscript 1 and the secondary by a subscript 2. Most of the uncertainties for quantities such as the velocity semi-amplitudes of each component and the orbital period are standard errors derived from least-squares determinations.

For the projected semi-major axes,

$$a_{1,2} \sin i = 1.3751 \times 10^4 \cdot (1-e^2)^{1/2} \cdot K_{1,2} \cdot P \text{ km},$$

where the symbols have the following meaning:-

"a" is the semi-major axis of the orbit (km),

"i" is the inclination of the orbit,

"e" is the eccentricity of the orbit,

"K" is the semi-amplitude of the radial-velocity curve (kms^{-1}),

"P" is the period of the orbit (days).

The corresponding fractional errors in $a_{1,2} \sin i$ are,

$$\left[\frac{\sigma_{a_{1,2} \sin i}}{a_{1,2} \sin i} \right]^2 = \left[\frac{\sigma_{K_{1,2}}}{K_{1,2}} \right]^2 + \frac{e^4}{(1-e^2)^2} \cdot \left[\frac{\sigma_e}{e} \right]^2 + \left[\frac{\sigma_P}{P} \right]^2.$$

Similarly, for the minimum masses,

$$m_{1,2} \sin^3 i = 1.0385 \times 10^{-7} \cdot (1-e^2)^{3/2} \cdot (K_1 + K_2)^2 \cdot K_{1,2} \cdot P M_\odot,$$

where,

"m" is the mass of the star.

The corresponding fractional errors in $m_{1,2} \sin^3 i$ are,

$$\left[\frac{\sigma_{m_{1,2} \sin^3 i}}{m_{1,2} \sin^3 i} \right]^2 = \left[\frac{\sigma_{K_{1,2}}}{K_{1,2}} \right]^2 + \left[\frac{2 \sigma_{K_{\text{sum}}}}{K_{\text{sum}}} \right]^2 + \frac{9e^4}{(1-e^2)^2} \cdot \left[\frac{\sigma_e}{e} \right]^2 + \left[\frac{\sigma_P}{P} \right]^2,$$

where,

$$\sigma_{K_{\text{sum}}}^2 = \sigma_{K_1}^2 + \sigma_{K_2}^2.$$

The spectroscopic mass ratio is defined as,

$$q = m_2 / m_1 = K_1 / K_2.$$

The corresponding fractional error in q is

$$\left[\frac{\sigma_q}{q} \right]^2 = \left[\frac{\sigma_{K_1}}{K_1} \right]^2 + \left[\frac{\sigma_{K_2}}{K_2} \right]^2.$$

References

- Aitken, R.G.. 1935. "The Binary Stars", McGraw-Hill, New York, 125.
- Barford, N.C.. 1967. "Experimental Measurement: Precision, Error and Truth", Addison-Wesley, London.
- Bevington, P.R., 1969. "Data Reduction and Error Analysis for the Physical Sciences", McGraw-Hill, New York, 237.
- Cousins, A.W.J.. 1983. S.A.A.O. Circ., 7, 36.
- Florentin-Neilsen, R., 1983. Inst. Theor. Astrophys. Oslo, Report No. 59, 141.
- Hill, G.. 1979. Publ. Dom. Astrophys. Obs., 15, 297.
- Hill, G., 1982. Publ. Dom. Astrophys. Obs., 16, 67.
- Hill, G., 1982. Publ. Dom. Astrophys. Obs., 16, 59.
- Hill, G. & Fisher, W.A.. 1982. Publ. Dom. Astrophys. Obs. 16, 159.
- Hill, G., Fisher, W.A. & Poeckert, R., 1982a. Publ. Dom. Astrophys. Obs., 16, 43.
- Hill, G., Ramsden, D., Fisher, W.A. & Morris, S.C.. 1982b. Publ. Dom. Astrophys. Obs., 16, 11.
- Hill, G., Fisher, W.A. & Poeckert, R., 1982c. Publ. Dom. Astrophys. Obs., 16, 27.
- Irwin, J.B., 1973. Astrophys. J., 179, 241.
- Kwee, K.K. & van Woerden, H., 1956. Bull. astr. Inst.

Netherlands, 12, 327.

Lehmann-Filhes, R., 1894. Astr. Nachr., 136, 17.

Malcolm, G.J. & Bell, S.A., 1986. Mon. Not. astr. Soc. South Africa, 45, No. 1 & 2.

Mochnecki, S.W., 1984. Astrophys. J. Suppl. Ser., 55, 551.

Popper, D.M., 1974. Astron. J., 79, 1307.

Powell, M.J.D., 1967. Report No. HL67/5309, AERE, Harwell.

Rucinski, S.M., 1973a. Acta astr., 23, 79.

Rucinski, S.M., 1973b. Acta astr., 24, 119.

Rucinski, S.M., 1976a. Publs. astr. Soc. Pacific, 88, 244.

Rucinski, S.M., 1976b. Acta astr., 26, 227.

Rucinski, S.M., 1976c. Publs. astr. Soc. Pacific, 88, 777.

Sterne, T.E., 1941. Proc. Nat. Acad. Sci. Am., 27, 175.

Wells, D.C., Greisen, E.W. & Harten, R.H., 1981. Astrophys. J. Suppl. Ser., 44, 363.

CHAPTER 3

Simultaneous differential photometry with the St. Andrews

Twin Photometric Telescope; I. - The eclipsing binary TT Aurigae.

Simultaneous differential photometry with the St. Andrews
Twin Photometric Telescope; I. - The eclipsing binary TT Aurigae.

S.A. Bell and R.W. Hilditch.
University Observatory, Buchanan Gardens, St. Andrews,
Fife, KY16 9LZ, Scotland.

Communicated by the Director, University Observatory, St. Andrews.

Received _____

Correspondence to:-

Dr. R.W. Hilditch,
University Observatory,
Buchanan Gardens,
St. Andrews, Fife,
KY16 9LZ,
Scotland.

Summary

The refurbished Twin Photometric Telescope at St. Andrews has been used to obtain a complete B light curve (~ 1150 observations) of the B-type interacting binary system TT Aurigae. Analysis of the light curve by the synthesis code LIGHT (Hill, 1979) results in an r.m.s. scatter of the individual observations about the theoretical model fit of $\pm 0.^m005$ magnitudes. The system is shown to be in a semi-detached state but with too large a mass ratio to be considered as a classical Algol system.

1) Introduction

Light curves of eclipsing binary stars are usually determined to a precision of the order of $0^m.01$ - $0^m.03$ depending upon the quality of the observing site, the stability of the photometric equipment, methods of reduction and the amount of intrinsic variability in the individual components of the binary systems. Even at the best photometric sites and with very stable equipment, the standard observing procedure of sequentially monitoring the variable and one or two comparison stars limits the precision of the resultant light curve and often demands that the same phases be re-observed in order to obtain an adequate number of observations per unit phase interval. For short-period systems with intrinsically variable components (e.g. W UMa systems, cataclysmic variables) the limitation on time resolution can become quite acute whilst the intrinsic variability may make the resultant light curves extremely difficult to analyse.

To some extent, these problems may be overcome by incorporating a second channel into an existing single-channel photometer (e.g. Grauer and Bond, 1981), or modifying a two-channel photometer (e.g. Bell, Hilditch and King, 1984) in order to obtain simultaneous observations of both the variable and comparison star. A large number of observations per unit phase interval is obtained and hence the non-repetitive nature of many light curves may be more readily determined. Such modifications allow many small observatories with less than ideal photometric conditions to obtain precision light curves but the main drawback of these techniques is the severe restriction on the separation (< 15 arc minutes) of the two stars on the celestial sphere.

Such limitations on simultaneous differential photometry of two stars have now been removed at St. Andrews with the use of the Twin Photometric Telescope (TPT). Originally, this telescope was designed for observations of photometric sequences in clusters (Reddish, 1966) but since being removed from the Royal Observatory, Edinburgh, and its subsequent refurbishment at St. Andrews, it has been employed in a programme of observations of contact and near-contact binary systems. In this first paper, we present a description of the system, the observing procedures, and a single-colour light curve of the B-type eclipsing binary system TT Aurigae. The light curve has been analysed using the physically realistic light-curve synthesis code LIGHT (Hill, 1979) resulting in an r.m.s. scatter of the individual observations about the theoretical model fit of $\pm 0.005^m$. In the light of this solution, the evolutionary state of this system is discussed briefly.

2) Observing technique

The Twin Photometric Telescope consists of two 40 cm f/15 Ritchey Chretien reflecting telescopes mounted on a single fork mounting. The reference telescope is fixed with respect to the mounting while the offset telescope can be moved by up to 5 degrees in both right ascension and declination with respect to the reference telescope. The two instruments are similar in their construction differing only in the fact that the reference telescope incorporates an autoguider and the offset telescope incorporates a wide field acquisition eyepiece. The photometers on both telescopes use matched S-20 response EMI 9863A/350 photomultipliers driven by a single EHT power supply and housed in thermoelectrically-controlled cold boxes. No relative drift of the zero-points of the photometers

has been observed through this season in excess of 0.003^m .

The whole instrument can be controlled from within the adjoining "warm" room. The pointing of the telescopes, the aperture diaphragm selection for the photomultipliers and dome and shutter positioning are controlled from this room and the observer need only leave the control console for final image acquisition.

Data logging is achieved using an LSI 11/2 mini-computer under FORTH control. Observations are stored on disk which allows the display of data in the control room at an observer interactive-graphics terminal.

3) Observational data

The eclipsing binary TT Aurigae (HD 33088) was discovered in 1907, though its EB-type light curve was not noted until photographic observations were obtained (Martin and Plummer, 1916; Jordan, 1929). A photometric and spectroscopic study by Joy and Sitterley (1934) provided a light curve using a polarizing photometer, which showed marked differences from the earlier observations, and a radial velocity curve with errors of more than 50kms^{-1} .

Joy and Sitterley classified the primary as B3 with a companion of similar spectral type. Intermediate band uvby photometry of this system by Hilditch and Hill (1975), corrected for the effects of reddening, indicate that the most likely spectral type for the primary to be B2 and the secondary to be between B4 and B6. Hill et al. (1975) classified this object to be $B2 \pm 1$. Classification of the secondary is hindered by the very diffuse nature of its spectrum and its lower luminosity. Popper (1981) indicates that he has a new

set of high-dispersion spectra of TT Aurigae in which the secondary component is weakly visible.

More recent photometric observations have been made by Kulkarni and Lokanadham (1978) in the UBV system. However, these observations were made over four observing seasons and show an average scatter of around $0.^m02-0.^m03$.

For the TPT observations, the comparison star was HD32989 ($m_B = 7.5$, B5) and the check star was the V-magnitude standard η Aur ($m_B = 3.00$, B3). The filter used for these observations was comparable with the Johnson "B" filter and the integration times were fixed at 60s. The observing procedure included regular observations of the comparison star with both telescopes as well as observations of the check star in one telescope and the comparison in the other. This provided a check on variations in the comparison star and drifts between the two telescope/photometer combinations.

The binary system was observed on five nights during 1983 November and December and 1984 February by SAB. The expectations of the observing procedure have been fully realised in that a high-quality light curve has been obtained even when results from nights affected by thin high cloud and mist have been used. A plot of the magnitudes of the two stars in their respective telescopes versus time on the night of 1983 November 29/30 has been made in Figure 1 as well as the differential magnitude in the sense variable minus comparison. It can be seen that the photometric quality of the night becomes increasingly poor as the night progresses although the differential magnitude remains unaffected by the prevailing weather conditions.

The reduction of the data has been described elsewhere (Hilditch, 1981) and the resultant light curve is shown in Figure 2. Data for the five nights are given in Table 2. The r.m.s. error of a least-squares cubic-spline fit to the light curve is less than 0.005^m , further emphasizing the advantages of this particular instrument.

A single time of minimum was determined from the data of 1983 November 29/30 using the method of Kwee and van Woerden (1956). Using the visual and photographic times of minima assembled by Plavec et al. (1960) and Klimek (1972) and the photoelectrically observed times of minima of Kulkarni and Lokanadham and our own, the period was improved by weighting the photoelectric observations significantly higher than the rest and making a least-squares fit to the data. The improved ephemeris is given below.

$$\text{Pri. Min.} = \text{M.J.D. } 45668.10863 + 1.3327342 E$$

$$\qquad \qquad \qquad \pm 7 \qquad \qquad \qquad \pm 1$$

The phases given in Table 2 have been calculated using this ephemeris. The refined period shows only a very small difference when compared with that calculated by Iwanowska (1934) of 1.3327333 days.

4) Analysis of the light curve

Primary minimum appears to be highly symmetric although the secondary minimum does not; egress appears to be slightly steeper than ingress. The remainder of the curve is ideal for an accurate determination of the geometry of the system.

The light curve was analysed using LIGHT (Hill, 1979), a physically realistic light-curve solution package incorporating Roche geometry and the model atmospheres of Kurucz (1978). The initial attempt used the parameters of Cester et al. (1981), who based their solution on the spectroscopic value of the mass ratio $q (= 0.80)$ calculated by Joy and Sitterley. This value of q proved to be inadequate and light-curve solutions were made using a range of mass ratios while allowing the inclination, the secondary temperature and the radii of the two component stars to vary. This procedure indicated that the inclination of the system could be fixed at 87.5° .

Solutions of the light curves were then sought with the two stellar radii, the mass ratio and temperature of the secondary component as free parameters. The temperature of the primary component was adopted from the tabulation of Popper (1980) whilst the "second order" parameters of limb-darkening coefficients and electron scattering fractions were taken from Carbon and Gingerich (1969) and Hutchings and Hill (1971) respectively. The best-fit solutions for both a B2 and a B3 primary are presented in Table 1 and as the solutions give apparently identical fits to the observed data, a single fit is plotted on Figure 2.

The solutions obtained are consistent with either a B2 primary and B4 secondary or a B3 primary and a B6 secondary. The major discrepancy between the analysis presented here and that of Cester et al. lies with the mass ratio. The implication of this solution is that the secondary lies extremely close to its critical Roche potential ($r_{\text{crit}} = 0.316$ for $q = 0.61$) making TT Aurigae a semi-detached system rather than a detached system. Confirmation of the semi-detached nature of the system requires new high-dispersion

spectroscopy.

5) Conclusions

The technique of simultaneous differential photometry has been shown to be most effective in establishing light curves of high precision. A direct consequence of this precision has been the accurate determination of the geometrical elements ($r_{\text{pri}}, r_{\text{sec}}, i, q$) of the binary system from which it is shown that TT Aurigae is in a semi-detached state with a high mass-ratio.

Popper (1980) and Eaton (1978a,b) have identified five hot semi-detached systems namely V Puppis, u Herculis, V356 Sagittarii, IU Aurigae and Z Vulpeculae, which have properties significantly different from the Algol systems. These five systems have early B-type primary components and early B- to early A-type secondary components, and high mass ratios (mean $q = 0.48 \pm 0.13$ s.d.). Clearly TT Aurigae belongs to this class of binary system. By contrast, the twelve Algol systems listed by Popper have lower total masses, much larger differences in spectral types between components and an average mass ratio of 0.22 ± 0.11 (s.d.).

There appears to be a general consensus that the evolutionary status of the Algol systems can be explained by non-conservative case B mass exchange but that there has been insufficient quantitative comparison of observation with theory (Plavec 1982 and references therein; Giuricin et al. 1982; Plavec 1983). However, there is a dearth of evolutionary models for early-type close binaries which presumably must evolve into contact or into semi-detached states some time during their main-sequence evolution (case A systems). Webbink (1976,1980) carried out some exploratory

calculations but we have been unable to find any evolutionary models which are directly comparable with this type of short-period (~ 2 days) massive semi-detached system. A detailed photometric and spectroscopic study of V Puppis by Andersen et al. (1983) reaches the same conclusion.

Acknowledgements

Our thanks are due to Professor D.W.N.Stibbs, Dr. R.P.Edwin, Messrs. D.M.Carr, W.Brown, J.Lindsay, G.Cunningham and D.Erskine without whom the TPT could not have been restored to such excellent order. Our thanks are also due to Mr. J.R.Stapleton for much of the data-logging software. SAB gratefully acknowledges the financial support of SERC in the form of a Research Studentship.

References

- Andersen, J., Clausen, J.V., Gimenez, A. & Nordstrom, B., 1983.
Astron. Astrophys., 128, 17.
- Bell, S.A., Hilditch, R.W. & King, D.J., 1984. Mon. Not. R. astr.
Soc., 208, 123.
- Carbon, D.F. & Gingerich, O.J., 1969. Theory and Observation of
Normal Stellar Atmospheres, ed. Gingerich, O.J. (M.I.T. press,
Cambridge), 377.
- Cester, B., Fedel, B., Giuricin, G., Mardirossian, F. & Mezzetti, M.,
1981. Astron. Astrophys. Suppl. Ser., 33, 91.
- Eaton, J.A., 1978a. Acta astr., 28, 63.
- Eaton, J.A., 1978b. Acta astr., 28, 601.
- Giuricin, G., Mardirossian, F. & Mezzetti, M., 1982. IAU Coll., 69,
183.
- Grauer, A.D. & Bond, H.E., 1981. Publ. astr. Soc. Pacific., 93,
388.
- Hilditch, R.W. & Hill, G., 1975. Mem. R. astr. Soc., 79, 101.
- Hilditch, R.W., 1981. Mon. Not. R. astr. Soc., 196, 305.
- Hill, G., Hilditch, R.W., Younger, P.F. & Fisher, W.A., 1975. Mem. R.
astr. Soc., 79, 131.
- Hill, G., 1979. Publ. Dom. Astrophys. Obs., 15, 297.
- Hutchings, J.B. & Hill, G., 1971. Astrophys. J., 167, 137.

- Iwanowska,W., 1934. Wilno Bull., 15, 3.
- Jordan,F.C., 1929. Publ. Allegheny Obs., 7, 177.
- Joy,A.H. & Sitterley,B.W., 1934. Astrophys. J., 73, 77.
- Klimek,Z., 1972. Info. Bull. Var. Stars., No. 637.
- Kulkarni,A.G. & Lokanadham,B., 1978. Contrib. Nizamiah & Japal-Rangapur Obs., 8.
- Kurucz,R.L., 1978. Astrophys. J. Suppl. Ser., 40, 1.
- Kwee,K.K. & van Woerden,H., 1956. Bull. astr. Inst. Netherlands, 12, 327.
- Martin,C. & Plummer,H.C., 1916. Mon. Not. R. astr. Soc., 76, 395.
- Plavec,M.J., Pekny,Z. & Smetanov,M., 1960. Bull. astr. Inst. Czechoslovakia, 11, 180.
- Plavec,M.J., 1982. IAU Coll., 69, 159.
- Plavec,M.J., 1983. J. Roy. Astron. Soc. Can., 77, 283.
- Popper,D.M., 1980. Ann. Rev. Astron. Astrophys., 18, 115.
- Popper,D.M., 1981. Astrophys. J. Suppl. Ser., 47, 339.
- Reddish,V.C., 1966. Sky & Telescope, 32, No. 3, 124.
- Webbink,R.F., 1976. Astrophys. J. Suppl. Ser., 32, 583.
- Webbink,R.F., 1980. IAU Symp., 88, 127.

Figure captions

Figure 1: Observations made on 1983 November 29/30. Triangles and inverted triangles represent the variable and comparison magnitudes respectively. The crosses are the corresponding differential magnitudes in the sense variable minus comparison.

Figure 2: The light curve of TT Aurigae. The crosses represent the individual observations and the solid line represents the theoretical-model fit.

Table 1 : Light-curve solutions for TT Aurigae.

B2 primary	B3 primary
$T_{\text{pri}} = 23120 \text{ K (fixed)}$	$T_{\text{pri}} = 19050 \text{ K (fixed)}$
$i = 87.5 \pm 0.1 \text{ (best fit)}$	$i = 87.5 \pm 0.1 \text{ (best fit)}$
$T_{\text{sec}} = 17280 \pm 70 \text{ K}$	$T_{\text{sec}} = 14350 \pm 55 \text{ K}$
$r_{\text{pri}} = 0.335 \pm 0.0005 \text{ (polar)}$	$r_{\text{pri}} = 0.334 \pm 0.0004 \text{ (polar)}$
$r_{\text{pri}} = 0.347 \pm 0.0005 \text{ (mean)}$	$r_{\text{pri}} = 0.346 \pm 0.0004 \text{ (mean)}$
$r_{\text{sec}} = 0.315 \pm 0.0007 \text{ (polar)}$	$r_{\text{sec}} = 0.314 \pm 0.0006 \text{ (polar)}$
$r_{\text{sec}} = 0.335 \pm 0.0007 \text{ (mean)}$	$r_{\text{sec}} = 0.334 \pm 0.0006 \text{ (mean)}$
$q = 0.614 \pm 0.034$	$q = 0.597 \pm 0.034$

Table 2 : Johnson B observations.

1983 Nov 29/30					
M. J. D.	Phase	(V-C)			
45667.85787	0.8119	0.442	45667.93513	0.8698	0.504
45667.85856	0.8124	0.451	45667.93583	0.8704	0.502
45667.85925	0.8129	0.442	45667.93652	0.8709	0.502
45667.85995	0.8134	0.443	45667.93722	0.8714	0.503
45667.86064	0.8139	0.445	45667.93791	0.8719	0.503
45667.86134	0.8145	0.449	45667.93861	0.8724	0.506
45667.86203	0.8150	0.442	45667.93930	0.8730	0.508
45667.86273	0.8155	0.447	45667.94000	0.8735	0.510
45667.86342	0.8160	0.451	45667.94069	0.8740	0.507
45667.86412	0.8166	0.446	45667.94138	0.8745	0.511
45667.86963	0.8207	0.448	45667.94691	0.8787	0.514
45667.87032	0.8212	0.448	45667.94760	0.8792	0.513
45667.87101	0.8217	0.448	45667.94829	0.8797	0.518
45667.87171	0.8223	0.447	45667.94899	0.8802	0.516
45667.87240	0.8228	0.449	45667.94968	0.8808	0.515
45667.87310	0.8233	0.454	45667.95038	0.8813	0.514
45667.87379	0.8238	0.453	45667.95107	0.8818	0.511
45667.87449	0.8243	0.453	45667.95177	0.8823	0.516
45667.87518	0.8249	0.454	45667.95246	0.8828	0.523
45667.87588	0.8254	0.453	45667.95316	0.8834	0.517
45667.88336	0.8310	0.459	45667.97242	0.8978	0.555
45667.88406	0.8315	0.455	45667.97312	0.8983	0.549
45667.88475	0.8320	0.457	45667.97382	0.8989	0.546
45667.88544	0.8326	0.463	45667.97451	0.8994	0.546
45667.88614	0.8331	0.468	45667.97520	0.8999	0.549
45667.88684	0.8336	0.459	45667.97590	0.9004	0.552
45667.88753	0.8341	0.465	45667.97659	0.9009	0.559
45667.88822	0.8346	0.461	45667.97729	0.9015	0.559
45667.88892	0.8352	0.463	45667.97798	0.9020	0.556
45667.88961	0.8357	0.467	45667.97868	0.9025	0.563
45667.90606	0.8480	0.481	45667.98356	0.9062	0.569
45667.90675	0.8485	0.485	45667.98425	0.9067	0.575
45667.90745	0.8491	0.478	45667.98495	0.9072	0.579
45667.90814	0.8496	0.479	45667.98564	0.9077	0.578
45667.90884	0.8501	0.479	45667.98634	0.9083	0.579
45667.90953	0.8506	0.480	45667.98703	0.9088	0.580
45667.91023	0.8512	0.482	45667.98773	0.9093	0.587
45667.91092	0.8517	0.484	45667.98842	0.9098	0.591
45667.91161	0.8522	0.481	45667.98912	0.9103	0.600
45667.91231	0.8527	0.486	45667.98981	0.9109	0.595
45667.92303	0.8608	0.490	45667.99851	0.9174	0.626
45667.92372	0.8613	0.492	45667.99921	0.9179	0.632
45667.92442	0.8618	0.489	45667.99990	0.9184	0.634
45667.92511	0.8623	0.497	45668.00060	0.9190	0.636
45667.92581	0.8628	0.491	45668.00129	0.9195	0.636
45667.92650	0.8634	0.495	45668.00198	0.9200	0.643
45667.92719	0.8639	0.495	45668.00268	0.9205	0.648
45667.92789	0.8644	0.497	45668.00338	0.9210	0.650
45667.92858	0.8649	0.498	45668.00407	0.9216	0.650
45667.92928	0.8654	0.499	45668.00476	0.9221	0.651
			45668.01066	0.9265	0.686
			45668.01136	0.9270	0.687
			45668.01206	0.9276	0.693
			45668.01275	0.9281	0.697
			45668.01344	0.9286	0.698

continued

45668.01414	0.9291	0.697	45668.08797	0.9845	1.359
45668.01483	0.9296	0.703	45668.08866	0.9850	1.357
45668.01553	0.9302	0.712	45668.08936	0.9856	1.370
45668.01622	0.9307	0.715	45668.09005	0.9861	1.380
45668.01691	0.9312	0.718	45668.09075	0.9866	1.387
45668.02187	0.9349	0.752	45668.09144	0.9871	1.395
45668.02257	0.9354	0.751	45668.09214	0.9876	1.406
45668.02326	0.9360	0.754	45668.09283	0.9882	1.407
45668.02395	0.9365	0.757	45668.09353	0.9887	1.412
45668.02465	0.9370	0.760	45668.09924	0.9930	1.471
45668.02534	0.9375	0.771	45668.09994	0.9935	1.477
45668.02603	0.9380	0.777	45668.10063	0.9940	1.481
45668.02673	0.9386	0.775	45668.10132	0.9945	1.488
45668.02743	0.9391	0.783	45668.10202	0.9951	1.490
45668.02812	0.9396	0.784	45668.10271	0.9956	1.488
45668.03173	0.9423	0.806	45668.10341	0.9961	1.508
45668.03243	0.9428	0.814	45668.10410	0.9966	1.502
45668.03312	0.9434	0.816	45668.10480	0.9971	1.506
45668.03381	0.9439	0.821	45668.10549	0.9977	1.510
45668.03451	0.9444	0.825	45668.10619	0.9982	1.520
45668.03520	0.9449	0.831	45668.10688	0.9987	1.518
45668.03590	0.9454	0.837	45668.10757	0.9992	1.517
45668.03659	0.9460	0.837	45668.10827	0.9998	1.523
45668.03729	0.9465	0.843	45668.10897	0.0003	1.522
45668.03798	0.9470	0.844	45668.10966	0.0008	1.520
45668.04168	0.9498	0.881	45668.11035	0.0013	1.518
45668.04238	0.9503	0.892	45668.11105	0.0018	1.521
45668.04307	0.9508	0.893	45668.11174	0.0024	1.519
45668.04377	0.9514	0.895	45668.11244	0.0029	1.515
45668.04446	0.9519	0.902	45668.11355	0.0037	1.510
45668.04516	0.9524	0.913	45668.11424	0.0042	1.507
45668.04585	0.9529	0.912	45668.11494	0.0048	1.500
45668.04655	0.9534	0.920	45668.11563	0.0053	1.502
45668.04724	0.9540	0.919	45668.11633	0.0058	1.494
45668.04793	0.9545	0.931	45668.11702	0.0063	1.481
45668.06520	0.9674	1.095	45668.11771	0.0068	1.483
45668.06590	0.9680	1.102	45668.11841	0.0074	1.476
45668.06659	0.9685	1.103	45668.11911	0.0079	1.480
45668.06728	0.9690	1.118	45668.11980	0.0084	1.465
45668.06798	0.9695	1.120	45668.12540	0.0126	1.385
45668.06868	0.9700	1.133	45668.12609	0.0131	1.400
45668.06937	0.9706	1.147	45668.12679	0.0136	1.377
45668.07006	0.9711	1.151	45668.12748	0.0142	1.372
45668.07076	0.9716	1.156	45668.12818	0.0147	1.373
45668.07145	0.9721	1.162	45668.12887	0.0152	1.363
45668.07701	0.9763	1.228	45668.12957	0.0157	1.350
45668.07770	0.9768	1.234	45668.13026	0.0163	1.348
45668.07840	0.9773	1.238	45668.13096	0.0168	1.328
45668.07909	0.9779	1.249	45668.13165	0.0173	1.330
45668.07979	0.9784	1.261	45668.13713	0.0214	1.256
45668.08048	0.9789	1.268	45668.13783	0.0219	1.252
45668.08118	0.9794	1.269	45668.13852	0.0225	1.254
45668.08187	0.9799	1.287	45668.13922	0.0230	1.238
45668.08256	0.9805	1.295	45668.13991	0.0235	1.224
45668.08326	0.9810	1.293	45668.14061	0.0240	1.222
45668.08728	0.9840	1.343	45668.14130	0.0245	1.215

continued

45673.88497	0.3342	0.447	45673.94833	0.3818	0.491
45673.88567	0.3347	0.443	45673.94902	0.3823	0.494
45673.88636	0.3353	0.447	45673.94972	0.3828	0.487
45673.88705	0.3358	0.451	45673.95041	0.3833	0.491
45673.88775	0.3363	0.449	45673.95110	0.3839	0.493
45673.88844	0.3368	0.447	45673.95180	0.3844	0.492
45673.89483	0.3416	0.454	45673.95249	0.3849	0.495
45673.89553	0.3421	0.453	45673.95318	0.3854	0.499
45673.89622	0.3427	0.451	45673.95388	0.3859	0.493
45673.89691	0.3432	0.453	45673.95458	0.3865	0.495
45673.89761	0.3437	0.448	45673.96601	0.3950	0.513
45673.89830	0.3442	0.453	45673.96671	0.3956	0.506
45673.89900	0.3448	0.453	45673.96740	0.3961	0.509
45673.89969	0.3453	0.456	45673.96809	0.3966	0.509
45673.90039	0.3458	0.460	45673.96879	0.3971	0.520
45673.90108	0.3463	0.456	45673.96948	0.3976	0.516
45673.90492	0.3492	0.462	45673.97018	0.3982	0.514
45673.90562	0.3497	0.466	45673.97087	0.3987	0.515
45673.90631	0.3502	0.465	45673.97157	0.3992	0.517
45673.90701	0.3508	0.461	45673.97226	0.3997	0.514
45673.90770	0.3513	0.461	45673.98250	0.4074	0.536
45673.90839	0.3518	0.466	45673.98320	0.4079	0.531
45673.90909	0.3523	0.454	45673.98389	0.4085	0.543
45673.90978	0.3528	0.461	45673.98459	0.4090	0.545
45673.91048	0.3534	0.467	45673.98528	0.4095	0.541
45673.91117	0.3539	0.465	45673.98597	0.4100	0.546
45673.91702	0.3583	0.471	45673.98667	0.4105	0.546
45673.91771	0.3588	0.468	45673.98737	0.4111	0.546
45673.91840	0.3593	0.463	45673.98806	0.4116	0.547
45673.91910	0.3598	0.468	45673.98875	0.4121	0.553
45673.91980	0.3604	0.471	45673.99238	0.4148	0.561
45673.92049	0.3609	0.470	45673.99307	0.4153	0.557
45673.92118	0.3614	0.464	45673.99377	0.4159	0.554
45673.92188	0.3619	0.469	45673.99446	0.4164	0.566
45673.92257	0.3624	0.473	45673.99515	0.4169	0.564
45673.92327	0.3630	0.470	45673.99585	0.4174	0.566
45673.92783	0.3664	0.476	45673.99654	0.4179	0.568
45673.92852	0.3669	0.477	45673.99724	0.4185	0.576
45673.92922	0.3674	0.477	45673.99793	0.4190	0.572
45673.92991	0.3679	0.475	45673.99863	0.4195	0.575
45673.93060	0.3685	0.480	45674.00247	0.4224	0.585
45673.93130	0.3690	0.482	45674.00316	0.4229	0.582
45673.93199	0.3695	0.478	45674.00386	0.4234	0.589
45673.93269	0.3700	0.481	45674.00455	0.4240	0.590
45673.93338	0.3706	0.485	45674.00525	0.4245	0.595
45673.93408	0.3711	0.480	45674.00594	0.4250	0.591
45673.93834	0.3743	0.483	45674.00663	0.4255	0.595
45673.93903	0.3748	0.488	45674.00733	0.4260	0.593
45673.93973	0.3753	0.486	45674.00803	0.4266	0.596
45673.94042	0.3758	0.489	45674.00872	0.4271	0.606
45673.94111	0.3764	0.486	45674.01608	0.4326	0.620
45673.94181	0.3769	0.483	45674.01677	0.4331	0.621
45673.94251	0.3774	0.480	45674.01747	0.4336	0.630
45673.94320	0.3779	0.492	45674.01817	0.4342	0.623
45673.94389	0.3784	0.483	45674.01886	0.4347	0.634
45673.94459	0.3790	0.488	45674.01955	0.4352	0.631

continued

45674.02025	0.4357	0.632	45674.08500	0.4843	0.910
45674.02094	0.4363	0.635	45674.08570	0.4848	0.919
45674.02163	0.4368	0.641	45674.08639	0.4854	0.917
45674.02233	0.4373	0.638	45674.08709	0.4859	0.921
45674.02604	0.4401	0.655	45674.09660	0.4930	0.965
45674.02674	0.4406	0.658	45674.09729	0.4935	0.964
45674.02744	0.4411	0.660	45674.09799	0.4941	0.963
45674.02813	0.4416	0.667	45674.09869	0.4946	0.962
45674.02882	0.4422	0.665	45674.09938	0.4951	0.967
45674.02952	0.4427	0.666	45674.10007	0.4956	0.966
45674.03021	0.4432	0.665	45674.10077	0.4961	0.973
45674.03091	0.4437	0.669	45674.10146	0.4967	0.971
45674.03160	0.4442	0.674	45674.10216	0.4972	0.975
45674.03230	0.4448	0.682	45674.10285	0.4977	0.974
45674.03624	0.4477	0.691	45674.10354	0.4982	0.975
45674.03693	0.4483	0.700	45674.10424	0.4988	0.972
45674.03763	0.4488	0.696	45674.10494	0.4993	0.981
45674.03833	0.4493	0.705	45674.10563	0.4998	0.980
45674.03902	0.4498	0.702	45674.10632	0.5003	0.978
45674.03971	0.4503	0.709	45674.10702	0.5008	0.976
45674.04041	0.4509	0.712	45674.10771	0.5014	0.972
45674.04110	0.4514	0.710	45674.10841	0.5019	0.974
45674.04180	0.4519	0.716	45674.10910	0.5024	0.973
45674.04249	0.4524	0.715	45674.10979	0.5029	0.968
45674.04608	0.4551	0.735	45674.11095	0.5038	0.968
45674.04677	0.4556	0.740	45674.11165	0.5043	0.967
45674.04747	0.4562	0.740	45674.11234	0.5048	0.966
45674.04816	0.4567	0.744	45674.11303	0.5054	0.968
45674.04886	0.4572	0.745	45674.11373	0.5059	0.959
45674.04955	0.4577	0.741	45674.11443	0.5064	0.967
45674.05025	0.4582	0.750	45674.11581	0.5074	0.953
45674.05094	0.4588	0.752	45674.11651	0.5080	0.956
45674.05164	0.4593	0.758	45674.11720	0.5085	0.956
45674.05233	0.4598	0.760	45674.12084	0.5112	0.939
45674.05654	0.4630	0.781	45674.12153	0.5117	0.938
45674.05724	0.4635	0.787	45674.12223	0.5123	0.933
45674.05793	0.4640	0.786	45674.12292	0.5128	0.937
45674.05863	0.4645	0.791	45674.12361	0.5133	0.931
45674.05932	0.4650	0.789			
45674.06002	0.4656	0.796			
45674.06071	0.4661	0.799			
45674.06141	0.4666	0.801			
45674.06210	0.4671	0.807			
45674.06279	0.4677	0.808	45674.77848	0.0047	1.485
45674.06672	0.4706	0.829	45674.77918	0.0052	1.487
45674.06741	0.4711	0.829	45674.77988	0.0057	1.472
45674.06950	0.4727	0.843	45674.78057	0.0062	1.473
45674.07019	0.4732	0.845	45674.78126	0.0068	1.462
45674.07088	0.4737	0.850	45674.78196	0.0073	1.465
45674.07158	0.4742	0.858	45674.78265	0.0078	1.454
45674.07227	0.4748	0.854	45674.78335	0.0083	1.456
45674.07297	0.4753	0.844	45674.78404	0.0088	1.449
45674.08223	0.4822	0.907	45674.78473	0.0094	1.440
45674.08292	0.4828	0.906	45674.78543	0.0099	1.431
45674.08362	0.4833	0.910	45674.78613	0.0104	1.426
45674.08431	0.4838	0.906	45674.78682	0.0109	1.431

1983 Dec 06/07

M.J.D. Phase (V-C)

continued

45674.78751	0.0114	1.417	45674.84448	0.0542	0.844
45674.78821	0.0120	1.409	45674.85458	0.0618	0.779
45674.79191	0.0147	1.359	45674.85528	0.0623	0.759
45674.79260	0.0153	1.361	45674.85597	0.0628	0.764
45674.79330	0.0158	1.346	45674.85667	0.0633	0.760
45674.79400	0.0163	1.341	45674.85736	0.0639	0.746
45674.79469	0.0168	1.336	45674.85806	0.0644	0.749
45674.79538	0.0173	1.318	45674.85875	0.0649	0.747
45674.79608	0.0179	1.310	45674.85945	0.0654	0.737
45674.79677	0.0184	1.306	45674.86014	0.0659	0.743
45674.79747	0.0189	1.300	45674.86083	0.0665	0.730
45674.79816	0.0194	1.301	45674.86153	0.0670	0.731
45674.79885	0.0199	1.284	45674.86222	0.0675	0.731
45674.79955	0.0205	1.281	45674.86292	0.0680	0.720
45674.80025	0.0210	1.278	45674.86361	0.0685	0.710
45674.80094	0.0215	1.263	45674.86431	0.0691	0.718
45674.80163	0.0220	1.254	45674.86785	0.0717	0.696
45674.80559	0.0250	1.203	45674.86854	0.0722	0.696
45674.80629	0.0255	1.198	45674.86924	0.0728	0.693
45674.80698	0.0260	1.183	45674.86993	0.0733	0.682
45674.80768	0.0266	1.182	45674.87063	0.0738	0.681
45674.80837	0.0271	1.174	45674.87132	0.0743	0.672
45674.80906	0.0276	1.170	45674.87202	0.0748	0.675
45674.80976	0.0281	1.155	45674.87271	0.0754	0.668
45674.81045	0.0287	1.144	45674.87340	0.0759	0.668
45674.81115	0.0292	1.157	45674.87410	0.0764	0.665
45674.81184	0.0297	1.144	45674.87479	0.0769	0.658
45674.81254	0.0302	1.132	45674.87549	0.0775	0.665
45674.81323	0.0307	1.119	45674.87618	0.0780	0.657
45674.81392	0.0313	1.117	45674.87688	0.0785	0.654
45674.81462	0.0318	1.106	45674.87757	0.0790	0.651
45674.81531	0.0323	1.098	45674.88254	0.0827	0.625
45674.81881	0.0349	1.064	45674.88323	0.0833	0.627
45674.81951	0.0354	1.060	45674.88392	0.0838	0.617
45674.82020	0.0360	1.046	45674.88462	0.0843	0.621
45674.82089	0.0365	1.039	45674.88531	0.0848	0.612
45674.82159	0.0370	1.036	45674.88601	0.0853	0.612
45674.82228	0.0375	1.031	45674.88670	0.0859	0.610
45674.82297	0.0380	1.026	45674.88740	0.0864	0.606
45674.82367	0.0386	1.018	45674.88809	0.0869	0.598
45674.82436	0.0391	1.007	45674.88879	0.0874	0.599
45674.82506	0.0396	1.004	45674.88948	0.0880	0.595
45674.83476	0.0469	0.919	45674.89017	0.0885	0.596
45674.83545	0.0474	0.914	45674.89087	0.0890	0.591
45674.83615	0.0479	0.911	45674.89156	0.0895	0.592
45674.83684	0.0485	0.898	45674.89226	0.0900	0.590
45674.83754	0.0490	0.897	45674.89566	0.0926	0.576
45674.83823	0.0495	0.888	45674.89636	0.0931	0.575
45674.83892	0.0500	0.880	45674.89705	0.0936	0.571
45674.83962	0.0505	0.876	45674.89775	0.0942	0.568
45674.84032	0.0511	0.872	45674.89844	0.0947	0.569
45674.84101	0.0516	0.867	45674.89913	0.0952	0.567
45674.84170	0.0521	0.864	45674.89983	0.0957	0.567
45674.84240	0.0526	0.860	45674.90052	0.0962	0.562
45674.84309	0.0531	0.850	45674.90121	0.0968	0.562
45674.84378	0.0537	0.848	45674.90191	0.0973	0.561

continued

45674.90261	0.0978	0.552	45674.96704	0.1461	0.483
45674.90330	0.0983	0.553	45674.96773	0.1467	0.486
45674.90399	0.0988	0.551	45674.96843	0.1472	0.487
45674.90469	0.0994	0.555	45674.96912	0.1477	0.483
45674.90538	0.0999	0.549	45674.96981	0.1482	0.480
45674.90895	0.1026	0.536	45674.97051	0.1487	0.483
45674.90964	0.1031	0.542	45674.97121	0.1493	0.481
45674.91034	0.1036	0.537	45674.97190	0.1498	0.486
45674.91103	0.1041	0.536	45674.97259	0.1503	0.477
45674.91173	0.1046	0.532	45674.97599	0.1529	0.479
45674.91242	0.1052	0.533	45674.97668	0.1534	0.477
45674.91312	0.1057	0.537	45674.97737	0.1539	0.477
45674.91381	0.1062	0.531	45674.97807	0.1544	0.475
45674.91450	0.1067	0.527	45674.97876	0.1549	0.474
45674.91520	0.1072	0.527	45674.97946	0.1555	0.478
45674.91589	0.1078	0.527	45674.98015	0.1560	0.478
45674.91659	0.1083	0.527	45674.98085	0.1565	0.475
45674.91728	0.1088	0.525	45674.98154	0.1570	0.475
45674.91798	0.1093	0.522	45674.98223	0.1575	0.473
45674.91867	0.1099	0.522	45674.98293	0.1581	0.471
45674.92309	0.1132	0.517	45674.98362	0.1586	0.471
45674.92379	0.1137	0.519	45674.98432	0.1591	0.473
45674.92448	0.1142	0.519	45674.98501	0.1596	0.466
45674.92517	0.1147	0.513	45674.98571	0.1602	0.465
45674.92587	0.1153	0.516	45674.98948	0.1630	0.472
45674.92656	0.1158	0.513	45674.99018	0.1635	0.467
45674.92726	0.1163	0.514	45674.99087	0.1640	0.463
45674.92795	0.1168	0.512	45674.99156	0.1645	0.467
45674.92865	0.1173	0.509	45674.99226	0.1651	0.468
45674.92934	0.1179	0.508	45674.99295	0.1656	0.470
45674.93004	0.1184	0.516	45674.99365	0.1661	0.464
45674.93073	0.1189	0.513	45674.99434	0.1666	0.469
45674.93142	0.1194	0.511	45674.99504	0.1672	0.465
45674.93212	0.1199	0.512	45674.99573	0.1677	0.469
45674.93281	0.1205	0.504	45674.99643	0.1682	0.463
45674.94243	0.1277	0.506	45674.99712	0.1687	0.468
45674.94313	0.1282	0.503	45674.99781	0.1692	0.467
45674.94382	0.1287	0.497	45674.99851	0.1698	0.468
45674.94451	0.1292	0.498	45674.99920	0.1703	0.463
45674.94521	0.1298	0.505	45675.00250	0.1728	0.462
45674.94591	0.1303	0.504	45675.00319	0.1733	0.462
45674.94660	0.1308	0.500	45675.00389	0.1738	0.459
45674.94729	0.1313	0.502	45675.00459	0.1743	0.461
45674.94799	0.1318	0.499	45675.00528	0.1748	0.464
45674.94868	0.1324	0.500	45675.00597	0.1754	0.458
45674.94937	0.1329	0.500	45675.00667	0.1759	0.460
45674.95007	0.1334	0.500	45675.00736	0.1764	0.461
45674.95077	0.1339	0.498	45675.00806	0.1769	0.459
45674.95146	0.1345	0.494	45675.00875	0.1774	0.460
45674.95215	0.1350	0.499	45675.00944	0.1780	0.459
45674.96287	0.1430	0.488	45675.01014	0.1785	0.456
45674.96357	0.1435	0.489	45675.01084	0.1790	0.461
45674.96426	0.1441	0.487	45675.01153	0.1795	0.459
45674.96495	0.1446	0.487	45675.01222	0.1800	0.457
45674.96565	0.1451	0.491	45675.02417	0.1890	0.455
45674.96634	0.1456	0.490	45675.02486	0.1895	0.449

continued

45675.02556	0.1901	0.447	45675.07515	0.2273	0.424
45675.02625	0.1906	0.449	45675.07585	0.2278	0.425
45675.02695	0.1911	0.453	45675.07960	0.2306	0.429
45675.02764	0.1916	0.452	45675.08029	0.2311	0.424
45675.02833	0.1921	0.447	45675.08099	0.2316	0.432
45675.02903	0.1927	0.451	45675.08168	0.2322	0.425
45675.02972	0.1932	0.452	45675.08237	0.2327	0.425
45675.03042	0.1937	0.442	45675.08307	0.2332	0.430
45675.03111	0.1942	0.449	45675.08376	0.2337	0.426
45675.03181	0.1947	0.445	45675.08446	0.2342	0.424
45675.03250	0.1953	0.447	45675.08515	0.2348	0.423
45675.03320	0.1958	0.446	45675.08585	0.2353	0.426
45675.03389	0.1963	0.445	45675.08654	0.2358	0.430
45675.03810	0.1995	0.444	45675.08723	0.2363	0.424
45675.03880	0.2000	0.442	45675.08793	0.2369	0.424
45675.03949	0.2005	0.443	45675.08862	0.2374	0.424
45675.04018	0.2010	0.444	45675.08932	0.2379	0.423
45675.04088	0.2016	0.441	45675.09438	0.2417	0.423
45675.04158	0.2021	0.437	45675.09507	0.2422	0.427
45675.04227	0.2026	0.437	45675.09577	0.2427	0.426
45675.04296	0.2031	0.438	45675.09646	0.2433	0.420
45675.04366	0.2036	0.439	45675.09715	0.2438	0.428
45675.04435	0.2042	0.442	45675.09785	0.2443	0.421
45675.04505	0.2047	0.437	45675.09854	0.2448	0.425
45675.04574	0.2052	0.442	45675.09924	0.2453	0.425
45675.04644	0.2057	0.437	45675.09993	0.2459	0.424
45675.04713	0.2062	0.439	45675.10063	0.2464	0.422
45675.04783	0.2068	0.436	45675.10132	0.2469	0.423
45675.05181	0.2097	0.437	45675.10202	0.2474	0.421
45675.05250	0.2103	0.439	45675.10271	0.2479	0.420
45675.05319	0.2108	0.435	45675.10340	0.2485	0.426
45675.05389	0.2113	0.435	45675.10410	0.2490	0.424
45675.05458	0.2118	0.431	45675.10489	0.2496	0.418
45675.05528	0.2124	0.437	45675.10558	0.2501	0.425
45675.05597	0.2129	0.434	45675.10627	0.2506	0.428
45675.05667	0.2134	0.433	45675.10697	0.2511	0.421
45675.05736	0.2139	0.429	45675.10766	0.2517	0.425
45675.05806	0.2144	0.429	45675.10836	0.2522	0.422
45675.05875	0.2150	0.434	45675.10905	0.2527	0.423
45675.05944	0.2155	0.433	45675.10975	0.2532	0.423
45675.06014	0.2160	0.433	45675.11044	0.2537	0.426
45675.06084	0.2165	0.434	45675.11114	0.2543	0.425
45675.06153	0.2170	0.430	45675.12285	0.2631	0.413
45675.06613	0.2205	0.427	45675.12354	0.2636	0.418
45675.06682	0.2210	0.429	45675.12424	0.2641	0.422
45675.06751	0.2215	0.429	45675.12493	0.2646	0.415
45675.06821	0.2221	0.426	45675.12563	0.2651	0.416
45675.06890	0.2226	0.425	45675.12632	0.2657	0.419
45675.06960	0.2231	0.433	45675.12701	0.2662	0.417
45675.07029	0.2236	0.426	45675.12771	0.2667	0.419
45675.07098	0.2241	0.427	45675.12841	0.2672	0.417
45675.07168	0.2247	0.431	45675.12910	0.2677	0.420
45675.07238	0.2252	0.426	45675.12979	0.2683	0.418
45675.07307	0.2257	0.427	45675.13049	0.2688	0.416
45675.07376	0.2262	0.425	45675.13118	0.2693	0.414
45675.07446	0.2267	0.429	45675.13188	0.2698	0.415

continued

45675.13257	0.2703	0.416
45675.14260	0.2779	0.424
45675.14330	0.2784	0.419
45675.14400	0.2789	0.421
45675.14469	0.2794	0.420
45675.14538	0.2800	0.417
45675.14608	0.2805	0.421
45675.14677	0.2810	0.419
45675.14747	0.2815	0.424
45675.14816	0.2820	0.424
45675.14885	0.2826	0.419
45675.14955	0.2831	0.422
45675.15025	0.2836	0.423
45675.15094	0.2841	0.426
45675.15163	0.2847	0.424
45675.15233	0.2852	0.418

1983 Dec 12/13

M. J. D.	Phase	(V-C)
45680.77942	0.5074	0.936
45680.78011	0.5079	0.946
45680.78081	0.5084	0.949
45680.78150	0.5090	0.943
45680.78220	0.5095	0.938
45680.78289	0.5100	0.929
45680.78359	0.5105	0.932
45680.78428	0.5110	0.928
45680.78498	0.5116	0.922
45680.78567	0.5121	0.925
45680.78699	0.5131	0.920
45680.78768	0.5136	0.921
45680.78838	0.5141	0.920
45680.78907	0.5146	0.922
45680.78977	0.5152	0.903
45680.79046	0.5157	0.917
45680.79115	0.5162	0.902
45680.79185	0.5167	0.890
45680.79254	0.5172	0.903
45680.79324	0.5178	0.890
45680.79732	0.5208	0.871
45680.79802	0.5213	0.877
45680.79871	0.5219	0.867
45680.79941	0.5224	0.857
45680.80010	0.5229	0.852
45680.80079	0.5234	0.857
45680.80149	0.5240	0.851
45680.80219	0.5245	0.849
45680.80288	0.5250	0.840
45680.80357	0.5255	0.850
45680.80427	0.5260	0.836
45680.80496	0.5266	0.834
45680.80566	0.5271	0.831
45680.80635	0.5276	0.833
45680.80705	0.5281	0.827

45680.81149	0.5315	0.805
45680.81218	0.5320	0.799
45680.81288	0.5325	0.785
45680.81357	0.5330	0.790
45680.81427	0.5335	0.791
45680.81496	0.5341	0.793
45680.81566	0.5346	0.781
45680.81635	0.5351	0.784
45680.81705	0.5356	0.781
45680.81774	0.5361	0.780
45680.81843	0.5367	0.769
45680.81913	0.5372	0.775
45680.81983	0.5377	0.763
45680.82052	0.5382	0.774
45680.84827	0.5591	0.642
45680.84897	0.5596	0.642
45680.84966	0.5601	0.637
45680.85035	0.5606	0.634
45680.85105	0.5611	0.635
45680.85175	0.5617	0.629
45680.85244	0.5622	0.627
45680.85313	0.5627	0.628
45680.85383	0.5632	0.627
45680.85452	0.5637	0.617
45680.85522	0.5643	0.622
45680.85591	0.5648	0.620
45680.85661	0.5653	0.609
45680.85730	0.5658	0.621
45680.85800	0.5664	0.602
45680.86303	0.5701	0.606
45680.86373	0.5707	0.608
45680.86442	0.5712	0.594
45680.86511	0.5717	0.595
45680.86581	0.5722	0.595
45680.86650	0.5727	0.591
45680.86720	0.5733	0.586
45680.86789	0.5738	0.586
45680.86858	0.5743	0.579
45680.86928	0.5748	0.585
45680.86998	0.5753	0.576
45680.87067	0.5759	0.586
45680.87136	0.5764	0.581
45680.87206	0.5769	0.573
45680.87275	0.5774	0.575
45680.87679	0.5805	0.568
45680.87748	0.5810	0.570
45680.87818	0.5815	0.558
45680.87888	0.5820	0.554
45680.87957	0.5825	0.556
45680.88026	0.5831	0.550
45680.88096	0.5836	0.556
45680.88165	0.5841	0.553
45680.88235	0.5846	0.550
45680.88304	0.5851	0.548
45680.88373	0.5857	0.550
45680.88443	0.5862	0.541

continued

45680.88513	0.5867	0.537	45736.96865	0.6683	0.453
45680.88582	0.5872	0.546	45736.96934	0.6688	0.450
45680.88651	0.5878	0.537	45736.97004	0.6693	0.442
45680.88721	0.5883	0.540	45736.97073	0.6698	0.445
45680.88790	0.5888	0.539	45736.97142	0.6704	0.450
45680.88860	0.5893	0.536	45736.97212	0.6709	0.447
45680.88929	0.5898	0.534	45736.97281	0.6714	0.451
45680.88999	0.5904	0.540	45736.97351	0.6719	0.446
45680.90096	0.5986	0.516	45736.97420	0.6725	0.446
45680.90165	0.5991	0.513	45736.97490	0.6730	0.448
45680.90235	0.5996	0.512	45736.97559	0.6735	0.444
45680.90304	0.6001	0.518	45736.97628	0.6740	0.441
45680.90374	0.6007	0.512	45736.97698	0.6745	0.446
45680.90443	0.6012	0.515	45736.97767	0.6751	0.446
45680.90513	0.6017	0.509	45736.97837	0.6756	0.446
45680.90582	0.6022	0.503	45736.97906	0.6761	0.441
45680.90651	0.6028	0.501	45736.97976	0.6766	0.443
45680.90721	0.6033	0.512	45736.98045	0.6771	0.443
45680.90790	0.6038	0.507	45736.98115	0.6777	0.450
45680.90860	0.6043	0.505	45737.01204	0.7008	0.431
45680.90929	0.6048	0.501	45737.01273	0.7014	0.430
45680.90999	0.6054	0.493	45737.01342	0.7019	0.425
45680.91068	0.6059	0.496	45737.01412	0.7024	0.425
45680.91425	0.6086	0.495	45737.01481	0.7029	0.428
45680.91495	0.6091	0.497	45737.01551	0.7035	0.432
45680.91565	0.6096	0.502	45737.01620	0.7040	0.419
45680.91634	0.6101	0.493	45737.01690	0.7045	0.427
45680.91703	0.6107	0.489	45737.01759	0.7050	0.435
45680.91773	0.6112	0.496	45737.01829	0.7055	0.428
45680.91842	0.6117	0.492	45737.01898	0.7061	0.430
			45737.01967	0.7066	0.427
			45737.02037	0.7071	0.425
			45737.02107	0.7076	0.429
			45737.02176	0.7081	0.433
			45737.02245	0.7087	0.425
			45737.02315	0.7092	0.422
			45737.02384	0.7097	0.425
			45737.02454	0.7102	0.422
			45737.02523	0.7107	0.425
			45737.05609	0.7339	0.423
			45737.05678	0.7344	0.425
			45737.05748	0.7349	0.420
			45737.05817	0.7355	0.423
			45737.05887	0.7360	0.414
			45737.05956	0.7365	0.419
			45737.06026	0.7370	0.424
			45737.06095	0.7375	0.419
			45737.06164	0.7381	0.422
			45737.06234	0.7386	0.420
			45737.06303	0.7391	0.414
			45737.06372	0.7396	0.426
			45737.06442	0.7402	0.417
			45737.06512	0.7407	0.416
			45737.06581	0.7412	0.423
			45737.06650	0.7417	0.427
			45737.06720	0.7422	0.413

1984 Feb 06/07

M.J.D.	Phase	(V-C)			
45736.94682	0.6519	0.456	45737.02176	0.7081	0.433
45736.94751	0.6524	0.460	45737.02245	0.7087	0.425
45736.94821	0.6530	0.457	45737.02315	0.7092	0.422
45736.94890	0.6535	0.459	45737.02384	0.7097	0.425
45736.94960	0.6540	0.454	45737.02454	0.7102	0.422
45736.95029	0.6545	0.454	45737.02523	0.7107	0.425
45736.95098	0.6550	0.458	45737.05609	0.7339	0.423
45736.95168	0.6556	0.458	45737.05678	0.7344	0.425
45736.95237	0.6561	0.459	45737.05748	0.7349	0.420
45736.95307	0.6566	0.457	45737.05817	0.7355	0.423
45736.95376	0.6571	0.454	45737.05887	0.7360	0.414
45736.95446	0.6576	0.457	45737.05956	0.7365	0.419
45736.95515	0.6582	0.457	45737.06026	0.7370	0.424
45736.95585	0.6587	0.452	45737.06095	0.7375	0.419
45736.95654	0.6592	0.456	45737.06164	0.7381	0.422
45736.95723	0.6597	0.448	45737.06234	0.7386	0.420
45736.95793	0.6602	0.450	45737.06303	0.7391	0.414
45736.95862	0.6608	0.456	45737.06372	0.7396	0.426
45736.95932	0.6613	0.458	45737.06442	0.7402	0.417
45736.96001	0.6618	0.456	45737.06512	0.7407	0.416
45736.96795	0.6678	0.449	45737.06581	0.7412	0.423
			45737.06650	0.7417	0.427
			45737.06720	0.7422	0.413

continued

45737.06789	0.7428	0.418
45737.06859	0.7433	0.422
45737.06928	0.7438	0.417
45737.07274	0.7464	0.418
45737.07344	0.7469	0.425
45737.07413	0.7474	0.419
45737.07483	0.7480	0.417
45737.07552	0.7485	0.419
45737.07622	0.7490	0.414
45737.07691	0.7495	0.423
45737.07899	0.7511	0.427
45737.08038	0.7521	0.417
45737.08177	0.7532	0.423
45737.08316	0.7542	0.419
45737.08385	0.7547	0.424
45737.08455	0.7553	0.426
45737.09949	0.7665	0.425
45737.10018	0.7670	0.419
45737.10088	0.7675	0.420
45737.10158	0.7680	0.434
45737.10227	0.7685	0.423
45737.10296	0.7691	0.419
45737.10366	0.7696	0.429
45737.10435	0.7701	0.429
45737.10504	0.7706	0.426
45737.10574	0.7712	0.434
45737.10644	0.7717	0.423
45737.10713	0.7722	0.425
45737.10782	0.7727	0.420
45737.10852	0.7732	0.426
45737.10921	0.7738	0.421
45737.10991	0.7743	0.424
45737.11060	0.7748	0.419
45737.11129	0.7753	0.421
45737.11199	0.7758	0.431
45737.11269	0.7764	0.425
45737.11778	0.7802	0.429
45737.11847	0.7807	0.433
45737.11916	0.7812	0.434
45737.11986	0.7818	0.431
45737.12056	0.7823	0.428
45737.12125	0.7828	0.424
45737.12194	0.7833	0.426
45737.12264	0.7838	0.433
45737.12333	0.7844	0.421
45737.12403	0.7849	0.422
45737.12472	0.7854	0.433
45737.12542	0.7859	0.423
45737.12611	0.7864	0.428
45737.12681	0.7870	0.425
45737.12750	0.7875	0.428

Differential Magnitude (V-C)

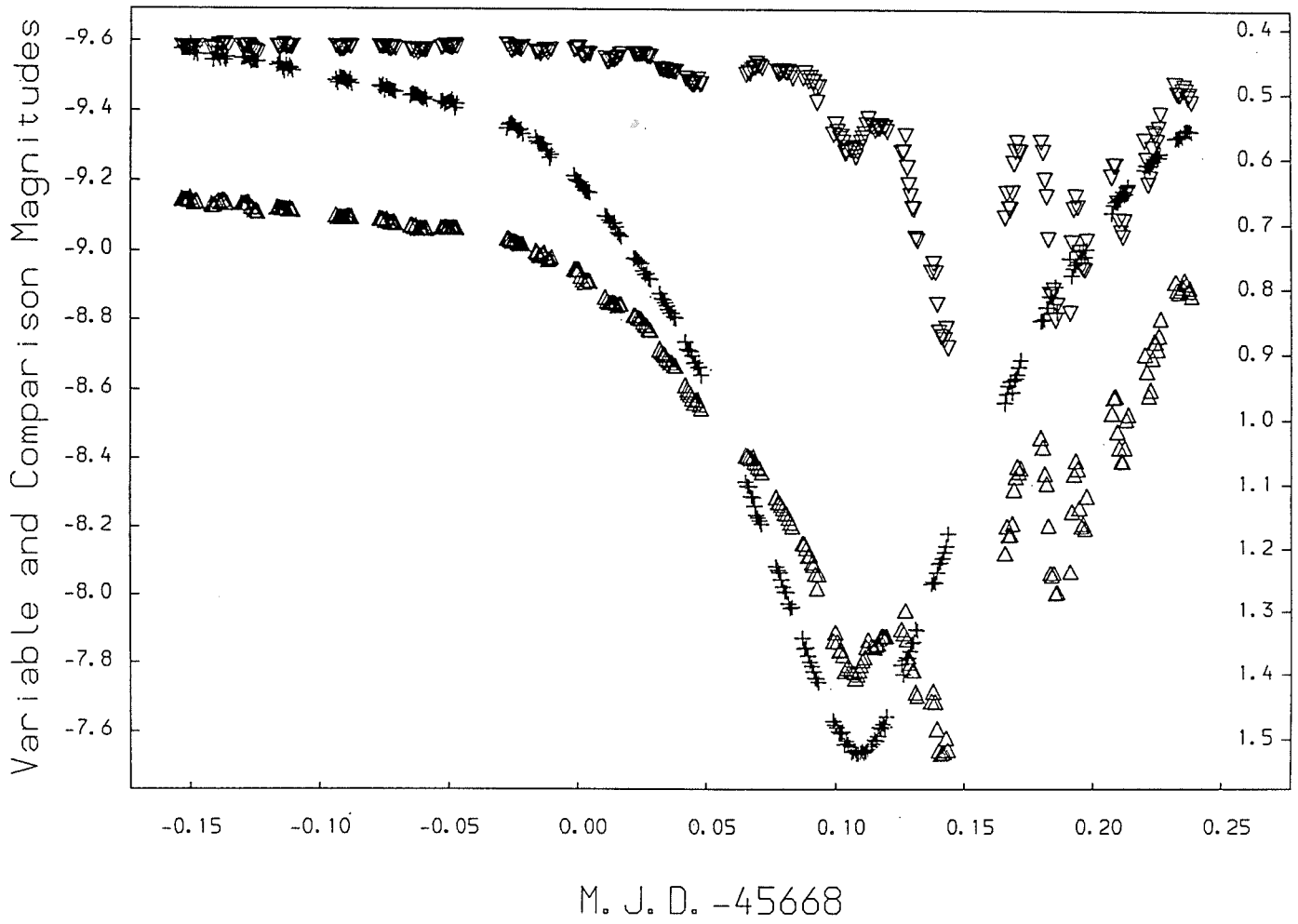


Figure 1.

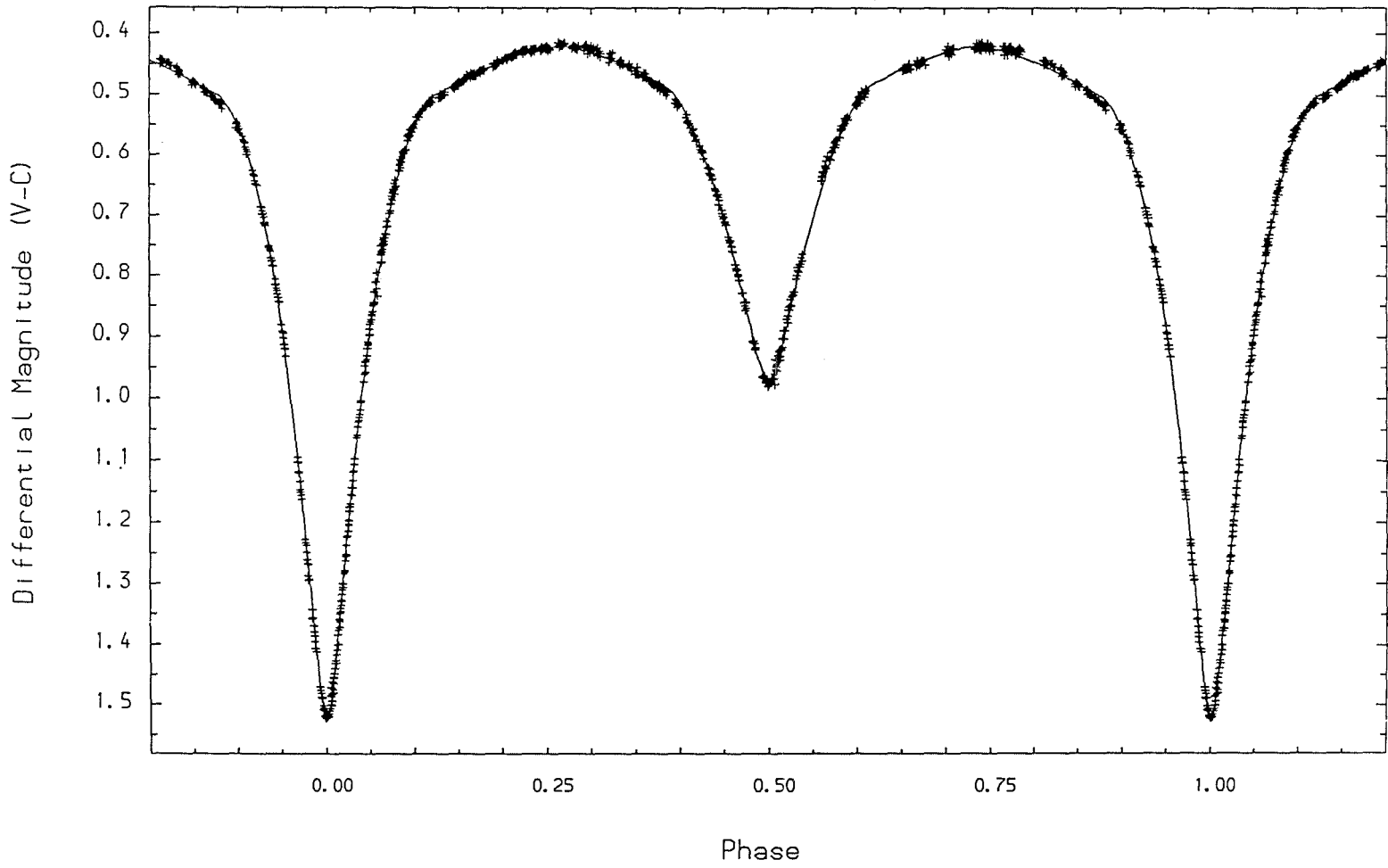


Figure 2.

CHAPTER 4

A photometric and spectroscopic study of the early-type binary

AH Cephei.

A photometric and spectroscopic study of the early-type binary

AH Cephei.

S.A.Bell, R.W.Hilditch and A.J.Adamson

University Observatory, Buchanan Gardens, St. Andrews,

Fife, KY16 9LZ, Scotland.

Received _____

Correspondence to:-

S.A.Bell,
University Observatory,
Buchanan Gardens,
St. Andrews, Fife,
KY16 9LZ,
Scotland.

Summary

We present new Strömgren photometry and medium dispersion spectroscopy of the early-type close binary AH Cephei. The masses and radii of the two components are found to be (18.1 ± 0.9) , (15.9 ± 0.8) solar masses and (6.7 ± 0.2) and (6.2 ± 0.2) solar radii respectively. Two possible values of the effective temperature of the primary component lead to two sets of possible luminosities for the components. Comparison with currently available evolutionary tracks for single stars suggests that this system could evolve into contact during its main-sequence lifetime.

1) Introduction

The early-type binary system AH Cephei (HD 216014, BD +64° 1717: Sp. type B0.5Vn + B0.5Vn) was discovered to be a spectroscopic binary by Plaskett and subsequently investigated by Pearce (1927), who found a period of 2.2875 days. Photometric observations by Huffer and Eggen (1947) revealed a light curve of the Beta Lyrae type with a period of 1.77473 days. Their analysis showed the system to be composed of two massive early B stars. The ambiguity over the period was resolved by Zverev (1933) by means of his own visual observations and a re-examination of Pearce's velocities. Pearce (1935) calculated a new spectroscopic orbit, based on the shorter period confirmed by Zverev, which showed a small eccentricity.

Nekrasova (1960) published photometric observations of the system obtained with blue and yellow filters and her subsequent analysis ruled out any orbital eccentricity. Cester et al. (1981) used these photometric data and obtained quite different solutions to those previously found. Their analysis cast doubts on the detached nature of the system mainly because they conclude that the radius of the primary is comparable with the corresponding Roche critical surface.

As part of a programme to investigate the properties of early-type close binaries with orbital periods less than 1.8 days, it was decided to include AH Cephei in our sample. A thorough photometric and spectroscopic investigation in conjunction with a fully-rigorous analysis would remove any doubt as to the nature of this eclipsing binary, and would clarify its evolutionary status.

2) Spectroscopy

2.1) Observations

The spectroscopic observations presented in this study were obtained from two different sources at two different times. A total of five spectrograms were obtained at double-lined phases by RWH during 1972 with the 1.8m telescope and Cassegrain spectrograph of the Dominion Astrophysical Observatory, Victoria. A dispersion of 15\AA mm^{-1} was employed (the 21121 configuration) and the spectra were recorded on baked IIIaJ emulsion.

The diffuse and rotationally broadened lines of HeI were measured for radial velocity using the ARCTURUS oscilloscope comparator at DAO. The two spectra were barely resolved at this dispersion, the intensity between the components of the same absorption line only just returning to the local continuum level.

The remaining ten spectra were obtained by SAB and AJA during the period 1985 August 28-30, at the Observatorio del Roque de los Muchachos, La Palma, using the 2.5m Isaac Newton Telescope in conjunction with the Intermediate Dispersion Spectrograph (IDS) and Image Photon Counting System (IPCS). The Jobin-Yvon 1200 grating and Camera 2 of the IDS provided spectra at a dispersion of 16.7\AA mm^{-1} . Observations were made using a slit width of $100\ \mu\text{m}$, or 0.55 arcseconds when projected on the sky, and neutral density filters to avoid saturating the IPCS. Each observation consisted of two spectra centred on 4040\AA and 4400\AA with typical exposure times of 500-600s for both wavelength ranges. All stellar integrations were alternated with comparison-source exposures by a Cu-Ar lamp for wavelength calibration purposes. The spectra were stored on disk and tape at the end of each exposure in FITS format (Wells, Greisen

and Harten, 1981).

On each night, observations were made of radial velocity standard stars covering a range in spectral type of F7-G8 in both wavelength ranges. Observations were also made of the secondary radial-velocity standard ADS 16472A (spectral type B3), selected from a compilation by Petrie (1953) of B-type secondary standards. The spectra of this star were subsequently used as comparison spectra in cross-correlation analyses of the spectra of AH Cephei.

2.2) Reduction and Analysis

The spectroscopic data were processed on the University of St. Andrews VAX computers, using the SPICA package to flat-field the spectra, effect the sky background subtraction and convert them into a form suitable for the spectroscopic image-processing package REDUCE (Hill et al., 1982a).

The spectra were linearised using REDUCE and smoothing and rectification were applied using FTSPLOTT, a program written by AJA. Smoothing was applied by taking running means over 5 pixels, and rectification was achieved by division into the spectrum of a heavily smoothed version of itself. The spectra were finally log-linearised using REDUCE in preparation for the cross-correlation analysis.

Cross correlations of the spectra of AH Cephei with the comparison star ADS 16472A were made using VCROSS (Hill, 1982a). To obtain the optimum cross-correlation function, windows were set up around the principal spectral lines showing splitting. The HeI lines at $\lambda\lambda 4026, 4144, 4388$ and 4471 were found to be the most

useful. Two He I lines were not used; $\lambda 4009$ was very weak and $\lambda 4120$ was occasionally blended with H δ . The Balmer lines, however, were omitted from the analysis due to their extremely Stark-broadened and rotationally broadened profiles. The lines of interstellar CaII were prominent in all the short wavelength spectra, the K line being extremely well defined but the H line being severely blended with H ϵ . The mean velocity derived from these lines using VELMEAS (Hill et al., 1982b) was $-28 \pm 8 \text{ km s}^{-1}$. These lines were also excluded from the analysis. The final radial velocities for both components of the binary are listed in Table 1 and the radial velocity curves are given in Figure 1.

The velocity of the secondary component of the system on exposure INTD237/13 shows a radial velocity residual of $\sim -90 \text{ km s}^{-1}$. This velocity has been excluded from the analysis since it shows a residual of four times the standard deviation of the fit and inclusion of this point would seriously detract from the quality of the fit to the rest of the data. However, if this point is included, the velocity semi-amplitude for the secondary component would be increased from $283 \pm 8 \text{ km s}^{-1}$ to $291 \pm 10 \text{ km s}^{-1}$.

Examination of the light curves for AH Cephei confirm Nekrasova's conclusion that the orbit is circular (Section 3.5). Adopting the procedures of Popper (1974), the circular orbital elements of AH Cephei were computed by separate analysis of each component. The velocity semi-amplitudes of the primary and secondary components, K_1 and K_2 respectively, the systemic velocity V_0 and the derived mass functions and projected semi-major axes of the orbits of the two components, together with their standard errors, are given in Table 2.

The projected rotational velocities have been estimated from the half-width of the HeI $\lambda 4471$ line for both components by means of the calibration of Slettebak et al. (1975). The only exposure showing a satisfactorily-resolved feature was INTD235/23 (Figure 2). Our estimates of the projected rotational velocities of 175 ± 15 and $180 \pm 20 \text{ km s}^{-1}$ for the primary and secondary components respectively, are in reasonable agreement with the study carried out by Olson (1984) who found $180 \pm 18 \text{ km s}^{-1}$ for the primary and $149 \pm 27 \text{ km s}^{-1}$ for the secondary. If synchronous rotation is adopted together with the final mean radii of the two stars (Table 7), then theoretical velocities of 179 and 164 km s^{-1} would be expected for the primary and secondary component respectively. Measurements of the equivalent width for the two components of the $\lambda 4471$ feature would imply a luminosity ratio of the secondary L_s to the primary L_p of 0.85 with an estimated error of approximately 10%. This compares quite favourably with the study made by Petrie (1950) whose spectroscopic magnitude difference between the two components leads to a luminosity ratio, L_s/L_p , of 0.78 ± 0.03 .

3) Photometry

3.1) Observations

Photoelectric photometry was obtained by SAB at the Observatorio del Sierra Nevada during the period 1984 September 19-25. Simultaneous observations were made in the Strömgren four-colour system using the 0.75m. Stevenson telescope and a Danish 6-channel uvby- β photometer. A 46 arcsecond aperture was used throughout this study and integration times were fixed at 60s for the monitoring sequence. The comparison star used was HD 215371

(B1.5V), which has been used in several previous studies of AH Cephei (Huffer and Eggen, 1947; Nekrasova, 1960; Guarnieri et al., 1975; Mayer, 1980). It was decided that a check star was not necessary as previous work had not revealed any evidence of variability in this star. A total of 687 observations in each colour were obtained. The instrumental magnitude differences relative to HD 215371 are given in Table 3. During each night between 15 and 20 uvby standard stars were observed to allow a transformation to the standard system to be made. Data for the variable and comparison stars are given in Table 5.

3.2) Reductions

The reduction to differential magnitudes was made using a computer program written by SAB incorporating L2FRES (Powell, 1967), a least-squares cubic-spline-fitting routine and INTEP (Hill, 1982b), a hermite interpolation routine. A spline function was fitted to the sky background readings and used for interpolating values of the background at the time of the stellar observations for subsequent subtraction from the stellar data. The extinction in each colour was determined using the comparison star data in the usual manner, but checks for azimuthal and time dependencies in the extinction coefficients were also made. After corrections for extinction were made, another spline function was fitted to the comparison star magnitudes and differential data were formed by subtracting the spline evaluated at the times of the variable-star observations.

The standard-star observations and associated sky backgrounds were simply subtracted and a second computer program written by SAB performed a least squares analysis to determine the transformation coefficients to the standard uvby system. Transformation equations were derived for the (b-y), (v-b) and (u-b) indices over a wide range of colour and for the V magnitude. Colour terms were evaluated relative to the (b-y) colour index. The extinction coefficients determined using the comparison star data were adopted and no appreciable time drifts were found in the analysis. The mean scale factors, colour terms and extinctions for the transformations are given in Table 4 and the standard magnitudes and colours for the comparison and variable stars are given in Table 5. The instrumental magnitudes were used for the subsequent analysis since corrections to the differential magnitudes due to the scale factors would be less than half the error on a single observation and make little or no difference to the solutions obtained from the light-curve analysis.

3.3) Ephemeris

Guarnieri et al. (1975) made a study of the available times of minima and concluded that a variation in the period had taken place but observations were too scarce to state its nature. For the older minima before HJD 2434714, they found a period of $P = 1.774736 \pm 0.000001$ days and for minima after that date they proposed the following ephemeris based on three points:

$$\text{Pri. Min.} = \text{H.J.D. } 2434989.404 + 1.774759 E$$

± 1

± 2

3.4) Colour indices

In compiling Stromgren four-colour observations of northern hemisphere binary systems, Hilditch and Hill (1975) observed AH Cephei on four occasions. Mean colour indices for $(b-y)$, m_1 and c_1 were de-reddened yielding intrinsic colours of $-0^m.127$, $0^m.092$ and $-0^m.109$, respectively. These values are in reasonable agreement with those given in Table 5 with the exception of c_0 , where a difference of $0^m.08$ was found, suggesting that the u-band observations made in 1984 are systematically brighter than those of Hilditch and Hill by $0^m.08$. The cause of this discrepancy is not clear. Zero-point determinations for the uvby standard stars from night to night were found to be consistent to less than $0^m.02$. The scale factor for the $(u-b)$ transformation was found to be slightly greater than unity (Table 4), consistent with the fact that the grating reflectivity falls off towards the blue end of the u filter band (Gronbech et al., 1976). An instrumental or atmospheric effect cannot be completely ruled out, but the possibility exists that this brightening is intrinsic to the system.

3.5) Analysis

The light curves for AH Cephei are of the Beta-Lyrae type and are slightly asymmetric, the maximum light level at $0^p.25$ being about $0^m.005$ higher than at $0^p.75$, whereas the colours are the same. The primary minimum for the u-band curve shows some asymmetry, having a steeper egress than ingress. It can be seen from inspection of Figure 4 that our light curve does not indicate any eccentricity since primary and secondary minima occur at phases $0^p.00$ and $0^p.50$ respectively.

The c_1 index showed no appreciable variation over the orbital cycle and because of the discrepancy outlined above, two values were adopted for the polar temperatures of the primary component employing the calibration of Davis and Shobbrook (1977). Using the c_0 index derived from the colours of Hilditch and Hill (1975), a temperature of 29900K was found whereas the photometry presented in this paper suggested a polar temperature of at least 34000K. In a survey of MK spectral types by Hill et al. (1975), the composite spectrum for AH Cephei was classified as being between O6 and O8. This corresponds to a temperature in excess of 35500K (Popper, 1980). Other published composite spectral types for this system are B0.5III (Roman, 1956), B0.5Vnn (Hiltner, 1956) and B0.2V (Olson, 1968), which are compatible with a primary temperature of 29900K. It was decided to solve the light curves for primary temperatures of 29900K (Solution I) and 35000K (Solution II).

Each light curve was analysed using LIGHT (Hill, 1979), fixing the mass ratio q at that determined from the spectroscopic analysis and the primary component temperature T_1 by photometric calibration. The fractional primary component radius r_1 , the secondary component temperature T_2 and fractional radius r_2 , and the inclination of the system i were kept as free parameters. As a first approximation, the solution of Cester et al. (1981) was used. Table 7 lists the results of the analysis for the two possible primary component temperatures.

The following assumptions were made for each analysis. Black-body fluxes were adopted because preliminary solutions using the model atmospheres of Kurucz (1979) gave inferior fits. Synchronous rotation was assumed since the projected synchronous rotational velocities computed from our final fit agreed quite well

with the observed values (Section 2.2). Gravity-darkening exponents (β_1 and β_2) were set at 0.25 for both components, and electron scattering fractions (Escat_1 and Escat_2) were taken from Hutchings and Hill (1971). The limb-darkening coefficients were calculated automatically within LIGHT at each iteration of the solution using interpolation from the tabulation by Carbon and Gingerich (1969).

Changing the primary temperature T_1 , had little effect on the solution except, of course, for T_2 . To determine how sensitive the solutions were to the adopted mass ratio, further solutions were made of the b-band light curve with q at the limits of the spectroscopic mass ratio suggested by the standard error derived from the errors in the velocity semi-amplitudes. All the free parameters showed variations of less than 1% which, in turn would indicate only a weak dependence upon the mass ratio.

The b-band light curve is plotted in Figure 4, with the fit using Solution II. Either fit could have been plotted as they differ by less than 0.0005^m . The (b-y) and (u-b) colours are plotted in Figure 5 using the same value of T_1 . Once again, both fits are very nearly indistinguishable, although Solution II did give very marginally better χ^2 statistics for the individual solutions (Table 7). The residuals for the individual light curves using Solution II are plotted in Figure 6. All the curves show a departure of approximately 0.005^m around second quadrature. The u-band curve also shows a trend through secondary minimum, being faintest at 0.4^P and brightest at 0.65^P . The other curves show an enhanced scatter around the same region. Unfortunately, the coverage is not extensive enough to show whether this effect is symptomatic of some activity at this phase. The u-band solutions indicate somewhat larger inclination than the other bands and this

may be a result of the use of black-body radiation and its inability to model the Balmer discontinuity. The luminosity ratios L_s/L_p for the b-band light curves of the hotter and cooler primaries of 0.88 and 0.86, respectively, compare favourably with the spectroscopically-derived value of 0.85. The final result for the two adopted primary temperatures from our photometric analysis of AH Cephei is given in Table 8.

4) Discussion

4.1) Spectroscopy and Photometry

It would be expected that the observed velocity amplitudes are affected by reflection between the two components and pair blending in the double spectral lines. Kitamura's technique (1953,1954) was used to estimate the effect of reflection on K_1 and K_2 ; the corrections were less than 1kms^{-1} . These corrections, in our opinion, must be taken as lower limits as they seem very low considering the temperature of the two components, although the assumptions made by this method are still reasonable given the detached nature of AH Cephei. The magnitude of the correction, however, is still small in comparison with the errors in the velocity semi-amplitudes. With $K_1 + K_2 > 530\text{kms}^{-1}$, blending of the diffuse He I lines probably has very little effect on the derived absolute dimensions (Andersen, 1975). All of these systematic effects would tend to make the observed velocity semi-amplitudes, and consequently the masses and radii of the two components, too small.

The absolute values of the effective temperatures may well be in error by up to 1000K in the case of Solution II, as they are based on the upper limit of the (c_o, T_{eff}) calibration. Each primary temperature has photometric and spectroscopic evidence to support it, although reference to the empirical mass-luminosity diagram for detached OB binaries would lend support to the adoption of a 35000K primary (Section 4.2).

Astrophysical data for AH Cephei are given in Table 9. The bolometric corrections quoted were obtained using the calibration of Davis and Shobbrook (1977), and the absolute visual magnitudes and distance were found from the data given in this paper.

4.2) Evolutionary state

The properties of the two components from Solution II suggest that the system is composed of an O8 primary and an O9 secondary, whose absolute magnitudes correspond well with the tabulation of unevolved O stars by Conti and Burnichon (1975). Solution I, however, requires the system to be composed of a B0 primary and a B0.5 secondary.

Using the compilation of properties of detached OB binaries given by Popper (1980, Table 4) and improvements made since its publication, empirical relationships have been plotted for the HR diagram, mass-luminosity and mass-radius planes in Figures 7, 8 and 9. In the HR diagram, both the O-type and B-type configurations lie close to an unweighted least-squares fit to the original data. The mass-luminosity diagram shows the O-type configuration to fit the relationship extremely well, whereas the B-type components are about 0.5^m too faint. The mass-radius diagram shows that the absolute

dimensions for both possible systems are compatible with the empirical relationship. Taking into account the marginally better fits obtained with LIGHT for Solution II, it would appear that the O-type system is the preferred configuration.

The equivalent-volume radii of the critical Roche lobes for the primary and secondary, expressed in units of the separation of the two components, are 0.390 ($7.3R_{\odot}$) and 0.368 ($6.9R_{\odot}$) respectively. Hence the primary fills 64% of its Roche lobe and the secondary fills 60% of its lobe. The two possible configurations were compared with models made by Maeder (1981) to evaluate the possibility that the system would evolve into contact before the end of its main-sequence lifetime. Interpolation between the 15 and $30M_{\odot}$ models is not appropriate as the main-sequence lifetimes of the two models differ by a factor of 2. However, assuming there is no mass loss, the $15M_{\odot}$ model will evolve to a radius of $7.3R_{\odot}$ in about 7×10^6 yrs and therefore provides a guide to the age of AH Cephei at the onset of contact. The $18M_{\odot}$ primary would evolve more rapidly than this, but the model grids available are not fine enough to improve this estimate.

The observed period changes (Section 3.3) suggest that either mass transfer or mass loss occurs in the system. In the case of conservative mass transfer, the period of the orbit changes at a rate proportional to the mass-transfer rate. If the lighter star loses mass then the orbital period will increase. Conversely, if the heavier star loses mass the orbital period decreases. From the O-C diagram (Figure 3), it is apparent that the orbital period has increased, implying mass transfer from the secondary. Our solutions, however, show quite clearly that the system is detached which would rule out this possibility.

It seems likely that the components of the system would exhibit evidence of mass loss due to stellar winds, particularly in the case of the late O-type system. If a stellar wind is present, resulting in a mass-loss rate of the order of $10^{-7} M_{\odot} \text{yr}^{-1}$ (de Loore et al., 1977), then the period will increase (cf. for example, Pringle, 1985). Over the main-sequence lifetime of 11×10^6 yrs, the period will lengthen by 0.1 and the semi-major axis will become $20R_{\odot}$. The primary would then have to expand to a radius of $7.6R_{\odot}$ to reach its critical Roche lobe. This stage could be reached after 90% of its main-sequence lifetime, allowing AH Cephei to evolve into a contact system before the end of hydrogen-core burning. If the mass-loss rate is a factor of 10 greater, then case A evolution could be prevented by increasing the separation of the two components as has already been suggested by Vanbeveren et al. (1979). Case B mass transfer may then bring about the common envelope stage of evolution.

In the B-type configuration, the secondary compares favourably with Maeder's $15M_{\odot}$ model with intermediate mass loss of approximately $10^{-7} M_{\odot} \text{yr}^{-1}$ at an age of about 6×10^6 yrs. If this is the case, then the primary could also be losing mass which would tend to delay or prevent case A evolution. The O-type configuration secondary appears to be unevolved, but the coarseness of the model grids makes the interpretation of the evolutionary state of the primary components difficult.

Assuming the mass-loss rate is not excessively high, the evolution of this system could proceed as follows. Before the end of core-hydrogen burning, the primary reaches its critical Roche lobe and a phase of rapid mass transfer follows. During this phase, the secondary radius will increase rapidly due to accretion of

matter from the primary and the system will take on a contact configuration. If the mass transfer is arrested for any reason, then AH Cephei may become a member of a small group of binaries with Roche lobe-filling secondaries and apparently normal primaries, such as V Puppis. If the mass transfer proceeds, then the evolution of the system depends on how much mass is lost to the system and on the behaviour of the secondary as a result of this mass transfer. At present, there are no theoretical models available to describe this behaviour with or without non-conservative mass exchange and stellar winds.

5) Conclusion

The new spectroscopic and photometric analysis has led to the reliable determination of the absolute dimensions of the components for AH Cephei and has shown the configuration of the system to be detached. There are, however, two choices of primary component temperature, affecting the evolutionary status in the following manner. The O-type system appears to be essentially unevolved whereas the cooler B-type system appears to be about halfway through its main-sequence lifetime assuming the mass loss rate is not excessive. More photometric observations are required to resolve which of the two possible primary temperatures is correct.

We have shown that Case A evolution is likely for this system although the magnitude of the mass-loss rate plays a decisive role in the evolutionary stage at which contact is likely to occur. The observed period changes indicate the possibility that mass loss has taken place in the system in the recent past. UV observations are required to confirm the existence of stellar winds from one or both

of the components. If, however, mass transfer has taken place then it could be interpreted as the precursor to the formation of a contact system. Further observations of times of minima are required to evaluate the changes in the orbital period.

Acknowledgements

The authors would like to express their gratitude for the hospitality and assistance extended to them by the staffs of the Instituto de Astrofísica de Andalucía, the Observatorio del Roche de los Muchachos and the Dominion Astrophysical Observatory during the observing runs. We acknowledge PATT for the allocations of observing time, and the SERC for financial support in the form of a research studentship for one of us (SAB). We would also like to thank Prof. D.W.N. Stibbs for the use of the facilities of the University Observatory, St. Andrews.

References

- Andersen, J., 1975. *Astron. Astrophys.*, 44, 355.
- Battistini, P., Bonifazi, A. & Guarnieri, A., 1973. *Info. Bull. Var. Stars*, No. 817.
- Carbon, D.F. & Gingerich, O.J., 1969. *Theory and Observations of Normal Stellar Atmospheres*, ed. Gingerich, O.J. (M.I.T. press, Cambridge), 377.
- Cester, B., Fedel, B., Giuricin, F., Mardirossian, F. & Mezzetti, M., 1981. *Astron. Astrophys. Suppl. Ser.*, 33, 91.
- Conti, P.S. & Burnichon, M.L., 1975. *Astron. Astrophys.*, 38, 467.
- Davis, J. & Shobbrook, R.R., 1977. *Mon. Not. R. astr. Soc.*, 178, 651.
- de Loore, C., De Grève, J.P. & Lamers, H.J.G.L.M., 1977. *Astron. Astrophys.* 61, 251.
- Gronbech, B., Olsen, E.H. & Strömberg, B., 1976. *Astron. Astrophys. Suppl. Ser.*, 26, 155.
- Guarnieri, A., Bonifazi, A. & Battistini, P., 1975. *Astron. Astrophys. Suppl. Ser.*, 20, 199.
- Hartigan, P. & Binzel, R.P., 1982. *J. AAVSO*, 11, 21.
- Hilditch, R.W. & Hill, G., 1975. *Mem. R. astr. Soc.*, 79, 101.
- Hill, G., 1979. *Publ. Dom. Astrophys. Obs.*, 15, 297.
- Hill, G., 1982a. *Publ. Dom. Astrophys. Obs.*, 16, 59.

- Hill,G., 1982b. Publ. Dom. Astrophys. Obs., 16, 67.
- Hill,G., Hilditch,R.W., Younger,F. & Fisher,W.A., 1975. Mem. R. astr. Soc., 79, 131.
- Hill,G., Fisher,W.A. & Poeckert,R., 1982a. Publ. Dom. Astrophys. Obs., 16, 43.
- Hill,G., Ramsden,D., Fisher,W.A. & Morris,S.C., 1982b. Publ. Dom. Astrophys. Obs., 16, 11.
- Hiltner,W.A., 1956. Astrophys. J. Suppl. Ser., 2, 389.
- Huffer,C.M. & Eggen,O.J., 1947. Astrophys. J., 106, 303.
- Hutchings,J.B. & Hill,G., 1971. Astrophys. J., 167, 137.
- Kitamura,M., 1953. Publ. astr. Soc. Japan, 5, 114.
- Kitamura,M., 1954. Publ. astr. Soc. Japan, 6, 217.
- Kwee,K.K. & van Woerden,H., 1956. Bull. astr. Inst. Netherlands, 12, 327.
- Kurucz,R.L., 1979. Astrophys. J. Suppl. Ser., 40, 1.
- Maeder,A., 1981. Astron. Astrophys., 102, 401.
- Mayer,P., 1980. Bull. astr. Inst. Czechoslovakia, 31, 292.
- Mayer,P. & Tremko,J., 1983. Info. Bull. Var. Stars, No. 2407.
- Moore,J.H., 1936. Lick Obs. Bull., No. 483, 16.
- Nekrasova,S.V., 1960. Perem. Zvezdy, 13, 157.
- Olson,E.C., 1968. Astrophys. J., 153, 187.

- Olson, E.C., 1984. Publ. astr. Soc. Pacific, 96, 376.
- Pearce, J.A., 1927. Publ. Dom. Astrophys. Obs., 3, 171.
- Pearce, J.A., 1935. J. Roy. astr. Soc. Canada, 43, 413.
- Petrie, R.M., 1950. Publ. Dom. Astrophys. Obs., 8, 319.
- Petrie, R.M., 1953. Publ. Dom. Astrophys. Obs., 9, 297.
- Popper, D.M., 1974. Astron. J., 79, 1307.
- Popper, D.M., 1980. Ann. Rev. Astron. Astrophys., 18, 115.
- Powell, M.J.D., 1967. Report No. HL67/5309, AERE, Harwell.
- Pringle, J.E., 1985. Interacting Binary Stars, ed. Pringle, J.E. & Wade, R.A. (Cambridge University Press, Cambridge), 1.
- Rafert, J.B., 1982. Publ. astr. Soc. Pacific, 94, 485.
- Roman, N.G., 1956. Astrophys. J., 123, 246.
- Slettebak, A., Collins, G.W., Boyce, P.B., White, N.M. & Parkinson, T.D., 1975. Astrophys. J. Suppl. Ser., 29, 137.
- Vanbeveren, D., De Grève, J.P., van Dessel, E.L. & de Loore, C., 1979. Astron. Astrophys., 73, 19.
- Wells, D.C., Greisen, E.W. & Harten, R.H., 1981. Astrophys. J. Suppl. Ser., 44, 363.
- Zverev, M., 1931. Beob. Zirk. der. Astron. Nachr., 13, 25.
- Zverev, M., 1933. Perem. Zvezdy, 4, 177.

Figure captions

Figure 1: Observed radial velocities and computed orbits for AH Cephei. Triangles represent D.A.O. data and circles represent I.N.T. data.

Figure 2: IPCS data for the region $\lambda\lambda 4300-4500$ in AH Cephei. The data were taken at first quadrature from run number INTD235/23.

Figure 3: Observed minus calculated times of minima in fractions of a day based on the ephemeris computed in this paper. Crosses represent photographic times of minima and circles those obtained photoelectrically.

Figure 4: b-magnitude differences in the sense variable minus comparison between AH Cephei and HD 215371 together with the final theoretical curve using Solution II.

Figure 5: (b-y) and (u-b) colour-index differences in the sense variable minus comparison between AH Cephei and HD 215371 together with the final theoretical curves using Solution II.

Figure 6: Residuals of the individual uvby observations from the final theoretical curves using Solution II.

Figure 7: Location of the components of AH Cephei in the HR diagram for detached OB binaries (Popper, 1980). The hotter primary solution is represented by circles, the cooler by triangles.

Figure 8: Location of the components of AH Cephei in the empirical mass-luminosity diagram for detached OB binaries (Popper, 1980). The hotter primary solution is represented by circles, the cooler by triangles.

Figure 9: Location of the components of AH Cephei in the empirical mass-radius diagram for detached OB binaries (Popper, 1980). The hotter primary solution is represented by circles, the cooler by triangles.

Table 1 : Radial-velocity data.

D.A.O. data.

Plate No.	H.J.D.	Phase	V_1 kms ⁻¹	n	O-C kms ⁻¹	V_2 kms ⁻¹	n	O-C kms ⁻¹
	-2400000							
72867	41529.9115	0.2981	-225	(6)	+33	+276	(4)	+27
72987	41538.8921	0.3583	-177	(7)	+37	+215	(6)	+15
73099	41552.8613	0.2293	-242	(7)	+25	+253	(5)	- 8
73204	41562.8663	0.8667	+182	(11)	+18	-216	(10)	+15
73340	41585.7343	0.7518	+233	(3)	+ 5	-289	(3)	+15

The column headed n indicates the number of lines measured for the mean velocity tabulated.

I.N.T. data.

Tape/Run No.	H.J.D.	Phase	V_1 kms ⁻¹	O-C kms ⁻¹	V_2 kms ⁻¹	O-C kms ⁻¹	Range
	-2400000						
INTD234/18	46306.5765	0.7391	+219	- 8	-309	- 6	Short
INTD234/20	46306.5905	0.7470	+239	+11	-341	-37	Long
INTD235/22	46307.4599	0.2369	-259	+ 9	+278	+16	Short
INTD235/23	46307.4662	0.2404	-305	-37	+289	+27	Long
INTD235/25	46307.4780	0.2471	-297	-27	+284	+21	Long
INTD235/26	46307.4849	0.2510	-277	- 8	+238	-24	Short
INTD235/60	46307.7155	0.3809	-180	-10	+125	-47	Short
INTD235/61	46307.7238	0.3856	-235	-51	+129	-37	Long
INTD237/12	46308.4176	0.7765	+227	+ 3	-266	+34	Short
INTD237/13*	46308.4252	0.7808	+197	-26	-389	-90	Long

* see Section 2.2.

The final column indicates the wavelength region used.

Table 2 : Orbital elements.

K_1 (kms ⁻¹)	= 249 ± 8
K_2 (kms ⁻¹)	= 283 ± 8 *1
$V_{o(1)}$ (kms ⁻¹)	= -21 ± 7
$V_{o(2)}$ (kms ⁻¹)	= -20 ± 7
V_o (kms ⁻¹)	= -21 ± 5
σ_1 (kms ⁻¹)	= 25 *2
σ_2 (kms ⁻¹)	= 26 *2
q (m_2/m_1)	= 0.88 ± 0.04
e	= 0 (adopted)
$a_1 \sin i$ (R_\odot)	= 8.7 ± 0.3
$a_2 \sin i$ (R_\odot)	= 9.9 ± 0.3
$a \sin i$ (R_\odot)	= 18.7 ± 0.4
$m_1 \sin^3 i$ (M_\odot)	= 14.8 ± 0.7
$m_2 \sin^3 i$ (M_\odot)	= 13.0 ± 0.7

*1 - See Section 2.2.

*2 - r.m.s. scatter of a single observation.

Table 3 : uvby observations.

1984 Sep 19/20		Differential Magnitude (v-c)			
H.J.D.	Phase	u	v	b	y
2445963.40419	0.3766	0.393	0.485	0.331	0.069
2445963.40516	0.3771	0.391	0.485	0.331	0.072
2445963.40600	0.3776	0.392	0.490	0.333	0.073
2445963.40721	0.3783	0.392	0.477	0.327	0.065
2445963.40801	0.3787	0.394	0.472	0.323	0.064
2445963.41477	0.3825	0.395	0.479	0.328	0.067
2445963.41559	0.3830	0.395	0.486	0.332	0.070
2445963.41644	0.3835	0.393	0.481	0.330	0.068
2445963.41726	0.3839	0.393	0.485	0.332	0.068
2445963.41807	0.3844	0.394	0.490	0.335	0.073
2445963.42255	0.3869	0.398	0.488	0.334	0.071
2445963.42338	0.3874	0.398	0.490	0.335	0.071
2445963.42418	0.3878	0.398	0.492	0.335	0.072
2445963.42500	0.3883	0.399	0.491	0.335	0.074
2445963.42582	0.3888	0.400	0.494	0.336	0.073
2445963.43396	0.3933	0.402	0.488	0.336	0.073
2445963.43479	0.3938	0.398	0.493	0.337	0.073
2445963.43560	0.3943	0.400	0.489	0.336	0.068
2445963.43643	0.3947	0.399	0.490	0.337	0.073
2445963.43724	0.3952	0.398	0.488	0.336	0.070
2445963.44156	0.3976	0.401	0.490	0.336	0.072
2445963.44237	0.3981	0.399	0.492	0.338	0.075
2445963.44321	0.3986	0.400	0.500	0.342	0.082
2445963.44402	0.3990	0.401	0.494	0.337	0.076
2445963.44484	0.3995	0.402	0.498	0.342	0.080
2445963.44891	0.4018	0.403	0.491	0.339	0.076
2445963.44975	0.4023	0.404	0.489	0.338	0.076
2445963.45056	0.4027	0.404	0.490	0.339	0.076
2445963.45137	0.4032	0.404	0.494	0.340	0.078
2445963.45220	0.4036	0.403	0.492	0.339	0.076
2445963.48511	0.4222	0.431	0.522	0.368	0.106
2445963.48596	0.4226	0.434	0.524	0.368	0.106
2445963.48677	0.4231	0.433	0.527	0.371	0.108
2445963.48758	0.4236	0.435	0.528	0.371	0.110
2445963.48843	0.4241	0.433	0.529	0.371	0.109
2445963.49518	0.4279	0.443	0.535	0.381	0.119
2445963.49601	0.4283	0.445	0.535	0.382	0.119
2445963.49682	0.4288	0.448	0.537	0.383	0.120
2445963.49762	0.4292	0.448	0.544	0.385	0.126
2445963.49843	0.4297	0.449	0.541	0.386	0.125
2445963.50257	0.4320	0.453	0.547	0.391	0.130
2445963.50338	0.4325	0.455	0.549	0.393	0.132
2445963.50421	0.4329	0.457	0.548	0.395	0.133
2445963.50505	0.4334	0.457	0.548	0.396	0.135
2445963.50586	0.4339	0.457	0.555	0.400	0.139
2445963.51360	0.4382	0.472	0.557	0.406	0.144

continued

2445963.51442	0.4387	0.472	0.563	0.411	0.146
2445963.51525	0.4392	0.475	0.563	0.412	0.146
2445963.51606	0.4396	0.475	0.560	0.409	0.144
2445963.51687	0.4401	0.477	0.566	0.413	0.147
2445963.52330	0.4437	0.487	0.574	0.422	0.156
2445963.52412	0.4442	0.488	0.581	0.428	0.160
2445963.52498	0.4446	0.488	0.583	0.427	0.162
2445963.52582	0.4451	0.490	0.582	0.428	0.160
2445963.52667	0.4456	0.492	0.586	0.431	0.161
2445963.53128	0.4482	0.504	0.585	0.436	0.170
2445963.53218	0.4487	0.501	0.588	0.435	0.171
2445963.53303	0.4492	0.503	0.590	0.437	0.172
2445963.53387	0.4497	0.504	0.595	0.441	0.175
2445963.53468	0.4501	0.504	0.592	0.440	0.176
2445963.55254	0.4602	0.538	0.619	0.468	0.207
2445963.55338	0.4606	0.537	0.618	0.467	0.206
2445963.55420	0.4611	0.540	0.623	0.471	0.209
2445963.55501	0.4616	0.538	0.627	0.473	0.213
2445963.55584	0.4620	0.540	0.627	0.472	0.213
2445963.56109	0.4650	0.549	0.630	0.481	0.215
2445963.56190	0.4654	0.548	0.633	0.482	0.217
2445963.56271	0.4659	0.550	0.641	0.490	0.223
2445963.56353	0.4664	0.552	0.645	0.493	0.226
2445963.56437	0.4668	0.552	0.648	0.495	0.225
2445963.56518	0.4673	0.554	0.647	0.494	0.229
2445963.56989	0.4699	0.557	0.646	0.497	0.229
2445963.57071	0.4704	0.563	0.652	0.504	0.232
2445963.57152	0.4709	0.563	0.660	0.510	0.237
2445963.57234	0.4713	0.565	0.653	0.507	0.230
2445963.57318	0.4718	0.565	0.654	0.509	0.234
2445963.57401	0.4723	0.574	0.670	0.524	0.251
2445963.58200	0.4768	0.578	0.662	0.512	0.251
2445963.58284	0.4772	0.577	0.664	0.514	0.250
2445963.58365	0.4777	0.578	0.664	0.514	0.249
2445963.58446	0.4781	0.580	0.667	0.515	0.250
2445963.58529	0.4786	0.579	0.672	0.520	0.256
2445963.58615	0.4791	0.583	0.670	0.518	0.255
2445963.59100	0.4818	0.587	0.687	0.532	0.269
2445963.59183	0.4823	0.589	0.685	0.528	0.265
2445963.59266	0.4828	0.591	0.691	0.538	0.274
2445963.59433	0.4837	0.590	0.691	0.535	0.274
2445963.60011	0.4870	0.598	0.684	0.530	0.269
2445963.60092	0.4874	0.592	0.685	0.529	0.269
2445963.60175	0.4879	0.600	0.697	0.540	0.279
2445963.60256	0.4883	0.599	0.694	0.540	0.276
2445963.60339	0.4888	0.597	0.692	0.536	0.273
2445963.60426	0.4893	0.601	0.699	0.542	0.282
2445963.61097	0.4931	0.606	0.688	0.538	0.270
2445963.61181	0.4936	0.605	0.689	0.539	0.273
2445963.61264	0.4940	0.602	0.689	0.539	0.270
2445963.61349	0.4945	0.602	0.685	0.537	0.268
2445963.61430	0.4950	0.605	0.687	0.538	0.269

continued

2445963.61879	0.4975	0.609	0.696	0.544	0.281
2445963.61962	0.4980	0.607	0.693	0.541	0.276
2445963.62048	0.4984	0.604	0.692	0.540	0.274
2445963.62129	0.4989	0.607	0.699	0.545	0.279
2445963.62211	0.4994	0.606	0.691	0.539	0.273
2445963.62294	0.4998	0.609	0.697	0.548	0.277
2445963.62853	0.5030	0.603	0.696	0.545	0.275
2445963.62935	0.5034	0.602	0.696	0.545	0.276
2445963.63019	0.5039	0.604	0.695	0.545	0.275
2445963.63104	0.5044	0.605	0.698	0.547	0.276
2445963.64401	0.5117	0.597	0.685	0.533	0.272
2445963.64491	0.5122	0.596	0.686	0.534	0.270
2445963.64579	0.5127	0.594	0.684	0.532	0.266
2445963.64666	0.5132	0.595	0.684	0.535	0.271
2445963.64754	0.5137	0.596	0.683	0.533	0.268
2445963.64837	0.5142	0.593	0.685	0.534	0.269
2445963.65372	0.5172	0.587	0.689	0.532	0.274
2445963.65459	0.5177	0.583	0.681	0.526	0.263
2445963.65543	0.5181	0.584	0.687	0.531	0.269
2445963.65711	0.5191	0.581	0.681	0.524	0.263
2445963.65795	0.5196	0.581	0.682	0.529	0.266
2445963.66330	0.5226	0.575	0.670	0.517	0.256
2445963.66413	0.5231	0.574	0.672	0.520	0.254
2445963.66499	0.5235	0.575	0.683	0.528	0.263
2445963.66585	0.5240	0.576	0.672	0.519	0.251
2445963.66671	0.5245	0.571	0.670	0.518	0.250
2445963.66754	0.5250	0.568	0.676	0.524	0.256
2445963.67331	0.5282	0.561	0.652	0.498	0.239
2445963.67418	0.5287	0.562	0.646	0.495	0.235
2445963.67503	0.5292	0.561	0.649	0.497	0.235
2445963.67585	0.5296	0.559	0.647	0.495	0.232
2445963.67667	0.5301	0.559	0.645	0.493	0.228
2445963.67749	0.5306	0.552	0.638	0.489	0.222
2445963.68261	0.5335	0.550	0.646	0.489	0.229
2445963.68353	0.5340	0.545	0.642	0.487	0.225
2445963.68440	0.5345	0.546	0.646	0.491	0.228
2445963.68527	0.5350	0.544	0.641	0.485	0.223
2445963.68614	0.5354	0.542	0.641	0.489	0.223
2445963.68697	0.5359	0.542	0.645	0.492	0.226
2445963.69182	0.5387	0.537	0.628	0.475	0.210
2445963.69263	0.5391	0.534	0.629	0.475	0.214
2445963.69344	0.5396	0.533	0.622	0.473	0.206
2445963.69427	0.5400	0.531	0.624	0.472	0.206
2445963.69511	0.5405	0.531	0.630	0.476	0.208
2445963.69592	0.5410	0.530	0.621	0.470	0.202
2445963.70088	0.5437	0.526	0.619	0.464	0.200
2445963.70171	0.5442	0.521	0.614	0.464	0.196
2445963.70254	0.5447	0.521	0.617	0.462	0.196
2445963.70336	0.5451	0.521	0.617	0.464	0.196
2445963.70417	0.5456	0.526	0.618	0.465	0.191
2445963.70844	0.5480	0.520	0.613	0.461	0.192
2445963.70931	0.5485	0.515	0.612	0.459	0.187

continued

2445963.71016	0.5490	0.515	0.609	0.458	0.186
2445963.71099	0.5494	0.508	0.605	0.455	0.181
2445963.71180	0.5499	0.505	0.605	0.453	0.179

1984 Sep 20/21

Differential Magnitude (v-c)

H.J.D.	Phase	u	v	b	y
2445964.37346	0.9227	0.433	0.519	0.372	0.106
2445964.37475	0.9234	0.437	0.522	0.373	0.107
2445964.37559	0.9239	0.433	0.522	0.372	0.109
2445964.37640	0.9244	0.440	0.523	0.377	0.112
2445964.37723	0.9249	0.435	0.525	0.372	0.111
2445964.37806	0.9253	0.434	0.527	0.373	0.113
2445964.38277	0.9280	0.439	0.532	0.379	0.119
2445964.38397	0.9286	0.441	0.536	0.380	0.121
2445964.38480	0.9291	0.445	0.537	0.383	0.122
2445964.38563	0.9296	0.444	0.539	0.384	0.123
2445964.38645	0.9300	0.446	0.543	0.385	0.127
2445964.38727	0.9305	0.446	0.542	0.383	0.126
2445964.39225	0.9333	0.460	0.545	0.394	0.134
2445964.39308	0.9338	0.464	0.547	0.396	0.135
2445964.39390	0.9342	0.463	0.548	0.396	0.135
2445964.39974	0.9375	0.465	0.559	0.404	0.143
2445964.40058	0.9380	0.466	0.564	0.405	0.143
2445964.40142	0.9385	0.466	0.563	0.406	0.144
2445964.41316	0.9451	0.494	0.588	0.430	0.169
2445964.41401	0.9456	0.494	0.591	0.431	0.171
2445964.41485	0.9460	0.495	0.595	0.436	0.175
2445964.41568	0.9465	0.497	0.595	0.435	0.173
2445964.41650	0.9470	0.498	0.595	0.437	0.178
2445964.41733	0.9474	0.503	0.599	0.441	0.178
2445964.42202	0.9501	0.512	0.601	0.444	0.185
2445964.42283	0.9505	0.512	0.609	0.451	0.193
2445964.42364	0.9510	0.513	0.606	0.448	0.187
2445964.42446	0.9515	0.515	0.612	0.453	0.194
2445964.42529	0.9519	0.515	0.615	0.455	0.195
2445964.42612	0.9524	0.516	0.615	0.456	0.196
2445964.43072	0.9550	0.524	0.618	0.463	0.201
2445964.43153	0.9554	0.525	0.618	0.463	0.201
2445964.43238	0.9559	0.529	0.621	0.465	0.202
2445964.43318	0.9564	0.530	0.622	0.466	0.204
2445964.43400	0.9568	0.530	0.629	0.472	0.210
2445964.43481	0.9573	0.531	0.624	0.469	0.206
2445964.44074	0.9606	0.544	0.631	0.479	0.217
2445964.44157	0.9611	0.544	0.633	0.479	0.218
2445964.44239	0.9616	0.547	0.640	0.484	0.224
2445964.45240	0.9672	0.561	0.655	0.501	0.239
2445964.45323	0.9677	0.565	0.657	0.503	0.240
2445964.45408	0.9681	0.566	0.660	0.506	0.242
2445964.45489	0.9686	0.568	0.661	0.506	0.243
2445964.46212	0.9727	0.580	0.663	0.512	0.247

continued

2445964.46294	0.9731	0.581	0.665	0.513	0.249
2445964.46375	0.9736	0.582	0.672	0.517	0.252
2445964.46458	0.9741	0.583	0.669	0.516	0.251
2445964.46539	0.9745	0.583	0.674	0.520	0.254
2445964.46623	0.9750	0.587	0.678	0.523	0.259
2445964.47129	0.9778	0.595	0.678	0.525	0.262
2445964.47212	0.9783	0.592	0.683	0.527	0.265
2445964.47297	0.9788	0.596	0.683	0.527	0.264
2445964.47378	0.9792	0.596	0.687	0.529	0.268
2445964.47463	0.9797	0.598	0.691	0.533	0.272
2445964.47547	0.9802	0.599	0.688	0.533	0.270
2445964.47708	0.9811	0.599	0.694	0.536	0.274
2445964.48139	0.9835	0.607	0.692	0.538	0.277
2445964.48224	0.9840	0.605	0.694	0.537	0.278
2445964.48305	0.9845	0.607	0.700	0.542	0.279
2445964.48388	0.9849	0.607	0.700	0.541	0.281
2445964.48471	0.9854	0.607	0.704	0.543	0.286
2445964.48556	0.9859	0.611	0.708	0.548	0.286
2445964.49314	0.9902	0.614	0.699	0.545	0.282
2445964.49396	0.9906	0.615	0.703	0.547	0.283
2445964.49480	0.9911	0.614	0.701	0.546	0.283
2445964.49563	0.9916	0.615	0.706	0.550	0.286
2445964.49645	0.9920	0.615	0.705	0.551	0.285
2445964.49726	0.9925	0.615	0.708	0.551	0.288
2445964.50279	0.9956	0.618	0.707	0.553	0.290
2445964.50362	0.9961	0.621	0.708	0.552	0.290
2445964.50444	0.9965	0.620	0.709	0.553	0.292
2445964.50610	0.9975	0.619	0.710	0.554	0.290
2445964.50693	0.9979	0.617	0.709	0.554	0.291
2445964.51287	0.0013	0.621	0.709	0.552	0.294
2445964.51370	0.0017	0.619	0.709	0.554	0.293
2445964.51451	0.0022	0.619	0.709	0.552	0.290
2445964.51533	0.0027	0.620	0.710	0.553	0.291
2445964.51615	0.0031	0.621	0.709	0.555	0.290
2445964.51696	0.0036	0.619	0.705	0.552	0.286
2445964.52371	0.0074	0.616	0.704	0.548	0.288
2445964.52453	0.0078	0.615	0.706	0.550	0.288
2445964.52537	0.0083	0.616	0.703	0.547	0.285
2445964.52624	0.0088	0.614	0.702	0.549	0.285
2445964.53447	0.0134	0.606	0.694	0.541	0.277
2445964.53533	0.0139	0.603	0.693	0.538	0.276
2445964.53615	0.0144	0.603	0.692	0.537	0.274
2445964.53696	0.0148	0.607	0.697	0.543	0.279

1984 Sep 21/22

Differential Magnitude (v-c)

H. J. D.	Phase	u	v	b	y
2445965.41932	0.5120	0.589	0.679	0.527	0.265
2445965.42014	0.5125	0.589	0.681	0.526	0.266
2445965.42098	0.5130	0.587	0.679	0.524	0.262
2445965.42180	0.5134	0.588	0.681	0.527	0.265

continued

2445965.42262	0.5139	0.588	0.686	0.528	0.267
2445965.42347	0.5144	0.585	0.679	0.524	0.262
2445965.42722	0.5165	0.585	0.676	0.520	0.260
2445965.42807	0.5170	0.582	0.677	0.521	0.261
2445965.43141	0.5188	0.583	0.668	0.521	0.253
2445965.43225	0.5193	0.584	0.668	0.519	0.250
2445965.43307	0.5198	0.580	0.668	0.517	0.252
2445965.43388	0.5202	0.579	0.666	0.516	0.247
2445965.43470	0.5207	0.577	0.666	0.514	0.248
2445965.43554	0.5212	0.577	0.665	0.515	0.246
2445965.44006	0.5237	0.569	0.657	0.506	0.240
2445965.44087	0.5242	0.570	0.659	0.509	0.240
2445965.44170	0.5246	0.568	0.662	0.508	0.244
2445965.44264	0.5252	0.566	0.658	0.507	0.238
2445965.44347	0.5256	0.569	0.662	0.510	0.245
2445965.44430	0.5261	0.572	0.667	0.513	0.246
2445965.44950	0.5290	0.563	0.647	0.498	0.234
2445965.45035	0.5295	0.556	0.648	0.495	0.233
2445965.45117	0.5300	0.558	0.645	0.493	0.229
2445965.45202	0.5304	0.555	0.647	0.493	0.232
2445965.45285	0.5309	0.553	0.647	0.492	0.232
2445965.45369	0.5314	0.553	0.643	0.489	0.226
2445965.45944	0.5346	0.549	0.634	0.483	0.221
2445965.46026	0.5351	0.545	0.631	0.481	0.216
2445965.46655	0.5386	0.534	0.623	0.471	0.210
2445965.46738	0.5391	0.533	0.623	0.470	0.209
2445965.46847	0.5397	0.531	0.623	0.469	0.210
2445965.46929	0.5402	0.533	0.622	0.467	0.207
2445965.47665	0.5443	0.517	0.607	0.455	0.192
2445965.47749	0.5448	0.515	0.604	0.453	0.189
2445965.47830	0.5452	0.512	0.601	0.450	0.186
2445965.47915	0.5457	0.513	0.601	0.449	0.185
2445965.47997	0.5462	0.509	0.600	0.449	0.185
2445965.48080	0.5467	0.507	0.595	0.447	0.182
2445965.48668	0.5500	0.499	0.589	0.438	0.176
2445965.48752	0.5504	0.497	0.590	0.436	0.174
2445965.48836	0.5509	0.497	0.592	0.440	0.178
2445965.48921	0.5514	0.494	0.587	0.435	0.170
2445965.49003	0.5519	0.498	0.596	0.438	0.178
2445965.49084	0.5523	0.493	0.593	0.435	0.176
2445965.49612	0.5553	0.485	0.574	0.423	0.161
2445965.49697	0.5558	0.483	0.573	0.422	0.157
2445965.50383	0.5596	0.472	0.566	0.413	0.151
2445965.50464	0.5601	0.486	0.584	0.429	0.167
2445965.50546	0.5606	0.475	0.573	0.418	0.155
2445965.50629	0.5610	0.483	0.585	0.427	0.165
2445965.50711	0.5615	0.488	0.588	0.431	0.171
2445965.50887	0.5625	0.467	0.563	0.410	0.148
2445965.50973	0.5630	0.466	0.562	0.409	0.144
2445965.51054	0.5634	0.470	0.569	0.416	0.153
2445965.51690	0.5670	0.452	0.540	0.391	0.124
2445965.51771	0.5675	0.451	0.541	0.388	0.126

continued

2445965.51855	0.5679	0.450	0.544	0.389	0.126
2445965.51938	0.5684	0.447	0.539	0.386	0.124
2445965.52019	0.5688	0.446	0.536	0.385	0.120
2445965.52100	0.5693	0.444	0.534	0.384	0.120
2445965.52746	0.5730	0.433	0.525	0.377	0.110
2445965.52829	0.5734	0.432	0.523	0.373	0.108
2445965.52911	0.5739	0.432	0.524	0.375	0.106
2445965.52994	0.5743	0.432	0.526	0.378	0.109
2445965.53076	0.5748	0.432	0.519	0.375	0.102
2445965.53158	0.5753	0.431	0.523	0.379	0.107
2445965.53659	0.5781	0.418	0.513	0.363	0.100
2445965.53742	0.5786	0.420	0.512	0.362	0.100
2445965.53823	0.5790	0.426	0.524	0.372	0.109
2445965.53905	0.5795	0.418	0.515	0.363	0.101
2445965.53987	0.5799	0.421	0.520	0.368	0.108
2445965.54068	0.5804	0.427	0.529	0.373	0.116
2445965.54705	0.5840	0.410	0.499	0.349	0.088
2445965.54788	0.5845	0.411	0.501	0.350	0.086
2445965.54870	0.5849	0.411	0.500	0.350	0.086
2445965.54951	0.5854	0.409	0.497	0.348	0.085
2445965.55738	0.5898	0.396	0.495	0.341	0.084
2445965.55935	0.5909	0.405	0.490	0.343	0.079
2445965.56277	0.5929	0.394	0.489	0.336	0.081
2445965.56362	0.5933	0.395	0.486	0.334	0.076
2445965.57006	0.5969	0.390	0.483	0.333	0.074
2445965.57091	0.5974	0.389	0.490	0.338	0.082
2445965.57174	0.5979	0.388	0.485	0.333	0.073
2445965.57256	0.5984	0.392	0.491	0.340	0.081
2445965.57467	0.5995	0.393	0.480	0.332	0.070
2445965.57550	0.6000	0.396	0.484	0.334	0.074
2445965.58090	0.6031	0.386	0.482	0.329	0.072
2445965.58174	0.6035	0.386	0.485	0.332	0.073
2445965.58256	0.6040	0.387	0.485	0.332	0.072
2445965.58379	0.6047	0.385	0.478	0.328	0.067
2445965.58460	0.6051	0.387	0.480	0.329	0.069
2445965.58542	0.6056	0.385	0.478	0.329	0.066
2445965.59385	0.6104	0.386	0.478	0.329	0.068
2445965.59467	0.6108	0.385	0.480	0.327	0.067
2445965.59550	0.6113	0.381	0.478	0.325	0.067
2445965.59631	0.6117	0.383	0.478	0.327	0.066
2445965.59715	0.6122	0.385	0.480	0.328	0.067
2445965.59797	0.6127	0.382	0.477	0.325	0.064
2445965.60791	0.6183	0.385	0.476	0.329	0.067
2445965.60876	0.6188	0.383	0.475	0.326	0.063
2445965.60958	0.6192	0.380	0.476	0.326	0.062
2445965.61039	0.6197	0.385	0.476	0.326	0.062
2445965.61122	0.6201	0.379	0.475	0.325	0.061
2445965.61208	0.6206	0.378	0.474	0.325	0.058
2445965.61891	0.6245	0.383	0.475	0.324	0.065
2445965.61974	0.6250	0.378	0.475	0.324	0.062
2445965.62056	0.6254	0.375	0.473	0.323	0.059
2445965.62335	0.6270	0.376	0.473	0.322	0.060

continued

2445965.62430	0.6275	0.377	0.471	0.322	0.058
2445965.62511	0.6280	0.374	0.472	0.321	0.059
2445965.62593	0.6284	0.374	0.473	0.322	0.060
2445965.63336	0.6326	0.373	0.472	0.321	0.062
2445965.63421	0.6331	0.372	0.472	0.319	0.062
2445965.63565	0.6339	0.374	0.470	0.318	0.059
2445965.63692	0.6346	0.377	0.467	0.318	0.057
2445965.63775	0.6351	0.374	0.470	0.319	0.058
2445965.65285	0.6436	0.370	0.464	0.314	0.056
2445965.65369	0.6441	0.372	0.465	0.316	0.055
2445965.65451	0.6445	0.368	0.462	0.312	0.051
2445965.65675	0.6458	0.367	0.460	0.311	0.053
2445965.65760	0.6463	0.370	0.464	0.315	0.054
2445965.65841	0.6467	0.368	0.465	0.314	0.052
2445965.66563	0.6508	0.367	0.461	0.308	0.052
2445965.66645	0.6513	0.363	0.464	0.311	0.054
2445965.66727	0.6517	0.365	0.460	0.309	0.049
2445965.66839	0.6524	0.370	0.462	0.313	0.050
2445965.66922	0.6528	0.362	0.460	0.309	0.047

1984 Sep 22/23

Differential Magnitude (v-c)

H.J.D.	Phase	u	v	b	y
2445966.34619	0.0343	0.573	0.653	0.499	0.239
2445966.34704	0.0347	0.573	0.659	0.502	0.240
2445966.34788	0.0352	0.573	0.652	0.499	0.238
2445966.34872	0.0357	0.570	0.656	0.499	0.238
2445966.34953	0.0361	0.568	0.658	0.499	0.237
2445966.35037	0.0366	0.566	0.651	0.494	0.233
2445966.35454	0.0390	0.558	0.641	0.487	0.222
2445966.35537	0.0394	0.555	0.643	0.488	0.224
2445966.35620	0.0399	0.555	0.638	0.486	0.220
2445966.35706	0.0404	0.553	0.640	0.485	0.221
2445966.35787	0.0409	0.551	0.641	0.485	0.222
2445966.35869	0.0413	0.549	0.638	0.482	0.219
2445966.36267	0.0436	0.540	0.625	0.471	0.209
2445966.36349	0.0440	0.541	0.630	0.474	0.211
2445966.36432	0.0445	0.537	0.622	0.467	0.205
2445966.36516	0.0450	0.536	0.622	0.466	0.205
2445966.36598	0.0454	0.536	0.625	0.468	0.207
2445966.36680	0.0459	0.534	0.621	0.465	0.202
2445966.37325	0.0495	0.518	0.601	0.447	0.187
2445966.37408	0.0500	0.519	0.603	0.448	0.187
2445966.37489	0.0504	0.517	0.602	0.447	0.187
2445966.37574	0.0509	0.519	0.603	0.447	0.185
2445966.37656	0.0514	0.513	0.599	0.444	0.183
2445966.37738	0.0518	0.511	0.607	0.446	0.188
2445966.38228	0.0546	0.503	0.590	0.435	0.174
2445966.38311	0.0551	0.502	0.597	0.439	0.176
2445966.38392	0.0555	0.502	0.591	0.433	0.172
2445966.38476	0.0560	0.499	0.594	0.435	0.173

continued

2445966.38559	0.0565	0.499	0.596	0.435	0.176
2445966.38640	0.0569	0.495	0.587	0.429	0.169
2445966.39144	0.0598	0.488	0.575	0.421	0.160
2445966.39228	0.0602	0.485	0.570	0.417	0.154
2445966.39309	0.0607	0.482	0.573	0.417	0.157
2445966.39393	0.0612	0.481	0.577	0.418	0.157
2445966.39474	0.0616	0.480	0.571	0.414	0.151
2445966.39555	0.0621	0.479	0.575	0.416	0.156
2445966.40603	0.0680	0.463	0.549	0.397	0.135
2445966.40688	0.0685	0.460	0.549	0.395	0.132
2445966.41299	0.0719	0.450	0.544	0.387	0.126
2445966.41384	0.0724	0.449	0.539	0.385	0.124
2445966.41466	0.0728	0.447	0.542	0.387	0.123
2445966.41547	0.0733	0.444	0.543	0.385	0.121
2445966.41629	0.0738	0.443	0.540	0.381	0.119
2445966.41723	0.0743	0.442	0.540	0.382	0.121
2445966.42234	0.0772	0.435	0.525	0.371	0.108
2445966.42320	0.0777	0.431	0.529	0.372	0.112
2445966.42402	0.0781	0.433	0.537	0.377	0.116
2445966.42486	0.0786	0.430	0.531	0.372	0.110
2445966.42569	0.0791	0.431	0.532	0.375	0.113
2445966.42650	0.0795	0.431	0.534	0.375	0.111
2445966.43166	0.0824	0.423	0.516	0.363	0.099
2445966.43248	0.0829	0.424	0.526	0.369	0.106
2445966.43332	0.0834	0.418	0.517	0.361	0.099
2445966.43414	0.0838	0.418	0.524	0.363	0.101
2445966.43601	0.0849	0.419	0.505	0.355	0.092
2445966.43686	0.0854	0.416	0.509	0.356	0.091
2445966.44334	0.0890	0.412	0.506	0.352	0.090
2445966.44415	0.0895	0.410	0.503	0.348	0.086
2445966.44498	0.0899	0.409	0.503	0.349	0.088
2445966.44579	0.0904	0.408	0.503	0.348	0.084
2445966.44673	0.0909	0.407	0.500	0.346	0.083
2445966.44755	0.0914	0.405	0.499	0.346	0.082
2445966.45429	0.0952	0.399	0.499	0.343	0.083
2445966.45515	0.0957	0.401	0.498	0.341	0.081
2445966.45599	0.0961	0.399	0.502	0.343	0.081
2445966.45736	0.0969	0.401	0.496	0.340	0.079
2445966.45820	0.0974	0.400	0.491	0.338	0.075
2445966.45903	0.0978	0.399	0.493	0.340	0.075
2445966.46442	0.1009	0.395	0.491	0.337	0.073
2445966.46523	0.1013	0.396	0.491	0.337	0.075
2445966.46606	0.1018	0.399	0.495	0.340	0.077
2445966.46747	0.1026	0.398	0.486	0.336	0.071
2445966.46829	0.1031	0.397	0.489	0.338	0.072
2445966.46912	0.1035	0.396	0.485	0.335	0.068
2445966.48000	0.1097	0.397	0.483	0.332	0.073
2445966.48084	0.1101	0.392	0.483	0.330	0.070
2445966.48827	0.1143	0.393	0.481	0.330	0.070
2445966.48912	0.1148	0.393	0.485	0.332	0.071
2445966.48994	0.1153	0.392	0.488	0.332	0.073
2445966.49105	0.1159	0.390	0.481	0.328	0.066

continued

2445966.49187	0.1164	0.391	0.483	0.329	0.068
2445966.49268	0.1168	0.390	0.484	0.330	0.070
2445966.49833	0.1200	0.388	0.485	0.330	0.072
2445966.49916	0.1205	0.387	0.480	0.327	0.068
2445966.50000	0.1209	0.389	0.484	0.328	0.070
2445966.50104	0.1215	0.388	0.484	0.329	0.072
2445966.50187	0.1220	0.387	0.481	0.327	0.069
2445966.50270	0.1224	0.388	0.481	0.326	0.066
2445966.50827	0.1256	0.385	0.481	0.328	0.069
2445966.50912	0.1261	0.386	0.485	0.330	0.073
2445966.50998	0.1266	0.385	0.486	0.331	0.073
2445966.51107	0.1272	0.386	0.477	0.324	0.063
2445966.51863	0.1314	0.386	0.472	0.321	0.060
2445966.51946	0.1319	0.383	0.473	0.321	0.061
2445966.52028	0.1324	0.382	0.473	0.321	0.061
2445966.52315	0.1340	0.381	0.475	0.319	0.064
2445966.52401	0.1345	0.382	0.472	0.319	0.061
2445966.52486	0.1349	0.382	0.471	0.317	0.061
2445966.53378	0.1400	0.381	0.472	0.319	0.062
2445966.53462	0.1404	0.378	0.473	0.317	0.060
2445966.53547	0.1409	0.381	0.468	0.316	0.060
2445966.53628	0.1414	0.378	0.471	0.317	0.059
2445966.53710	0.1418	0.378	0.476	0.320	0.064
2445966.53799	0.1423	0.377	0.469	0.315	0.060
2445966.54541	0.1465	0.374	0.472	0.317	0.059
2445966.54627	0.1470	0.375	0.469	0.316	0.054
2445966.55304	0.1508	0.370	0.466	0.314	0.050
2445966.55386	0.1513	0.372	0.469	0.317	0.052
2445966.55469	0.1517	0.372	0.467	0.316	0.051
2445966.55553	0.1522	0.371	0.470	0.317	0.051
2445966.58064	0.1664	0.365	0.459	0.308	0.048
2445966.58149	0.1668	0.364	0.462	0.309	0.048
2445966.58231	0.1673	0.361	0.456	0.307	0.044
2445966.58315	0.1678	0.363	0.458	0.309	0.047
2445966.59224	0.1729	0.362	0.459	0.305	0.048
2445966.59310	0.1734	0.363	0.454	0.302	0.041
2445966.59394	0.1739	0.363	0.459	0.305	0.047
2445966.59476	0.1743	0.363	0.460	0.306	0.046
2445966.59559	0.1748	0.362	0.458	0.306	0.043
2445966.59640	0.1752	0.361	0.458	0.304	0.043
2445966.60284	0.1789	0.357	0.450	0.299	0.039
2445966.60369	0.1794	0.357	0.455	0.304	0.040
2445966.60450	0.1798	0.356	0.450	0.300	0.036
2445966.60534	0.1803	0.355	0.449	0.299	0.037
2445966.60615	0.1807	0.354	0.456	0.303	0.041
2445966.60697	0.1812	0.354	0.449	0.300	0.036
2445966.61141	0.1837	0.355	0.456	0.303	0.045
2445966.61224	0.1842	0.354	0.455	0.341	0.040
2445966.61306	0.1846	0.352	0.453	0.301	0.042
2445966.61388	0.1851	0.353	0.451	0.299	0.040
2445966.61471	0.1856	0.351	0.455	0.302	0.042
2445966.61553	0.1860	0.355	0.451	0.301	0.038

continued

2445966.62251	0.1900	0.350	0.445	0.294	0.033
2445966.62337	0.1905	0.349	0.443	0.295	0.033
2445966.62419	0.1909	0.350	0.444	0.294	0.034
2445966.62503	0.1914	0.352	0.445	0.295	0.033
2445966.62584	0.1918	0.350	0.447	0.297	0.032
2445966.62666	0.1923	0.351	0.445	0.295	0.035
2445966.63299	0.1959	0.349	0.444	0.292	0.036
2445966.63384	0.1964	0.347	0.450	0.297	0.037
2445966.63469	0.1968	0.351	0.443	0.295	0.036
2445966.63556	0.1973	0.349	0.443	0.294	0.033
2445966.63638	0.1978	0.352	0.446	0.297	0.035
2445966.63721	0.1982	0.349	0.442	0.293	0.031
2445966.64297	0.2015	0.350	0.445	0.295	0.035
2445966.64379	0.2020	0.346	0.444	0.293	0.031
2445966.64461	0.2024	0.348	0.444	0.294	0.034
2445966.64545	0.2029	0.345	0.445	0.295	0.035
2445966.64626	0.2033	0.352	0.450	0.299	0.037
2445966.64707	0.2038	0.348	0.446	0.298	0.036
2445966.65950	0.2108	0.345	0.442	0.290	0.030
2445966.66032	0.2113	0.345	0.443	0.291	0.032
2445966.66828	0.2158	0.343	0.438	0.286	0.027
2445966.66913	0.2162	0.341	0.440	0.289	0.026
2445966.67052	0.2170	0.344	0.438	0.288	0.023
2445966.67133	0.2175	0.342	0.436	0.288	0.024
2445966.67215	0.2179	0.342	0.439	0.290	0.024
2445966.67300	0.2184	0.344	0.435	0.290	0.022
2445966.67700	0.2207	0.339	0.436	0.286	0.026
2445966.67782	0.2211	0.341	0.442	0.290	0.029
2445966.67865	0.2216	0.337	0.435	0.285	0.024
2445966.67949	0.2221	0.341	0.439	0.291	0.027
2445966.68031	0.2225	0.339	0.443	0.292	0.029
2445966.68113	0.2230	0.341	0.437	0.288	0.025

1984 Sep 24/25

Differential Magnitude (v-c)

H. J. D.	Phase	u	v	b	y
2445968.41810	0.2017	0.357	0.449	0.298	0.039
2445968.41891	0.2022	0.351	0.445	0.293	0.036
2445968.42023	0.2029	0.354	0.442	0.291	0.034
2445968.42104	0.2034	0.350	0.443	0.289	0.032
2445968.42185	0.2038	0.349	0.440	0.289	0.030
2445968.42819	0.2074	0.343	0.436	0.284	0.024
2445968.42900	0.2078	0.343	0.436	0.284	0.024
2445968.42983	0.2083	0.344	0.441	0.287	0.025
2445968.43178	0.2094	0.356	0.444	0.295	0.033
2445968.43262	0.2099	0.355	0.445	0.296	0.034
2445968.43346	0.2103	0.356	0.448	0.298	0.035
2445968.44751	0.2183	0.346	0.439	0.288	0.027
2445968.44841	0.2188	0.343	0.439	0.287	0.024
2445968.47348	0.2329	0.348	0.436	0.288	0.027
2445968.47488	0.2337	0.345	0.436	0.286	0.022

continued

2445968.47569	0.2342	0.345	0.436	0.285	0.024
2445968.47652	0.2346	0.345	0.437	0.287	0.025
2445968.48552	0.2397	0.348	0.436	0.286	0.025
2445968.48637	0.2402	0.342	0.435	0.284	0.022
2445968.48719	0.2406	0.348	0.438	0.289	0.026
2445968.48812	0.2411	0.343	0.433	0.286	0.024
2445968.49667	0.2460	0.345	0.435	0.283	0.026
2445968.49752	0.2464	0.349	0.443	0.289	0.031
2445968.49834	0.2469	0.352	0.445	0.291	0.031
2445968.49916	0.2474	0.344	0.438	0.285	0.026
2445968.49997	0.2478	0.343	0.440	0.286	0.028
2445968.50079	0.2483	0.340	0.434	0.281	0.023
2445968.50697	0.2518	0.340	0.433	0.281	0.023
2445968.50783	0.2523	0.339	0.435	0.280	0.022
2445968.50868	0.2527	0.340	0.439	0.284	0.027
2445968.50949	0.2532	0.338	0.435	0.282	0.024
2445968.51033	0.2537	0.340	0.437	0.284	0.026
2445968.51116	0.2541	0.337	0.438	0.282	0.026
2445968.52612	0.2626	0.339	0.434	0.278	0.025
2445968.52695	0.2630	0.346	0.440	0.287	0.031
2445968.52781	0.2635	0.339	0.437	0.282	0.027
2445968.52865	0.2640	0.339	0.434	0.279	0.022
2445968.54054	0.2707	0.341	0.440	0.284	0.028
2445968.54229	0.2717	0.345	0.445	0.291	0.032
2445968.54310	0.2721	0.344	0.445	0.291	0.032
2445968.54392	0.2726	0.340	0.441	0.287	0.028
2445968.54593	0.2737	0.349	0.442	0.290	0.033
2445968.55511	0.2789	0.346	0.440	0.288	0.032
2445968.55594	0.2794	0.346	0.441	0.288	0.029
2445968.55677	0.2798	0.349	0.443	0.291	0.033
2445968.55758	0.2803	0.346	0.443	0.290	0.032
2445968.55840	0.2807	0.347	0.444	0.292	0.033
2445968.56017	0.2818	0.350	0.442	0.292	0.031
2445968.56101	0.2822	0.348	0.440	0.290	0.030
2445968.56186	0.2827	0.353	0.440	0.293	0.031

1984 Sep 25/26

Differential Magnitude (v-c)

H. J. D.	Phase	u	v	b	y
2445969.35285	0.7284	0.350	0.442	0.290	0.030
2445969.35377	0.7289	0.350	0.444	0.290	0.030
2445969.35460	0.7294	0.350	0.448	0.293	0.032
2445969.35543	0.7298	0.351	0.448	0.292	0.032
2445969.36252	0.7338	0.347	0.442	0.290	0.028
2445969.36333	0.7343	0.346	0.440	0.288	0.025
2445969.37149	0.7389	0.350	0.438	0.288	0.027
2445969.37230	0.7393	0.348	0.442	0.287	0.027
2445969.37317	0.7398	0.345	0.439	0.286	0.028
2445969.37407	0.7403	0.347	0.444	0.289	0.028
2445969.38163	0.7446	0.347	0.442	0.287	0.028
2445969.38249	0.7451	0.347	0.443	0.288	0.029

continued

2445969.38332	0.7456	0.345	0.446	0.291	0.029
2445969.38413	0.7460	0.348	0.448	0.293	0.031
2445969.39137	0.7501	0.346	0.439	0.287	0.027
2445969.39220	0.7506	0.345	0.442	0.288	0.029
2445969.39304	0.7510	0.346	0.448	0.292	0.032
2445969.39391	0.7515	0.345	0.444	0.290	0.030
2445969.39997	0.7549	0.346	0.444	0.288	0.029
2445969.40079	0.7554	0.347	0.446	0.291	0.030
2445969.40163	0.7559	0.346	0.451	0.294	0.035
2445969.40247	0.7563	0.345	0.449	0.292	0.031
2445969.40955	0.7603	0.345	0.442	0.287	0.028
2445969.41048	0.7609	0.343	0.440	0.288	0.028
2445969.41561	0.7637	0.344	0.439	0.289	0.027
2445969.41646	0.7642	0.343	0.437	0.287	0.026
2445969.42455	0.7688	0.343	0.436	0.287	0.026
2445969.42541	0.7693	0.344	0.440	0.289	0.027
2445969.42624	0.7697	0.346	0.445	0.290	0.030
2445969.42709	0.7702	0.347	0.441	0.289	0.028
2445969.43411	0.7742	0.348	0.439	0.288	0.029
2445969.43495	0.7747	0.346	0.444	0.291	0.032
2445969.43577	0.7751	0.347	0.441	0.292	0.032
2445969.43661	0.7756	0.346	0.444	0.291	0.031
2445969.44251	0.7789	0.349	0.441	0.291	0.034
2445969.44333	0.7794	0.345	0.446	0.294	0.035
2445969.45275	0.7847	0.349	0.443	0.290	0.032
2445969.45361	0.7852	0.350	0.442	0.292	0.031
2445969.45445	0.7856	0.349	0.443	0.291	0.031
2445969.45528	0.7861	0.348	0.449	0.294	0.034
2445969.46249	0.7902	0.349	0.444	0.292	0.035
2445969.46335	0.7907	0.346	0.440	0.290	0.030
2445969.46417	0.7911	0.348	0.446	0.294	0.031
2445969.46501	0.7916	0.349	0.450	0.297	0.035
2445969.47122	0.7951	0.349	0.438	0.291	0.027
2445969.47204	0.7955	0.349	0.442	0.292	0.028
2445969.47285	0.7960	0.348	0.443	0.293	0.027
2445969.47371	0.7965	0.352	0.446	0.296	0.031
2445969.48104	0.8006	0.353	0.442	0.293	0.029
2445969.48188	0.8011	0.352	0.446	0.294	0.033
2445969.48819	0.8047	0.354	0.440	0.293	0.029
2445969.48903	0.8051	0.354	0.444	0.295	0.032
2445969.49642	0.8093	0.355	0.444	0.296	0.035
2445969.49730	0.8098	0.355	0.450	0.299	0.036
2445969.49815	0.8103	0.355	0.451	0.300	0.035
2445969.49902	0.8107	0.357	0.452	0.301	0.038
2445969.50599	0.8147	0.355	0.449	0.297	0.037
2445969.50683	0.8151	0.356	0.453	0.299	0.037
2445969.50798	0.8158	0.359	0.448	0.297	0.036
2445969.50881	0.8163	0.358	0.450	0.297	0.038
2445969.51883	0.8219	0.360	0.445	0.297	0.038
2445969.51966	0.8224	0.362	0.454	0.303	0.043
2445969.52049	0.8228	0.361	0.457	0.302	0.042
2445969.52133	0.8233	0.360	0.455	0.301	0.042

continued

2445969.53163	0.8291	0.366	0.454	0.303	0.048
2445969.53247	0.8296	0.365	0.450	0.301	0.041
2445969.53329	0.8301	0.364	0.450	0.301	0.040
2445969.53411	0.8305	0.367	0.452	0.303	0.042
2445969.54306	0.8356	0.366	0.461	0.309	0.049
2445969.54389	0.8360	0.367	0.452	0.307	0.041
2445969.54473	0.8365	0.368	0.453	0.307	0.038
2445969.54556	0.8370	0.366	0.454	0.308	0.042
2445969.55457	0.8421	0.371	0.455	0.307	0.047
2445969.55545	0.8425	0.371	0.456	0.309	0.047
2445969.55628	0.8430	0.371	0.456	0.309	0.046
2445969.55715	0.8435	0.369	0.459	0.310	0.048
2445969.56477	0.8478	0.373	0.463	0.310	0.052
2445969.56563	0.8483	0.371	0.461	0.311	0.048
2445969.57262	0.8522	0.375	0.462	0.311	0.053
2445969.57349	0.8527	0.373	0.464	0.313	0.053
2445969.57432	0.8532	0.374	0.462	0.312	0.049
2445969.57520	0.8537	0.376	0.462	0.313	0.049
2445969.58365	0.8584	0.378	0.466	0.315	0.054
2445969.58448	0.8589	0.374	0.467	0.318	0.052
2445969.58532	0.8594	0.374	0.463	0.318	0.046
2445969.58616	0.8599	0.375	0.464	0.319	0.048
2445969.59289	0.8636	0.379	0.469	0.318	0.059
2445969.59376	0.8641	0.376	0.467	0.316	0.053
2445969.59458	0.8646	0.381	0.470	0.319	0.060
2445969.59543	0.8651	0.379	0.472	0.319	0.060
2445969.60423	0.8700	0.382	0.468	0.321	0.061
2445969.60508	0.8705	0.383	0.469	0.321	0.061
2445969.60591	0.8710	0.383	0.469	0.322	0.058
2445969.60676	0.8715	0.381	0.469	0.322	0.058
2445969.61710	0.8773	0.384	0.477	0.326	0.067
2445969.61796	0.8778	0.385	0.478	0.326	0.065
2445969.61878	0.8782	0.384	0.477	0.326	0.065
2445969.61962	0.8787	0.387	0.480	0.331	0.069
2445969.62617	0.8824	0.389	0.475	0.327	0.066
2445969.62701	0.8829	0.388	0.475	0.328	0.064
2445969.62783	0.8833	0.390	0.477	0.329	0.065
2445969.62867	0.8838	0.389	0.479	0.329	0.066
2445969.63505	0.8874	0.387	0.481	0.330	0.071
2445969.63587	0.8879	0.388	0.484	0.333	0.069
2445969.63671	0.8883	0.390	0.485	0.332	0.070
2445969.63753	0.8888	0.389	0.484	0.334	0.067

Table 4 : Transformation equations.

The transformation equations are of the form :-

$$C_{std} = \text{Zero point} + C_{inst} \cdot \text{Scale factor} + \text{Colour term} \cdot (b-y)_{std}$$

where C_{inst} and C_{std} refer to the instrumental extinction corrected and standard colours respectively.

Colour	Scale factor	Colour term	Mean extinction
V	1.000	0.056 ± 0.005	0.13 ± 0.01
(b-y)	1.015 ± 0.003	0.000	0.05 ± 0.02
(v-b)	0.982 ± 0.002	0.001 ± 0.003	0.09 ± 0.01
(u-b)	1.065 ± 0.002	0.049 ± 0.005	0.30 ± 0.05

Table 5 : Data for AH Cephei and HD 215371.

	AH Cephei	HD 215371
SAO no.	20247	20214
BD no.	+64° 1717	+64° 1704
R.A. (1950)	22 ^h 46 ^m 04 ^s	22 ^h 41 ^m 19 ^s
Dec. (1950)	+64° 47' 53"	+65° 04' 26"
Sp. type	B0.5Vn+B0.5Vn	B1.5V
V	6 ^m .794 (0 ^p .25) 7 ^m .057 (0 ^p .00) 7 ^m .039 (0 ^p .50)	6 ^m .752 ± 0 ^m .006
(b-y)	0 ^m .310 (0 ^p .25)	0 ^m .045 ± 0 ^m .006
m ₁	-0 ^m .048 (0 ^p .25)	0 ^m .066 ± 0 ^m .007
c ₁	-0 ^m .097 (0 ^p .25)	0 ^m .134 ± 0 ^m .008
(b-y) _o	-0 ^m .134 (0 ^p .25)	-0 ^m .105
m _o	0 ^m .094 (0 ^p .25)	0 ^m .114
c _o	-0 ^m .186 (0 ^p .25)	0 ^m .103
E(b-y)	0 ^m .444	0 ^m .147

Table 6 : Times of minima.

H.J.D.	Error (days)	Epoch (cycles)	O-C (days)	Source reference
-2400000				
15500.11		-17164.5	0.2621	Zverev, 1933.
24076.621		-12332.0	0.2398	Moore, 1936.
24078.326		-12331.0	0.1700	Zverev, 1933.
25388.089		-11593.0	0.1593	Huffer and Eggen, 1947.
25835.345		-11341.0	0.1755	Zverev, 1933.
25836.27		-11340.5	0.2131	Zverev, 1931.
26440.487		-11000.0	0.1239	Zverev, 1933.
26564.728		-10930.0	0.1316	Zverev, 1933.
26985.34		-10630.0	0.1252	Zverev, 1933.
34714.309		-6338.0	0.0094	Nekrasova, 1960.
34981.420	± 0.002	-6187.5	0.0188	Guarnieri et al., 1975.
34989.404	± 0.001	-6183.0	0.0164	Guarnieri et al., 1975.
40873.619	± 0.001	-2867.5	0.0108	Battistini et al., 1973.
34779.813	± 0.011	-1230.0	0.0334	Hartigan and Binzel, 1982.
43815.313	± 0.001	-1210.0	0.0382	Mayer, 1980. *
44101.532	± 0.002	-1100.0	0.0334	Mayer and Tremko, 1983.
45200.499	± 0.002	-429.5	0.0231	Mayer and Tremko, 1983.
45223.570	± 0.002	-416.5	0.0222	Mayer and Tremko, 1983.
45562.538	± 0.0006	-225.5	0.0108	Mayer and Tremko, 1983.
45579.398	± 0.003	-216.0	0.0106	Mayer and Tremko, 1983.
45963.6323	± 0.0003	0.5	0.0000	This paper.

* Re-analysed for this paper.

Table 7 : Light-curve solutions.

Adopted primary temperature 29900K

Colour	u	v	b	y
i (degrees)	69.37 ±7	69.11 ±9	69.12 ±7	69.23 ±8
T ₂ K (polar)	28450 ±150	28590 ±180	28990 ±140	28260 ±140
r ₁ (polar)	0.325 ±3	0.323 ±3	0.318 ±3	0.326 ±2
r ₁ (mean)	0.338 ±3	0.336 ±3	0.331 ±3	0.340 ±2
r ₂ (polar)	0.297 ±3	0.300 ±4	0.303 ±3	0.293 ±3
r ₂ (mean)	0.308 ±3	0.311 ±4	0.314 ±3	0.303 ±3
χ ² (mmag.) ²	22.64	35.27	20.93	22.21
L ₂ /L ₁	0.762	0.799	0.862	0.735
r.m.s. error (mmag.)	4.4	5.5	4.2	4.4

Adopted primary temperature 35000K

Colour	u	v	b	y
i (degrees)	69.31 ±7	69.05 ±9	69.06 ±6	69.15 ±8
T ₂ K (polar)	32970 ±170	33130 ±230	33740 ±140	32810 ±170
r ₁ (polar)	0.326 ±2	0.324 ±3	0.317 ±3	0.326 ±2
r ₁ (mean)	0.340 ±2	0.337 ±3	0.329 ±3	0.340 ±2
r ₂ (polar)	0.298 ±3	0.300 ±4	0.305 ±3	0.294 ±3
r ₂ (mean)	0.309 ±3	0.312 ±4	0.318 ±3	0.305 ±3
χ ² (mmag.) ²	22.21	34.56	20.58	21.68
L ₂ /L ₁	0.751	0.790	0.883	0.741
r.m.s. error (mmag.)	4.3	5.4	4.1	4.3

Table 8 : Adopted light-curve solutions.

T_1 K (polar)	29900	35000
q (spectroscopic)	0.878	0.878
Escat ₁ (adopted)	0.50	0.60
Escat ₂ (adopted)	0.48	0.55
β_1 (adopted)	0.25	0.25
β_2 (adopted)	0.25	0.25
i (degrees)	69.21 ± 12	69.14 ± 12
T_2 K (polar)	28570 ± 310	33160 ± 410
r_1 (polar)	0.323 ± 3	0.323 ± 4
r_1 (mean)	0.336 ± 3	0.337 ± 4
r_2 (polar)	0.298 ± 4	0.299 ± 5
r_2 (mean)	0.309 ± 4	0.311 ± 5

Table 9 : Astrophysical data for AH Cephei.

Absolute dimensions:	Primary	Secondary
M/M	18.1 ± 0.9	15.9 ± 0.8
R/R $_{\odot}$	6.7 ± 0.2	6.2 ± 0.2
log g (cgs)	4.04 ± 0.03	4.06 ± 0.03

Photometric data: Solution I

T $_{\text{eff}}$ (K)	29900 (adopted)	28600 ± 300
M $_{\text{bol}}$	$-6.^{\text{m}}59 \pm 0.^{\text{m}}09$	$-6.^{\text{m}}21 \pm 0.^{\text{m}}10$
log (L/L $_{\odot}$)	4.51 ± 0.04	4.36 ± 0.04
B.C.	$-2.^{\text{m}}90$	$-2.^{\text{m}}80$
M $_{\text{V}}$	$-3.^{\text{m}}69 \pm 0.^{\text{m}}09$	$-3.^{\text{m}}41 \pm 0.^{\text{m}}10$
E $_{(b-y)}$	$0.^{\text{m}}44$	
Distance (pc)	680 ± 30	

Photometric data: Solution II

T $_{\text{eff}}$ (K)	35000 (adopted)	33200 ± 400
M $_{\text{bol}}$	$-7.^{\text{m}}31 \pm 0.^{\text{m}}14$	$-6.^{\text{m}}86 \pm 0.^{\text{m}}15$
log (L/L $_{\odot}$)	4.78 ± 0.05	4.62 ± 0.06
B.C.	$<-3.^{\text{m}}3$	$-3.^{\text{m}}15$
M $_{\text{V}}$	$-4.^{\text{m}}01 \pm 0.^{\text{m}}14$	$-3.^{\text{m}}71 \pm 0.^{\text{m}}15$
E $_{(b-y)}$	$0.^{\text{m}}44$	
Distance (pc)	790 ± 50	

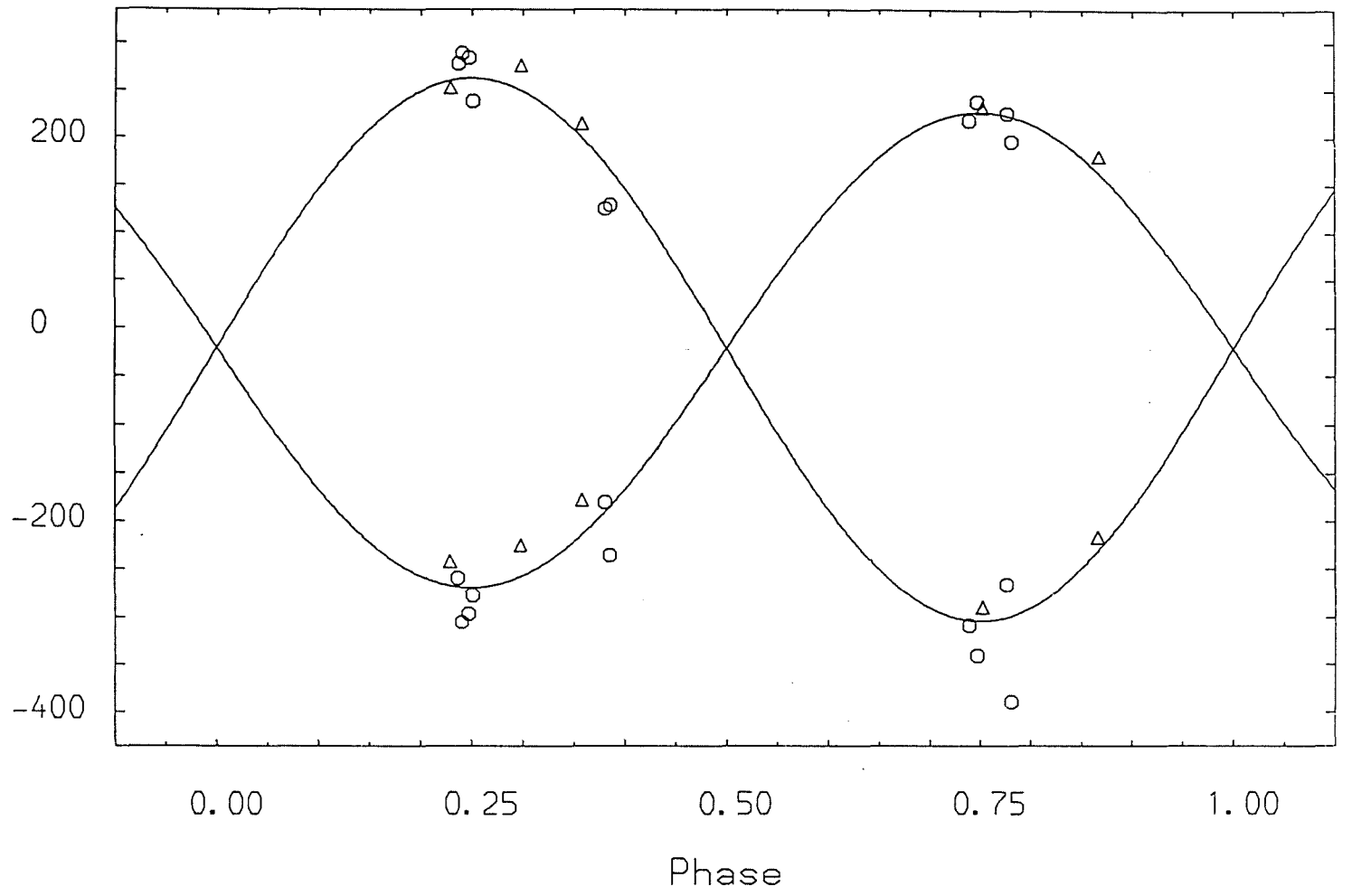


Figure 1.

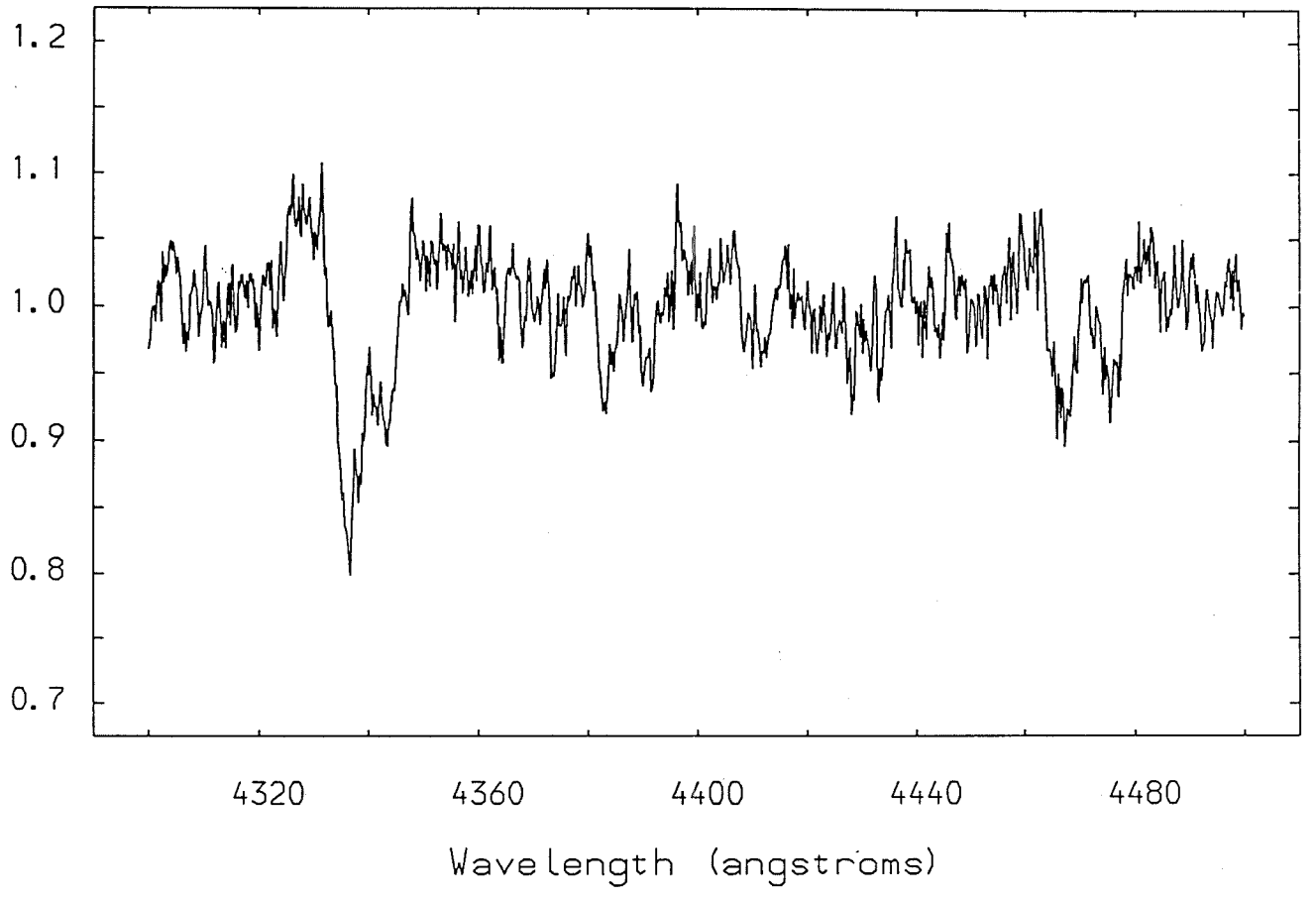


Figure 2.

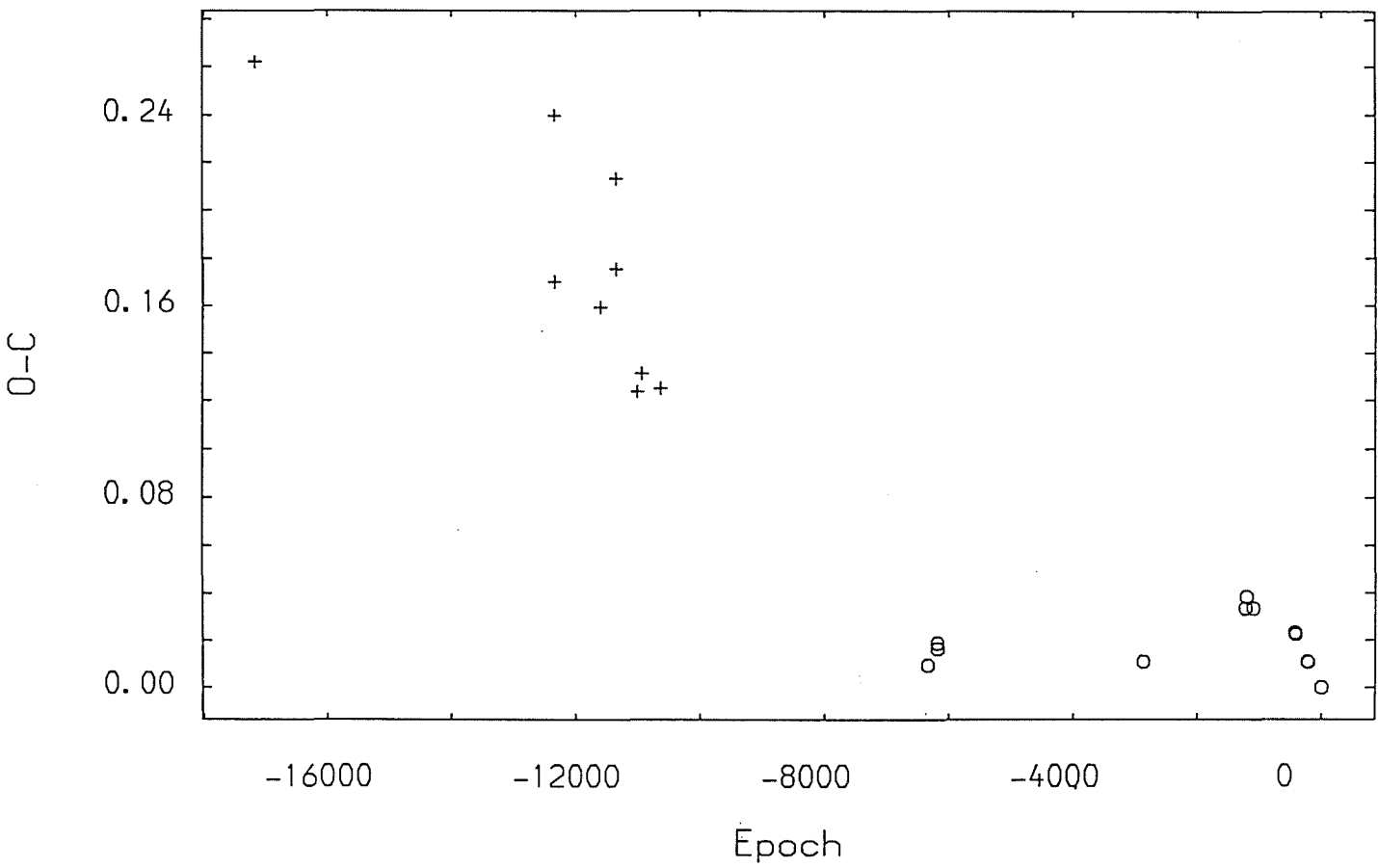


Figure 3.

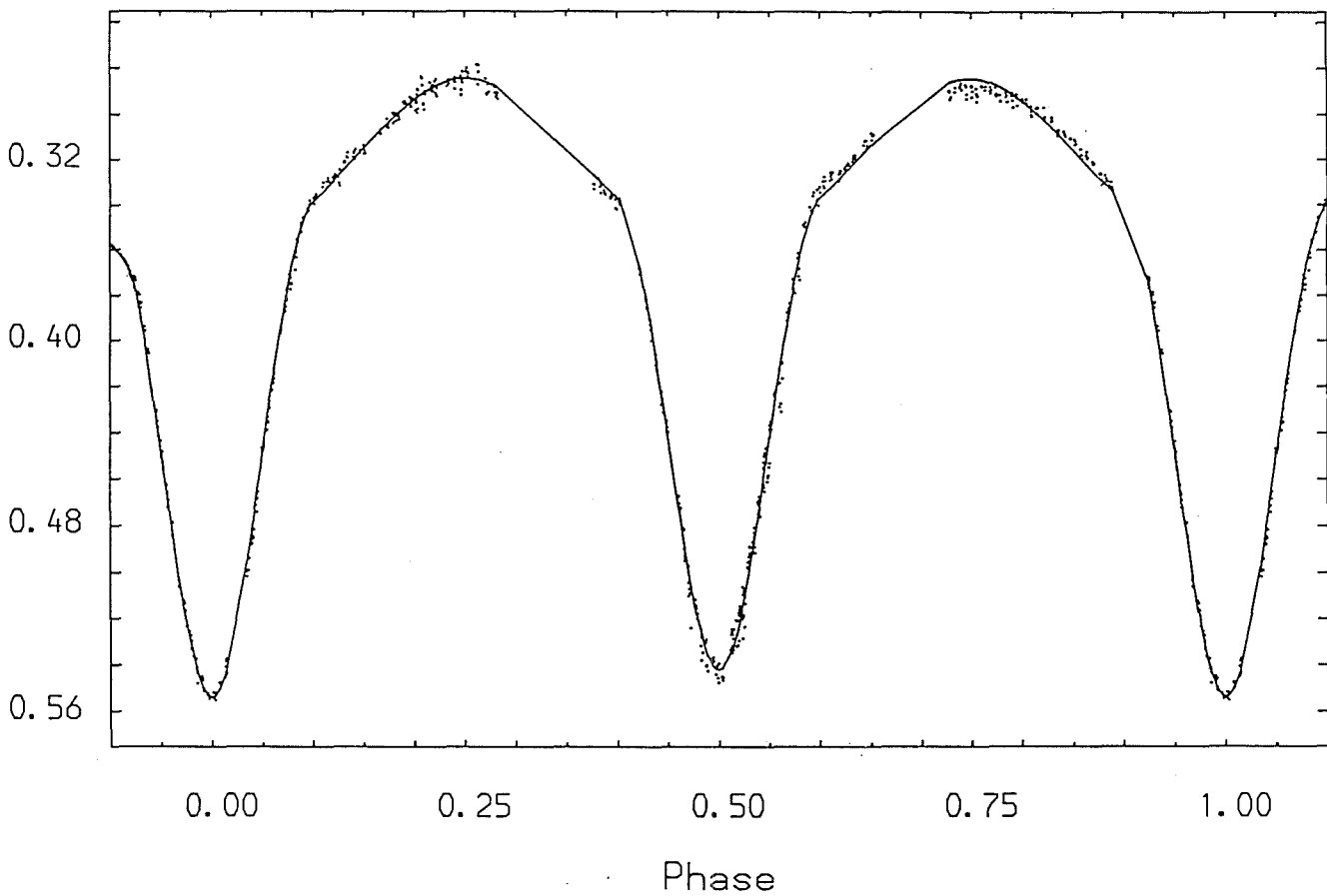


Figure 4.

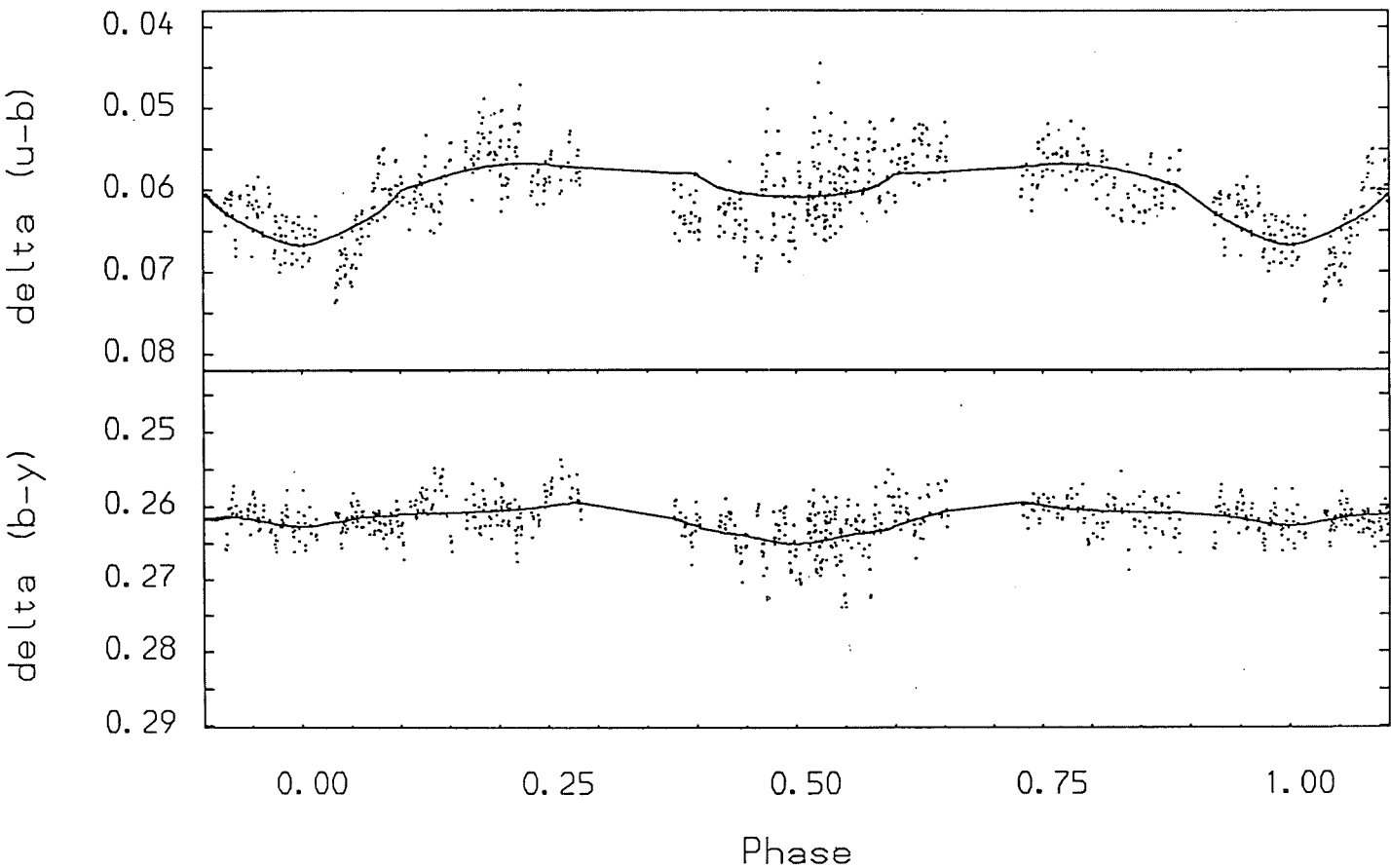
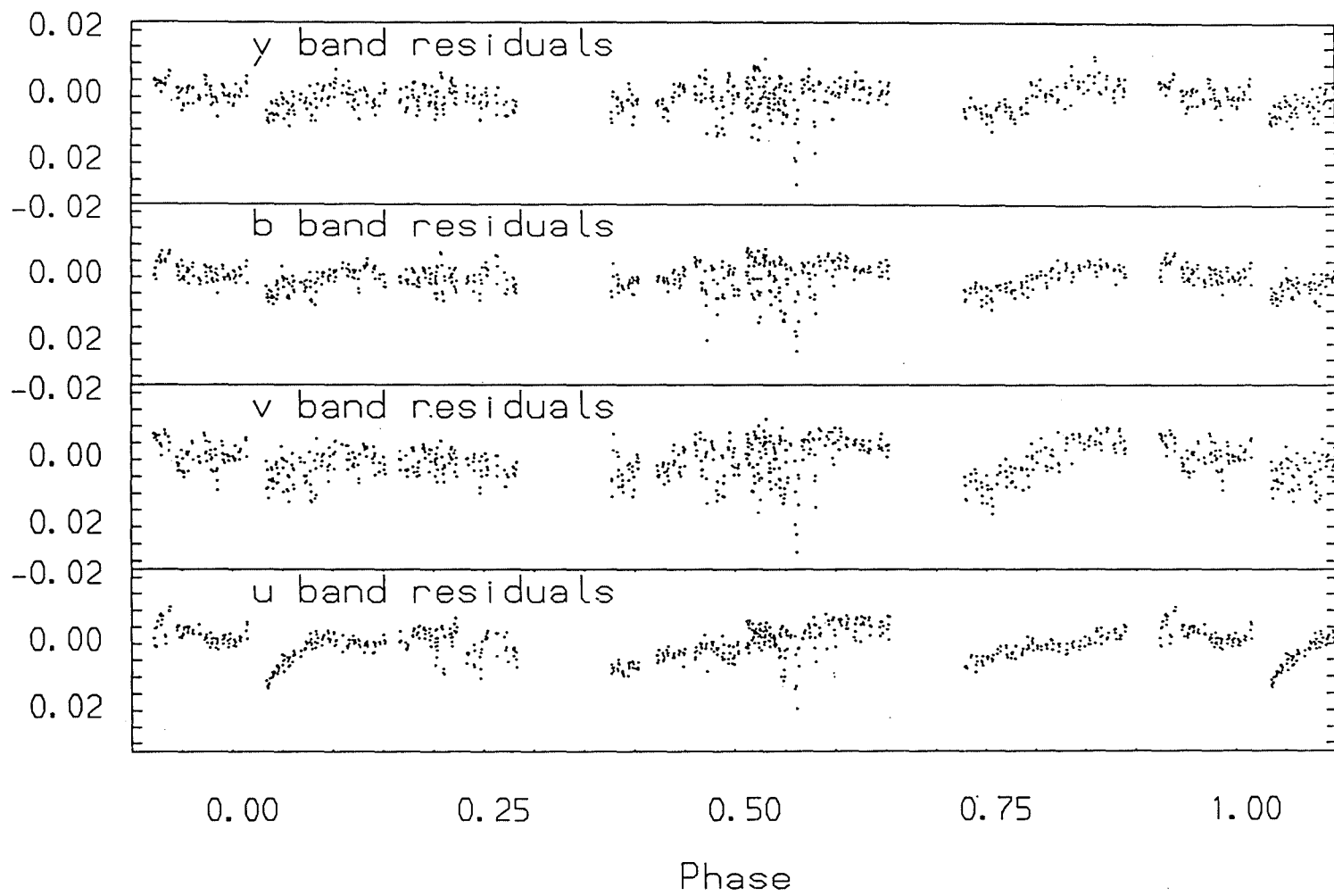


Figure 5.

Figure 6.



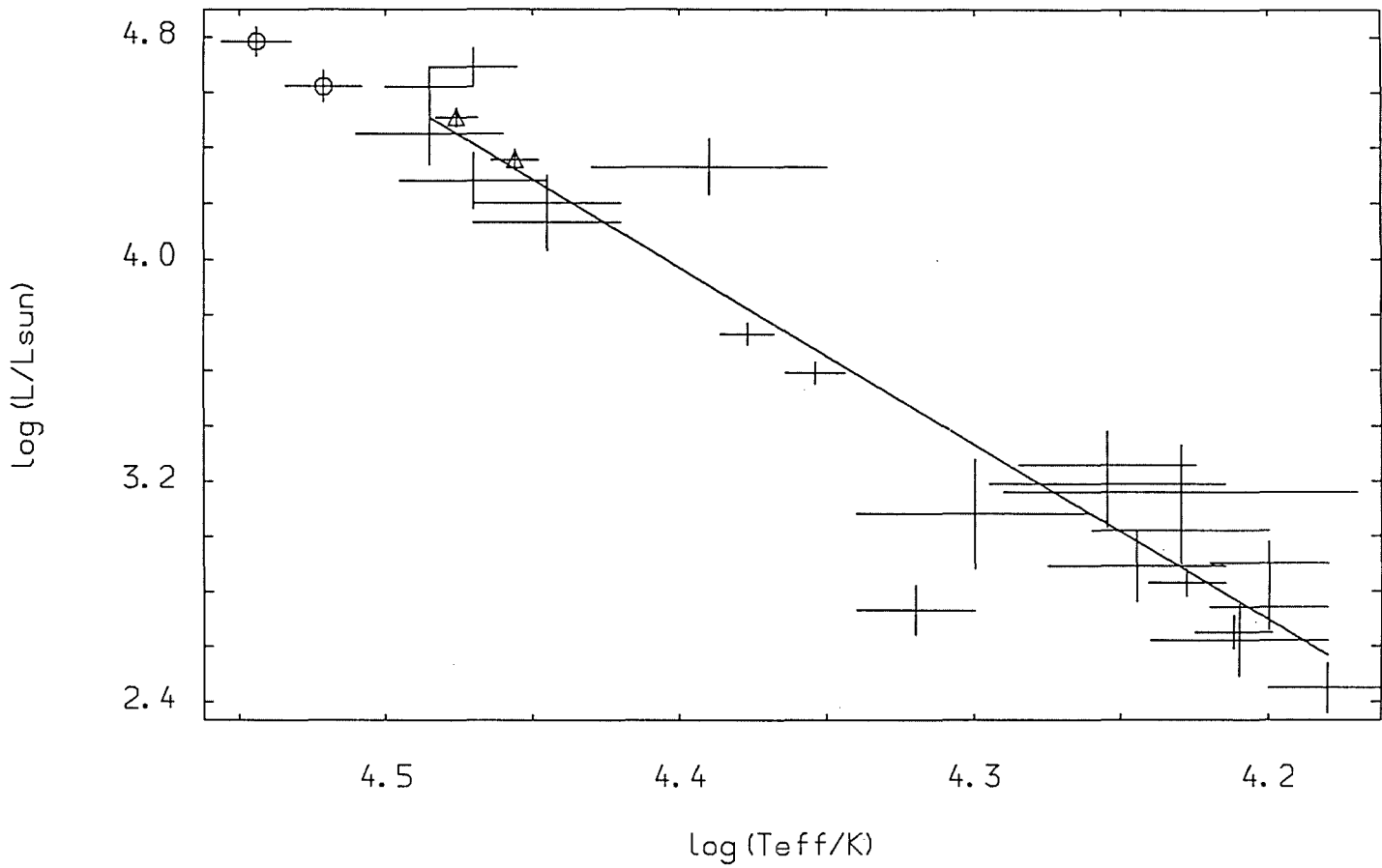


Figure 7.

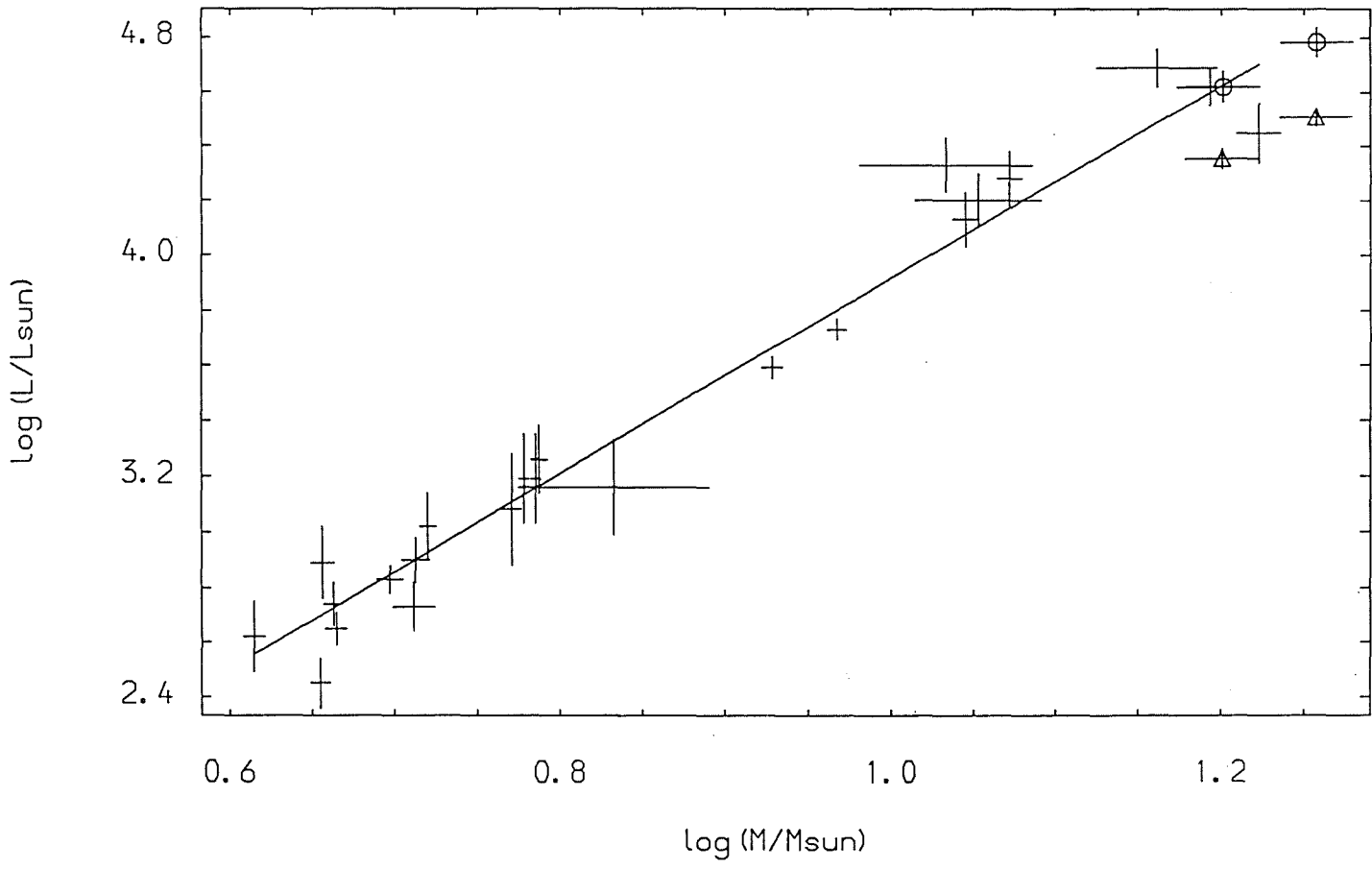


Figure 8.

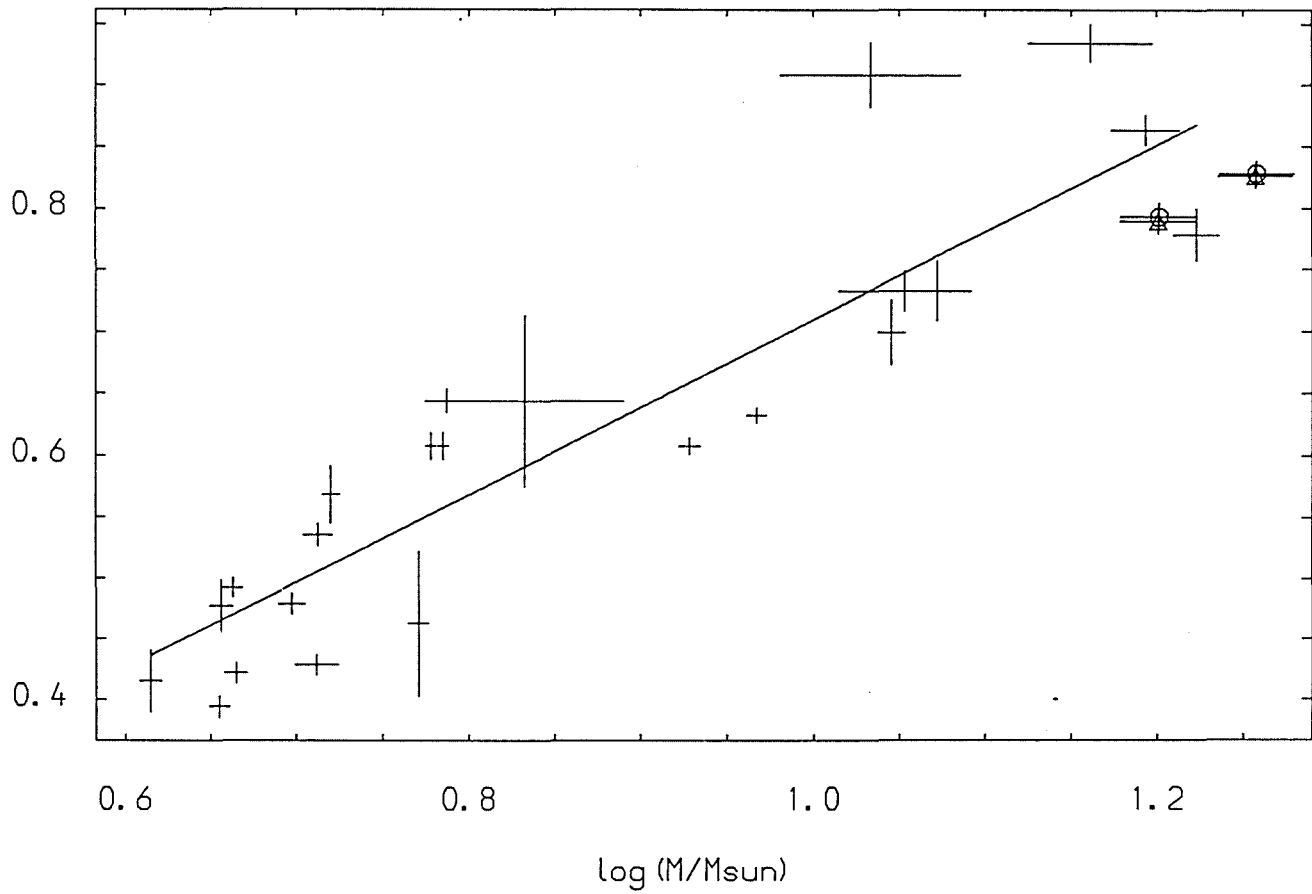


Figure 9.

CHAPTER 5

Simultaneous differential photometry with the St. Andrews

Twin Photometric Telescope:

II. - The eclipsing binaries SX Aurigae & TT Aurigae.

Simultaneous differential photometry with the St. Andrews

Twin Photometric Telescope:

II. - The eclipsing binaries SX Aurigae & TT Aurigae.

S.A. Bell, A.J. Adamson and R.W. Hilditch.

University Observatory, Buchanan Gardens, St. Andrews,

Fife, KY16 9LZ, Scotland.

Received _____

Correspondence to:-

S.A. Bell,
University Observatory,
Buchanan Gardens,
St. Andrews, Fife,
KY16 9LZ,
Scotland.

Summary

The Twin Photometric Telescope at St. Andrews has been used to obtain a complete B light curve (~ 1000 observations) of the B-type interacting binary system SX Aur. Spectroscopic data have also been obtained with the Isaac Newton Telescope of SX Aur and TT Aur to confirm the previous spectroscopic observations by Popper (1943) and Wachmann et al. (1985) respectively. Complete analyses of the data for both systems result in determinations of the masses and radii of the two components to accuracies better than 4% and 2% respectively. In the HR diagram, comparisons with the evolutionary tracks for single stars published by Hejlesen (1980) show that a chemical composition of ($X = 0.70$, $Z = 0.02$) provides good agreement with the location of the primary component of TT Aur, and for SX Aur, provided that the temperature of the primary component is adopted to be 25000K.

Both systems appear to have passed through a stage of case A mass-ratio reversal since both secondaries fill their respective Roche lobes and are substantially overluminous for their masses. TT Aur is currently in the slow phase of mass transfer with the present primary being close to the ZAMS, whilst the shorter-period system SX Aur is approaching a contact state as a result of the expansion by main-sequence evolution of the present primary component.

1) Introduction

The variability of SX Aur (HD 33357, SAO 40094, BD +41^o1101) was discovered by Leavitt (1907), and its period was correctly determined by Hertzsprung (1928). A complete photographic light curve was obtained by Oosterhoff (1933), who also calculated orbital elements for the system. These elements were later revised by Wyse (1934). Photoelectric observations have been obtained by Lavrov (1960), Fliegel (1963), Bondarenko (1974) and Chambliss and Leung (1979; hereafter CL). Analyses were made by Fliegel and CL using their own data as well as Giuricin et al. (1982) using the observations of Bondarenko. The solutions found by CL and Giuricin et al. are in reasonable agreement with each other, but differ from previous solutions as to the Roche configuration and the nature of primary eclipse. Spectroscopic data were obtained by Popper (1943), who found SX Aur to be a double-lined spectroscopic binary, and also by Petrie (1956). It was decided that the configuration of this system would be better understood by the analysis of a high-precision light curve of the type provided by the Twin Photometric Telescope and more modern intermediate-dispersion spectroscopy.

Bell and Hilditch (1984; hereafter Paper I), presented a high-precision light curve of the close binary TT Aur and an analysis of the observations. No modern spectroscopy was available at that time and the determination of the mass ratio of the system could only be described as provisional. Wachmann et al. (1985; hereafter WPC), have since presented B and V photoelectric observations and medium-resolution spectroscopy of the system. Their analysis showed the system to be semi-detached and the secondary to be the larger component whereas the solution in Paper I

found a similar configuration with the secondary smaller than the primary component. As WPC point out, this discrepancy must be resolved before the nature of TT Aur can be said to be satisfactorily understood.

2) Spectroscopy

2.1) Observations

The spectroscopic observations presented in this paper were obtained by SAB and AJA during the period 1985 August 25-30, at the Observatorio del Roque de los Muchachos, La Palma, using the 2.5m Isaac Newton Telescope in conjunction with the Intermediate Dispersion Spectrograph (IDS) and Image Photon Counting System (IPCS). A dispersion of 16.7 \AA mm^{-1} was used, each observation consisting of two spectra centred on 4040 \AA and 4400 \AA . A more detailed description of the observational technique has been given elsewhere (Bell et al., 1986).

2.2) Reduction and Analysis

The spectroscopic data were processed in the manner described by Bell et al. (1986) using the spectroscopic image-processing package REDUCE (Hill et al., 1982a). Cross-correlation analysis using VCROSS (Hill, 1982) was attempted using the B3V secondary radial-velocity standard star ADS16472A. The amplitude of the noise on the spectra is approximately 6% of the continuum height whereas the depths of the weak secondary features are of the order of 10% of the continuum height which made identification of the cross-correlation peak due to the secondary component very

difficult. For this reason, it was necessary to measure the radial velocities of the two components by visual inspection. The errors on the primary and secondary radial velocities are estimated to be 15 and 20kms^{-1} respectively.

The principal spectral lines showing splitting were the HeI lines at $\lambda\lambda 4026, 4144, 4388$ and 4471 and these proved to be the most useful. Two other He I lines were occasionally used in the analysis; $\lambda 4009$ was clearly visible in the primary component at spectra close to secondary minimum and $\lambda 4120$ was used when interference from H δ was minimal. The measurements of these lines to determine the radial velocities of the components of SX Aur and TT Aur were made using VELMEAS (Hill et al., 1982b) by visual inspection of the line centres. The Balmer lines, however, were omitted from the analysis due to their extremely rotationally and Stark-broadened profiles. The lines of interstellar CaII were clearly visible in the short wavelength spectra, the K line being especially well defined. The H line, however was always severely blended with H ϵ .

2.2.1) SX Aurigae

Over an interval of eighteen months Popper (1943) obtained 37 spectrograms of SX Aur at a dispersion of 76\AA mm^{-1} at H γ . He classified both components to be of spectral type B3.5 and made 22 primary and 17 secondary component velocity measurements. After weighting these data and assuming that the orbit was circular, he obtained velocity semi-amplitudes for the primary component K_1 and the secondary component K_2 of 172 ± 4 and $322 \pm 7\text{kms}^{-1}$ respectively. From the primary component velocities he also obtained a systemic

velocity V_o of $3 \pm 4 \text{ km s}^{-1}$. Measurements of the interstellar K line led to a velocity of $7.6 \pm 1.0 \text{ km s}^{-1}$. He also calculated a mean ratio of the secondary luminosity L_s to that of the primary L_p of 0.45. Crude measurements of the equivalent widths for the two components of the $\lambda 4026$ feature on the only suitable quadrature spectrum (INTD237/50) would imply a luminosity ratio of 0.3 with an estimated error of 0.1. It would be unwise to place too much confidence in this determination. In a recent study of rotational velocity changes in eclipsing binary systems, Olson (1984) found rotational velocities of 201 ± 5 and $92 \pm 29 \text{ km s}^{-1}$ for the primary and secondary components of SX Aur respectively.

We have obtained 9 spectra of SX Aur yielding 9 primary component and 7 secondary component velocities. The final radial velocities for both components are given in Table 1. The interstellar CaII lines gave a velocity of $4.9 \pm 0.9 \text{ km s}^{-1}$. Our spectroscopic data covers first quadrature only but it is sufficient to show that there are no significant systematic differences between the two sets of observations. We have therefore re-calculated K_1 , K_2 and V_o using Popper's unity and half-weighted points and our data excluding two primary velocities close to secondary minimum which may be affected by rotational distortion. The re-analysis of the data in terms of K_1 , K_2 , V_o and the derived mass functions and projected semi-major axes, together with their standard errors are given in Table 2. The radial-velocity curves and re-computed orbits are given in Figure 1.

2.2.2) TT Aurigae

WPC presented new spectroscopic data obtained over the interval 1971 to 1983 in their investigation of TT Aur. Twenty five spectrograms at a dispersion of 16.2 \AA mm^{-1} were measured giving velocity semi-amplitudes for the primary and secondary components of 175 ± 2 and $259 \pm 3 \text{ kms}^{-1}$ respectively. Their analysis compared favourably with the original spectroscopic study of Joy and Sitterley (1931) made at a lower dispersion. They obtained a mean systemic velocity of $2 \pm 2 \text{ kms}^{-1}$ and a velocity of $4.2 \pm 0.4 \text{ kms}^{-1}$ for the interstellar CaII lines.

We present the results of the analysis of 10 spectra obtained at both quadratures for this system consisting of 10 primary and 8 secondary component velocities. The interstellar CaII lines gave a velocity of $4.4 \pm 1.4 \text{ kms}^{-1}$. Once again, no significant systematic effects can be found between the two sets of observations. The final radial velocities have been phased using the ephemeris given in Paper I and are listed in Table 1. The results of the re-analysis of both sets of data are given in Table 2. The resulting orbits and radial-velocity curves are presented in Figure 2. The spectra for TT Aur were not of sufficient quality to enable an estimate of the spectroscopic luminosity ratio to be made.

3) Photometry

3.1) Observations

The photometric observations for SX Aur were obtained by SAB using the Twin Photometric Telescope (TPT) at St. Andrews on four nights during 1984 February and 1985 January. The observing

technique has already been described in detail in Paper I. For the observations of SX Aur, the comparison star was HD 33411 ($m_B = 8.2$, B8) and the check star was the V-magnitude standard η Aur ($m_B = 3.00$, B3). The filter used for these measurements was comparable with the Johnson 'B' filter and the observations were made using a 46 arcsecond aperture with the duration of the integration fixed at 60s. The data for the four nights are given in Table 3 and the resultant light curve is shown in Figure 3. The data presented in Table 3 were reduced using a computer program written by SAB which follows a method described more thoroughly elsewhere (Hilditch, 1981).

The light curve of SX Aur appears to be slightly brighter at $0^P.25$ than at $0^P.75$ in agreement with the observations made by CL whilst the primary minimum appears to be very slightly asymmetric, though not to the extent reported by Bondarenko (1974). As with TT Aur, the asymmetry in the minimum is suggestive of non-photospheric matter in the system; however, IUE observations of SX Aur by Peters et al. (1985) find no evidence for a circumstellar envelope. There is no phase shift for secondary minimum from $0^P.5$ and the assumption of a circular orbit for this analysis appears to be reasonable.

3.2) Ephemeris

Two new times of minima have been obtained and a new ephemeris has been calculated using the published photoelectric times of minima given in Table 4. The method of Kwee and van Woerden (1956) has been used for the calculation of the time of minimum in both cases and an unweighted least-squares analysis for the evaluation of

between $(B-V)_0$ and the assigned spectral type.

By means of the Strömgen photometry of Hilditch and Hill (1975) and the (c_0, T_{eff}) calibration of Davis and Shobbrook (1977), a polar primary temperature of 23600K was adopted for TT Aur, with an estimated error of 1000K. This is in good agreement with the spectral classification by Hill et al. (1975) of $B2 \pm 1$. The HeI line at $\lambda 4009$ can be seen clearly only at the same phase as SX Aur, lending further support to the B2 classification of the primary. However, WPC adopt a polar temperature of 24800K for the primary using an iterative procedure to match the observed colour indices with the temperature averaged over the entire surface of the star.

Both light curves were analysed using LIGHT (Hill, 1979), fixing the mass ratio q at that determined from the spectroscopic analysis and the primary component temperature T_1 by photometric calibration or spectral classification. The fractional primary-component radius r_1 , the secondary-component temperature T_2 and fractional radius r_2 , and the inclination of the system i were kept as free parameters. The fractional radii are expressed in terms of the separation a of the two components. As a first approximation, the solution obtained by CL was used for SX Aur and that of WPC was used for TT Aur. Tables 5 and 6 list the results of the analyses for SX Aur and TT Aur respectively. The solutions for SX Aur and TT Aur are shown in Figures 3 & 4 respectively and the residuals are shown in Figures 5 & 6. As expected, there are no significant differences between the two solutions for SX Aur using the two adopted primary-component temperatures except, of course, for the final values of the luminosities of both components and the temperature of the secondary component.

The following assumptions were made for each analysis. Black-body fluxes were adopted because preliminary solutions using the model atmospheres of Kurucz (1979) gave noticeably inferior fits. In our experience of solving the light curves of early B-type systems, this has always been the case. Gravity-darkening exponents (β_1 and β_2) were set at 0.25 for both components, and electron scattering fractions (Escat_1 and Escat_2) were taken from Hutchings and Hill (1971). The limb-darkening coefficients were calculated automatically within LIGHT at each iteration of the solution using interpolation from the tabulation by Carbon and Gingerich (1969).

The data obtained for this paper were unsuitable for determinations of the projected rotational velocities of the components of each system for the reasons outlined in Section 2.2. In the case of TT Aur, no data are available and synchronous rotation was assumed. The primary component of SX Aur shows reasonable agreement between the observed projected rotational velocity found by Olson (1984) and that predicted by our solution (215kms^{-1}). The secondary component, however, rotates at $92 \pm 27\text{kms}^{-1}$ which corresponds to about half the velocity required for synchronism predicted by our solution (165kms^{-1}). It must be pointed out that because the secondary component is substantially less luminous than the primary, the error in measuring its rotational velocity is large and the value should be treated with caution. However, a solution was attempted using this rotational velocity and is given in Table 5. Further discussion of the validity of this solution is given in Section 4.2.1.

In the case of SX Aur, the solution with synchronous rotation for both components proved to be insensitive to changes in the mass ratio within the error limits derived from the velocity semi-amplitudes. A grid of solutions was generated for q in steps of 0.005 between 0.52 and 0.56 which showed only minimal changes in the free parameters of the order of the formal errors of the solution quoted in Table 5. This was not the case for TT Aur. The solution for TT Aur presented in Paper I yielded a mass ratio of 0.61 with the inclination fixed at $87^{\circ}.5$ which made the primary component the larger of the two stars. WPC found the situation reversed with a mass ratio of 0.68 and an inclination of $86^{\circ}.4$. The solution presented here shows the inclination to be $86^{\circ}.9$ and the two stars to be of comparable sizes with the secondary component marginally larger than the primary. The discrepancy between the Paper I and WPC solutions can be largely eliminated by a good spectroscopic determination of q and demonstrates the need for high-quality radial velocities for systems such as this to distinguish between equally-good photometric solutions.

4) Discussion

4.1) Spectroscopy and Photometry

The effects of blending in the diffuse HeI lines probably have a more marked effect in TT Aur than in SX Aur due to the smaller velocity separation between the two components. WPC suggest that corrections of 5% and 10% in K_1 and K_2 respectively should be made for TT Aur. We have adopted these corrections in our analysis (see Section 4.2.2). The effects of reflection on the velocity semi-amplitudes will also give systematically low masses and radii.

The distorted nature of the components of these systems makes corrections for this effect difficult although they are unlikely to be greater than about $2\text{-}3\text{kms}^{-1}$.

The largest source of error is the temperature of the primary component. Despite good photometry, the distortion of the stars makes the choice of temperature difficult. WPC computed a value of 24800K for TT Aur and it seems likely that the primary temperature lies between 23600K and 24800K. For SX Aur, the primary temperatures adopted for our analysis were based (i) upon the $(B-V)_0$ colour index rather than the spectral classification used by CL of B3.5, which was made before the introduction of the MK classification system, and (ii) upon the spectral class of B1 given by Morgan et al. (1955) and Hiltner (1956). Suitable Strömgren photometry of this system could not be found and no better estimate of the primary temperature could be made. For both systems we have adopted an error of 1000K for each primary component. Astrophysical data for SX Aur based on synchronous rotation for both components, and for TT Aur using the corrected velocity semi-amplitudes, are given in Tables 7 & 8 respectively.

4.2) Evolutionary state

4.2.1) SX Aurigae

Three solutions have been presented for SX Aur involving two temperatures for the primary component and synchronous and non-synchronous rotation of the secondary component. The non-synchronous rotation of the secondary yields an unrealistic result, producing a secondary filling 122% of its Roche lobe. This would involve an over-contact configuration which is clearly not

supported by the UV observations of the system by Peters et al. (1985), who did not find any evidence for a common envelope. Peters et al. also noted that there was some evidence for a stellar wind with a velocity of 600kms^{-1} whose source is the primary component. It seems likely that the period change found by Kreiner and Tremko (1978) is attributable to mass loss of $4 \times 10^{-7} M_{\odot} \text{yr}^{-1}$ rather than mass transfer. Other than this, there is no obvious indication of mass transfer in the system at present.

In the HR diagram, comparisons with the evolutionary tracks for single stars published by Hejlesen (1980) show that a chemical composition of ($X = 0.70$, $Z = 0.02$) provides good agreement with the location of the primary component on the appropriate mass track at an age of 1×10^7 yrs if the higher temperature is adopted. The primary component appears to be $\sim 1.0^m$ underluminous for the lower value of the temperature. At the higher temperature, the secondary is overluminous for its mass by $\sim 0.8^m$ and has remarkably similar properties to the secondary of TT Aur. At the lower-temperature, the secondary component of SX Aur is on an evolutionary track appropriate to its mass near the end of core-hydrogen burning and with an age of $\sim 5 \times 10^7$ yrs. Alternatively, if a composition of ($X = 0.80$, $Z = 0.02$) is adopted, the lower temperature solution makes the primary component appear to be normal and unevolved whilst the secondary is overluminous for its mass by $\sim 0.7^m$. However, the work of Andersen et al. (1983) on other B-type systems shows that the model with the higher helium content is to be preferred. Accordingly, we express a preference for the solution with the higher value adopted for the temperature of the primary component. Therefore, the system seems most likely to have evolved through a case A mass-transfer process leading to mass-ratio reversal and the

current primary has evolved into contact. SX Aur is then at a similar stage of evolution to the system V Pup (Andersen et al., 1983) in its evolution into contact.

4.2.2) TT Aurigae

It has already been pointed out that TT Aur probably belongs to a small group of semi-detached systems which have properties significantly different from Algol systems (Bell and Hilditch, 1984).

Using the uncorrected velocity semi-amplitudes, the components of TT Aur were too bright by $\sim 1.5^m$ for their observed masses and too hot by $\sim 5000\text{K}$ using the theoretical models of Hejlesen (1980) assuming a composition of ($X = 0.70$, $Z = 0.02$) This discrepancy can be removed for the primary component by using the corrected values of K_1 and K_2 , thus increasing the masses of the primary by $2M_{\odot}$ and the secondary by $1M_{\odot}$. The masses of the two components corrected for blending have been used in the subsequent analysis. In the case of the primary component, it becomes indistinguishable from a normal single star approximately halfway through its main-sequence lifetime. Its radius is about 20% larger than the ZAMS value and its temperature and surface gravity match those of the model for the corrected mass with an age of $\sim 10^7$ yrs.

The secondary component, however, is still $\sim 0.8^m$ brighter and $\sim 40\%$ larger than a normal star of its mass. A normal star of the required mass would have an effective temperature of 19100K and a radius of $3.0R_{\odot}$. In spite of the good agreement of the primary component with the theoretical models, it cannot be used to derive the age of the system because neither component has followed the

normal evolutionary course of a single star. It seems probable that this system has evolved through a phase of case A rapid mass exchange and reversal of the mass ratio. Slow mass exchange may still be in progress if the period fluctuations reported by WPC are real.

5) Conclusion

We have presented a new light curve of SX Aur and medium resolution spectroscopy of SX Aur and TT Aur. The radial velocities show good agreement with previous studies and photometric analyses of TPT light curves have been made on both systems using the spectroscopic mass ratios. The light curve of TT Aur presented in Paper I has been re-analysed with the new spectroscopic mass ratio as opposed to the "best-fit" photometric value and, as a result, the discrepancy between Paper I and the work of WPC has been removed. This system is found to be semi-detached with a Roche-lobe filling secondary component a little larger than the primary component. SX Aur, however, is shown to be a marginal contact system like V Pup which has reached a more advanced stage of evolution than TT Aur.

Acknowledgements

The authors would like to express their gratitude for the hospitality and assistance extended to them by the staff of the Observatorio del Roche de los Muchachos. We acknowledge PATT for the allocations of observing time, and the SERC for financial support in the form of a research studentship for one of us (SAB). We would also like to thank Prof. D.W.N. Stibbs for the use of the facilities of the University Observatory, St. Andrews and SAB wishes

to thank the workshop staff for their technical support of the Twin
Photometric Telescope.

References

- Andersen, J., Clausen, J.V., Gimenez, A. & Nordstrom, B., 1983.
Astron. Astrophys., 128, 17.
- Bell, S.A. & Hilditch, R.W., 1984. Mon. Not. R. astr. Soc., 211,
229. (Paper I)
- Bell, S.A., Hilditch, R.W. & Adamson, A.J., 1986. Submitted to Mon.
Not. R. astr. Soc.
- Böhm-Vitense, E., 1981. Ann. Rev. Astron. Astrophys., 19, 295.
- Bondarenko, I.I., 1974. Perem. Zvezdy Prilozh, 2, 51.
- Carbon, D.F. & Gingerich, O.J., 1969. Theory and Observations of
Normal Stellar Atmospheres, ed. Gingerich, O.J. (M.I.T. press,
Cambridge), 377.
- Chambliss, C.R., 1977. Inf. Bull. var. Stars, No. 1278.
- Chambliss, C.R. & Leung, K.-C., 1979. Astrophys. J., 228, 828.
(CL)
- Davis, J. & Shobbrook, R.R., 1977. Mon. Not. R. astr. Soc., 178,
651.
- Fliegel, H.F., 1963. Ph.D. dissertation, University of
Pennsylvania, Philadelphia.
- Giuricin, G., Mardirossian, F. & Mezzetti, M., 1982. Astron. Nachr.,
303, 311.
- Hejlesen, P.M., 1980. Astron. Astrophys. Suppl. Ser., 39, 347.
- Hertzsprung, E., 1928. Bull. astr. Inst. Netherlands., 4, 178.

- Hilditch, R.W., 1981. Mon. Not. R. astr. Soc., 196, 305.
- Hill, G., 1979. Publ. Dom. Astrophys. Obs., 15, 297.
- Hill, G., 1982. Publ. Dom. Astrophys. Obs., 16, 59.
- Hilditch, R.W. & Hill, G., 1975. Mem. R. astr. Soc., 79, 101.
- Hill, G., Hilditch, R.W., Younger, F. & Fisher, W.A., 1975. Mem. R. astr. Soc., 79, 131.
- Hill, G., Fisher, W.A. & Poeckert, R., 1982a. Publ. Dom. Astrophys. Obs., 16, 43.
- Hill, G., Ramsden, D., Fisher, W.A. & Morris, S.C., 1982b. Publ. Dom. Astrophys. Obs., 16, 11.
- Hiltner, W.A., 1956. Astrophys. J. Suppl. Ser., 2, 389.
- Hutchings, J.B. & Hill, G., 1971. Astrophys. J., 167, 137.
- Joy, A.H. & Sitterley, B.W., 1934. Astrophys. J., 73, 77.
- Kizilirmak, A., & Pohl, E., 1970. Inf. Bull. var. Stars., No. 456.
- Kizilirmak, A., & Pohl, E., 1974. Inf. Bull. var. Stars., No. 937.
- Kizilirmak, A., & Pohl, E., 1975. Inf. Bull. var. Stars., No. 1053.
- Kreiner, J.M. & Tremko, J., 1978. Acta astr., 28, 179.
- Kurucz, R.L., 1979. Astrophys. J. Suppl. Ser., 40, 1.
- Kwee, K.K. & van Woerden, H., 1956. Bull. astr. Inst. Netherlands, 12, 327.
- Lavrov, M.I., 1960. Engelhardt Obs. Bull., No. 35, 69.

Leavitt, H.S., 1907. Harvard Obs. Circ., No. 130.

Morgan, W.W., Code, A.D. & Whitford, A.E., 1955. Astrophys. J. Suppl. Ser., 2, 41.

Olson, E.C., 1984. Publ. astr. Soc. Pacific, 96, 376.

Oosterhoff, P.T., 1933. Bull. astr. Inst. Netherlands, 7, 107.

Peters, G.J., Polidan, R.S. & Linnell, A.P., 1985. Bull. Amer. astr. Soc., 17, 584.

Petrie, R.M., 1956. Publ. Dom. Astrophys. Obs., 10, 287.

Popper, D.M., 1943. Astrophys. J., 97, 394.

Popper, D.M. & Dumont, P.J., 1977. Astron. J., 82, 216.

Strzalkowski, A. & Piotrowski, S., 1951. Acta astr., 4, 132.

Wachmann, A.A., Popper, D.M. & Clausen, J.V., 1986. Astron. Astrophys., 162, 62.

Wyse, A.B., 1934. Publ. astr. Soc. Pacific, 46, 176.

Figure captions

Figure 1: Observed radial velocities and computed orbits for SX Aur. Squares represent I.N.T. data and diamonds represent Popper's unity-weighted data. Popper's half and quarter-weighted data are represented by crosses and dots respectively.

Figure 2: Observed radial velocities and computed orbits for TT Aur. Squares represent I.N.T. data and diamonds represent the data of Wachmann et al. (1986).

Figure 3: B-magnitude differences in the sense variable minus comparison between SX Aur and HD 33411 together with the final theoretical curve.

Figure 4: B-magnitude differences in the sense variable minus comparison between TT Aur and HD 32989 together with the final theoretical curve.

Figure 5: Residuals of the individual observations for SX Aur from the final theoretical curve.

Figure 6: Residuals of the individual observations for TT Aur from the final theoretical curve.

Table 1 : Radial-velocity data for SX Aur and TT Aur.

SX Aur data.

Tape/Run	H.J.D.	Phase	V_1	n	O-C	V_2	n	O-C	
No.	-2400000		kms^{-1}		kms^{-1}	kms^{-1}		kms^{-1}	Range
INTD231/47	46303.6574	0.1382	-138	(2)	- 5	+270	(1)	+14	Long
INTD231/48	46303.6664	0.1457	-148	(3)	-10	+285	(2)	+20	Short
INTD231/50	46303.6782	0.1555	-155	(4)	-10	+292	(1)	+15	Short
INTD235/52	46307.6654	0.4504	- 47	(2)	--	---	-	--	Short
INTD235/53	46307.6723	0.4562	- 26	(2)	--	---	-	--	Long
INTD237/50	46308.6453	0.2602	-190	(4)	-16	+343	(2)	+11	Short
INTD237/51	46308.6523	0.2660	-180	(2)	- 6	+324	(2)	- 7	Long
INTD237/53	46308.6627	0.2746	-177	(2)	- 4	+320	(2)	- 9	Long
INTD237/54	46308.6703	0.2809	-181	(2)	-10	+318	(2)	- 8	Short

TT Aur data.

Tape/Run	H.J.D.	Phase	V_1	n	O-C	V_2	n	O-C	
No.	-2400000		kms^{-1}		kms^{-1}	kms^{-1}		kms^{-1}	Range
INTD232/46	46304.6505	0.2459	-155	(2)	+16	+260	(2)	- 2	Long
INTD232/47	46304.6582	0.2516	-169	(2)	+ 2	+270	(2)	+ 8	Short
INTD232/49	46304.6686	0.2595	-159	(3)	+11	+265	(3)	+ 3	Short
INTD232/50	46304.6769	0.2657	-165	(2)	+ 9	+268	(2)	+ 7	Long
INTD234/31	46306.6466	0.7436	+193	(2)	+15	-243	(2)	+11	Long
INTD234/33	46306.6577	0.7519	+189	(3)	+11	-248	(3)	+ 6	Short
INTD235/48	46307.6390	0.4883	+ 19	(2)	--	---	-	--	Long
INTD235/49	46307.6473	0.4945	- 10	(3)	--	---	-	--	Short
INTD237/62	46308.7169	0.2970	-166	(2)	- 3	+243	(2)	- 8	Long
INTD237/63	46308.7231	0.3017	-154	(3)	+ 8	+248	(3)	- 1	Short

The columns headed n indicate the number of lines measured for the mean velocity tabulated. The final column indicates the wavelength region used.

Table 2 : Orbital elements for SX Aur and TT Aur.

		SX Aur	TT Aur
K_1 (kms ⁻¹)	=	175 ± 5	175 ± 2
K_2 (kms ⁻¹)	=	323 ± 7	258 ± 2
$V_o(1)$ (kms ⁻¹)	=	0 ± 5	4 ± 2
$V_o(2)$ (kms ⁻¹)	=	10 ± 7	4 ± 2
V_o (kms ⁻¹)	=	5 ± 4	4 ± 1
σ_1 (kms ⁻¹) *	=	21	11
σ_2 (kms ⁻¹) *	=	25	11
q (m_2/m_1)	=	0.54 ± 0.02	0.68 ± 0.01
e	=	0 (adopted)	0 (adopted)
$a_1 \sin i$ (R)	=	4.2 ± 0.1	4.60 ± 0.06
$a_1 \sin i$ (R ^o)	=	7.7 ± 0.2	6.80 ± 0.06
$a_2 \sin i$ (R ^o)	=	11.9 ± 0.2	11.39 ± 0.08
$m_1 \sin^3 i$ (M)	=	10.0 ± 0.4	6.7 ± 0.1
$m_2 \sin^3 i$ (M ^o)	=	5.4 ± 0.2	4.52 ± 0.08

* - r.m.s. scatter of a single observation.

Table 3: Johnson B observations.

1984 Feb 08/09					
H.J.D.	Phase	(V-C)			
45739.30925	0.7652	0.168	45739.38027	0.8239	0.218
45739.31032	0.7661	0.166	45739.38096	0.8244	0.214
45739.31102	0.7666	0.174	45739.38165	0.8250	0.218
45739.31171	0.7672	0.170	45739.38235	0.8256	0.221
45739.31241	0.7678	0.165	45739.38304	0.8262	0.219
45739.31310	0.7684	0.171	45739.38374	0.8267	0.222
45739.31379	0.7689	0.171	45739.38443	0.8273	0.222
45739.31449	0.7695	0.177	45739.38513	0.8279	0.222
45739.31519	0.7701	0.172	45739.38582	0.8285	0.220
45739.31588	0.7707	0.173	45739.38652	0.8290	0.224
45739.31657	0.7712	0.180	45739.38721	0.8296	0.227
45739.31727	0.7718	0.177	45739.39645	0.8372	0.226
45739.31796	0.7724	0.175	45739.39714	0.8378	0.232
45739.31866	0.7730	0.175	45739.39783	0.8384	0.228
45739.31935	0.7735	0.170	45739.39853	0.8390	0.231
45739.32004	0.7741	0.176	45739.39922	0.8395	0.230
45739.32074	0.7747	0.171	45739.39992	0.8401	0.227
45739.32144	0.7753	0.178	45739.40061	0.8407	0.234
45739.32213	0.7758	0.177	45739.40131	0.8413	0.230
45739.32282	0.7764	0.169	45739.40200	0.8418	0.235
45739.32352	0.7770	0.170	45739.40270	0.8424	0.228
45739.33433	0.7859	0.174	45739.40339	0.8430	0.230
45739.33502	0.7865	0.173	45739.40399	0.8436	0.233
45739.33572	0.7871	0.177	45739.40408	0.8436	0.233
45739.33641	0.7876	0.181	45739.40478	0.8441	0.235
45739.33711	0.7882	0.180	45739.40547	0.8447	0.233
45739.33780	0.7888	0.180	45739.40617	0.8453	0.236
45739.33849	0.7893	0.175	45739.40686	0.8459	0.234
45739.33919	0.7899	0.179	45739.40756	0.8464	0.239
45739.33989	0.7905	0.179	45739.40825	0.8470	0.235
45739.34058	0.7911	0.178	45739.40895	0.8476	0.243
45739.34127	0.7916	0.179	45739.40964	0.8481	0.243
45739.34197	0.7922	0.179	45739.42184	0.8582	0.259
45739.34266	0.7928	0.181	45739.42253	0.8588	0.264
45739.34335	0.7934	0.175	45739.42323	0.8594	0.264
45739.34405	0.7939	0.177	45739.42392	0.8599	0.266
45739.34474	0.7945	0.183	45739.42462	0.8605	0.265
45739.34544	0.7951	0.184	45739.42531	0.8611	0.268
45739.34613	0.7957	0.186	45739.42601	0.8617	0.266
45739.34683	0.7962	0.180	45739.42670	0.8622	0.269
45739.34752	0.7968	0.178	45739.42740	0.8628	0.269
45739.37402	0.8187	0.213	45739.42809	0.8634	0.267
45739.37471	0.8193	0.215	45739.42878	0.8640	0.267
45739.37540	0.8199	0.212	45739.42948	0.8645	0.268
45739.37610	0.8204	0.218	45739.42948	0.8645	0.268
45739.37679	0.8210	0.215	45739.43017	0.8651	0.265
45739.37749	0.8216	0.213	45739.43087	0.8657	0.279
45739.37818	0.8221	0.220	45739.43156	0.8663	0.271
45739.37888	0.8227	0.215	45739.43226	0.8668	0.272
45739.37957	0.8233	0.215	45739.43295	0.8674	0.273
			45739.43365	0.8680	0.273
			45739.43434	0.8686	0.277
			45739.43503	0.8691	0.274
			45739.43891	0.8723	0.287
			45739.43960	0.8729	0.286
			45739.44030	0.8735	0.285
			45739.44100	0.8741	0.291

continued

45739.44169	0.8746	0.295	45739.54115	0.9568	0.685
45739.44238	0.8752	0.293	45739.54185	0.9574	0.690
45739.44308	0.8758	0.297	45739.54255	0.9580	0.688
45739.44377	0.8764	0.294	45739.54324	0.9586	0.698
45739.44447	0.8769	0.296	45739.54393	0.9591	0.701
45739.44516	0.8775	0.296	45739.54463	0.9597	0.707
45739.44586	0.8781	0.298	45739.54532	0.9603	0.717
45739.44655	0.8786	0.297	45739.54602	0.9608	0.718
45739.44725	0.8792	0.309	45739.54671	0.9614	0.726
45739.44794	0.8798	0.307	45739.54740	0.9620	0.724
45739.44863	0.8804	0.308	45739.54810	0.9626	0.739
45739.44933	0.8809	0.310	45739.54880	0.9631	0.730
45739.45002	0.8815	0.311	45739.54949	0.9637	0.745
45739.45071	0.8821	0.313	45739.55018	0.9643	0.744
45739.45141	0.8827	0.314	45739.55088	0.9649	0.755
45739.45211	0.8832	0.313	45739.55157	0.9654	0.757
45739.46458	0.8935	0.341	45739.55227	0.9660	0.768
45739.46528	0.8941	0.340	45739.55296	0.9666	0.768
45739.46597	0.8947	0.349	45739.55366	0.9672	0.773
45739.46667	0.8953	0.350	45739.57547	0.9852	0.903
45739.46736	0.8958	0.348	45739.57617	0.9858	0.905
45739.46805	0.8964	0.349	45739.57686	0.9863	0.910
45739.46875	0.8970	0.355	45739.57756	0.9869	0.914
45739.46944	0.8976	0.353	45739.57825	0.9875	0.915
45739.47014	0.8981	0.360	45739.57895	0.9881	0.923
45739.47083	0.8987	0.359	45739.57964	0.9886	0.922
45739.47152	0.8993	0.359	45739.58034	0.9892	0.932
45739.47222	0.8999	0.359	45739.58103	0.9898	0.933
45739.47292	0.9004	0.371	45739.58668	0.9944	0.929
45739.47361	0.9010	0.367	45739.58737	0.9950	0.935
45739.47430	0.9016	0.366	45739.58806	0.9956	0.931
45739.47500	0.9022	0.366	45739.58876	0.9962	0.934
45739.47569	0.9027	0.377	45739.58946	0.9967	0.932
45739.47639	0.9033	0.379	45739.59015	0.9973	0.942
45739.47708	0.9039	0.379	45739.59084	0.9979	0.937
45739.52357	0.9423	0.579	45739.59154	0.9985	0.939
45739.52426	0.9429	0.584	45739.59223	0.9990	0.942
45739.52495	0.9434	0.582	45739.59293	0.9996	0.940
45739.52565	0.9440	0.580	45739.59362	0.0002	0.937
45739.52634	0.9446	0.593	45739.59432	0.0008	0.938
45739.52704	0.9452	0.599	45739.59501	0.0013	0.934
45739.52773	0.9457	0.604	45739.59571	0.0019	0.939
45739.52842	0.9463	0.607	45739.59640	0.0025	0.942
45739.52912	0.9469	0.610	45739.59795	0.0038	0.932
45739.52982	0.9475	0.614	45739.59864	0.0043	0.933
45739.53051	0.9480	0.620	45739.59934	0.0049	0.936
45739.53120	0.9486	0.618	45739.60004	0.0055	0.929
45739.53190	0.9492	0.625	45739.60073	0.0061	0.926
45739.53259	0.9498	0.632	45739.60142	0.0066	0.926
45739.53328	0.9503	0.634	45739.60212	0.0072	0.928
45739.53398	0.9509	0.642	45739.60281	0.0078	0.924
45739.53468	0.9515	0.646	45739.60350	0.0084	0.921
45739.53537	0.9520	0.646	45739.60420	0.0089	0.927
45739.53606	0.9526	0.651	45739.60489	0.0095	0.917
45739.53676	0.9532	0.656	45739.60559	0.0101	0.922
45739.54046	0.9563	0.684	45739.60628	0.0107	0.912

continued

45739.60698	0.0112	0.910	45749.33224	0.0481	0.642
45739.60767	0.0118	0.910	45749.34661	0.0600	0.569
45739.61215	0.0155	0.898	45749.34730	0.0605	0.557
45739.61285	0.0161	0.897	45749.34800	0.0611	0.551
45739.61354	0.0166	0.897	45749.34869	0.0617	0.556
45739.61423	0.0172	0.884	45749.34939	0.0623	0.553
45739.61493	0.0178	0.886	45749.35008	0.0628	0.549
45739.61562	0.0184	0.884	45749.35078	0.0634	0.542
45739.61632	0.0189	0.871	45749.35147	0.0640	0.542
45739.61701	0.0195	0.868	45749.35217	0.0646	0.545
45739.61771	0.0201	0.864	45749.35286	0.0651	0.534
45739.61840	0.0207	0.859	45749.35355	0.0657	0.539
45739.61910	0.0212	0.860	45749.35425	0.0663	0.530
45739.61979	0.0218	0.865	45749.35494	0.0669	0.517
45739.62048	0.0224	0.853	45749.35564	0.0674	0.514
45739.62118	0.0230	0.852	45749.35633	0.0680	0.515
45739.62188	0.0235	0.844	45749.35703	0.0686	0.512
45739.63323	0.0329	0.763	45749.35772	0.0692	0.510
45739.63392	0.0335	0.758	45749.35842	0.0697	0.501
45739.63462	0.0341	0.757	45749.35911	0.0703	0.505
45739.63531	0.0346	0.747	45749.35980	0.0709	0.497
45739.63601	0.0352	0.750	45749.36361	0.0740	0.490
45739.63670	0.0358	0.734	45749.36431	0.0746	0.476
45739.63740	0.0364	0.740	45749.36500	0.0752	0.483
45739.63809	0.0369	0.722	45749.36570	0.0757	0.479
45739.63878	0.0375	0.723	45749.36639	0.0763	0.461
45739.63948	0.0381	0.723	45749.36708	0.0769	0.470
45739.64017	0.0387	0.722	45749.36778	0.0775	0.459
45739.64087	0.0392	0.712	45749.36848	0.0780	0.465
45739.64156	0.0398	0.705	45749.36917	0.0786	0.450
45739.64226	0.0404	0.707	45749.36986	0.0792	0.456
45739.64295	0.0410	0.699	45749.37056	0.0798	0.452
			45749.37125	0.0803	0.461
			45749.37195	0.0809	0.450
			45749.37264	0.0815	0.439
			45749.37333	0.0821	0.446
			45749.37403	0.0826	0.438
			45749.37473	0.0832	0.434
			45749.37542	0.0838	0.440
			45749.37611	0.0844	0.433
			45749.37681	0.0849	0.422
			45749.38704	0.0934	0.406
			45749.38773	0.0940	0.396
			45749.38843	0.0945	0.390
			45749.38912	0.0951	0.379
			45749.38982	0.0957	0.393
			45749.39051	0.0963	0.383
			45749.39121	0.0968	0.376
			45749.39190	0.0974	0.374
			45749.39259	0.0980	0.375
			45749.39329	0.0985	0.357
			45749.39398	0.0991	0.363
			45749.39467	0.0997	0.373
			45749.39537	0.1003	0.366
			45749.39607	0.1008	0.364
			45749.39676	0.1014	0.360

1984 Feb 18/19

H. J. D.

Phase

(V-C)

continued

45749.39745	0.1020	0.360	46077.30926	0.0856	0.414
45749.39815	0.1026	0.365	46077.30995	0.0862	0.411
45749.39884	0.1031	0.357	46077.31065	0.0868	0.415
45749.39954	0.1037	0.357	46077.31134	0.0874	0.403
45749.40023	0.1043	0.351	46077.31204	0.0879	0.408
45749.41696	0.1181	0.316	46077.31273	0.0885	0.402
45749.41765	0.1187	0.294	46077.31342	0.0891	0.407
45749.41834	0.1193	0.311	46077.31412	0.0897	0.398
45749.41904	0.1198	0.320	46077.31481	0.0902	0.398
45749.41974	0.1204	0.308	46077.31943	0.0940	0.389
45749.42043	0.1210	0.304	46077.32013	0.0946	0.387
45749.42112	0.1216	0.303	46077.32082	0.0952	0.378
45749.42182	0.1221	0.301	46077.32151	0.0958	0.371
45749.42251	0.1227	0.302	46077.32221	0.0963	0.381
45749.42321	0.1233	0.306	46077.32290	0.0969	0.378
45749.42390	0.1238	0.292	46077.32360	0.0975	0.375
45749.42460	0.1244	0.302	46077.32429	0.0981	0.370
45749.42529	0.1250	0.308	46077.32499	0.0986	0.370
45749.42598	0.1256	0.290	46077.32568	0.0992	0.362
45749.42668	0.1261	0.301	46077.32638	0.0998	0.363
45749.42737	0.1267	0.293	46077.32707	0.1004	0.349
45749.42807	0.1273	0.298	46077.32776	0.1009	0.363
45749.42876	0.1279	0.293	46077.32846	0.1015	0.349
45749.42945	0.1284	0.287	46077.32915	0.1021	0.341
45749.43015	0.1290	0.282	46077.32985	0.1027	0.346
45749.44099	0.1380	0.280	46077.33124	0.1038	0.347
45749.44169	0.1385	0.277	46077.33193	0.1044	0.353
45749.44238	0.1391	0.273	46077.33263	0.1049	0.355
45749.44308	0.1397	0.269	46077.36180	0.1291	0.278
45749.44377	0.1403	0.276	46077.36250	0.1296	0.275
45749.44447	0.1408	0.270	46077.36319	0.1302	0.279
45749.44516	0.1414	0.262	46077.36389	0.1308	0.279
45749.44586	0.1420	0.268	46077.36458	0.1314	0.273
45749.44655	0.1426	0.260	46077.36527	0.1319	0.279
45749.44724	0.1431	0.264	46077.36596	0.1325	0.270
45749.44794	0.1437	0.264	46077.36665	0.1331	0.265
45749.44864	0.1443	0.263	46077.36735	0.1336	0.268
45749.44933	0.1449	0.271	46077.36804	0.1342	0.270
45749.45002	0.1454	0.263	46077.36873	0.1348	0.273
45749.45072	0.1460	0.272	46077.36943	0.1354	0.271
45749.45141	0.1466	0.254	46077.37013	0.1359	0.269
45749.45211	0.1472	0.260	46077.37082	0.1365	0.266
45749.45280	0.1477	0.254	46077.37151	0.1371	0.270
45749.45349	0.1483	0.252	46077.37221	0.1377	0.267
45749.45419	0.1489	0.265	46077.37290	0.1382	0.265
			46077.37360	0.1388	0.263
			46077.37429	0.1394	0.260
			46077.37498	0.1399	0.260
			46077.38642	0.1494	0.245
			46077.38712	0.1500	0.248
			46077.38781	0.1506	0.245
			46077.38851	0.1511	0.241
			46077.38920	0.1517	0.240
			46077.38989	0.1523	0.244
			46077.39059	0.1528	0.244
			46077.39128	0.1534	0.243

1985 Jan 11/12

H. J. D.	Phase	(V-C)
46077.30509	0.0822	0.435
46077.30579	0.0828	0.439
46077.30648	0.0833	0.428
46077.30717	0.0839	0.419
46077.30787	0.0845	0.422
46077.30856	0.0851	0.421

continued

46077.39198	0.1540	0.243	46077.45443	0.2056	0.181
46077.39267	0.1546	0.241	46077.45513	0.2062	0.183
46077.39337	0.1551	0.241	46077.45582	0.2068	0.182
46077.39406	0.1557	0.239	46077.45652	0.2073	0.186
46077.39474	0.1563	0.235	46077.45721	0.2079	0.183
46077.39544	0.1569	0.235	46077.45790	0.2085	0.178
46077.39613	0.1574	0.238	46077.45860	0.2090	0.177
46077.39683	0.1580	0.238	46077.45929	0.2096	0.176
46077.39752	0.1586	0.233	46077.45999	0.2102	0.183
46077.39822	0.1591	0.232	46077.46068	0.2108	0.186
46077.39891	0.1597	0.230	46077.46138	0.2113	0.176
46077.39960	0.1603	0.236	46077.46207	0.2119	0.180
46077.40591	0.1655	0.229	46077.46276	0.2125	0.174
46077.40661	0.1661	0.228	46077.46346	0.2131	0.174
46077.40730	0.1667	0.226	46077.46415	0.2136	0.173
46077.40799	0.1672	0.227	46077.46485	0.2142	0.173
46077.40869	0.1678	0.231	46077.47233	0.2204	0.172
46077.40939	0.1684	0.226	46077.47302	0.2210	0.176
46077.41008	0.1690	0.226	46077.47371	0.2215	0.168
46077.41077	0.1695	0.224	46077.47441	0.2221	0.173
46077.41147	0.1701	0.227	46077.47510	0.2227	0.173
46077.41215	0.1707	0.222	46077.47580	0.2233	0.171
46077.41285	0.1712	0.217	46077.47649	0.2238	0.172
46077.41354	0.1718	0.222	46077.47718	0.2244	0.170
46077.41424	0.1724	0.220	46077.47788	0.2250	0.172
46077.41493	0.1730	0.216	46077.47858	0.2256	0.172
46077.41562	0.1735	0.217	46077.47927	0.2261	0.171
46077.41632	0.1741	0.216	46077.47996	0.2267	0.170
46077.41701	0.1747	0.212	46077.48066	0.2273	0.169
46077.41770	0.1753	0.219	46077.48135	0.2279	0.169
46077.41840	0.1758	0.211	46077.48205	0.2284	0.172
46077.41910	0.1764	0.214	46077.48274	0.2290	0.168
46077.42598	0.1821	0.201	46077.48344	0.2296	0.170
46077.42668	0.1827	0.208	46077.48413	0.2301	0.167
46077.42737	0.1832	0.202	46077.48483	0.2307	0.170
46077.42806	0.1838	0.203	46077.48552	0.2313	0.170
46077.42876	0.1844	0.208	46077.49121	0.2360	0.169
46077.42946	0.1850	0.202	46077.49191	0.2366	0.168
46077.43015	0.1855	0.205	46077.49260	0.2372	0.167
46077.43084	0.1861	0.206	46077.49330	0.2377	0.168
46077.43154	0.1867	0.207	46077.49399	0.2383	0.166
46077.43223	0.1873	0.201	46077.49469	0.2389	0.161
46077.43293	0.1878	0.203	46077.49538	0.2394	0.162
46077.43362	0.1884	0.194	46077.49607	0.2400	0.164
46077.43431	0.1890	0.195	46077.49677	0.2406	0.163
46077.43501	0.1896	0.193	46077.49746	0.2412	0.166
46077.43571	0.1901	0.196	46077.49816	0.2417	0.164
46077.43640	0.1907	0.191	46077.49885	0.2423	0.165
46077.43709	0.1913	0.197	46077.49955	0.2429	0.162
46077.43779	0.1919	0.199	46077.50024	0.2435	0.158
46077.43848	0.1924	0.198	46077.50094	0.2440	0.164
46077.43918	0.1930	0.191	46077.50163	0.2446	0.163
46077.45165	0.2033	0.184	46077.50232	0.2452	0.163
46077.45235	0.2039	0.180	46077.50302	0.2458	0.160
46077.45304	0.2045	0.178	46077.50372	0.2463	0.166
46077.45374	0.2050	0.176	46077.50441	0.2469	0.161

continued

46077.50844	0.2502	0.156	46077.58155	0.3107	0.186
46077.50913	0.2508	0.153	46077.58224	0.3112	0.184
46077.50982	0.2514	0.157	46077.58294	0.3118	0.188
46077.51052	0.2520	0.154	46077.58363	0.3124	0.184
46077.51121	0.2525	0.152	46077.58433	0.3130	0.193
46077.52359	0.2628	0.167	46077.58502	0.3135	0.178
46077.52427	0.2633	0.169	46077.58572	0.3141	0.191
46077.52496	0.2639	0.169	46077.58641	0.3147	0.184
46077.52566	0.2645	0.161	46077.58710	0.3152	0.184
46077.52635	0.2650	0.170	46077.59309	0.3202	0.185
46077.52705	0.2656	0.167	46077.59378	0.3208	0.201
46077.52774	0.2662	0.164	46077.59448	0.3213	0.187
46077.52844	0.2668	0.167	46077.59517	0.3219	0.193
46077.52913	0.2673	0.161	46077.59587	0.3225	0.191
46077.52982	0.2679	0.165	46077.59654	0.3230	0.199
46077.53052	0.2685	0.167	46077.59723	0.3236	0.198
46077.53122	0.2691	0.170	46077.59793	0.3242	0.188
46077.53190	0.2696	0.168	46077.59862	0.3248	0.201
46077.53259	0.2702	0.160	46077.59932	0.3253	0.197
46077.53328	0.2708	0.167	46077.60001	0.3259	0.197
46077.53398	0.2713	0.166	46077.60070	0.3265	0.198
46077.53467	0.2719	0.161	46077.60140	0.3271	0.202
46077.53537	0.2725	0.166	46077.60209	0.3276	0.197
46077.53606	0.2731	0.157	46077.60279	0.3282	0.200
46077.53676	0.2736	0.166	46077.60348	0.3288	0.192
46077.54304	0.2788	0.166	46077.60418	0.3294	0.200
46077.54373	0.2794	0.166	46077.60487	0.3299	0.208
46077.54443	0.2800	0.174	46077.60557	0.3305	0.208
46077.54513	0.2806	0.166	46077.60626	0.3311	0.193
46077.54582	0.2811	0.171	46077.62379	0.3456	0.213
46077.54651	0.2817	0.171	46077.62449	0.3461	0.217
46077.54721	0.2823	0.171	46077.62518	0.3467	0.216
46077.54789	0.2828	0.170	46077.62588	0.3473	0.214
46077.54858	0.2834	0.168	46077.62657	0.3479	0.219
46077.54928	0.2840	0.168	46077.62727	0.3484	0.215
46077.54998	0.2846	0.167	46077.62796	0.3490	0.224
46077.55067	0.2851	0.168	46077.62866	0.3496	0.210
46077.55136	0.2857	0.168	46077.62935	0.3502	0.219
46077.55206	0.2863	0.167	46077.63004	0.3507	0.222
46077.55275	0.2869	0.167	46077.63074	0.3513	0.221
46077.55345	0.2874	0.172	46077.63143	0.3519	0.217
46077.55414	0.2880	0.172	46077.63213	0.3525	0.224
46077.55484	0.2886	0.167	46077.63282	0.3530	0.220
46077.55553	0.2892	0.169	46077.63352	0.3536	0.217
46077.55623	0.2897	0.171	46077.63421	0.3542	0.217
46077.57391	0.3043	0.182	46077.63491	0.3547	0.222
46077.57460	0.3049	0.182	46077.63560	0.3553	0.221
46077.57530	0.3055	0.181	46077.63629	0.3559	0.224
46077.57599	0.3061	0.180	46077.63699	0.3565	0.220
46077.57669	0.3066	0.180	46077.64222	0.3608	0.235
46077.57738	0.3072	0.180	46077.64291	0.3614	0.226
46077.57808	0.3078	0.181	46077.64361	0.3619	0.245
46077.57877	0.3084	0.177	46077.64431	0.3625	0.234
46077.57947	0.3089	0.176	46077.64500	0.3631	0.233
46077.58016	0.3095	0.189	46077.64569	0.3637	0.237
46077.58085	0.3101	0.180	46077.64639	0.3642	0.226

continued

46092.34417	0.5104	0.633	46092.39701	0.5540	0.470
46092.34487	0.5109	0.629	46092.39770	0.5546	0.469
46092.34556	0.5115	0.630	46092.39839	0.5552	0.463
46092.34625	0.5121	0.627	46092.39909	0.5557	0.467
46092.34695	0.5127	0.625	46092.41447	0.5685	0.418
46092.34764	0.5132	0.625	46092.41516	0.5690	0.409
46092.34833	0.5138	0.626	46092.41586	0.5696	0.409
46092.34902	0.5144	0.620	46092.41655	0.5702	0.410
46092.34969	0.5149	0.627	46092.41725	0.5708	0.404
46092.35038	0.5155	0.621	46092.41794	0.5713	0.397
46092.35108	0.5161	0.615	46092.41863	0.5719	0.398
46092.35178	0.5166	0.623	46092.41933	0.5725	0.401
46092.35247	0.5172	0.616	46092.42002	0.5730	0.397
46092.35316	0.5178	0.612	46092.42071	0.5736	0.396
46092.35386	0.5184	0.614	46092.42140	0.5742	0.388
46092.35455	0.5189	0.614	46092.42210	0.5748	0.383
46092.35525	0.5195	0.608	46092.42279	0.5753	0.389
46092.35593	0.5201	0.607	46092.42348	0.5759	0.384
46092.35662	0.5207	0.606	46092.42418	0.5765	0.375
46092.35732	0.5212	0.606	46092.42488	0.5771	0.375
46092.36206	0.5252	0.594	46092.42557	0.5776	0.375
46092.36275	0.5257	0.586	46092.42626	0.5782	0.377
46092.36344	0.5263	0.585	46092.42696	0.5788	0.374
46092.36413	0.5269	0.583	46092.42765	0.5794	0.372
46092.36483	0.5274	0.585	46092.43310	0.5839	0.355
46092.36553	0.5280	0.584	46092.43379	0.5844	0.353
46092.36622	0.5286	0.572	46092.43449	0.5850	0.352
46092.36691	0.5292	0.579	46092.43518	0.5856	0.349
46092.36761	0.5297	0.579	46092.43587	0.5861	0.349
46092.36830	0.5303	0.571	46092.43656	0.5867	0.349
46092.36899	0.5309	0.573	46092.43724	0.5873	0.348
46092.36969	0.5315	0.567	46092.43793	0.5878	0.351
46092.37038	0.5320	0.567	46092.43863	0.5884	0.338
46092.37108	0.5326	0.562	46092.43932	0.5890	0.343
46092.37177	0.5332	0.563	46092.44001	0.5896	0.346
46092.37247	0.5337	0.560	46092.44071	0.5901	0.340
46092.37316	0.5343	0.555	46092.44140	0.5907	0.343
46092.37386	0.5349	0.561	46092.44210	0.5913	0.338
46092.37455	0.5355	0.554	46092.44279	0.5919	0.335
46092.37524	0.5360	0.549	46092.44347	0.5924	0.338
46092.38597	0.5449	0.512	46092.44417	0.5930	0.335
46092.38666	0.5455	0.512	46092.44486	0.5936	0.324
46092.38735	0.5460	0.504	46092.44556	0.5941	0.330
46092.38805	0.5466	0.504	46092.44625	0.5947	0.326
46092.38874	0.5472	0.498	46092.45175	0.5993	0.312
46092.38943	0.5478	0.501	46092.45245	0.5998	0.314
46092.39013	0.5483	0.497	46092.45311	0.6004	0.310
46092.39082	0.5489	0.493	46092.45380	0.6010	0.303
46092.39151	0.5495	0.494	46092.45450	0.6015	0.300
46092.39220	0.5501	0.492	46092.45520	0.6021	0.307
46092.39290	0.5506	0.489	46092.45589	0.6027	0.301
46092.39356	0.5512	0.485	46092.45658	0.6033	0.301
46092.39425	0.5517	0.481	46092.45728	0.6038	0.301
46092.39492	0.5523	0.477	46092.45797	0.6044	0.291
46092.39562	0.5529	0.474	46092.45867	0.6050	0.297
46092.39631	0.5535	0.471	46092.45935	0.6055	0.300

continued

46092.46005	0.6061	0.293	46092.53219	0.6657	0.205
46092.46074	0.6067	0.295	46092.53288	0.6663	0.204
46092.46143	0.6073	0.294	46092.53357	0.6669	0.201
46092.46213	0.6078	0.294	46092.53426	0.6675	0.205
46092.46282	0.6084	0.291	46092.53496	0.6680	0.203
46092.46352	0.6090	0.289	46092.53564	0.6686	0.201
46092.46421	0.6096	0.283	46092.53634	0.6692	0.204
46092.46491	0.6101	0.282	46092.53703	0.6697	0.208
46092.48241	0.6246	0.249	46092.53772	0.6703	0.200
46092.48311	0.6252	0.251	46092.53871	0.6711	0.202
46092.48380	0.6258	0.245	46092.53940	0.6717	0.195
46092.48450	0.6263	0.244	46092.54010	0.6723	0.201
46092.48519	0.6269	0.245	46092.54079	0.6728	0.195
46092.48589	0.6275	0.249	46092.54148	0.6734	0.204
46092.48657	0.6280	0.245	46092.54217	0.6740	0.199
46092.48727	0.6286	0.245	46092.54286	0.6746	0.198
46092.48797	0.6292	0.245	46092.54356	0.6751	0.202
46092.48866	0.6298	0.242	46092.54425	0.6757	0.201
46092.48935	0.6303	0.245	46092.54495	0.6763	0.200
46092.49004	0.6309	0.240	46092.54563	0.6769	0.201
46092.49074	0.6315	0.245	46092.54633	0.6774	0.200
46092.49143	0.6321	0.241	46092.54702	0.6780	0.192
46092.49212	0.6326	0.233	46092.55598	0.6854	0.186
46092.49281	0.6332	0.244	46092.55667	0.6860	0.185
46092.49350	0.6338	0.241	46092.55737	0.6866	0.189
46092.49419	0.6343	0.239	46092.55806	0.6871	0.188
46092.49489	0.6349	0.235	46092.55876	0.6877	0.186
46092.49558	0.6355	0.234	46092.55945	0.6883	0.184
46092.50684	0.6448	0.224	46092.56015	0.6888	0.187
46092.50754	0.6454	0.216	46092.56084	0.6894	0.181
46092.50823	0.6459	0.221	46092.56153	0.6900	0.183
46092.50892	0.6465	0.221	46092.56222	0.6906	0.186
46092.50961	0.6471	0.218	46092.56291	0.6911	0.184
46092.51031	0.6477	0.217	46092.56361	0.6917	0.192
46092.51100	0.6482	0.214	46092.56430	0.6923	0.185
46092.51169	0.6488	0.217	46092.56500	0.6929	0.178
46092.51239	0.6494	0.218	46092.56569	0.6934	0.180
46092.51308	0.6500	0.217	46092.56638	0.6940	0.181
46092.51378	0.6505	0.214	46092.56708	0.6946	0.181
46092.51445	0.6511	0.209	46092.56778	0.6951	0.189
46092.51512	0.6516	0.222	46092.56847	0.6957	0.183
46092.51667	0.6529	0.215	46092.56916	0.6963	0.181
46092.51736	0.6535	0.216	46092.57680	0.7026	0.185
46092.51805	0.6541	0.220	46092.57749	0.7032	0.178
46092.51875	0.6546	0.218	46092.57818	0.7037	0.183
46092.51944	0.6552	0.217	46092.57886	0.7043	0.172
46092.52013	0.6558	0.218	46092.57956	0.7049	0.181
46092.52082	0.6563	0.217	46092.58024	0.7055	0.175
46092.52151	0.6569	0.210	46092.58094	0.7060	0.176
46092.52221	0.6575	0.212	46092.58163	0.7066	0.171
46092.52290	0.6581	0.211	46092.58232	0.7072	0.177
46092.52360	0.6586	0.212	46092.58302	0.7077	0.175
46092.52429	0.6592	0.219	46092.58371	0.7083	0.177
46092.53011	0.6640	0.205	46092.58440	0.7089	0.179
46092.53080	0.6646	0.212	46092.58509	0.7095	0.175
46092.53150	0.6652	0.208	46092.58579	0.7100	0.179

continued

46092.58649	0.7106	0.178
46092.58718	0.7112	0.175
46092.58787	0.7118	0.174
46092.58857	0.7123	0.169
46092.58926	0.7129	0.171
46092.58996	0.7135	0.174
46092.59722	0.7195	0.164
46092.59791	0.7201	0.168
46092.59861	0.7206	0.169
46092.59931	0.7212	0.167
46092.60000	0.7218	0.165
46092.60069	0.7223	0.170
46092.60137	0.7229	0.170
46092.60207	0.7235	0.172
46092.60276	0.7241	0.166
46092.60345	0.7246	0.162
46092.60415	0.7252	0.167
46092.60484	0.7258	0.165
46092.60551	0.7263	0.174
46092.60620	0.7269	0.167
46092.60690	0.7275	0.163
46092.60759	0.7281	0.166
46092.60829	0.7286	0.169
46092.60898	0.7292	0.169
46092.60968	0.7298	0.161

Table 4 : Photoelectric times of minima.

H.J.D.	Error (days)	Epoch (cycles)	Source reference
-2400000			
33187.434		-5764.0	Strzalkowski and Piotrowski, 1951.
35525.3101		-3832.0	Lavrov, 1960.
39955.413	± 0.0007	-171.0	Kreiner and Tremko, 1978.
40162.3358		0.0	Kizilirmak and Pohl, 1970.
40175.6479	± 0.0003	11.0	Kreiner and Tremko, 1978.
40200.453	± 0.002	31.5	Kreiner and Tremko, 1978.
40201.665	± 0.002	32.5	Kreiner and Tremko, 1978.
40204.6895	± 0.001	35.0	Kreiner and Tremko, 1978.
40271.241		90.0	Kreiner and Tremko, 1978.
40289.396		105.0	Kizilirmak and Pohl, 1970.
40315.4147	± 0.0005	126.5	Kreiner and Tremko, 1978.
40491.478		272.0	Kizilirmak and Pohl, 1970.
40640.321		395.0	Bondarenko, 1974.
40683.277		430.5	Bondarenko, 1974.
41677.3552		1252.0	Kizilirmak and Pohl, 1974.
41691.271		1263.5	Kizilirmak and Pohl, 1974.
41692.4819		1264.5	Kizilirmak and Pohl, 1974.
41763.275		1323.0	Kizilirmak and Pohl, 1974.
41769.3242		1328.0	Kizilirmak and Pohl, 1974.
41775.372		1333.0	Kizilirmak and Pohl, 1974.
41957.4886		1483.5	Kizilirmak and Pohl, 1974.
42132.3431		1628.0	Kizilirmak and Pohl, 1975.
42403.4045		1852.0	Kizilirmak and Pohl, 1975.
42790.6298		2172.0	Chambliss, 1977.
42793.6549		2174.5	Chambliss, 1977.
43099.8040		2427.5	Chambliss, 1977.
43113.7212		2439.0	Chambliss, 1977.
43192.3749	± 0.0008	2504.0	Kreiner and Tremko, 1978.
43510.6275		2767.0	Chambliss and Leung, 1979
45739.5929	± 0.0002	4609.0	This paper.
46092.3328	± 0.0002	4900.5	This paper.

Table 5 : Light-curve solutions for SX Aur.

Secondary rotation	Synchronous	Synchronous	Non-synchronous
q (spectroscopic)	0.542	0.542	0.542
T ₁ K (polar)	22000 (adopted)	25000 (adopted)	22000 (adopted)
Escat ₁ (adopted)	0.31	0.38	0.31
Escat ₂ (adopted)	0.20	0.27	0.20
β ₁ (adopted)	0.25	0.25	0.25
β ₂ (adopted)	0.25	0.25	0.25
i (degrees)	82.82 ±7	82.87 ±6	81.32 ±10
T ₂ K (polar)	16900 ±20	18850 ±20	16660 ±30
r ₁ (polar)	0.4062 ±3	0.4069 ±3	0.4008 ±8
r ₁ (mean)	0.4315 ±3	0.4324 ±3	0.4246 ±8
r ₂ (polar)	0.3058 ±4	0.3054 ±4	0.3242 ±9
r ₂ (mean)	0.3254 ±4	0.3254 ±4	0.3503 ±9
χ ² (mmag.) ²	44.00	43.98	46.98
L ₂ /L ₁	0.346	0.345	0.399
r.m.s. error (mmag.)	5.6	5.6	5.7

The mean radii of the components presented here should be compared with the Roche-lobe radii of the primary and secondary for q=0.542 of 0.4328 and 0.3274 respectively.

Table 6 : Light-curve solutions for TT Aur.

Blending correction	Included	Not included
q (spectroscopic)	0.645	0.676
T ₁ K (polar)	23600 (adopted)	23600 (adopted)
Escat ₁ (adopted)	0.34	0.34
Escat ₂ (adopted)	0.22	0.22
β ₁ (adopted)	0.25	0.25
β ₂ (adopted)	0.25	0.25
i (degrees)	86.717 ±1	86.79 ±2
T ₂ K (polar)	18460 ±10	18400 ±10
r ₁ (polar)	0.3199 ±1	0.3220 ±1
r ₁ (mean)	0.3297 ±1	0.3325 ±1
r ₂ (polar)	0.3185 ±2	0.3202 ±3
r ₂ (mean)	0.3385 ±2	0.3398 ±3
χ ² (mmag.) ²	58.60	58.91
L ₂ /L ₁	0.641	0.631
r.m.s. error (mmag.)	6.0	6.1

The mean radii of the components in this table should be compared with the Roche-lobe radii for the primary and secondary of 0.4174 and 0.3417 respectively (q=0.645) and similarly 0.4132 and 0.3456 respectively (q=0.676).

Table 7 : Astrophysical data for SX Aur.

Absolute dimensions:	Primary	Secondary
M/M_{\odot}	10.3 ± 0.4	5.6 ± 0.3
R/R_{\odot}	5.17 ± 0.09	3.90 ± 0.07
$\log g$ (cgs)	4.02 ± 0.03	4.00 ± 0.03
Photometric data for the 22000K primary:		
$T_{\text{eff}}(\text{K})$	22000 ± 1000	16900 ± 1000
M_{bol}	$-4.^{\text{m}}68 \pm 0.^{\text{m}}20$	$-2.^{\text{m}}92 \pm 0.^{\text{m}}26$
$\log (L/L_{\odot})$	3.75 ± 0.08	3.05 ± 0.10
B.C.	$-2.^{\text{m}}23$	$-1.^{\text{m}}65$
M_{v}	$-2.^{\text{m}}45 \pm 0.^{\text{m}}20$	$-1.^{\text{m}}28 \pm 0.^{\text{m}}26$
$E_{\text{(B-V)}}$	$0.^{\text{m}}24$ (Chambliss and Leung, 1979)	
Distance (pc)	1200 ± 200	
Photometric data for the 25000K primary:		
$T_{\text{eff}}(\text{K})$	25000 ± 1000	18900 ± 1000
M_{bol}	$-5.^{\text{m}}24 \pm 0.^{\text{m}}18$	$-3.^{\text{m}}40 \pm 0.^{\text{m}}23$
$\log (L/L_{\odot})$	3.97 ± 0.07	3.24 ± 0.09
B.C.	$-2.^{\text{m}}50$	$-1.^{\text{m}}89$
M_{v}	$-2.^{\text{m}}74 \pm 0.^{\text{m}}19$	$-1.^{\text{m}}50 \pm 0.^{\text{m}}23$
$E_{\text{(B-V)}}$	$0.^{\text{m}}24$ (Chambliss and Leung, 1979)	
Distance (pc)	1400 ± 200	

Table 8 : Astrophysical data for TT Aur.

Absolute dimensions:	Primary	Secondary
M/M _☉	8.58 ± 0.1	5.56 ± 0.1
R/R _☉	4.06 ± 0.03	4.17 ± 0.03
log g (cgs)	4.16 ± 0.01	3.94 ± 0.01
Photometric data:		
T _{eff} (K)	23600 ± 1000	18500 ± 1000
M _{bol}	-4. ^m 46 ± 0. ^m 18	-3. ^m 46 ± 0. ^m 24
log (L/L _☉)	3.66 ± 0.07	3.26 ± 0.09
B.C.	-2. ^m 37	-1. ^m 84
M _V	-2. ^m 09 ± 0. ^m 19	-1. ^m 62 ± 0. ^m 24
E _(B-V)	0. ^m 285 (Popper and Dumont, 1977)	
Distance (pc)	1100 ± 200	

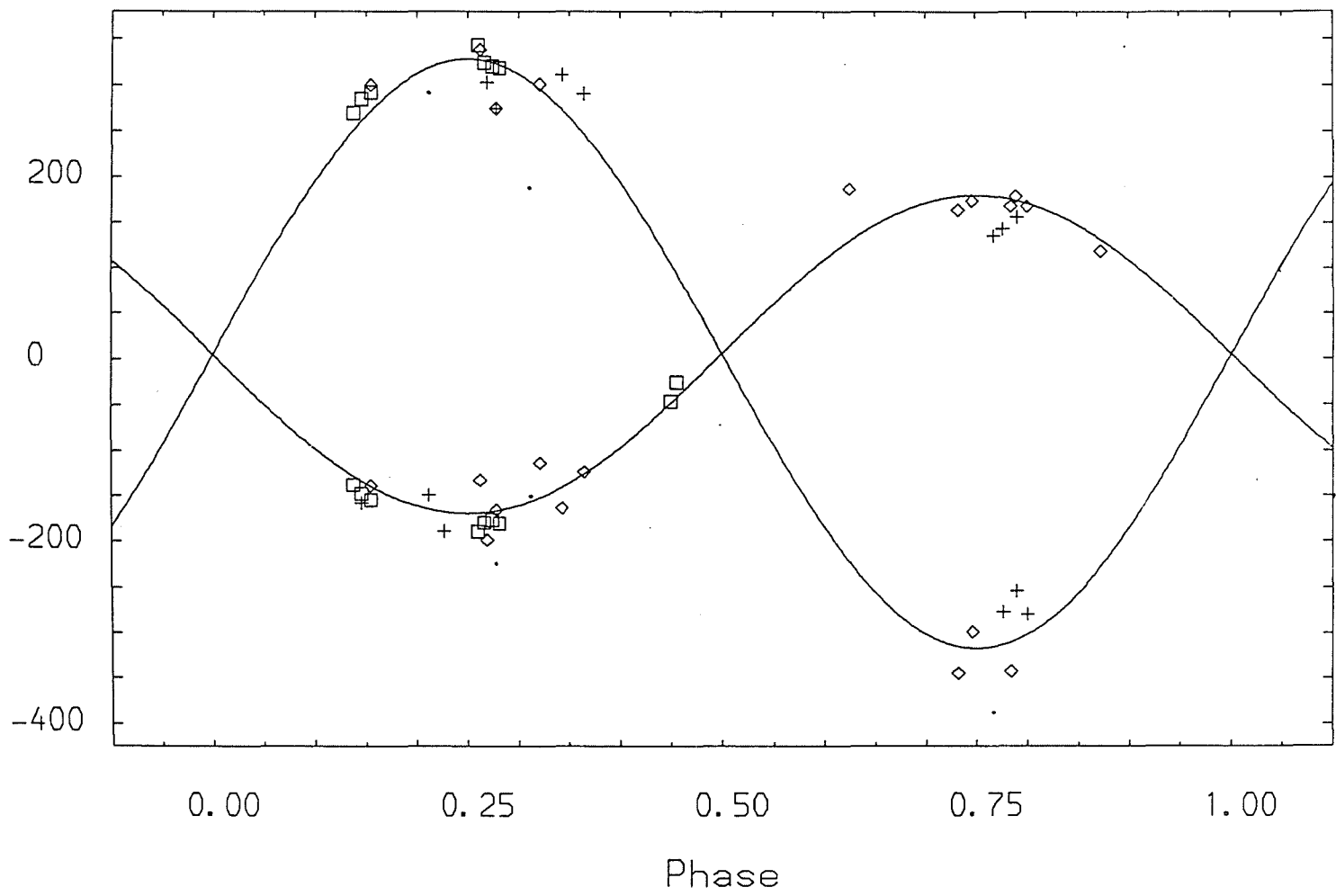


Figure 1.

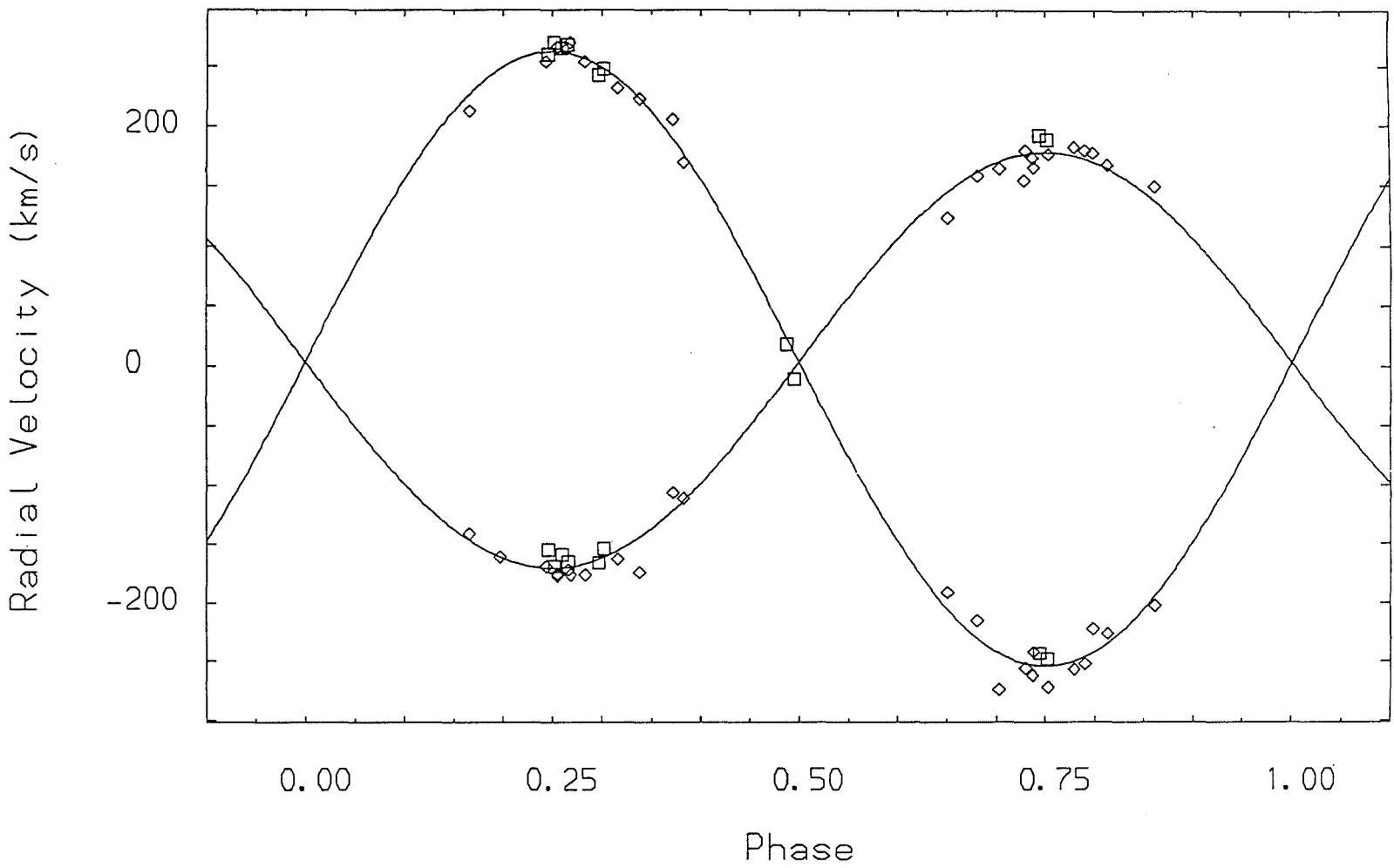


Figure 2.

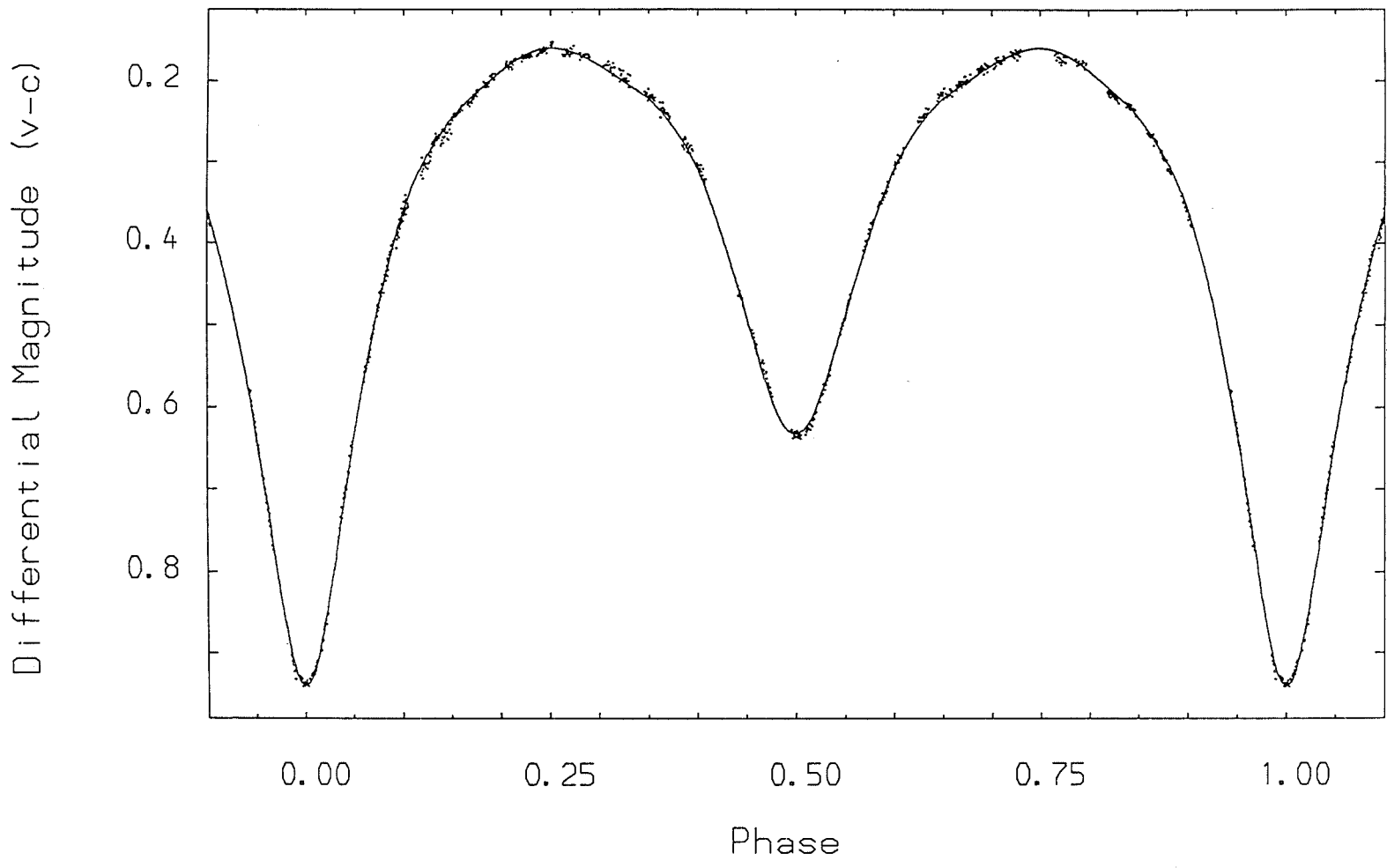


Figure 3.

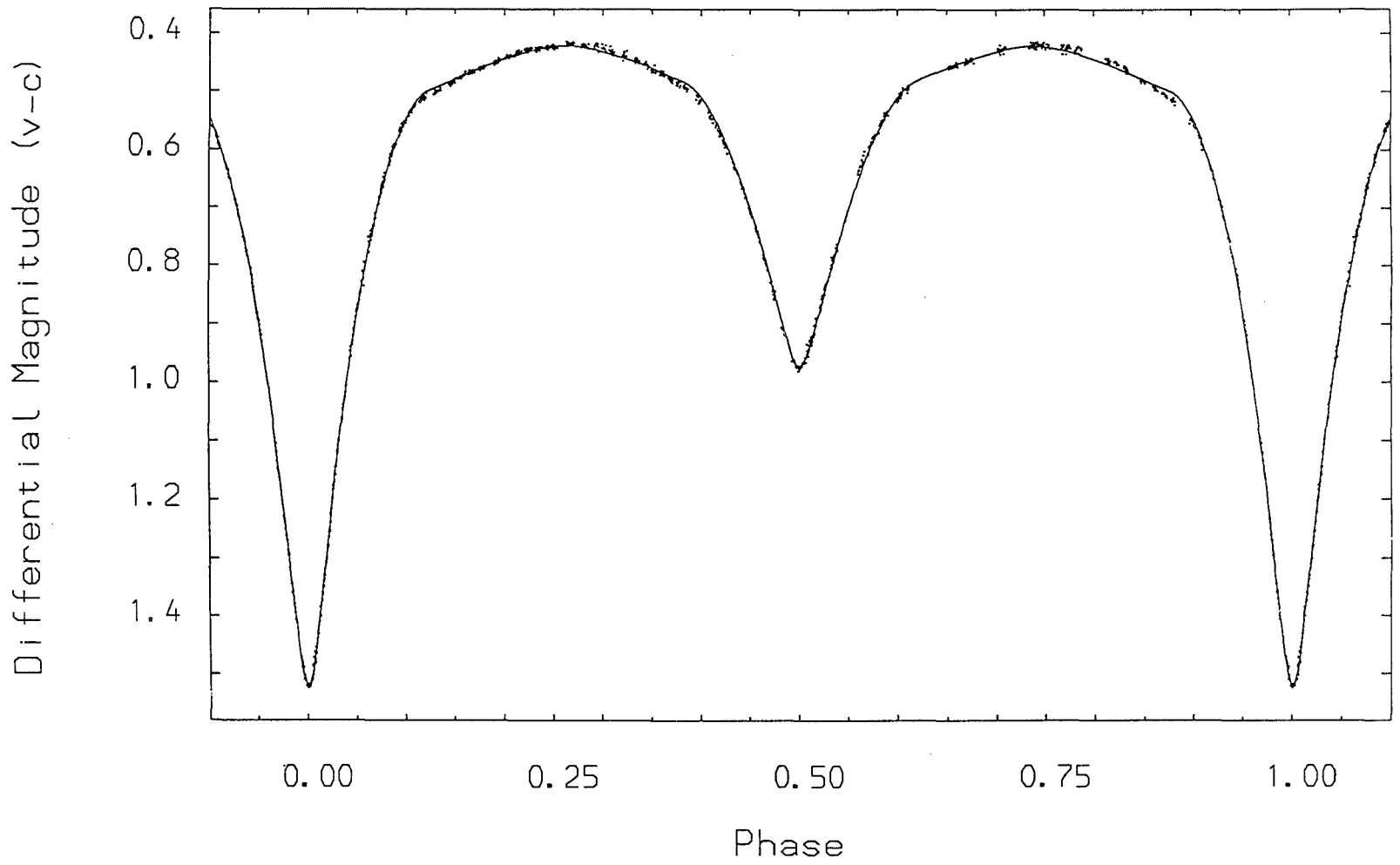


Figure 4.

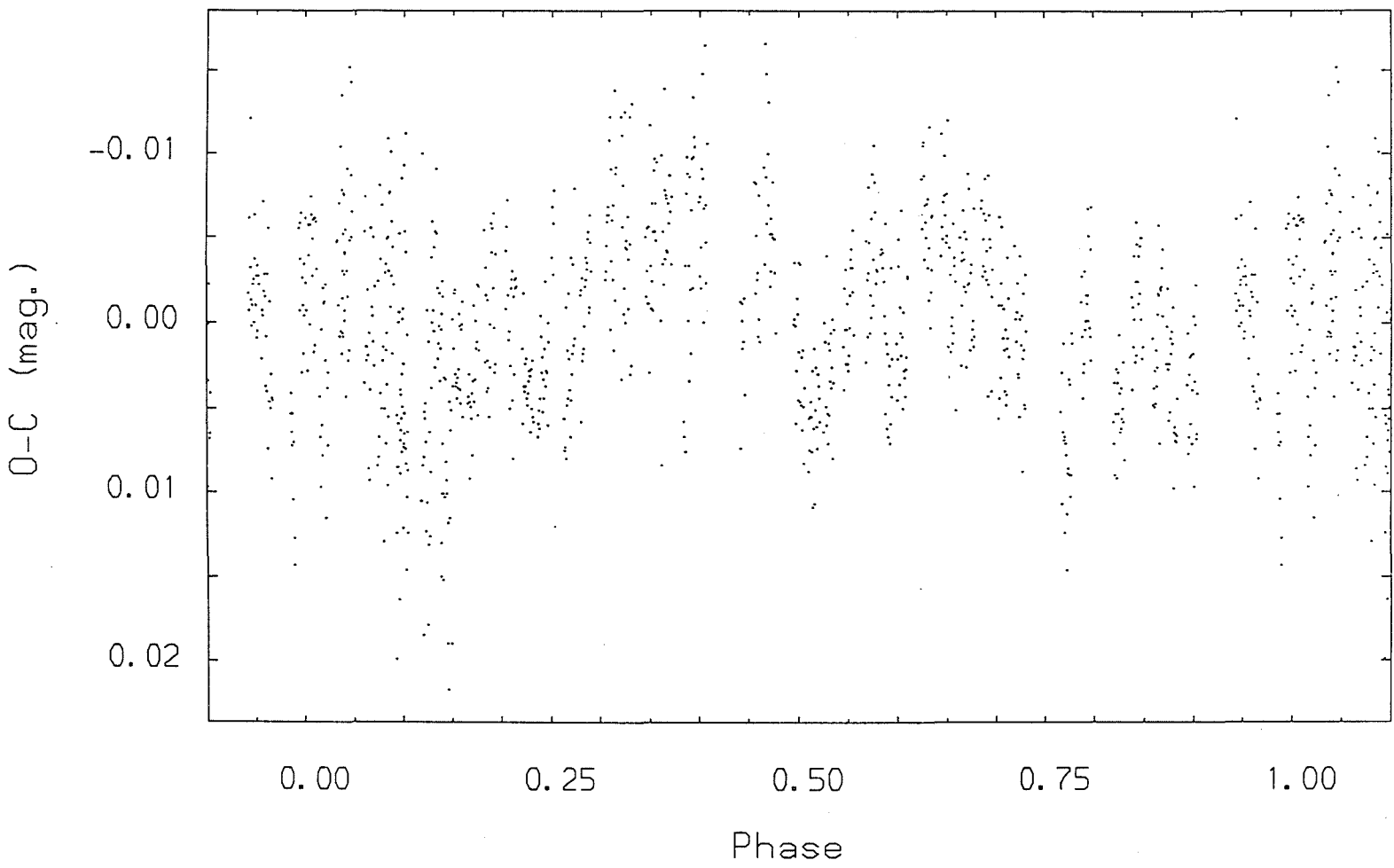


Figure 5.

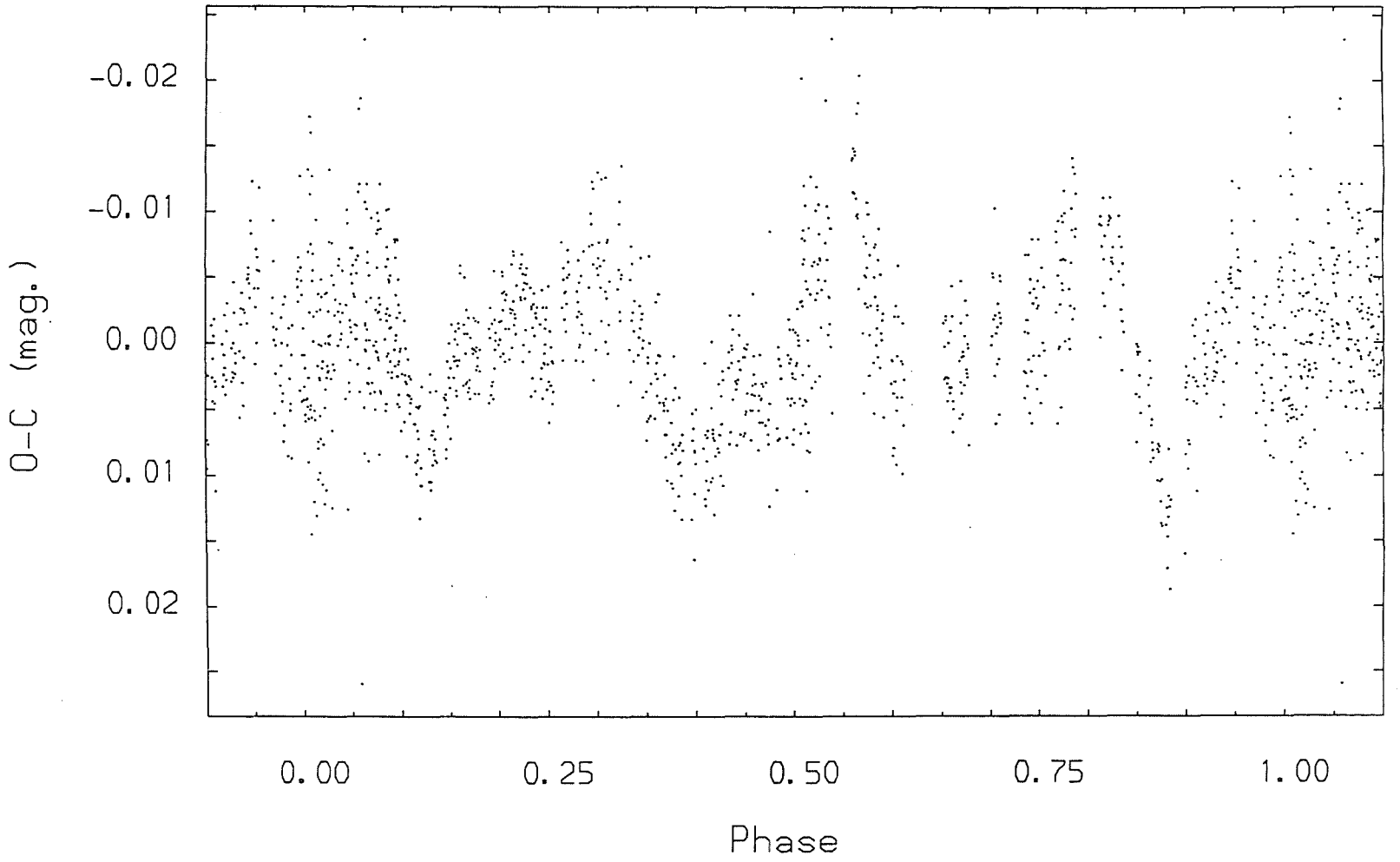


Figure 6.

CHAPTER 6

A photometric and spectroscopic study of the early-type binary
V1182 Aquilae.

A photometric and spectroscopic study of the early-type binary

V1182 Aquilae.

S.A.Bell, R.W.Hilditch and A.J.Adamson

University Observatory, Buchanan Gardens, St. Andrews,

Fife, KY16 9LZ, Scotland.

Received _____

Correspondence to:-

S.A.Bell,
University Observatory,
Buchanan Gardens,
St. Andrews, Fife,
KY16 9LZ,
Scotland.

Summary

We present new Strömgren photometry and medium dispersion spectroscopy of the early-type binary V1182 Aql. The masses and radii of the two components are found to be (37.8 ± 1.6) and (13.5 ± 0.5) solar masses and (8.8 ± 0.2) and (5.9 ± 0.1) solar radii respectively. A lower limit to the primary temperature has been established and interpretation of the evolutionary status of the system is closely linked to the adopted primary temperature.

1) Introduction

The early-type binary system V1182 Aql (HD 175514, SAO 124049: Sp. type O8V + B3) has been the subject of spectroscopic and photometric studies by Vitrichenko (1971), who improved the previous preliminary results of studies by Vitrichenko (1967) and Burnashey and Vitrichenko (1970). A single-lined radial velocity curve was obtained by Vitrichenko (1971), from which he concluded that the orbit was of small eccentricity and that the mass function $f(m) = 0.63$. Vitrichenko estimated a mass ratio of 0.38 based on the effect of the hydrogen lines of the secondary component on the composite hydrogen spectrum. Secondary lines have been detected in the spectra of V1182 Aql by Vitrichenko, but proved to be too weak to yield reliable velocities.

The only existing photoelectric light curve was obtained by Vitrichenko (1971), whose unfiltered observations indicated a Beta-Lyrae type light curve with little evidence of the eccentric orbit found from the solution to the radial velocity curve. His subsequent analysis showed the system to be of low inclination with a partial transit at primary eclipse. The results of the spectroscopic and photometric analyses showed the system to have a semi-detached configuration consisting of a primary in contact with its critical Roche lobe and a detached secondary.

By means of the program WINK (Wood, 1972), Giuricin and Mardirossian (1981) found a solution at variance with that of Vitrichenko. They found a lower inclination for the system as well as a smaller primary radius but a secondary whose temperature was indicative of a B1 star. Both components showed good agreement with a normal unevolved O9 + B1 main-sequence system. The more massive

primary component appeared to be in close proximity to its critical Roche surface which led to the suggestion by Giuricin and Mardirossian that the system bears some resemblance to BF Aur (Schneider et al., 1979), which is one of the strongest candidates for a system passing through a short-lived semi-detached phase at the beginning of case A mass transfer.

The possibility that this system could be at the beginning of case A mass transfer warranted its inclusion in our program to study the properties and evolutionary state of early-type close binaries. As observational data for this system were scarce, it was concluded that a new spectroscopic and photometric study of V1182 Aql would be beneficial in determining the absolute dimensions and evolutionary state of the system.

2) Spectroscopy

2.1) Observations

A total of twelve single-lined spectra were obtained by RWH in the period 1983 July 22-28 with the 1.8m telescope and the Cassegrain spectrograph of the Dominion Astrophysical Observatory, Victoria. An EMI 3-stage image tube was employed together with a grating and two different sets of optics giving dispersions of 32\AA mm^{-1} and 38\AA mm^{-1} respectively. The spectra were recorded on unbaked IIA-0 emulsion and were subsequently scanned using the DAO PDS machine and stored on magnetic tape in a format suitable for immediate reduction by REDUCE (see Section 2.2).

The remaining nine spectra, of which five were double-lined were obtained by SAB and AJA during the period 1985 August 27-30, at the Observatorio del Roque de los Muchachos, La Palma, using the 2.5m Isaac Newton Telescope (INT) in conjunction with the Intermediate Dispersion Spectrograph (IDS) and Image Photon Counting System (IPCS). The Jobin-Yvon 1200 grating and Camera 2 of the IDS provided spectra at a dispersion of 16.7 \AA mm^{-1} . Integrations were made using a slit width of $100 \mu\text{m}$, or 0.55 arcseconds when projected on the sky, and neutral-density filters to avoid saturating the IPCS. Observations consisted of pairs of spectra centred on 4040 \AA and 4400 \AA which provided useful spectral ranges of 480 \AA . Typical exposure times of 500-600s were employed for both wavelength ranges. All stellar integrations were alternated with comparison-source exposures by a Cu-Ar lamp for wavelength calibration purposes. The spectra were stored on disk and tape at the end of each exposure in FITS format (Wells et al., 1981).

To ensure that the observations made on both telescopes were on the standard system, two or three observations of radial velocity standard stars covering a range in spectral type of F7-G8 were made on each night. The observed radial velocities of these stars confirmed that they were on the standard system with an rms scatter of approximately 5 km s^{-1} . Observations were also made of the secondary radial-velocity standards ADS 16472A (Sp. type B3) at the INT and HD 160762 (Sp. type B3IV) at the DAO, selected from a compilation by Petrie (1953) of B-type secondary radial-velocity standards. The spectra of these stars could then be used as templates in subsequent cross-correlation analyses with the observations of V1182 Aql.

2.2) Reduction and Analysis

The INT spectroscopic data were processed on the University of St. Andrews VAX computers, using the STARLINK package SPICA to flat-field the spectra, effect the sky-background subtraction and convert them into a form suitable for the spectroscopic image-processing package REDUCE (Hill et al., 1982a).

The spectra were linearised using REDUCE and smoothing and rectification were applied using FTSPLOTT, a program written by AJA. Smoothing was applied by taking running means over 1.2\AA (5 pixels), and rectification was achieved by division into the spectrum of a heavily smoothed version of itself. The spectra were finally log-linearised using REDUCE in preparation for the cross-correlation analysis.

Cross-correlation analysis using VCROSS (Hill, 1982) was attempted using the B3V secondary radial-velocity standard star ADS 16472A for the INT spectra. The amplitude of the noise on the spectra is approximately 7% of the continuum height whereas the depths of the weak secondary features are of the order of 12% of the continuum height which made identification of the cross-correlation peak due to the secondary component very difficult. This procedure was abandoned in favour of the direct measurement of each feature.

The principal spectral lines showing splitting were the HeI lines at $\lambda\lambda 4026$, 4144 , 4388 and 4471 and these proved to be the most useful. Occasionally the HeI line at $\lambda 4009$ was used in the analysis and similarly the HeI line at $\lambda 4120$ was used when interference from H δ was minimal. The rest wavelengths adopted for this analysis have been taken from the list by Petrie (1953). The measurements of these lines to determine the radial velocities of

the components of V1182 Aql were made by fitting parabolae to single features and double-gaussian profiles to those features showing splitting using VELMEAS (Hill et al., 1982b) and VLINE (Hill et al., 1982c) respectively. In all cases, the spectra were smoothed prior to measurement. The primary and secondary radial velocities are given in Table 1 with estimated errors of 10 and 20kms⁻¹ respectively. The Balmer lines, however, were omitted from the analysis due to their extremely rotationally and Stark-broadened profiles.

The DAO spectra were somewhat noisier than those from the INT; they were therefore measured by visual inspection of the line centres using VELMEAS. The inferior dispersion and poorer signal-to-noise meant that features from the secondary could not be detected. However, primary-component velocities were obtained with an estimated error of approximately 20kms⁻¹ and are given in Table 1.

The lines of interstellar CaII were clearly visible in the INT short-wavelength-region spectra and in the DAO data, the K line being especially well defined. The H line, however, was always severely blended with H ϵ . The K line velocity was measured by parabola fitting using VELMEAS. The velocity of this interstellar line was determined to be $1 \pm 7\text{kms}^{-1}$ and $2 \pm 6\text{kms}^{-1}$ from the DAO and INT measures respectively.

Vitrichenko (1971) found a small eccentricity in his velocity curve of the primary component which was not clearly supported by the light curve he obtained. We find no evidence from our photoelectric and spectroscopic data for any eccentricity. Adopting the procedures of Popper (1974), the circular orbital elements of

V1182 Aq1 were computed by separate analysis of each component. All the data were used excluding those radial-velocity determinations less than 0.1 from either minimum to remove possible systematic errors in the radial velocities due to rotational distortion. The velocity semi-amplitude K_1 of the primary component and the systemic velocity V_0 were determined by means of a least-squares analysis from the velocity curve of the primary component. The velocity semi-amplitude K_2 of the secondary was determined in a similar manner using the radial velocities of the secondary, however no attempt was made to determine V_0 from these data. The mass functions and projected semi-major axes of the orbits of the two components were then derived and are summarised in Table 2. Another, most effective, technique was also developed to determine K_1 and K_2 directly from spectra obtained at both quadratures. This method involved the cross-correlation of selected features from these spectra and is described in detail in Appendix A. The results from this technique, given in Table 2, provide independent confirmation of the determinations made from the radial-velocity curves.

The projected rotational velocities have been estimated from the half-widths of both components of the HeI $\lambda 4026$ feature by means of the calibration provided by Olson (1984). The only satisfactorily-resolved $\lambda 4026$ feature was on spectrum no. INTD235/34 from which we have estimated projected rotational velocities of $220 \pm 30 \text{ km s}^{-1}$ for the primary and $150 \pm 40 \text{ km s}^{-1}$ for the secondary. These values compare quite favourably with the theoretical values of 240 and 160 km s^{-1} for the primary and secondary components respectively, assuming that circular orbits and synchronous rotation are applicable. While equivalent widths for

the HeI $\lambda 4026$ features in both components can be measured (the ratio of secondary to primary being 0.51), estimates of the luminosity ratio derived from these quantities are too seriously limited by the inherent errors in the relative line strengths of HeI $\lambda 4026$ in O and early B stars (Underhill, 1966a), to provide a reliable comparison with the photometrically determined luminosity ratio.

3) Photometry

3.1) Observations

Differential photoelectric photometry was obtained by SAB and AJA during the period 1985 July 16-28 at the Observatorio del Sierra Nevada, Spain. Simultaneous observations were made in the Strömrgren four-colour system using a Danish 6-channel uvby- β photometer and the 0.75m Steavenson telescope. A 46 arcsecond aperture was used throughout this study and integration times were fixed at 60s for the monitoring sequence.

The comparison star used was HD 175469 and the check star was HD 175406, both of which were used by Vitrichenko (1971) in his photometric study of V1182 Aql. At the time of the observations, the presence of Sahara dust in the atmosphere prevented any form of all sky photometry and hence no transformation could be made to the standard system. Since all three stars are separated by less than 10 arcminutes, differential photometry could still be obtained successfully. To minimise the effect of rapid extinction changes due to the dust and ensure good-quality light curves, observations of the comparison and check stars were made every 5 to 10 minutes.

A total of 451 observations in each colour were obtained. The instrumental magnitude differences relative to HD 175469 are given in Table 3. Data for the variable and comparison stars are given in Table 4. The estimated error on each observation is less than 0.01^m .

3.2) Reductions

The reduction to differential magnitudes was made using a computer program written by SAB and described in detail elsewhere (Bell et al., 1986). No variation in the differential magnitude between the comparison star and the check star has been detected exceeding 0.01^m .

Careful examination of the extinction curves confirmed the decision not to observe standard stars showing strong dependencies on azimuth, altitude and time, supporting the view that dust was present in non-uniform layers in the atmosphere during the two-week observing run. Under these conditions, it is unlikely that an accurate transformation to the standard system could have been made although differential photometry appears to have been successful.

Transformation equations derived by Morrison (1986) for observations made during 1985 August show no appreciable change in the scale factors from those obtained by Bell et al. (1986) in their study of AH Cep. Instrumental magnitudes have been used in the following analysis since corrections due to the scale factors derived by Morrison amount to less than 0.002^m on a single observation. These corrections would make no appreciable difference to the solutions obtained from the light-curve analysis.

3.3) Ephemeris

Two primary and two secondary minima were observed during the session and the times at which these minima took place were determined using the method of Kwee and van Woerden (1956). The mean times of minima for the four light curves are given in Table 5. The uncertainty in these determinations have been derived from the interagreement between the times of minima for the different colours. Observational data for this system are very scarce and the derived ephemeris must be regarded as a provisional one. Vitrichenko (1971) calculated the following ephemeris based upon his own observations:

$$\text{Pri. Min.} = \text{H.J.D. } 2439651.716 + 1.62192 E$$

$\pm 1 \qquad \pm 2$

A least-squares determination of the period was made by combining the times of minima derived from our observations and those obtained by Vitrichenko. The data presented in Tables 1 and 3, and plotted in Figures 1, 2 and 3 were phased according this period and the most accurately determined time of minimum:

$$\text{Pri. Min.} = \text{H.J.D. } 2446267.4027 + 1.621887 E$$

$\pm 4 \qquad \pm 1$

The paucity of observational data makes any analysis of the available times of minima extremely uncertain. Many more determinations of times of minima will be required to provide a better ephemeris for V1182 Aql and reveal any possible period changes.

3.4) Colour indices

It has already been pointed out that the prevailing weather conditions at the time the observations were made precluded the determination of standard Strömgren colour indices. UBV photometry, however, is available for this system although the phase at which these measurements were made is unknown. It can be seen from Figure 3 that there is no appreciable colour change in (b-y) and only a small change of less than $0.^m01$ at primary minimum in (u-b). In a catalogue of homogeneous UBV photometry, Nicolet (1978), gives $(B-V) = 0.59$ and $(U-B) = -0.45$ for V1182 Aql showing it to be a heavily reddened system. Using the method outlined by Underhill (1966b), we have derived the intrinsic colours given in Table 4.

3.5) Analysis

A preliminary inspection of the photometric data for V1182 Aql shows the system to have light curves of the Beta-Lyrae type. The depths of primary and secondary minimum are $0.^m17$ and $0.^m12$ respectively. There are no indications of any asymmetry in the four light curves. As secondary minimum occurs at $0.^p5$, we have adopted circular orbits for our analysis.

There appears to be a very small change in (b-y) at primary minimum and there is no reason to expect that the change in (B-V) would be larger. Assuming that the dominant contribution to the observed (B-V) colour can be ascribed to the primary, a lower limit to the temperature of the primary can be found using $(B-V)_0$ for the system and the calibration of Popper (1980). As a check on the published spectral type of O8V given by Vitrichenko (1971), we obtained a spectrogram of V1182 Aql at 80\AA mm^{-1} on baked IIa-0

emulsion using the 0.5m Leslie Rose telescope and spectrograph of the University Observatory, St. Andrews. Visual comparison of this spectrogram with MK standard stars observed with the same equipment confirmed the spectral type O8-O9V, in good agreement with the photometrically determined minimum temperature of 35600K. It must be noted, however, that the high rotational velocity of the primary component broadened and weakened the absorption lines and could result in the assignment of a later temperature type than would otherwise be the case. Making similar assumptions for $(U-B)_0$ as for $(B-V)_0$ and employing the calibration of Schmidt-Kaler (1965), further justification for the choice of this temperature can be made. We estimate an error of 1500K on this minimum temperature.

Each light curve was analysed by means of LIGHT (Hill, 1979), fixing the mass ratio q at that determined from the spectroscopic analysis and the primary component temperature T_1 by the method outlined above. The fractional primary-component radius r_1 , the secondary-component temperature T_2 and fractional radius r_2 , and the inclination of the system i were kept as free parameters. As a first approximation, the solution from Giuricin and Mardirossian (1981) was used. Table 6 lists the results of the analysis for the four light curves and the residuals of the individual uvby observations from the final theoretical curves are shown in Figure 4.

The following assumptions were made for each analysis. Black-body fluxes were adopted because preliminary solutions using the model atmospheres of Kurucz (1979) gave inferior fits. Synchronous rotation was assumed since the projected synchronous rotational velocities computed from our final fit agreed quite well with the observed values (Section 2.2). Gravity-darkening exponents

(β_1 and β_2) were set at 0.25 for both components, and electron scattering fractions (Escat_1 and Escat_2) were taken from Hutchings and Hill (1971). The limb-darkening coefficients were calculated automatically within LIGHT at each iteration of the solution using interpolation from the tabulation by Carbon and Gingerich (1969).

To determine how sensitive the solutions were to the adopted primary temperature and mass ratio, further solutions were made of the b-band light curve. The value of T_1 was adjusted by $\pm 1500\text{K}$ as suggested above and q was set at the limits of the spectroscopic mass ratio suggested by the standard error derived from the errors in the velocity semi-amplitudes. Varying the primary temperature T_1 , had little effect on the solution except, of course, for T_2 . The changes made to q had a similarly small effect. All the free parameters showed variations of less than 0.5% which would indicate only weak dependence upon T_1 and q . The final result of our photometric analysis is given in Table 7.

4) Discussion

4.1) Spectroscopy and Photometry

The velocity separation of more than 600kms^{-1} for the two components of V1182 Aql is probably large enough for the effects of blending of the diffuse HeI lines to have a minimal effect on the derived absolute dimensions (Andersen, 1975). The effect of reflection will systematically reduce the velocity semi-amplitudes of the two components. Employing Kitamura's treatment (1953, 1954), we find corrections of 2 and 3kms^{-1} for K_1 and K_2 respectively. The assumptions made by this method are probably still reasonable, given the detached nature of V1182 Aql. No appreciable changes in the

absolute dimensions result from the implementation of these corrections.

Astrophysical data for this system are given in Table 8. The bolometric corrections quoted here were obtained using the tabulation of Popper (1980). The derived absolute magnitude for the primary shows reasonable agreement with those of unevolved O stars observed by Conti and Burnichon (1975).

The largest source of error in this analysis is the estimate of the primary-component temperature. It seems likely that, had standard colours been available for this system, they would have been of little use in determining the primary temperature because of the low inclination of the system and the necessity for extrapolation of the colour-temperature relation (Popper, 1980). The UV photometry presented by Thompson et al. (1978) using the TD1 satellite in conjunction with the calibrations of Humphries et al. (1973) and Nandy et al. (1974) confirmed the late O-type classification for V1182 Aql. However, the quality of the observations and the small number of O stars defining the relation between spectral type and colour index prevented a critical determination of the spectral type of the primary component.

The broadening of inherently weak features in the spectra of O stars by rapid rotation makes the spectra appear later than they would otherwise be. If this is the case for V1182 Aql then the primary may be as early as O6. Unfortunately, the two spectral ranges observed with the IDS did not include the HeII lines at $\lambda 4200$ and $\lambda 4541$ and consequently the spectral type of the primary component could not be determined using the ratio of the equivalent widths of HeI $\lambda 4471$ with the HeII lines referred to above (see

Underhill, 1956). Underhill (1984) has described the difficulties involved in assigning temperatures to stars as early as the primary component. If, however, the O8 classification for the primary is correct, then our estimate of a temperature of $35600 \pm 1500\text{K}$ is in good agreement with Underhill's Figure 1. The inherent difficulties in assigning temperatures to O stars earlier than this by means of spectral classification makes the choice of primary temperature little better than an informed guess.

4.2) Evolutionary state

Our analysis would indicate that V1182 Aql is a detached system with the primary and secondary components filling 66% and 79% of their respective critical Roche lobes. The system would appear to be composed of an O8 primary and a B1 secondary.

We have compared the derived physical properties of the two stars with currently available models for single stars. Comparing the properties of the secondary with models produced by Hejlesen (1980) and Maeder (1981) show the secondary to be somewhat evolved from the zero-age main sequence about a quarter of the way through its main-sequence lifetime (cf. Figure 6).

The situation is not so clearly defined for the primary. Interpolation between the $30M_{\odot}$ and $60M_{\odot}$ tracks shows the primary to be $\sim 0.9^m$ underluminous for its mass; indeed the luminosity of the primary is compatible with a star of less than $30M_{\odot}$ (cf. Figure 7). Increasing the temperature of the primary to 42000K gives good agreement with the properties of a star of the order of $38M_{\odot}$ about one quarter of the way through its main-sequence lifetime. A solution of the b light curve adopting this primary temperature did

not change the fractional radii of the stars or the inclination of the system but increased the secondary temperature to 31900K. Adopting this alternative value of the secondary temperature made the secondary component overluminous by $\sim 0.8^m$. The secondary temperature and luminosity would then be best represented by a zero-age main sequence $17M_{\odot}$ star which would not be acceptable.

The radius of a star appropriate to the mass of the primary component is $8.7R_{\odot}$, making the primary about $0.1R_{\odot}$ larger than that predicted by the mass-radius relation derived from the ZAMS models of Maeder. The secondary is also $0.7R_{\odot}$ larger than that predicted for a $13.5M_{\odot}$ star by the same mass-radius relation. Therefore the anomalous luminosity of the primary component cannot be explained by an under-sized primary. The positions of the components of V1182 Aql in the mass-radius diagram (Figure 7) would support the view that the system is slightly evolved from the zero-age main sequence.

The evolutionary course of this system is consequently difficult to establish. We cannot be sure whether the system will pass through case A or case B evolution until the question of the primary temperature is resolved. If the higher temperature can be invoked then case A evolution may be prevented by the presence of a strong stellar wind. Using the expressions given by Lamers et al. (1980), the mass loss rate for such a star would be of the order of $10^{-6}M_{\odot}\text{yr}^{-1}$. For the cooler primary temperature, the mass loss rate is a factor of 2 smaller thereby increasing the possibility of case A mass transfer. Lamers et al. have pointed out that this relation is only approximate for stars of $M_{\text{bol}} > -9.0^m$ and the mass loss rates could be quite substantially smaller than this.

5) Conclusion

The new spectroscopic and photometric analysis has led to the reliable determination of the absolute dimensions of the components of V1182 Aql and has shown the system to be detached. There are some difficulties in assigning a temperature to the primary component whose spectral type is probably earlier than O8-O9. The evolutionary state of the system is difficult to assess and the possibility of case A or case B evolution is still open to question.

Acknowledgements

The authors would like to express their gratitude for the hospitality and assistance extended to them by the staffs of the Instituto de Astrofísica de Andalucía, the Observatorio del Roque de los Muchachos and the Dominion Astrophysical Observatory during the observing runs. We acknowledge PATT for the allocations of observing time, and the SERC for financial support in the form of a research studentship for one of us (SAB). We should also like to thank Prof. D.W.N. Stibbs for the use of the facilities of the University Observatory, St. Andrews.

References

- Andersen, J., 1975. *Astron. Astrophys.*, 44, 355.
- Bell, S.A., Hilditch, R.W. & Adamson, A.J., 1986. *Mon. Not. R. astr. Soc.* in print.
- Burnashey, V.I. & Vitrichenko, E.A., 1970. *Perem. Zvedzy*, 17, 502.
- Carbon, D.F. & Gingerich, O.J., 1969. *Theory and Observations of Normal Stellar Atmospheres*, ed. Gingerich, O.J. (M.I.T. Press, Cambridge), 377.
- Conti, P.S. & Burnichon, M.L., 1975. *Astron. Astrophys.*, 38, 467.
- Giuricin, G. & Mardirossian, F., 1981. *Astron. Astrophys. Suppl. Ser.*, 45, 499.
- Hejlesen, P.M., 1980. *Astron. Astrophys. Suppl. Ser.*, 39, 347.
- Hill, G., 1979. *Publ. Dom. Astrophys. Obs.*, 15, 297.
- Hill, G., 1982. *Publ. Dom. Astrophys. Obs.*, 16, 59.
- Hill, G., Fisher, W.A. & Poeckert, R., 1982a. *Publ. Dom. Astrophys. Obs.*, 16, 43.
- Hill, G., Ramsden, D., Fisher, W.A. & Morris, S.C., 1982b. *Publ. Dom. Astrophys. Obs.*, 16, 11.
- Hill, G., Fisher, W.A. & Poeckert, R., 1982c. *Publ. Dom. Astrophys. Obs.*, 16, 27.
- Humphries, C.M., Nandy, K. & Thompson, G.I., 1973. *Mon. Not. R. astr. Soc.*, 163, 1.

- Nandy,K., Humphries,C.M. & Thompson,G.I., 1974. Mon. Not. R. astr. Soc., 166, 297.
- Hutchings,J.B. & Hill,G., 1971. Astrophys. J., 167, 137.
- Kitamura,M., 1953. Publ. astr. Soc. Japan, 5, 114.
- Kitamura,M., 1954. Publ. astr. Soc. Japan, 6, 217.
- Kwee,K.K. & van Woerden,H., 1956. Bull. astr. Inst. Netherlands, 12, 327.
- Kurucz,R.L., 1979. Astrophys. J. Suppl. Ser., 40, 1.
- Lamers,H.J.G.L.M, Paerels,F.B.S. & De Loore,C., 1980. Astron. Astrophys., 87, 68.
- Maeder,A., 1981. Astron. Astrophys., 102, 401.
- Morrison,K., 1986. Submitted to Mon. Not. R. astr. Soc.
- Nicolet,B., 1978. Astron. Astrophys. Suppl. Ser., 34, 1.
- Olson,E.C., 1984. Publ. astr. Soc. Pacific, 96, 376.
- Petrie,R.M., 1953. Publ. Dom. Astrophys. Obs., 9, 297.
- Popper,D.M., 1974. Astron. J., 79, 1307.
- Popper,D.M., 1980. Ann. Rev. Astron. Astrophys., 18, 115.
- Schmidt-Kaler,Th., 1965. Landolt-Bornstein Tables, Group IV (Springer-Verlag, Berlin), 298.
- Schneider,D.P., Darland,J.J. & Leung,K.-C., 1979, Astron. J., 84, 236.
- Thompson,G.I., Nandy,K., Jamar,C., Monfils,A., Houziaux,L.,

Carnochan,D.J. & Wilson,R., 1978. Catalogue of Stellar Ultraviolet Fluxes (Science Research Council), 337.

Underhill,A.B., 1956. Publ. Dom. Astrophys. Obs., 10, 169.

Underhill,A.B., 1966a. In "The Early Type Stars", (Reidel, Dordrecht), 17.

Underhill,A.B., 1966b. In "The Early Type Stars", (Reidel, Dordrecht), 62.

Underhill,A.B., 1984. In "The MK Process and Stellar Classification", ed. Garrison,R.F. (University of Toronto, Toronto), 60.

Vitrichenko,E.A., 1967. Astron. Circ. No. 448, 6.

Vitrichenko,E.A., 1971. Publ. Crim. Astron. Obs., 43, 76.

Wells,D.C., Greisen,E.W. & Harten,R.H., 1981. Astrophys. J. Suppl. Ser., 44, 363.

Wood,D.B., 1972, A Computer program for Modelling Non-Spherical Eclipsing Binary Systems, Goddard Space Flight Centre, Greenbelt, Maryland, U.S.A.

Figure captions

Figure 1: Observed radial velocities and computed orbits for V1182 Aql. Primary component data obtained from the DAO and the INT are represented by crosses and squares respectively. Circles represent INT secondary component data.

Figure 2: b-magnitude differences in the sense variable minus comparison between V1182 Aql and HD 175469 together with the final theoretical curve.

Figure 3: (b-y) and (u-b) colour-index differences in the sense variable minus comparison between V1182 Aql and HD 175469 together with the final theoretical curves.

Figure 4: Residuals of the individual uvby observations from the final theoretical curves.

Figure 5: Cross-correlation functions obtained using the technique described in Appendix A. The upper diagram shows INTD235/34 (2^{nd} quadrature) cross-correlated against INTD237/04 (1^{st} quadrature). The lower plot shows the 1^{st} quadrature features of HeI $\lambda 3819$ and $\lambda 4026$ cross-correlated against those of 2^{nd} quadrature.

Figure 6: The locations of the two components of V1182 Aql in the theoretical HR diagram. The evolution tracks from Maeder (1981) are shown for three initial masses and each for no mass loss (solid line) and with mass loss (Maeder's case B: dashed line, and case C:

dot-dashed line). The crosses and dots represent the positions of V1182 Aql adopting a 35600K primary and a 42000K primary respectively.

Figure 7: The mass-radius relation using the theoretical ZAMS models of Maeder (1981). Data for a number of detached systems taken from a compilation of binaries with well-determined absolute dimensions (Popper, 1980) have also been plotted for comparison.

Appendix A

We have investigated a method for deriving the values of K_1 and K_2 , which retains all the advantages of the cross-correlation technique, but avoids the use of a standard star and hence problems caused by mis-matching of the chosen template with one or other (or both) components of the binary under study. The method requires spectra obtained at each quadrature for optimum results.

The idea is very simple to apply; the spectrum at one quadrature is cross-correlated against that taken at the other. The usual selection of wavelength ranges is performed to isolate the best-resolved features from both components (the HeI lines at $\lambda 3819$ and $\lambda 4026$ in this case). The observed velocities of the components at first and second quadratures are $[V_0 - K_1, V_0 + K_2]$ and $[V_0 + K_1, V_0 - K_2]$ respectively; the resulting cross-correlation function therefore contains four peaks :-

Primary vs Primary	at	$-2K_1$
Secondary vs Secondary	at	$+2K_2$
Primary vs secondary	at	$K_2 - K_1$
Secondary vs Primary	at	$-K_1 - (-K_2)$,

the latter two of which are seen to interfere constructively, reducing the complexity to three peaks. The sign of these velocity shifts depends only upon which spectrum is chosen as the fixed template, and the systemic velocity naturally cancels out because it shifts both spectra and we are dealing with relative shifts between the two.

Application of this method has a number of advantages. Firstly, the usual improvement of signal-to-noise of the cross-correlation process is retained; secondly, the line widths are matched as well as possible; and finally the primary/secondary peak allows a check on the K_1 and K_2 velocities derived separately from the primary/primary and secondary/secondary peaks, although the primary and secondary components of the chosen lines may not be as well matched.

The process is illustrated in Figure 5, where we show the two cross-correlation functions resulting with either quadrature spectrum as template; one is the mirror of the other. The three peaks anticipated above are plainly evident, their strengths reflecting the luminosity ratio of the two component stars: the secondary/secondary peak (at $2K_2$) is weak, the primary/primary at $2K_1$ dominates, and the "cross-term" peak at $K_2 - K_1$ is of intermediate strength; the rather ragged appearance of the latter may result from some mismatching between lines arising in the primary and secondary components. It is worth noting that the $K_2 - K_1$ peak would be dominant in the case of a less extreme luminosity ratio.

Table 1 : Radial-velocity data.

DAO data.

Plate No.	H.J.D. -2400000	Phase	V_1 kms ⁻¹	O-C kms ⁻¹	Dispersion Åmm ⁻¹
91899	45538.8605	0.8058	+124	-20	38
91900	45538.8640	0.8080	+162	+18	38
91901	45538.8668	0.8097	+142	- 1	38
91902	45538.8699	0.8116	+137	+ 5	38
91926	45544.7299	0.4247	- 60	+13	32
91927	45544.7334	0.4269	- 70	+ 1	32
91931	45544.7661	0.4470	- 59	- 6	32
91932	45544.7695	0.4491	- 25	+26	32
91941	45544.8317	0.4875	- 8	+ 6	32
91942	45544.8352	0.4896	- 19	- 7	32
91971	45545.7671	0.0842	- 33	+48	32
91981	45545.8435	0.1113	-110	- 8	32

INT data.

Tape/Run No.	H.J.D. -2400000	Phase	V_1 kms ⁻¹	O-C kms ⁻¹	V_2 kms ⁻¹	O-C kms ⁻¹	Range
INTD233/22	46305.5352	0.5112	+ 10	+ 1	---	--	Short
INTD234/02	46306.4632	0.0833	- 41	+39	---	--	Short
INTD234/03	46306.4729	0.0893	- 51	+34	---	--	Long
INTD235/33	46307.5270	0.7393	+142	-11	-409	+23	Long
INTD235/34	46307.4780	0.7448	+158	+ 5	-449	-17	Short
INTD235/36	46307.4849	0.7521	+165	+11	-414	+18	Long
INTD237/04	46308.3630	0.2547	-161	- 3	+431	- 5	Short
INTD237/08	46308.3950	0.2744	-154	+ 2	---	--	Long
INTD237/09	46308.4033	0.2796	-150	+ 5	+451	+22	Short

The final column indicates the wavelength region used.

Table 2 : Orbital elements.

K_1 (kms ⁻¹)	= 156 ± 3 *1
K_2 (kms ⁻¹)	= 435 ± 10 *1
V_0 (kms ⁻¹)	= -2 ± 3 *1
σ_1 (kms ⁻¹)	= 11 *2
σ_2 (kms ⁻¹)	= 19 *2
q (m_2/m_1)	= 0.36 ± 0.01
e	= 0 (adopted)
$a_1 \sin i$ (R)	= 5.0 ± 0.1
$a_2 \sin i$ (R _⊙)	= 13.9 ± 0.3
$a \sin i$ (R _⊙)	= 18.9 ± 0.3
$m_1 \sin^3 i$ (M)	= 25.5 ± 1.0
$m_2 \sin^3 i$ (M _⊙)	= 9.1 ± 0.4

Cross-correlation analysis (see Appendix A).

K_1 (kms ⁻¹)	= 155 ± 10 *3
K_2 (kms ⁻¹)	= 446 ± 30 *3
$K_1 - K_2$ (kms ⁻¹)	= 283 ± 30 *3

*1 - Using least-squares analysis.

*2 - r.m.s. scatter of a single observation.

*3 - For comparison purposes only. Uncertainties are estimated errors.

Table 3 : uvby observations.

1985 Jul 16/17		Differential Magnitude (v-c)			
H.J.D.	Phase	u	v	b	y
2446263.39233	0.5274	-0.891	0.127	0.009	-0.332
2446263.39452	0.5287	-0.902	0.129	0.006	-0.326
2446263.39633	0.5298	-0.889	0.127	0.009	-0.337
2446263.40134	0.5329	-0.899	0.118	-0.004	-0.347
2446263.40312	0.5340	-0.899	0.118	-0.001	-0.343
2446263.40508	0.5352	-0.895	0.119	-0.002	-0.349
2446263.42128	0.5452	-0.912	0.110	-0.014	-0.354
2446263.42305	0.5463	-0.907	0.105	-0.015	-0.363
2446263.42724	0.5489	-0.915	0.107	-0.015	-0.362
2446263.43161	0.5516	-0.917	0.102	-0.023	-0.371
2446263.43356	0.5528	-0.917	0.103	-0.017	-0.362
2446263.43556	0.5540	-0.914	0.108	-0.020	-0.363
2446263.44754	0.5614	-0.927	0.089	-0.035	-0.374
2446263.44937	0.5625	-0.923	0.090	-0.031	-0.373
2446263.45122	0.5637	-0.933	0.089	-0.036	-0.379
2446263.45877	0.5683	-0.930	0.085	-0.040	-0.387
2446263.46085	0.5696	-0.937	0.093	-0.039	-0.379
2446263.46543	0.5724	-0.945	0.082	-0.047	-0.391
2446263.47543	0.5786	-0.950	0.063	-0.052	-0.399
2446263.47731	0.5797	-0.949	0.070	-0.053	-0.396
2446263.47907	0.5808	-0.952	0.065	-0.058	-0.405
2446263.48612	0.5852	-0.952	0.061	-0.062	-0.398
2446263.48784	0.5862	-0.950	0.064	-0.056	-0.401
2446263.48966	0.5874	-0.956	0.063	-0.060	-0.397
2446263.49947	0.5934	-0.959	0.063	-0.062	-0.401
2446263.50126	0.5945	-0.960	0.058	-0.063	-0.407
2446263.50325	0.5957	-0.955	0.059	-0.060	-0.403
2446263.50965	0.5997	-0.955	0.058	-0.066	-0.408
2446263.51148	0.6008	-0.964	0.051	-0.066	-0.410
2446263.51336	0.6020	-0.962	0.057	-0.064	-0.407
2446263.52262	0.6077	-0.966	0.058	-0.067	-0.413
2446263.52457	0.6089	-0.962	0.057	-0.063	-0.408
2446263.52663	0.6102	-0.952	0.055	-0.060	-0.406
2446263.53049	0.6125	-0.970	0.057	-0.064	-0.410
2446263.53232	0.6137	-0.957	0.058	-0.059	-0.407
2446263.53430	0.6149	-0.962	0.053	-0.068	-0.412
2446263.54429	0.6210	-0.974	0.055	-0.071	-0.408
2446263.54615	0.6222	-0.954	0.054	-0.065	-0.407
2446263.54802	0.6233	-0.968	0.049	-0.071	-0.412
2446263.55313	0.6265	-0.976	0.049	-0.071	-0.415
2446263.55611	0.6283	-0.976	0.049	-0.076	-0.418
2446263.55799	0.6295	-0.976	0.053	-0.073	-0.416
2446263.56748	0.6353	-0.974	0.039	-0.080	-0.423
2446263.56933	0.6365	-0.978	0.044	-0.075	-0.420
2446263.57116	0.6376	-0.955	0.046	-0.068	-0.418
2446263.58006	0.6431	-0.966	0.043	-0.079	-0.421

continued

2446263.58200	0.6443	-0.957	0.044	-0.073	-0.419
2446263.58385	0.6454	-0.961	0.047	-0.077	-0.425

1985 Jul 19/20

Differential Magnitude (v-c)

H. J. D.	Phase	u	v	b	y
2446266.38237	0.3709	-0.972	0.048	-0.065	-0.416
2446266.38411	0.3720	-0.978	0.045	-0.077	-0.420
2446266.38770	0.3742	-0.983	0.045	-0.076	-0.421
2446266.38958	0.3754	-0.960	0.053	-0.061	-0.409
2446266.39135	0.3764	-0.978	0.046	-0.076	-0.423
2446266.40241	0.3833	-0.973	0.050	-0.074	-0.415
2446266.40419	0.3844	-0.966	0.043	-0.073	-0.419
2446266.40599	0.3855	-0.968	0.052	-0.066	-0.415
2446266.40979	0.3878	-0.958	0.055	-0.067	-0.416
2446266.41204	0.3892	-0.963	0.054	-0.068	-0.411
2446266.41380	0.3903	-0.961	0.056	-0.069	-0.409
2446266.42426	0.3967	-0.959	0.047	-0.065	-0.409
2446266.42601	0.3978	-0.977	0.046	-0.073	-0.418
2446266.42773	0.3989	-0.974	0.052	-0.070	-0.410
2446266.43135	0.4011	-0.974	0.045	-0.073	-0.415
2446266.43338	0.4024	-0.967	0.052	-0.071	-0.410
2446266.43510	0.4034	-0.958	0.053	-0.058	-0.403
2446266.44577	0.4100	-0.958	0.060	-0.063	-0.403
2446266.44750	0.4111	-0.939	0.066	-0.051	-0.393
2446266.44926	0.4121	-0.945	0.066	-0.050	-0.392
2446266.45287	0.4144	-0.945	0.066	-0.050	-0.397
2446266.45477	0.4155	-0.933	0.078	-0.040	-0.382
2446266.45648	0.4166	-0.943	0.071	-0.047	-0.392
2446266.48363	0.4333	-0.925	0.093	-0.029	-0.376
2446266.48540	0.4344	-0.921	0.091	-0.026	-0.372
2446266.48715	0.4355	-0.926	0.092	-0.028	-0.374
2446266.49292	0.4391	-0.921	0.093	-0.026	-0.374
2446266.49466	0.4401	-0.917	0.105	-0.020	-0.363
2446266.49640	0.4412	-0.909	0.103	-0.017	-0.362
2446266.50527	0.4467	-0.915	0.102	-0.014	-0.359
2446266.50700	0.4477	-0.917	0.099	-0.021	-0.366
2446266.50873	0.4488	-0.919	0.105	-0.018	-0.361
2446266.51243	0.4511	-0.908	0.111	-0.013	-0.354
2446266.51487	0.4526	-0.897	0.118	-0.004	-0.352
2446266.51664	0.4537	-0.905	0.114	-0.005	-0.346
2446266.52693	0.4600	-0.897	0.118	0.002	-0.343
2446266.52867	0.4611	-0.894	0.123	0.001	-0.343
2446266.53044	0.4622	-0.907	0.120	-0.001	-0.340
2446266.53412	0.4645	-0.878	0.132	0.012	-0.333
2446266.53662	0.4660	-0.891	0.131	0.008	-0.331
2446266.53866	0.4673	-0.885	0.134	0.018	-0.324
2446266.54753	0.4727	-0.885	0.139	0.017	-0.322
2446266.54937	0.4739	-0.864	0.141	0.024	-0.324
2446266.55111	0.4749	-0.878	0.141	0.020	-0.328
2446266.55472	0.4772	-0.882	0.131	0.014	-0.329

continued

2446266.55679	0.4784	-0.889	0.137	0.010	-0.332
2446266.55853	0.4795	-0.889	0.132	0.011	-0.328
2446266.56786	0.4853	-0.872	0.144	0.021	-0.322
2446266.56959	0.4863	-0.875	0.142	0.022	-0.323
2446266.57132	0.4874	-0.858	0.150	0.029	-0.314
2446266.57518	0.4898	-0.873	0.145	0.020	-0.325
2446266.57765	0.4913	-0.872	0.154	0.030	-0.319
2446266.57941	0.4924	-0.853	0.154	0.033	-0.313
2446266.59255	0.5005	-0.866	0.150	0.031	-0.316
2446266.59429	0.5016	-0.879	0.143	0.020	-0.319
2446266.59611	0.5027	-0.857	0.152	0.028	-0.320
2446266.60007	0.5051	-0.886	0.140	0.012	-0.327
2446266.60183	0.5062	-0.862	0.155	0.035	-0.313
2446266.60406	0.5076	-0.880	0.146	0.026	-0.317
2446266.61301	0.5131	-0.865	0.153	0.031	-0.314
2446266.61480	0.5142	-0.890	0.130	0.008	-0.333
2446266.61662	0.5153	-0.889	0.150	0.021	-0.321
2446266.62055	0.5178	-0.874	0.145	0.023	-0.322
2446266.62235	0.5189	-0.880	0.139	0.012	-0.330
2446266.62412	0.5200	-0.878	0.137	0.016	-0.334
2446266.63369	0.5259	-0.881	0.147	0.020	-0.326
2446266.63535	0.5269	-0.874	0.137	0.014	-0.332
2446266.63859	0.5289	-0.906	0.120	0.002	-0.343
2446266.64344	0.5319	-0.885	0.134	0.014	-0.336

1985 Jul 20/21

Differential Magnitude (v-c)

H.J.D.	Phase	u	v	b	y
2446267.36295	0.9755	-0.872	0.154	0.036	-0.301
2446267.36609	0.9774	-0.847	0.164	0.045	-0.299
2446267.37258	0.9814	-0.850	0.173	0.048	-0.292
2446267.37422	0.9824	-0.839	0.175	0.052	-0.288
2446267.37745	0.9844	-0.826	0.186	0.062	-0.282
2446267.37910	0.9855	-0.830	0.187	0.056	-0.286
2446267.38426	0.9886	-0.840	0.177	0.059	-0.290
2446267.39315	0.9941	-0.825	0.190	0.062	-0.282
2446267.39487	0.9952	-0.818	0.193	0.070	-0.281
2446267.40519	0.0015	-0.820	0.187	0.068	-0.283
2446267.40700	0.0027	-0.821	0.191	0.063	-0.284
2446267.40873	0.0037	-0.822	0.185	0.068	-0.282
2446267.41413	0.0071	-0.822	0.184	0.061	-0.282
2446267.41589	0.0081	-0.831	0.176	0.056	-0.293
2446267.42489	0.0137	-0.829	0.177	0.054	-0.284
2446267.42658	0.0147	-0.830	0.181	0.056	-0.289
2446267.42833	0.0158	-0.830	0.173	0.058	-0.288
2446267.43196	0.0180	-0.836	0.181	0.055	-0.288
2446267.43378	0.0192	-0.825	0.176	0.061	-0.289
2446267.43553	0.0202	-0.836	0.177	0.060	-0.294
2446267.44679	0.0272	-0.826	0.179	0.055	-0.290
2446267.44855	0.0283	-0.828	0.182	0.053	-0.293
2446267.45122	0.0299	-0.837	0.180	0.049	-0.290

continued

2446267.45487	0.0322	-0.854	0.165	0.040	-0.300
2446267.45660	0.0332	-0.853	0.166	0.043	-0.302
2446267.45832	0.0343	-0.848	0.158	0.039	-0.303
2446267.46674	0.0395	-0.878	0.143	0.017	-0.322
2446267.46848	0.0406	-0.893	0.131	0.007	-0.336
2446267.47023	0.0416	-0.884	0.125	0.012	-0.328
2446267.47551	0.0449	-0.887	0.122	0.006	-0.338
2446267.47726	0.0460	-0.886	0.126	0.007	-0.342
2446267.47900	0.0471	-0.883	0.145	0.016	-0.331
2446267.50315	0.0619	-0.900	0.111	-0.005	-0.348
2446267.50494	0.0630	-0.913	0.100	-0.019	-0.363
2446267.50674	0.0642	-0.916	0.103	-0.019	-0.369
2446267.51042	0.0664	-0.908	0.099	-0.021	-0.364
2446267.51219	0.0675	-0.919	0.100	-0.023	-0.368
2446267.51518	0.0694	-0.914	0.101	-0.025	-0.366
2446267.52578	0.0759	-0.924	0.098	-0.025	-0.365
2446267.52791	0.0772	-0.910	0.093	-0.023	-0.371
2446267.53045	0.0788	-0.908	0.094	-0.024	-0.362
2446267.53450	0.0813	-0.929	0.092	-0.036	-0.375
2446267.53624	0.0823	-0.914	0.090	-0.030	-0.377
2446267.53800	0.0834	-0.922	0.090	-0.033	-0.379
2446267.54638	0.0886	-0.936	0.083	-0.043	-0.387
2446267.54812	0.0897	-0.943	0.079	-0.047	-0.385
2446267.54986	0.0907	-0.933	0.072	-0.046	-0.389
2446267.55374	0.0931	-0.948	0.078	-0.045	-0.392
2446267.55546	0.0942	-0.937	0.078	-0.049	-0.390
2446267.55719	0.0953	-0.935	0.078	-0.047	-0.389
2446267.56564	0.1005	-0.935	0.082	-0.042	-0.390
2446267.56739	0.1015	-0.946	0.078	-0.045	-0.393
2446267.56914	0.1026	-0.928	0.078	-0.040	-0.388
2446267.57280	0.1049	-0.951	0.070	-0.057	-0.397
2446267.57459	0.1060	-0.941	0.069	-0.053	-0.393
2446267.57634	0.1071	-0.957	0.058	-0.061	-0.402
2446267.58686	0.1136	-0.962	0.066	-0.057	-0.394
2446267.58861	0.1146	-0.946	0.063	-0.051	-0.399
2446267.59077	0.1160	-0.958	0.055	-0.064	-0.403
2446267.59930	0.1212	-0.947	0.061	-0.057	-0.400
2446267.60105	0.1223	-0.960	0.059	-0.063	-0.401
2446267.61025	0.1280	-0.959	0.055	-0.066	-0.413
2446267.61198	0.1290	-0.971	0.051	-0.072	-0.412
2446267.61758	0.1325	-0.976	0.041	-0.073	-0.418
2446267.62996	0.1401	-0.951	0.058	-0.062	-0.405
2446267.63171	0.1412	-0.967	0.044	-0.076	-0.419

1985 Jul 21/22

Differential Magnitude (v-c)

H. J. D.	Phase	u	v	b	y
2446268.38778	0.6074	-0.960	0.050	-0.069	-0.413
2446268.39314	0.6107	-0.960	0.047	-0.066	-0.413
2446268.39491	0.6118	-0.965	0.048	-0.066	-0.412
2446268.39664	0.6128	-0.960	0.053	-0.066	-0.415

continued

2446268.40515	0.6181	-0.968	0.048	-0.069	-0.417
2446268.40692	0.6192	-0.955	0.054	-0.062	-0.404
2446268.40866	0.6202	-0.957	0.050	-0.064	-0.410
2446268.41483	0.6241	-0.978	0.049	-0.075	-0.414
2446268.41664	0.6252	-0.953	0.056	-0.062	-0.413
2446268.41866	0.6264	-0.963	0.048	-0.071	-0.414
2446268.42753	0.6319	-0.974	0.050	-0.075	-0.419
2446268.42932	0.6330	-0.973	0.045	-0.081	-0.424
2446268.43106	0.6341	-0.978	0.048	-0.081	-0.425
2446268.43802	0.6384	-0.979	0.045	-0.080	-0.422
2446268.43981	0.6395	-0.979	0.046	-0.081	-0.426
2446268.44153	0.6405	-0.973	0.046	-0.074	-0.417
2446268.44996	0.6457	-0.966	0.047	-0.077	-0.422
2446268.45175	0.6468	-0.974	0.044	-0.075	-0.427
2446268.45349	0.6479	-0.980	0.042	-0.079	-0.429
2446268.45878	0.6512	-0.975	0.047	-0.078	-0.427
2446268.46050	0.6522	-0.971	0.040	-0.078	-0.421
2446268.46227	0.6533	-0.970	0.043	-0.080	-0.424
2446268.48191	0.6654	-0.977	0.040	-0.078	-0.424
2446268.50958	0.6825	-0.997	0.025	-0.093	-0.443
2446268.51134	0.6836	-0.999	0.024	-0.101	-0.442
2446268.52035	0.6891	-1.003	0.022	-0.097	-0.443
2446268.52209	0.6902	-1.003	0.028	-0.092	-0.445
2446268.52382	0.6913	-0.992	0.022	-0.097	-0.440
2446268.52863	0.6942	-1.001	0.028	-0.097	-0.441
2446268.53035	0.6953	-1.000	0.022	-0.093	-0.444
2446268.53208	0.6963	-0.993	0.025	-0.092	-0.440
2446268.54056	0.7016	-0.994	0.023	-0.098	-0.447
2446268.54275	0.7029	-1.002	0.018	-0.104	-0.440
2446268.54940	0.7070	-0.987	0.019	-0.094	-0.443
2446268.55116	0.7081	-0.995	0.027	-0.098	-0.442

1985 Jul 22/23

Differential Magnitude (v-c)

H.J.D.	Phase	u	v	b	y
2446269.38388	0.2215	-0.997	0.025	-0.095	-0.441
2446269.38561	0.2226	-0.991	0.030	-0.090	-0.442
2446269.38731	0.2236	-0.999	0.024	-0.096	-0.442
2446269.40300	0.2333	-1.001	0.027	-0.096	-0.440
2446269.40467	0.2344	-0.990	0.024	-0.090	-0.442
2446269.40956	0.2374	-0.988	0.030	-0.093	-0.440
2446269.42004	0.2438	-0.990	0.029	-0.092	-0.440
2446269.42173	0.2449	-0.985	0.028	-0.088	-0.438
2446269.42636	0.2477	-1.007	0.016	-0.104	-0.449
2446269.42807	0.2488	-1.007	0.022	-0.104	-0.445
2446269.43768	0.2547	-1.004	0.018	-0.108	-0.450
2446269.43942	0.2558	-1.004	0.014	-0.106	-0.449
2446269.47547	0.2780	-0.994	0.020	-0.103	-0.444
2446269.48175	0.2819	-0.995	0.015	-0.102	-0.448
2446269.49278	0.2887	-0.992	0.022	-0.095	-0.444
2446269.49446	0.2897	-0.990	0.020	-0.098	-0.443

continued

2446269.49919	0.2926	-0.984	0.023	-0.096	-0.442
2446269.50091	0.2937	-0.988	0.028	-0.096	-0.438
2446269.50949	0.2990	-0.995	0.016	-0.102	-0.442
2446269.51127	0.3001	-0.990	0.015	-0.101	-0.440
2446269.51639	0.3032	-0.989	0.021	-0.098	-0.439
2446269.51819	0.3043	-0.981	0.025	-0.092	-0.437
2446269.52645	0.3094	-0.985	0.027	-0.095	-0.439
2446269.52817	0.3105	-0.993	0.024	-0.098	-0.439
2446269.53338	0.3137	-0.982	0.024	-0.094	-0.440
2446269.53511	0.3148	-0.975	0.027	-0.085	-0.436
2446269.54333	0.3198	-0.976	0.036	-0.078	-0.430
2446269.54506	0.3209	-0.977	0.037	-0.084	-0.427
2446269.54968	0.3238	-0.980	0.034	-0.088	-0.430
2446269.55137	0.3248	-0.974	0.039	-0.084	-0.428
2446269.56164	0.3311	-0.978	0.041	-0.087	-0.422
2446269.56338	0.3322	-0.987	0.045	-0.082	-0.423
2446269.56813	0.3351	-0.966	0.043	-0.078	-0.422
2446269.56982	0.3362	-0.982	0.034	-0.089	-0.434
2446269.58243	0.3440	-0.979	0.041	-0.081	-0.417
2446269.58422	0.3451	-0.984	0.039	-0.086	-0.423
2446269.59138	0.3495	-0.975	0.042	-0.080	-0.418
2446269.59309	0.3505	-0.969	0.042	-0.078	-0.422

1985 Jul 23/24

Differential Magnitude (v-c)

H.J.D.	Phase	u	v	b	y
2446270.38418	0.8383	-0.966	0.048	-0.070	-0.412
2446270.38596	0.8394	-0.983	0.039	-0.084	-0.423
2446270.38767	0.8404	-0.989	0.037	-0.084	-0.425
2446270.39255	0.8434	-0.974	0.045	-0.072	-0.419
2446270.39479	0.8448	-0.972	0.048	-0.078	-0.418
2446270.40188	0.8492	-0.963	0.055	-0.068	-0.409
2446270.40358	0.8502	-0.959	0.060	-0.064	-0.416
2446270.40532	0.8513	-0.972	0.054	-0.073	-0.420
2446270.41459	0.8570	-0.961	0.054	-0.064	-0.409
2446270.41629	0.8581	-0.974	0.051	-0.064	-0.413
2446270.41803	0.8592	-0.972	0.060	-0.071	-0.412
2446270.42286	0.8621	-0.953	0.063	-0.060	-0.400
2446270.42459	0.8632	-0.957	0.057	-0.065	-0.411
2446270.43599	0.8702	-0.967	0.056	-0.063	-0.408
2446270.43771	0.8713	-0.946	0.067	-0.054	-0.399
2446270.44399	0.8752	-0.950	0.062	-0.054	-0.404
2446270.44583	0.8763	-0.968	0.057	-0.065	-0.404
2446270.45411	0.8814	-0.952	0.063	-0.056	-0.403
2446270.45583	0.8825	-0.942	0.068	-0.048	-0.395
2446270.45780	0.8837	-0.940	0.070	-0.052	-0.395
2446270.46256	0.8866	-0.942	0.070	-0.049	-0.395
2446270.47474	0.8941	-0.940	0.076	-0.045	-0.395
2446270.47642	0.8952	-0.941	0.074	-0.046	-0.397
2446270.48153	0.8983	-0.946	0.069	-0.051	-0.401
2446270.48325	0.8994	-0.949	0.063	-0.051	-0.402

continued

2446270.49205	0.9048	-0.929	0.072	-0.044	-0.388
2446270.49378	0.9059	-0.938	0.079	-0.046	-0.390
2446270.49548	0.9069	-0.944	0.085	-0.046	-0.383
2446270.50262	0.9113	-0.925	0.090	-0.035	-0.374
2446270.50436	0.9124	-0.928	0.089	-0.035	-0.372
2446270.52726	0.9265	-0.896	0.113	-0.012	-0.354
2446270.53629	0.9321	-0.885	0.124	0.002	-0.341
2446270.53805	0.9332	-0.899	0.111	-0.010	-0.350
2446270.54624	0.9382	-0.902	0.110	-0.011	-0.356
2446270.54795	0.9393	-0.910	0.114	-0.009	-0.344
2446270.54968	0.9403	-0.888	0.122	0.007	-0.344
2446270.55661	0.9446	-0.885	0.127	0.010	-0.333
2446270.55835	0.9457	-0.882	0.122	0.009	-0.342
2446270.56692	0.9510	-0.877	0.143	0.018	-0.323
2446270.56866	0.9520	-0.874	0.135	0.017	-0.326
2446270.57041	0.9531	-0.866	0.140	0.024	-0.328
2446270.57509	0.9560	-0.862	0.155	0.033	-0.317
2446270.57686	0.9571	-0.860	0.161	0.035	-0.309
2446270.58619	0.9628	-0.850	0.170	0.047	-0.306
2446270.58791	0.9639	-0.848	0.161	0.040	-0.308
2446270.58962	0.9650	-0.856	0.162	0.042	-0.306
2446270.59619	0.9690	-0.862	0.155	0.038	-0.311
2446270.59792	0.9701	-0.862	0.157	0.038	-0.310
2446270.60761	0.9760	-0.840	0.172	0.054	-0.293
2446270.60937	0.9771	-0.848	0.167	0.051	-0.293
2446270.61108	0.9782	-0.835	0.181	0.059	-0.289
2446270.61818	0.9826	-0.838	0.180	0.062	-0.288
2446270.61983	0.9836	-0.847	0.182	0.059	-0.283
2446270.62170	0.9847	-0.830	0.181	0.064	-0.282

1985 Jul 24/25

Differential Magnitude (v-c)

H. J. D.	Phase	u	v	b	y
2446271.38120	0.4530	-0.894	0.114	-0.005	-0.351
2446271.38292	0.4541	-0.879	0.121	0.006	-0.344
2446271.39125	0.4592	-0.887	0.121	0.005	-0.344
2446271.39297	0.4603	-0.900	0.119	0.001	-0.343
2446271.40162	0.4656	-0.895	0.125	0.008	-0.344
2446271.40331	0.4666	-0.898	0.130	0.009	-0.341
2446271.41269	0.4724	-0.878	0.137	0.017	-0.332
2446271.41442	0.4735	-0.886	0.143	0.021	-0.330
2446271.42323	0.4789	-0.888	0.136	0.012	-0.327
2446271.42490	0.4800	-0.885	0.137	0.014	-0.328
2446271.43338	0.4852	-0.879	0.145	0.020	-0.323
2446271.43508	0.4862	-0.871	0.137	0.014	-0.329
2446271.44370	0.4915	-0.872	0.135	0.015	-0.325
2446271.44538	0.4926	-0.875	0.138	0.016	-0.329
2446271.45366	0.4977	-0.879	0.143	0.014	-0.320
2446271.45537	0.4987	-0.877	0.131	0.020	-0.323
2446271.46402	0.5041	-0.877	0.144	0.016	-0.324
2446271.46574	0.5051	-0.878	0.132	0.013	-0.326

continued

2446271.47574	0.5113	-0.880	0.142	0.017	-0.325
2446271.47835	0.5129	-0.879	0.136	0.016	-0.328
2446271.48685	0.5182	-0.883	0.129	0.007	-0.339
2446271.48857	0.5192	-0.882	0.126	0.006	-0.339
2446271.49689	0.5243	-0.894	0.122	0.004	-0.344
2446271.49862	0.5254	-0.892	0.119	-0.001	-0.346
2446271.50738	0.5308	-0.891	0.116	0.003	-0.344
2446271.50908	0.5319	-0.897	0.121	-0.003	-0.347
2446271.51865	0.5378	-0.898	0.117	-0.003	-0.352
2446271.52057	0.5389	-0.898	0.110	-0.002	-0.351
2446271.52924	0.5443	-0.906	0.108	-0.010	-0.355
2446271.53096	0.5454	-0.911	0.111	-0.010	-0.357
2446271.53972	0.5508	-0.917	0.105	-0.018	-0.358
2446271.54154	0.5519	-0.923	0.109	-0.012	-0.356
2446271.55044	0.5574	-0.930	0.090	-0.026	-0.371
2446271.55228	0.5585	-0.932	0.089	-0.030	-0.374
2446271.56105	0.5639	-0.933	0.106	-0.022	-0.366
2446271.56296	0.5651	-0.924	0.088	-0.033	-0.380
2446271.57157	0.5704	-0.939	0.066	-0.048	-0.394
2446271.57336	0.5715	-0.941	0.076	-0.046	-0.390
2446271.58281	0.5773	-0.944	0.072	-0.050	-0.393
2446271.58452	0.5784	-0.938	0.068	-0.047	-0.396
2446271.59711	0.5861	-0.955	0.069	-0.054	-0.402
2446271.59906	0.5873	-0.948	0.057	-0.059	-0.408
2446271.60753	0.5926	-0.951	0.054	-0.064	-0.407
2446271.60926	0.5936	-0.967	0.059	-0.062	-0.412

1985 Jul 25/26

Differential Magnitude (v-c)

H.J.D.	Phase	u	v	b	y
2446272.49132	0.1375	-0.957	0.061	-0.064	-0.403
2446272.49303	0.1385	-0.952	0.068	-0.055	-0.401
2446272.50399	0.1453	-0.952	0.058	-0.061	-0.403
2446272.50577	0.1464	-0.971	0.052	-0.073	-0.412
2446272.51395	0.1514	-0.970	0.051	-0.072	-0.414
2446272.51566	0.1525	-0.976	0.047	-0.080	-0.416
2446272.52390	0.1576	-0.981	0.045	-0.081	-0.418
2446272.52561	0.1586	-0.968	0.046	-0.076	-0.419
2446272.53387	0.1637	-0.967	0.040	-0.080	-0.422
2446272.53557	0.1648	-0.969	0.041	-0.084	-0.427
2446272.54400	0.1700	-0.970	0.040	-0.076	-0.421
2446272.54568	0.1710	-0.963	0.043	-0.072	-0.415
2446272.55376	0.1760	-0.975	0.041	-0.081	-0.424
2446272.55546	0.1770	-0.989	0.035	-0.083	-0.423
2446272.56368	0.1821	-1.002	0.025	-0.095	-0.435
2446272.56539	0.1831	-0.992	0.027	-0.094	-0.433

1985 Jul 26/27

Differential Magnitude (v-c)

H.J.D.	Phase	u	v	b	y
2446273.38785	0.6902	-0.995	0.022	-0.096	-0.438

continued

2446273.38959	0.6913	-0.985	0.027	-0.093	-0.437
2446273.39127	0.6924	-0.986	0.030	-0.088	-0.438
2446273.39958	0.6975	-0.983	0.028	-0.093	-0.436
2446273.40135	0.6986	-0.991	0.026	-0.097	-0.439
2446273.40304	0.6996	-0.996	0.026	-0.103	-0.445
2446273.41150	0.7048	-0.994	0.023	-0.095	-0.438
2446273.41319	0.7059	-0.982	0.031	-0.088	-0.437
2446273.41491	0.7069	-0.996	0.026	-0.102	-0.441
2446273.42328	0.7121	-1.000	0.018	-0.103	-0.446
2446273.42498	0.7131	-1.004	0.026	-0.104	-0.443
2446273.42667	0.7142	-0.996	0.024	-0.099	-0.444
2446273.43502	0.7193	-0.996	0.017	-0.099	-0.447
2446273.43671	0.7204	-0.997	0.020	-0.097	-0.446
2446273.43929	0.7220	-0.997	0.020	-0.102	-0.448
2446273.44820	0.7275	-0.992	0.021	-0.099	-0.441
2446273.45015	0.7287	-0.996	0.020	-0.101	-0.440
2446273.45188	0.7297	-0.987	0.021	-0.095	-0.436
2446273.46229	0.7361	-0.996	0.022	-0.099	-0.435
2446273.46400	0.7372	-0.995	0.019	-0.105	-0.440
2446273.49089	0.7538	-1.002	0.020	-0.102	-0.443
2446273.49258	0.7548	-0.987	0.021	-0.093	-0.437
2446273.49429	0.7559	-0.990	0.021	-0.100	-0.444
2446273.50475	0.7623	-0.998	0.023	-0.100	-0.448
2446273.50644	0.7634	-0.986	0.027	-0.090	-0.445
2446273.50814	0.7644	-0.997	0.024	-0.097	-0.447
2446273.51641	0.7695	-0.996	0.024	-0.098	-0.443
2446273.51812	0.7706	-0.995	0.024	-0.099	-0.443
2446273.51983	0.7716	-0.988	0.023	-0.096	-0.442
2446273.52814	0.7767	-0.993	0.025	-0.100	-0.441
2446273.52989	0.7778	-0.984	0.026	-0.095	-0.440
2446273.53162	0.7789	-0.980	0.028	-0.089	-0.440
2446273.54410	0.7866	-0.983	0.023	-0.091	-0.438
2446273.54579	0.7876	-0.993	0.021	-0.097	-0.440
2446273.54751	0.7887	-0.987	0.024	-0.095	-0.440
2446273.55571	0.7937	-0.989	0.030	-0.091	-0.432
2446273.55740	0.7948	-0.994	0.024	-0.093	-0.436
2446273.55914	0.7959	-0.978	0.028	-0.083	-0.427
2446273.57082	0.8031	-0.994	0.039	-0.087	-0.425
2446273.57253	0.8041	-0.983	0.031	-0.090	-0.437
2446273.57423	0.8052	-0.978	0.034	-0.086	-0.429
2446273.58559	0.8122	-0.969	0.045	-0.075	-0.425
2446273.58730	0.8132	-0.990	0.036	-0.085	-0.428
2446273.58929	0.8144	-0.981	0.038	-0.084	-0.427
2446273.59873	0.8203	-0.988	0.042	-0.084	-0.422
2446273.60043	0.8213	-0.981	0.039	-0.081	-0.424
2446273.60221	0.8224	-0.967	0.041	-0.078	-0.421
2446273.61056	0.8276	-0.965	0.043	-0.074	-0.423
2446273.61228	0.8286	-0.978	0.041	-0.083	-0.421
2446273.61399	0.8297	-0.981	0.037	-0.081	-0.426

continued

1985 Jul 28/29

Differential Magnitude (v-c)

H.J.D.	Phase	u	v	b	y
2446275.38023	0.9187	-0.918	0.085	-0.023	-0.375
2446275.38199	0.9198	-0.921	0.087	-0.030	-0.377
2446275.39220	0.9261	-0.910	0.105	-0.020	-0.357
2446275.39392	0.9271	-0.905	0.107	-0.018	-0.361
2446275.40225	0.9323	-0.908	0.106	-0.019	-0.361
2446275.40395	0.9333	-0.888	0.115	-0.008	-0.352
2446275.41223	0.9384	-0.883	0.125	0.009	-0.346
2446275.41396	0.9395	-0.893	0.126	0.008	-0.347
2446275.42361	0.9454	-0.877	0.129	0.011	-0.335
2446275.42537	0.9465	-0.879	0.146	0.015	-0.326
2446275.43379	0.9517	-0.879	0.144	0.020	-0.317
2446275.43546	0.9527	-0.868	0.144	0.023	-0.322
2446275.44398	0.9580	-0.854	0.151	0.034	-0.309
2446275.44598	0.9592	-0.852	0.160	0.037	-0.311
2446275.45475	0.9646	-0.846	0.165	0.043	-0.296
2446275.45646	0.9657	-0.847	0.165	0.041	-0.300
2446275.46493	0.9709	-0.829	0.174	0.052	-0.292
2446275.46672	0.9720	-0.838	0.168	0.048	-0.294
2446275.47524	0.9773	-0.844	0.181	0.055	-0.286
2446275.47696	0.9783	-0.834	0.174	0.054	-0.293
2446275.48546	0.9836	-0.834	0.180	0.057	-0.287
2446275.48716	0.9846	-0.832	0.178	0.057	-0.285
2446275.49587	0.9900	-0.832	0.182	0.060	-0.286
2446275.49758	0.9910	-0.837	0.176	0.055	-0.288
2446275.50833	0.9977	-0.828	0.181	0.064	-0.281
2446275.51006	0.9987	-0.826	0.184	0.063	-0.287
2446275.52144	0.0057	-0.829	0.184	0.061	-0.285
2446275.52319	0.0068	-0.815	0.191	0.066	-0.283
2446275.53213	0.0123	-0.828	0.182	0.059	-0.282
2446275.53389	0.0134	-0.826	0.185	0.059	-0.285
2446275.55174	0.0244	-0.846	0.154	0.037	-0.314

Table 4 : Data for V1182 Aq1, HD 175469 and HD 175406.

	V1182 Aq1	HD 175469	HD 175406
SAO no.	124049	124045	124043
BD no.	+09 ^o 3928	+09 ^o 3925	+09 ^o 3923
R.A. (1950)	18 ^h 53 ^m 00 ^s	18 ^h 52 ^m 49 ^s	18 ^h 52 ^m 32 ^s
Dec. (1950)	+09 ^o 16' 54"	+09 ^o 10' 29"	+09 ^o 10' 13"
Sp. type	O9Vnn+B3V	B9V	A5V
V	8 ^m .5 (0 ^p .25)	8 ^m .8	8 ^m .6
(B-V)	0 ^m .59	----	----
(U-B)	-0 ^m .45	----	----
(B-V) _o	-0 ^m .30	----	----
(U-B) _o	-1 ^m .12	----	----
E(B-V)	0 ^m .89	----	----
E(U-B)	0 ^m .67	----	----

Table 5 : Times of minima.

H.J.D.	Error (days)	Epoch (cycles)	Source reference
-2400000			
39651.716	± 0.001	-4079.0	Vitrichenko, 1971.
39652.537	± 0.005	-4078.5	Vitrichenko, 1971.
46266.5848	± 0.001	-0.5	This paper.
46267.4027	± 0.0004	0.0	This paper.
46271.4498	± 0.0007	2.5	This paper.
46275.5060	± 0.0009	5.0	This paper.

Table 6 : Light-curve solutions.

Adopted primary temperature 35600K

Colour	u	v	b	y
i (degrees)	61.6 ±3	61.6 ±2	61.3 ±2	61.1 ±2
T ₂ K (polar)	27310 ±480	27750 ±340	27500 ±320	27340 ±290
r ₁ (polar)	0.397 ±6	0.390 ±4	0.391 ±4	0.390 ±4
r ₁ (mean)	0.414 ±6	0.406 ±4	0.408 ±4	0.407 ±4
r ₂ (polar)	0.255 ±5	0.258 ±3	0.259 ±3	0.261 ±3
r ₂ (mean)	0.268 ±5	0.272 ±3	0.273 ±3	0.276 ±3
χ^2 (mmag.) ²	80.69	45.23	40.02	35.58
L ₂ /L ₁	0.270	0.308	0.311	0.324
r.m.s. error (mmag.)	8.4	6.3	6.0	5.6

Table 7 : Adopted light-curve solutions.

T_1 K (polar)	35600
q (spectroscopic)	0.36
Escat ₁ (adopted)	0.61
Escat ₂ (adopted)	0.44
β_1 (adopted)	0.25
β_2 (adopted)	0.25
i (degrees)	61.3 +2
T_2 K (polar)	27470 +200
r_1 (polar)	0.392 +3
r_1 (mean)	0.409 +3
r_2 (polar)	0.258 +3
r_2 (mean)	0.272 +3

Table 8 : Astrophysical data for V1182 Aql.

Absolute dimensions:	Primary	Secondary
M/M _☉	37.8 ± 1.6	13.5 ± 0.5
R/R _☉	8.8 ± 0.2	5.9 ± 0.1
log g (cgs)	4.12 ± 0.03	4.03 ± 0.03
Photometric data:		
T _{eff} (K)	35600 ± 1500	27500 ± 1500
M _{bol}	-7. ^m 93 ± 0. ^m 19	-5. ^m 9 ± 0. ^m 2
log (L/L _☉)	5.05 ± 0.08	4.3 ± 0.1
B.C.	-3. ^m 40	-2. ^m 73
M _V	-4. ^m 53 ± 0. ^m 19	-3. ^m 2 ± 0. ^m 2
E _(B-V)	0. ^m 89	
Distance (pc)	1240 ± 220	

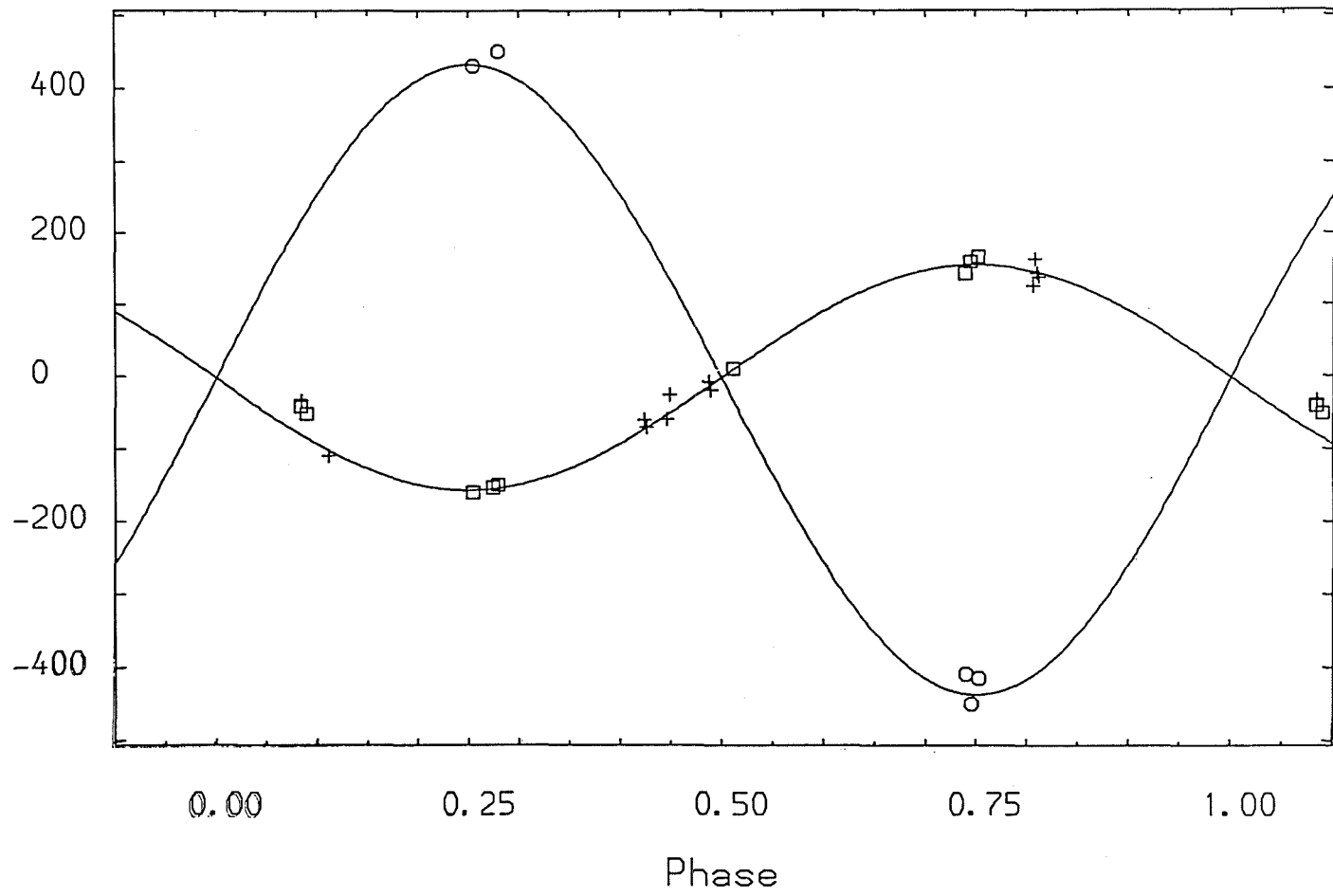


Figure 1.

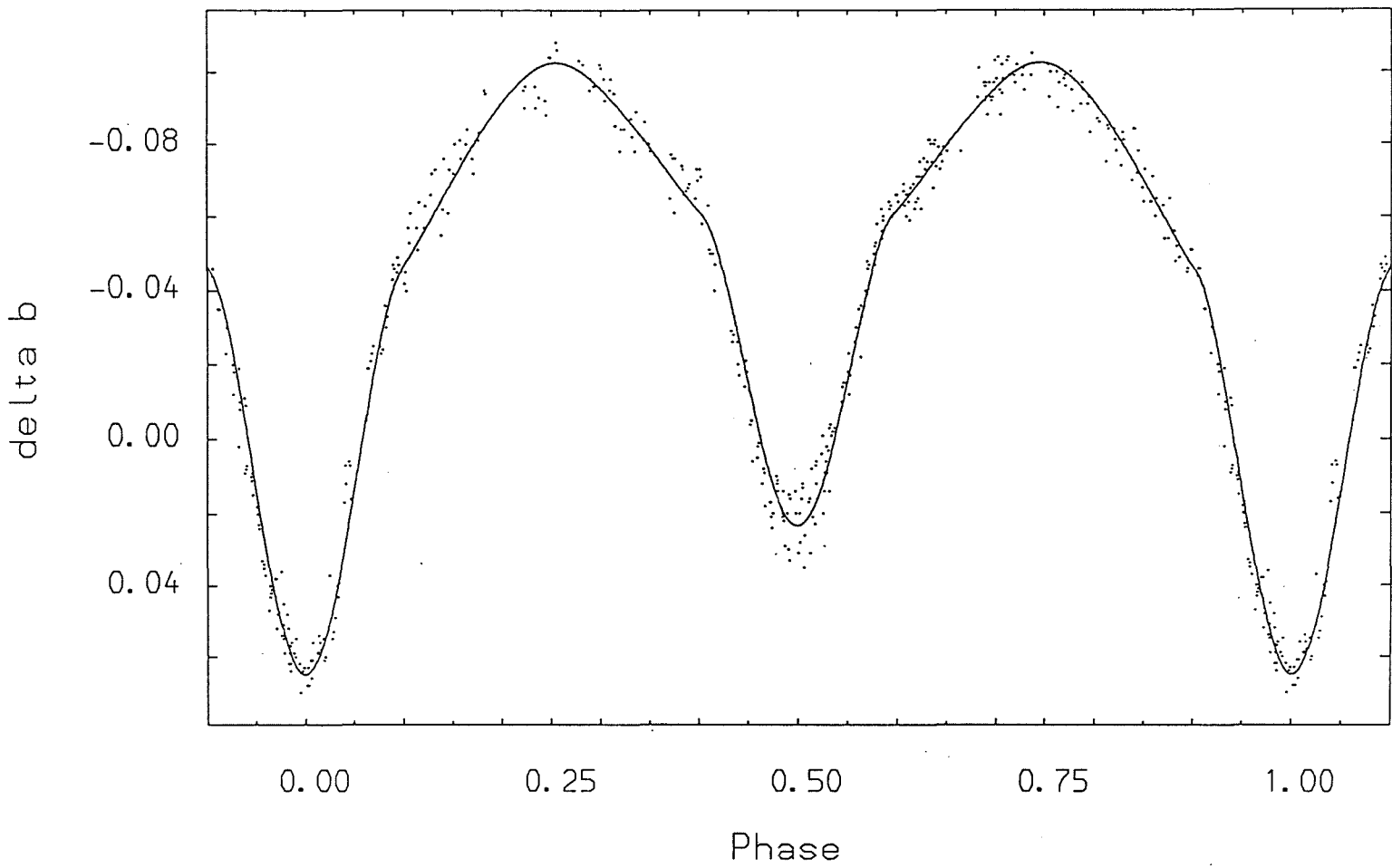


Figure 2.

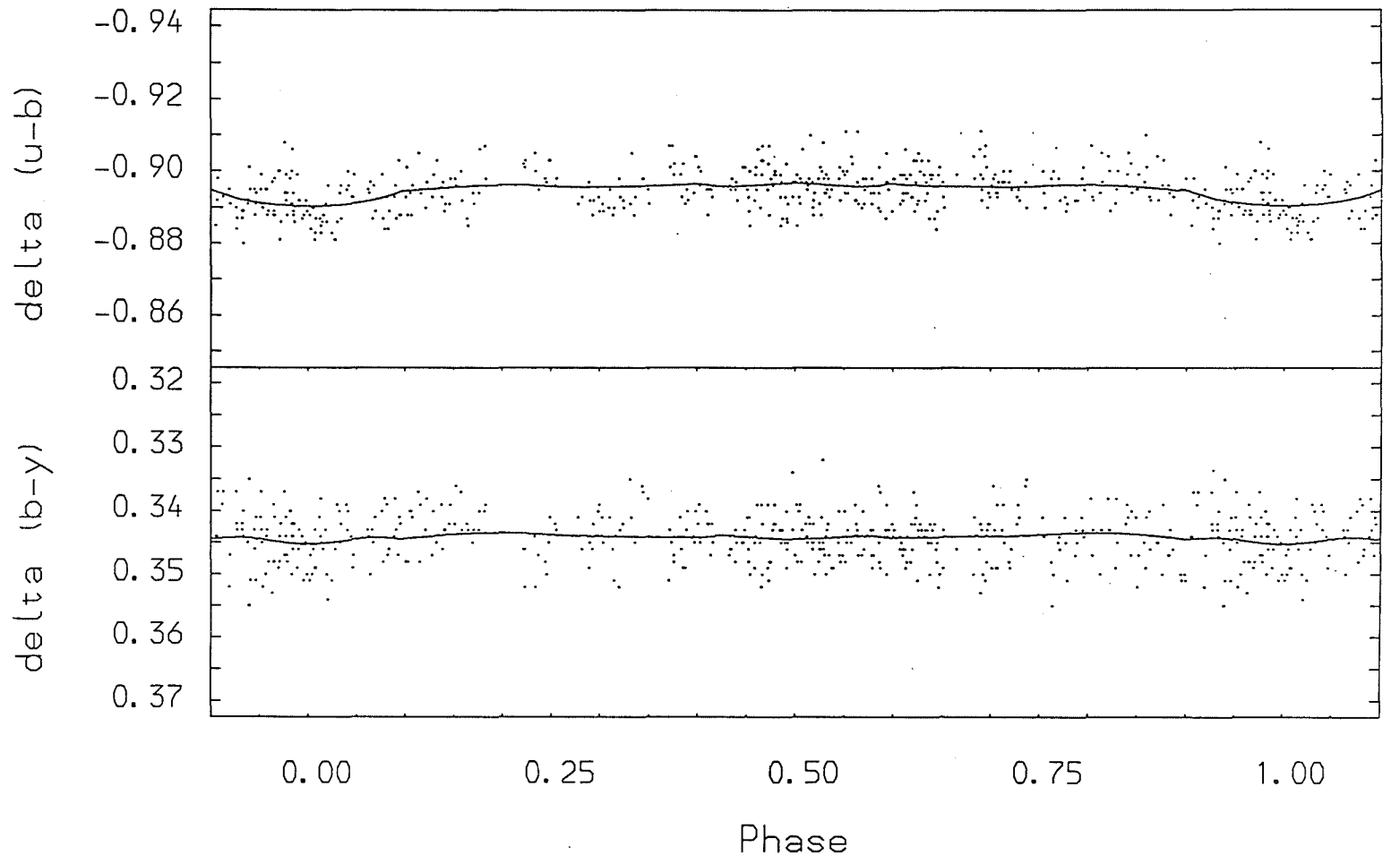
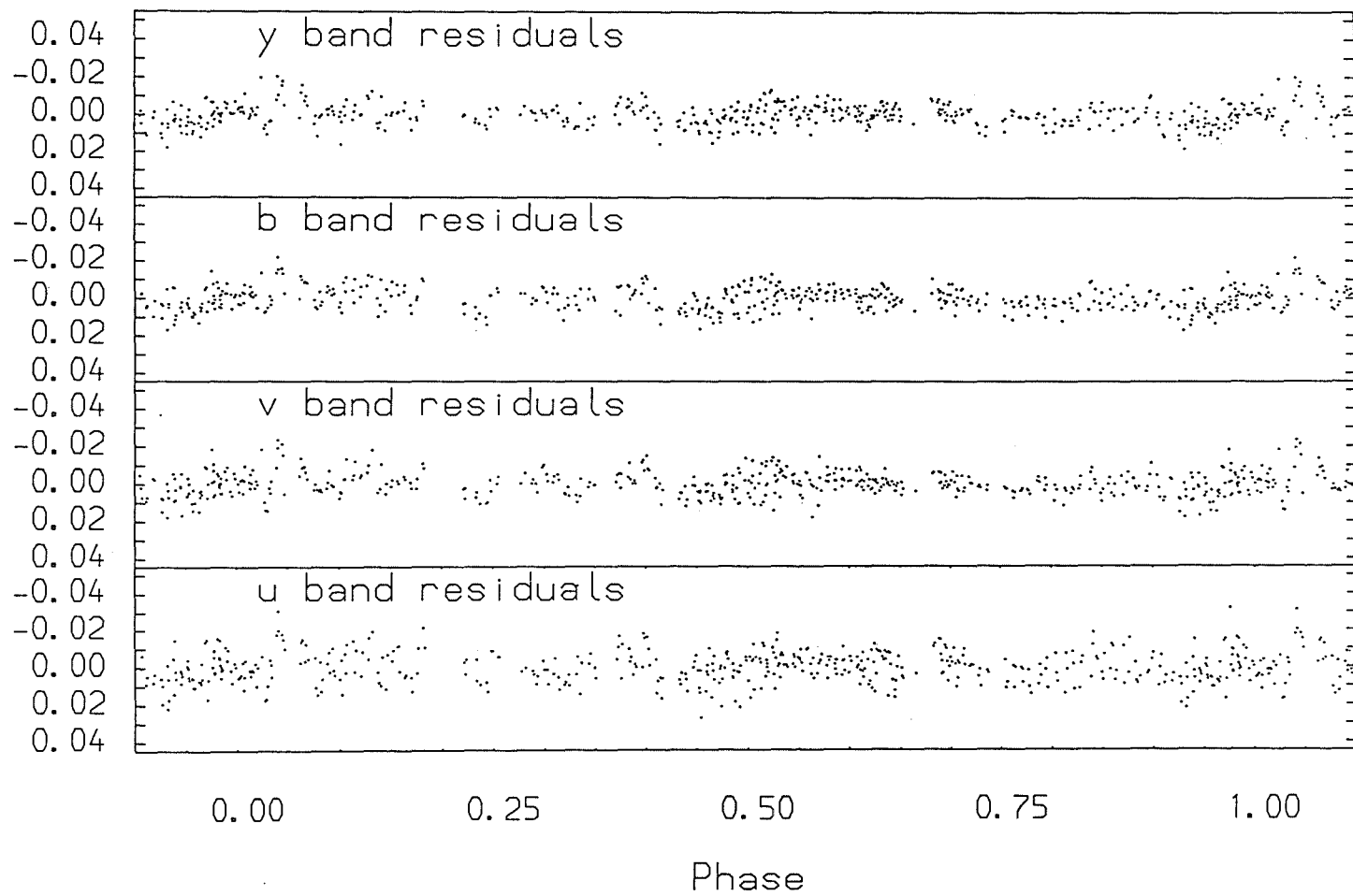


Figure 3.

Figure 4.



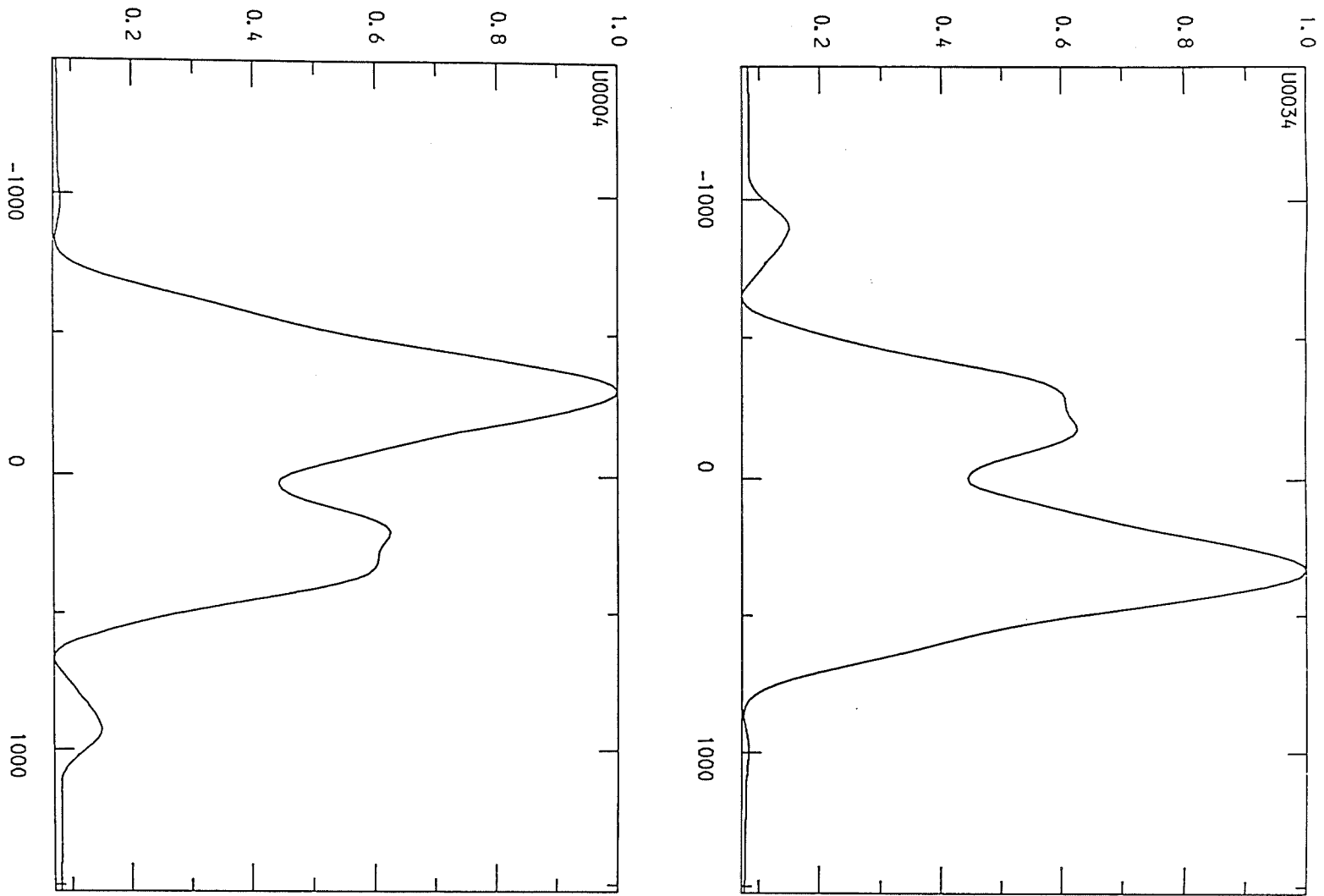


Figure 5.

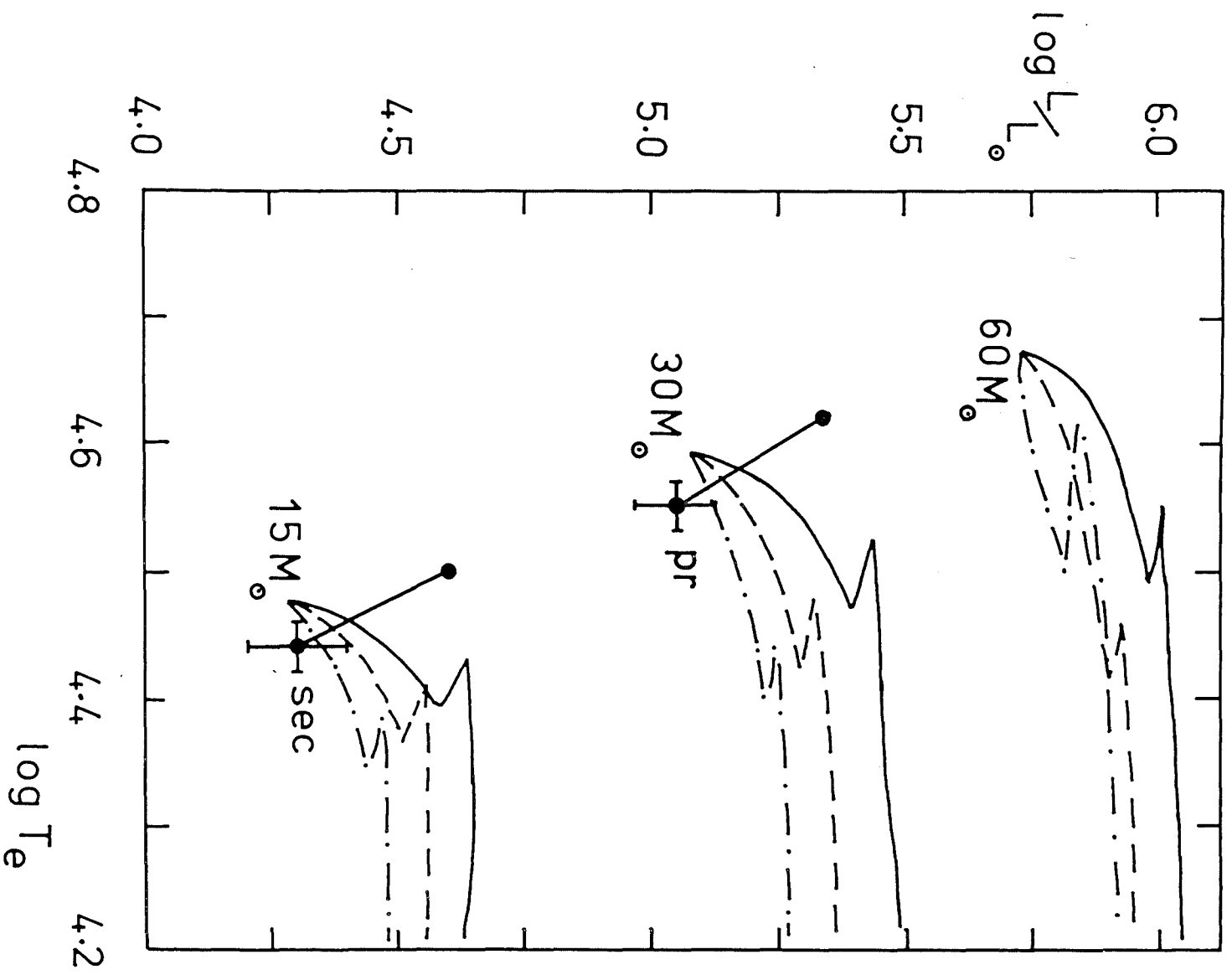


Figure 6.

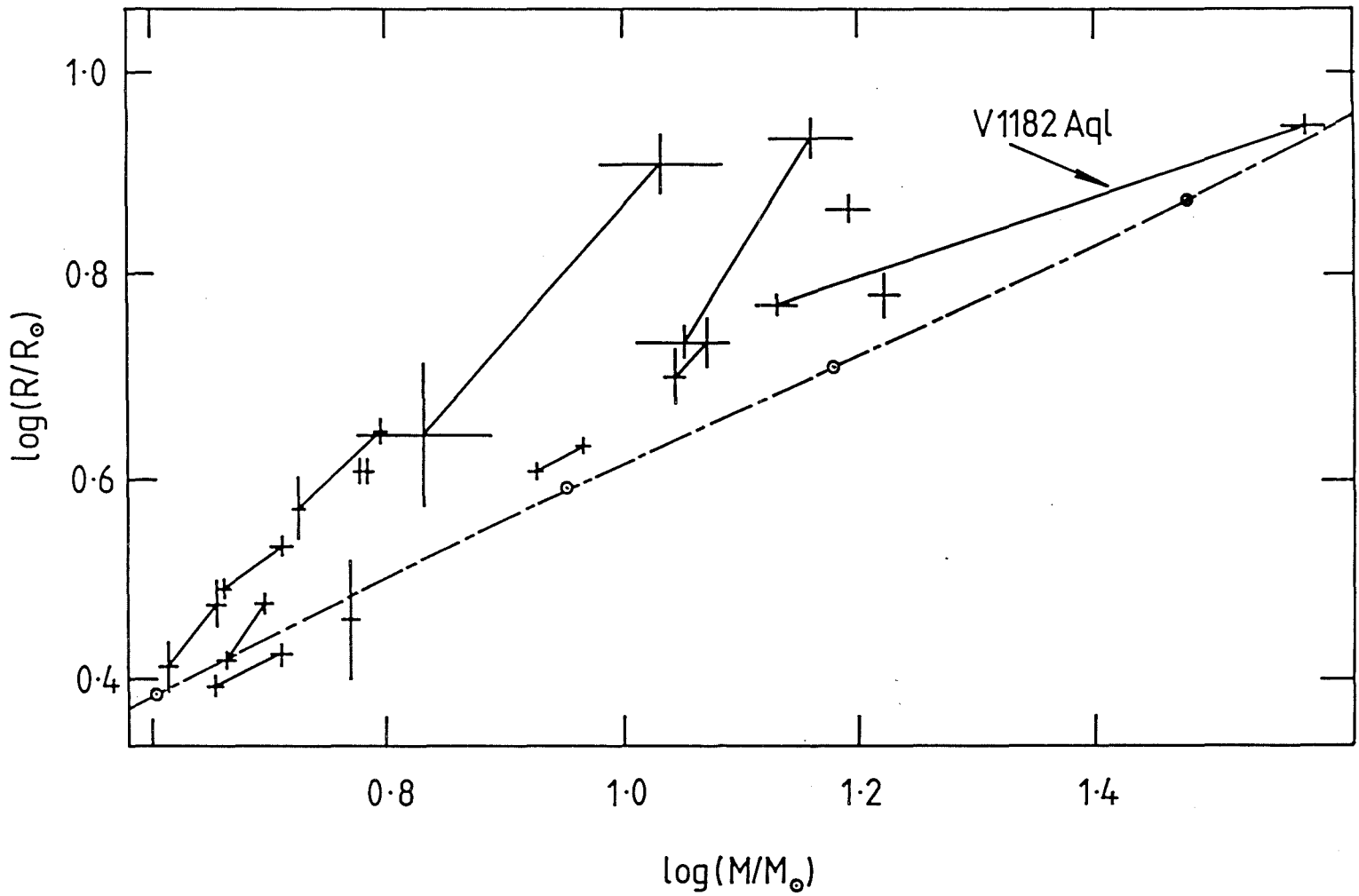


Figure 7.

CHAPTER 7

A photometric and spectroscopic study of the early-type binary

AI Crucis.

A photometric and spectroscopic study of the early-type binary

AI Crucis.

S.A.Bell, University Observatory, Buchanan Gardens, St. Andrews,
Fife, KY16 9LZ, Scotland.

D.Kilkenny, South African Astronomical Observatory, PO Box 9,
Observatory 7935, Cape, South Africa.

G.J.Malcolm, Boyden Observatory, Institute of Astronomy,
University of the Orange Free State, PO Box 339,
Bloemfontein 9300, South Africa.

Received _____

Correspondence to :-

S.A.Bell,
University Observatory,
Buchanan Gardens,
St. Andrews, Fife,
KY16 9LZ,
Scotland.

Summary

We present new Strömgren photometry and medium-dispersion spectroscopy of the early-type eclipsing binary AI Cru. The masses and radii of the two components are found to be (9.8 ± 0.5) and (5.8 ± 0.3) solar masses and (4.9 ± 0.1) and (4.4 ± 0.1) solar radii respectively. We confirm the semi-detached nature of the system noted by Russo (1980) and show by comparison with stationary models by Horn et al. (1970) that AI Cru has probably passed through the rapid phase of case A mass transfer. We suggest that the original system may have had a period of about 1.3^d and that the roles of the current primary and secondary components were at that time reversed.

1) Introduction

The early-type binary system AI Cru (CPD -60° 3273, CoD -60° 3971: Sp. type B2IV) was discovered to be an eclipsing binary by Oosterhoff (1933). His brightness estimates from 388 photographic plates formed a mean light curve of period 1.4177073 days whose depths of primary and secondary minimum were $1^m.0$ and $0^m.4$ respectively. Ollongren (1956) published an analysis of the photoelectric observations obtained by Oosterhoff and noted that AI Cru is probably a member of the open cluster NGC 4103. His analysis suggested that the system was composed of a B5 primary and a smaller, cooler and fainter B8 secondary. He also found the eclipses to be total but required third light, corresponding to 2% of the total light of the system, to secure a plausible fit to secondary minimum.

A more recent analysis of the original photoelectric data was made by Giuricin et al. (1980) using the program WINK (Wood, 1972). They found significant differences between their own analysis and that of Ollongren. They were able to confirm that the primary minimum was a transit but ruled out the need for third light to obtain a satisfactory fit to the light curve. As no spectroscopic study was then available, a "best-fit" photometric mass ratio of 0.8 was derived which suggested that the system was detached although both components were not far away from their respective critical Roche lobes.

A third analysis of Ollongren's data has been made by Russo (1980) using the method of Wilson and Devinney (1971). His solution showed good agreement with that obtained from the less physically realistic model of Giuricin et al. (1980). The most significant

difference between the two solutions was the photometric mass ratio for which Russo had determined a value of 0.6. He concluded that the system was semi-detached with the secondary component in contact with its critical Roche lobe.

The data on which all these analyses rest are not of the highest quality as Ollongren has pointed out. A thorough spectroscopic and photometric study would provide the necessary absolute dimensions for AI Cru to evaluate which of the two possible configurations is correct and also allow the evolutionary status of the system to be determined. If AI Cru is a member of NGC 4103, then it will establish an upper limit to the age of the system and place more rigorous constraints on theoretical calculations with which the components of the system can be compared.

2) Spectroscopy

2.1) Observations

The spectroscopic data for AI Cru were obtained using the 1.9m telescope at SAAO, Sutherland in conjunction with the Image Tube Spectrograph and Reticon Photon Counting System (RPCS). A total of 18 spectra was obtained by SAB during the period 1986 February 18-24 and by DK between 1986 April 5-8 of which 11 were double-lined. Grating 3 was employed in the second order to give a dispersion of 30 \AA mm^{-1} and provide spectra over a usable spectral range of 500 \AA centred on 4200 \AA . A slit width of $100 \mu\text{m}$ was used corresponding to 0.9 arcseconds projected on the sky and dekker 3 was employed to define star and sky "holes" on arrays A and B of the RPCS respectively for all the stellar observations. Stellar exposures were made using integration times of 600s and were alternated with

Cu-Ar comparison arc exposures for calibration purposes. Neutral density filters were also used to prevent the saturation of the RPCS whenever necessary.

On each night, several observations were made of radial-velocity standard stars to ensure the observations were commensurate with the standard system. The observed radial velocities of these standard stars showed an rms scatter of 4kms^{-1} about the standard system. Observations were also made of three B stars which had been selected for use as template spectra for subsequent cross-correlation analyses. SAO 217922, SAO 198315 and SAO 235690 were chosen from a compilation of radial velocities for early type stars by Zentelis (1983) because they showed good agreement with previous observations, for example those made by Andersen and Nordstrom (1983).

2.2) Reduction and Analysis

Wesselink (1969) gave a spectral type of B2IV for the primary component of AI Cru but noted that Lloyd Evans and Thackeray found some evidence that the spectral type should be revised to B2IVe. However, no evidence has been found in the spectra obtained for this study to confirm the existence of any emission features.

The spectroscopic data were processed on the University of St. Andrews VAX computers, using the STARLINK package FIGARO to flat-field the spectra, effect the sky background subtraction and convert them into a form suitable for the spectroscopic image-processing package REDUCE (Hill et al., 1982a).

As the star and sky observations were made in different arrays of the RPCS, checks were made for systematic shifts between the two arrays before sky subtraction was made. Small shifts were found (~ 0.8 pixels), but the sky background signal was so small that these shifts had no appreciable effect on the final radial velocity measurements.

Smoothing, rectification and log-linearisation were applied in the manner described elsewhere by Bell et al. (1986a). Cross-correlation analysis using VCROSS (Hill, 1982) was attempted employing the spectrum of the B4V star SAO 235690 as a template. This method proved to be too susceptible to the inherent noise in the data and to the mis-matching of the sharp standard star lines with the extremely rotationally-broadened features of AI Cru. The amplitude of this noise was approximately 6% of the continuum height, whereas the depths of the weak secondary features were of the order of 12% of the continuum height making identification of the cross-correlation peak corresponding to the secondary component very difficult.

Attempts were made to use VLINE (Hill et al, 1982b) to obtain radial velocities for both components by fitting double-gaussian profiles to several of the combined He I features. The susceptibility of VLINE to noise spikes severely restricted the use of this technique. For these reasons, it was necessary to measure the radial velocities of the two components using VELMEAS (Hill et al., 1982c) by fitting parabolae to those features which could be visually resolved and were not badly affected by noise spikes. An alternative method for determining the radial velocities of secondary features affected by noise spikes employed visual inspection of the lines centres using VELMEAS. The errors on the

primary and secondary radial velocities are estimated to be approximately 15kms^{-1} for this technique.

The principal spectral features showing splitting were the HeI lines at $\lambda\lambda 4009, 4026, 4120, 4144, 4388$ and 4471 . A section of the spectrum of AI Cru at first quadrature is shown in Figure 1 (SAA02/21). The rest wavelengths adopted for this analysis have been taken from the list by Petrie (1953). The measurement of these lines for radial velocity proved consistent, with the exception of $\lambda 4026$ and $\lambda 4471$ which were found to be blue-shifted by up to 8kms^{-1} relative to the mean radial velocity of the other He I lines. This may be attributed to rotational effects on these triplet lines. These determinations have been included in the subsequent analysis as the measuring uncertainty is of the same order as the velocity discrepancy.

The Balmer lines were omitted from the analysis due to their extremely Stark-broadened and rotationally-broadened profiles. The final radial velocities for both components of AI Cru are listed in Table 1 and the radial velocity curves are given in Figure 2. As the interstellar K line appeared at the blue end of the wavelength region being observed, no reliable measurements of the radial velocity of this feature could be made due to uncertainties in the wavelength calibration.

Examination of the v, b and y light curves for AI Cru show no evidence for any eccentricity in the orbit and we have assumed a circular orbit for the subsequent analysis. Adopting the procedures of Popper (1974), the circular orbital elements of AI Cru were computed by separate analysis of each component. Only double-lined measurements have been used in these analyses in order to avoid

systematic errors arising from the effects of blending and rotational distortion in the radial velocity determinations. Eleven primary component velocity measurements have been used in the least-squares analysis to determine the velocity semi-amplitude of the primary K_1 and the systemic velocity V_0 . The secondary velocity semi-amplitude K_2 was evaluated in a similar manner to K_1 using the secondary-component velocities but without making a determination for V_0 . The derived mass functions and projected semi-major axes of the orbits of the two components, together with their standard errors, are given in Table 2.

Using a technique to determine directly K_1 and K_2 from spectra obtained at quadratures described by Bell et al. (1986b), we have found values of the velocity semi-amplitudes in good agreement with those determined from the measurement of discrete features. The most suitable spectra for this determination were SAA01/012 and SAA02/252 using the HeI feature at $\lambda 4026$. Corrections have been applied to the results to allow for the fact that one of the spectra had been obtained at $0^{\text{P}}16$. Velocity semi-amplitudes of $169 \pm 10 \text{ km s}^{-1}$ and $271 \pm 15 \text{ km s}^{-1}$ were found for the primary and secondary components respectively, which provide independent confirmation of the determinations made from the radial-velocity curves given in Table 2.

By means of the measurement of the half-widths of both components of the HeI $\lambda 4471$ feature using VLINE, we have estimated the projected rotational velocities for both stars using the calibration of Slettebak et al. (1975). The exposure showing the most satisfactorily-resolved feature was SAA01/018, and from this spectrum we estimate the projected rotational velocities of the primary and secondary components to be 170 ± 10 and $150 \pm 10 \text{ km s}^{-1}$

respectively. If the assumption of synchronous rotation is made and the final mean radii of the two stars derived from the corrected velocity semi-amplitudes are adopted (see Table 8), then theoretical projected rotational velocities of 175 and 156kms^{-1} would be expected for the primary and secondary components respectively.

Measurements of the equivalent widths for the two components of the $\lambda 4471$ feature on SAA01/18 would imply a luminosity ratio of the secondary L_s to the primary L_p of 0.48 with an estimated error of approximately 10% assuming the intrinsic line strengths for the primary and secondary components are similar. This compares quite favourably with the luminosity ratio obtained photometrically of 0.43 for the b light curve.

3) Photometry

3.1) Observations

The photoelectric photometry for AI Cru was obtained by SAB during the period 1985 February 14-22 by means of the 0.5m telescope at SAAO, Sutherland, using the single channel Modular Photometer with an EMI 6256QA tube and uvby filters. A 30 arcsecond diaphragm was used throughout the observations and integration times were fixed at 60s for the monitoring sequence. A complete light curve was obtained with the exception of an interval of approximately 25 minutes around primary minimum. On those nights when primary minimum was obtainable, poor weather conditions prevented the determination of the depth of the minimum. The comparison star chosen for its proximity to AI Cru for this study was CPD -60° 3727 and the check star was CPD -60° 3746; data for the variable and comparison stars are given in Table 4. Both the comparison and the

check stars were found to be constant in brightness to considerably better than 0.01^m . During each night, between 15 and 25 uvby standard stars were observed to allow the observations to be transformed to the standard system.

The confirmation of the depth of primary minimum was made using the 0.41m telescope at Boyden Observatory by GJM and SAB. The photometer and data acquisition system used for these observations have been described fully elsewhere (Malcolm and Bell, 1986). Observations were made using UBV filters on three separate occasions to determine the shape and depth of primary minimum. Observations of E-region standards were also made before and after the monitoring sequence to facilitate the transformation of the data to the standard system. The star CPD -60° 3727 was again employed as the comparison star using a 30 arcsecond diaphragm. However, the integration times were shortened to 30s to provide better coverage of the minima.

3.2) Reductions

The SAAO photometric reduction package was used to reduce the Stromgren data to instrumental magnitudes and transform the observations to the standard system. Differential magnitudes with respect to CPD -60° 3727 were formed using a spline-fitting program written by SAB. The resultant differential magnitudes in the standard system and the corresponding mean times of observation are given in Table 3. A total of 207 uvby observations were made in each colour and the resulting b light curve and colour index changes are given in Figures 3 and 4 respectively.

The observations made at Boyden were reduced using the methods outlined by Bell et al. (1986a) and transformed to the standard UBV system. These observations show that primary minimum in the V passband is approximately 0.^m03 fainter than the deepest part of the transformed y light curve obtained at SAAO. Assuming that the transformed y and V light curves are comparable and there is little colour change in the missing section of the light curves, it is possible to establish the depth of primary minimum of the u,v and b light curves. The quoted magnitude for 0.^p0 for AI Cru given in Table 4 is based on the observed V magnitude of primary minimum obtained at Boyden.

3.3) Ephemeris

Ollongren (1956) provided the following ephemeris for AI Cru based on both photographic and photoelectric data. However, it is worth noting that he was unable to determine a time of primary minimum directly and therefore calculated the time of minimum based on the older ephemeris of Oosterhoff (1933) and the partial coverage of a primary minimum on the date given below.

$$\text{Pri. Min.} = \text{H.J.D. } 2433466.3358 + 1.4177073 E$$

± 2
 ± 7

Ollongren found no evidence for any significant fluctuations in the period of the system during the 25 years for which photographic minima were available. A total of three new times of primary minima have been obtained from Johnson V and B band observations made at Boyden, and a new ephemeris has been calculated using the published photoelectric times of minima given in Table 5. The method of Kwee and van Woerden (1956) has been used for the calculation of all of

the times of minima. An unweighted least-squares analysis was made to determine the period using the tabulated photoelectric times of minima. The time of minimum calculated by Ollongren has been included in our analysis as it shows no appreciable residual in the period determination. The new photometric and spectroscopic data presented in this paper for AI Cru have been phased using the ephemeris given below.

$$\text{Pri. Min.} = \text{H.J.D. } 2446567.4063 + 1.4177112 \text{ E}$$
$$\qquad \qquad \qquad \pm 1 \qquad \qquad \qquad \pm 1$$

As observational data for this system are sparse, analysis of the times of minima given in Table 5 cannot provide reliable evidence for variations in the period of AI Cru. Further observations will be required to confirm the provisional ephemeris given here.

3.4) Colour indices

The observed and de-reddened colour indices for AI Cru and both of the comparison stars are given in Table 4. There appears to be little change in the (b-y) and (v-b) colour indices with orbital phase for AI Cru. However, (u-b) shows very marked changes at both minima. The asymmetries in the light curves discussed in Section 3.5 introduce considerable phase shifts into the colour curves. In particular, the (u-b) curve (see Figure 4) is badly affected by distortions in the u curve. Less pronounced asymmetries in the y curve have correspondingly smaller effects on the (b-y) curve at secondary minimum.

Good agreement between the colour excess in (b-y) for AI Cru and that of the comparison star can be seen, but the check-star colour excess is 50% larger. Using the relationship $E(b-y) = 0.74 E(B-V)$, excellent agreement between the mean colour excess for NGC 4103 of $0.^m.30$ calculated by Wesselink (1969) in (B-V) and that of the variable and comparison of $0.^m.224$ in (b-y) can be obtained.

3.5) Analysis

A preliminary inspection of the photometric data for AI Cru shows that the system has light curves indicative of strongly distorted components of significantly different temperatures. The v and b curves show no evidence of asymmetry in either minimum whereas some evidence for small-scale distortions in the secondary minimum of the y curve can be seen. All the light curves do exhibit a noticeable $0.^m.02$ "dip" between $0.^p.15$ and $0.^p.19$. However, the secondary minimum of the u curve shows very marked distortion on the egress from secondary minimum. There is also evidence for a similar effect in the primary minimum. The effect of the distorted u curve is most clearly seen in the (u-b) colour curve in Figure 4. The primary minimum occurs earlier in (u-b) than in the other colour curves; the opposite is found to be the case for secondary minimum. As the observations were made on a single channel photometer, corrections have been applied to the phasing of the individual light curves corresponding to the difference between the mean time of a set of uvby observations and the actual time of observation for an individual band. This correction amounts to approximately $0.^p.001$ and cannot be the cause of the asymmetries in the u curve noted above.

The (b-y) colour index shows no appreciable variation over the orbital cycle. The (u-b) colour index, however, shows quite marked changes at both minima. The light-curve solutions show clearly that the flux from the secondary component at 0.5^P is of the order of a few per cent and we have therefore estimated the primary temperature from the colours at this phase. Using the (c_o, T_{eff}) calibration of Davis and Shobbrook (1977), we have adopted a primary temperature of 24200K. This temperature is considerably higher than that used in previous analyses and can be ascribed to a star of spectral type B1.5. We have estimated that the error in the primary-component temperature is approximately 500K.

Each light curve was analysed using LIGHT (Hill, 1979), fixing the mass ratio q at that determined from the spectroscopic analysis and the primary component-temperature T_1 by the photometric calibration outlined above. The fractional primary-component radius r_1 , the secondary-component temperature T_2 and fractional radius r_2 , and the inclination of the system i were kept as free parameters. As a first approximation, the solution of Russo (1980) was used. Table 6 lists the results of the analysis for the four light curves.

The following assumptions were made for each analysis. Black-body fluxes were adopted because preliminary solutions using the model atmospheres of Kurucz (1979) gave inferior fits. Synchronous rotation was assumed since the projected synchronous rotational velocities computed from our final fit agreed quite well with the observed values (see Section 2.2). Gravity-darkening exponents (β_1 and β_2) were set at 0.25 for both components, and electron scattering fractions (Escat_1 and Escat_2 for the primary and secondary components respectively) were taken from Hutchings and Hill (1971). The limb-darkening coefficients were calculated

automatically within LIGHT at each iteration of the solution, using interpolation from the tabulation by Carbon and Gingerich (1969).

The final results of our light-curve solutions are given in Table 7. The u-curve solution has a secondary temperature of the order of 1000K cooler than the other solutions. The solution also requires a smaller primary component and a larger secondary component. The distortions in the u curve have a pronounced effect on the solution using this light curve and for these reasons, our adopted final solution is based on the results of the analyses for the v, b and y curves only. The residuals of the uvby observations from the theoretical curves for each passband are shown in Figure 5. Further solutions were made to evaluate the sensitivity of the solutions on the adopted primary temperature and mass ratio. Changes to the primary temperature had no effect on the solution, with the exception of the calculated secondary temperature. Variations in the mass ratio of ± 0.05 at intervals of 0.01 made no significant difference to the solutions obtained, and there would appear to be only a weak dependence on the adopted mass ratio for this system.

4) Discussion

4.1) Spectroscopy and Photometry

The velocity separation of approximately 450kms^{-1} for the two components of AI Cru is probably not large enough for the effects of blending of the diffuse HeI lines to be ignored (Andersen, 1975). The effects of reflection and blending will systematically reduce the velocity semi-amplitudes of the two components. Employing the method of Kitamura (1953, 1954) to allow for reflection effects, we

find corrections of 1 and 2kms^{-1} for K_1 and K_2 respectively. The assumptions made by this method are probably still reasonable, given the nature of AI Cru. In order to compensate for the effects of reflection and blending we have applied a total correction of 5% to the primary and secondary velocity semi-amplitudes. This correction is based on experience with other systems but must be regarded as a rough estimate. The orbital elements determined from the corrected values of the velocity semi-amplitudes are given in Table 2.

Astrophysical data for this system are given in Table 8. Data based on both the observed and corrected velocity semi-amplitudes are tabulated. The bolometric corrections quoted in Table 8 are taken from the calibration of Davis and Shobbrook (1977). The errors quoted in Table 8 are derived from the formal errors of the spectroscopic and photometric analyses. They are likely to be underestimates of the real errors because they do not take into account the uncertainties in such quantities as the blending correction which is at best a rough estimate and the distribution of radial-velocity and photometric data whose analyses may provide somewhat optimistic formal errors. It is probably more realistic to increase the error estimates on the masses, radii and luminosities of the two components by a factor of two for the radii and luminosities and three for the masses.

4.2) Membership of NGC 4103

Wesselink (1969) calculated a mean colour excess in (B-V) of 0.30^m for NGC 4103 and a distance of 1600pc. We find a comparable colour excess in (b-y) and a distance of $1980 \pm 180\text{pc}$. Although our estimate of the distance is larger than that of Wesselink, it is in

good agreement with the distance of 1880pc determined by Balona and Shobbrook (1984), and it seems extremely likely that AI Cru is a member of NGC 4103. The same cannot be said for the check star which Wesselink classified as being of spectral type B0; this is confirmed by its c_0 colour index. He noted that there were probably no stars earlier than spectral type B2 in the cluster, and our colour excess for the check star would suggest that it is considerably more distant than the cluster itself.

The isochrone for 25×10^6 yrs in the theoretical HR diagram of Hejlesen (1980) for a composition of ($X = 0.70$, $Z = 0.02$) is in good agreement with the colour-magnitude diagram given by Wesselink in the range $15^m.0 > V > 9^m.0$. Stars beyond $(B-V) = 0^m.3$ and in the range $16^m.7 > V > 15^m.0$ are still contracting towards the main sequence and cannot therefore lie on this isochrone. Our estimate of $(25 \pm 5) \times 10^6$ yrs for the age of this cluster is in good agreement with that determined by Wesselink, namely 27×10^6 yrs, and can be considered as an upper limit to the age of AI Cru itself.

4.3) Evolutionary state

Adopting the corrected masses for the two components, comparisons with the evolutionary tracks for single stars published by Hejlesen (1980) show that a chemical composition of ($X = 0.70$, $Z = 0.02$) provides good agreement with the locations of the primary and secondary components. However, the age determinations using the temperature and surface gravity of the two stars show a large discrepancy. The primary component lies on an evolutionary track appropriate to its mass at an age of 11×10^6 yrs, but the secondary component is in agreement with the mass track for a $6M_{\odot}$ star at an

age of 38×10^6 yrs. Assuming AI Cru is a member of NGC 4103, the secondary cannot be older than the age of the cluster determined in Section 4.2. If the uncorrected masses are used, both stars are overluminous by $\sim 0.5^m$ for their respective masses.

Alternatively, if a composition of ($X = 0.80$, $Z = 0.02$) is adopted in conjunction with the corrected masses, then both components would again appear to be overluminous by $\sim 0.5^m$. The change of composition for the models has no effect on the age discrepancy described above. The masses of both components would have to be increased by $\sim 10\%$ to provide a good fit to the required temperature and luminosity, but justification for such a correction would prove difficult to find. The work of Andersen et al. (1983) on other B-type systems shows that the model with a higher helium content is to be preferred.

Comparing the mass and radius of the two components with the zero-age main sequence relation derived from the models of Hejlesen, it is clear that both stars are evolved. In the case of the primary component, the radius is $0.7R_{\odot}$ larger than that of a zero-age main-sequence star of similar mass. The situation for the secondary is more marked with the star being $1.3R_{\odot}$ larger than the corresponding zero-age main-sequence star (see Figure 6). However, if the two stars are considered individually, both components appear to be main-sequence objects.

The primary and secondary components of AI Cru fill 65% and 92% of their Roche lobes respectively and, in view of the age discrepancy between the two components, it seems very probable that this system has evolved through the rapid phase of case A mass exchange and a reversal of the mass ratio has taken place. The

stationary models representing the end of this rapid phase of mass exchange by Horn et al. (1970) have been used to make comparisons with the absolute dimensions of AI Cru. The phase of rapid mass transfer takes place in the order of 10^5 yrs, and it is unlikely that the system will be observed during this interval. It is more likely, however, that the system will be observed in the slow phase of mass transfer that follows. Caution should be exercised in the interpretation of these models as the parameters of the system may change during this interval.

Assuming there has been no mass loss from the system, the original mass of AI Cru must have been around $16M_{\odot}$. This can be conveniently compared with the models of total mass $15.75M_{\odot}$, initial primary mass $9M_{\odot}$ and a mass ratio of 0.75. The observed absolute dimensions of AI Cru and the two models giving the best agreement with these data are given in Table 9. These models represent the system at two possible ages after the rapid mass-transfer phase. The masses and temperatures of both components, the primary radius, the period, the mass ratio and separation can be compared with the observed parameters. It can be seen that the absolute dimensions of AI Cru show better agreement with the older model. It is possible that the model for AI Cru before mass-ratio reversal may have involved a $9M_{\odot}$ primary and a $6.6M_{\odot}$ secondary with a period of approximately 1.3 d. After an interval of about 10^7 yrs, the rapid phase of case A mass exchange took place which lasted of the order of 10^5 yrs. The slow phase of mass transfer may still be in progress as the asymmetries in the light curve are suggestive of photospheric matter in the system. Plavec et al. (1968) suggest that this phase lasts at least 2.5×10^6 yrs, based on their model of an $9M_{\odot} + 8M_{\odot}$ system. It would appear that the roles of the two components have

been reversed with the final mass ratio being slightly more extreme than that for the original system.

5) Conclusion

We have presented new Strömgren photometry and medium-resolution spectroscopy of AI Cru. A reliable determination of the absolute dimensions of the components of the system has been made, and we have confirmed the semi-detached nature of the system with a Roche lobe-filling secondary component. This analysis is in good agreement with the study made by Russo (1980). It is probable that case A evolution has taken place in this system and that it may now be in the slow phase of mass transfer. There are insufficient observational data available to detect any period change. However, there is some photometric evidence of photospheric activity which may be caused by mass flow in the system.

Comparing the observed parameters of the system with models by Horn et al. (1970) suggest that the original system may have had a marginally shorter period and that roles of the two stars have reversed as a result of case A mass transfer. It should be noted that these older computations of conservative mass transfer have, in general, been found to be inadequate in explaining the properties of semi-detached systems. However, it would be of considerable interest to compare the current state of AI Cru with more modern evolutionary models to confirm this scenario.

Acknowledgements

The authors would like to express their thanks for the hospitality and assistance extended to them by the staffs of the South African Astronomical Observatory and the Institute of Astronomy of the University of the Orange Free State during the observing runs. We acknowledge PATT for the allocations of observing time at SAAO, and the SERC for financial support in the form of a research studentship for one of us (SAB). SAB gratefully acknowledges a visiting fellowship from the University of the Orange Free State and financial assistance made available by the University of St. Andrews. He also wishes to express his gratitude to Prof. A.H. Jarrett and Prof. D.W.N. Stibbs for the use of the facilities of the Boyden Observatory and the University Observatory, St. Andrews respectively and to Dr. R.W. Hilditch for many helpful and lively discussions during the course of this study. We would also like to express our gratitude to Dr. J. Andersen for his constructive criticism of our analysis.

References

- Andersen, J., 1975. *Astron. Astrophys.*, 44, 355.
- Andersen, J., Clausen, J.V., Gimenez, A. & Nordstrom, B., 1983. *Astron. Astrophys.*, 128, 17.
- Andersen, J. & Nordstrom, B., 1983. *Astron. Astrophys. Suppl. Ser.*, 52, 471.
- Balona, L.A. & Shobbrook, R.R., 1984. *Mon. Not. R. astr. Soc.*, 211, 375.
- Bell, S.A., Hilditch, R.W. & Adamson, A.J., 1986a. *Mon. Not. R. astr. Soc.*, 223, 513.
- Bell, S.A., Hilditch, R.W. & Adamson, A.J., 1986b. *Mon. Not. R. astr. Soc.* in press.
- Bell, S.A., Adamson, A.J. & Hilditch, R.W., 1986c. *Mon. Not. R. astr. Soc.* in press.
- Carbon, D.F. & Gingerich, O.J., 1969. *Theory and Observations of Normal Stellar Atmospheres*, ed. Gingerich, O.J. (M.I.T. press, Cambridge), 377.
- Davis, J. & Shobbrook, R.R., 1977. *Mon. Not. R. astr. Soc.*, 178, 651.
- Giuricin, G., Mardirossian, F., Mezzetti, M. & Predolin, F., 1980. *Astrophys. Space Sci.*, 71, 411.
- Hejlesen, P.M., 1980. *Astron. Astrophys. Suppl. Ser.*, 39, 347.
- Hilditch, R.W., 1984. *Mon. Not. R. astr. Soc.*, 211, 943.

- Hill,G., 1979. Publ. Dom. Astrophys. Obs., 15, 297.
- Hill,G., 1982a. Publ. Dom. Astrophys. Obs., 16, 59.
- Hill,G., Fisher,W.A. & Poeckert,R., 1982a. Publ. Dom. Astrophys. Obs., 16, 43.
- Hill,G., Fisher,W.A. & Poeckert,R., 1982b. Publ. Dom. Astrophys. Obs., 16, 27.
- Hill,G., Ramsden,D., Fisher,W.A. & Morris,S.C., 1982c. Publ. Dom. Astrophys. Obs., 16, 11.
- Horn,J., Kriz,S. & Plavec,M., 1968. Bull. astr. Inst. Czechoslovakia, 21, 45.
- Hutchings,J.B. & Hill,G., 1971. Astrophys. J., 167, 137.
- Kitamura,M., 1953. Publ. astr. Soc. Japan, 5, 114.
- Kitamura,M., 1954. Publ. astr. Soc. Japan, 6, 217.
- Kwee,K.K. & van Woerden,H., 1956. Bull. astr. Inst. Netherlands, 12, 327.
- Kurucz,R.L., 1979. Astrophys. J. Suppl. Ser., 40, 1.
- Landolt,A.U., 1970. Inf. Bull. Var. Stars, No. 446.
- Malcolm,G.J. & Bell,S.A., 1986. Mon. Not. astr. Soc. South Africa, 45, No. 1 & 2.
- Ollongren,A., 1956. Bull. astr. Inst. Netherlands., 12, 313.
- Oosterhoff,P.Th., 1933. Bull. Astr. Inst. Netherlands., 9, 73.
- Petrie,R.M., 1953. Publ. Dom. Astrophys. Obs., 9, 297.

Plavec, M., Kriz, S., Harmanec, P. & Horn, J., 1968. Bull. astr. Inst. Czechoslovakia, 19, 24.

Popper, D.M., 1974. Astron. J., 79, 1307.

Russo, G., 1981. Astrophys. Space Sci., 77, 197.

Slettebak, A., Collins, G.W., Boyce, P.B., White, N.M. & Parkinson, T.D., 1975. Astrophys. J. Suppl. Ser., 29, 137.

Wells, D.C., Greisen, E.W. & Harten, R.H., 1981. Astrophys. J. Suppl. Ser., 44, 363.

Wesselink, A.J., 1969. Mon. Not. R. astr. Soc., 146, 329.

Wilson, R.E. & Devinney, E.J., 1971. Astrophys. J., 166, 605.

Wood, D.B., 1972, A Computer program for Modelling Non-Spherical Eclipsing Binary Systems, Goddard Space Flight Centre, Greenbelt, Maryland, U.S.A.

Zentelis, N., 1983. Astron. Astrophys. Suppl. Ser., 53, 445.

Figure captions

Figure 1: The spectrum of AI Cru in the wavelength range $\lambda\lambda 4000-4150$. This spectrum (SAA02/21) was taken at first quadrature during the second RPCS run.

Figure 2: Observed radial velocities and computed orbits for AI Cru. Primary-component data are represented by squares and secondary-component data by circles.

Figure 3: b-magnitude differences in the sense variable minus comparison between AI Cru and CPD $-60^\circ 3727$ together with the final theoretical curve.

Figure 4: (b-y) and (u-b) colour-index differences in the sense variable minus comparison between AI Cru and CPD $-60^\circ 3727$ together with the final theoretical curves.

Figure 5: Residuals of the individual uvby observations from the final theoretical curves.

Figure 6: The mass-radius relation using the theoretical ZAMS models of Maeder (1981). Data for a number of semi-detached systems with well-determined absolute dimensions have also been plotted for comparison with AI Cru (Popper, 1980; Andersen et al., 1983; Hilditch, 1984; Bell et al., 1986c).

Table 1 : Radial-velocity data for AI Cru.

Tape/Run	H.J.D.	Phase	V_1	n	O-C	V_2	n	O-C
No.	-2400000		kms^{-1}		kms^{-1}	kms^{-1}		kms^{-1}
SAA01/012	46480.5244	0.7168	+161	(4)	+ 5	-287	(3)	+ 1
SAA01/014	46480.5387	0.7269	+164	(4)	+ 6	-293	(3)	- 3
SAA01/016	46480.5540	0.7376	+164	(5)	+ 5	-298	(4)	- 6
SAA01/018	46480.5967	0.7678	+150	(3)	-10	-281	(4)	+11
SAA01/020	46480.6106	0.7776	+154	(6)	- 3	-262	(4)	+27
SAA01/073	46481.5404	0.4334	- 75	(4)	+ 7	----		---
SAA01/075	46481.5491	0.4396	- 62	(3)	+14	----		---
SAA01/249	46486.4660	0.9078	+ 73	(4)	-10	----		---
SAA01/251	46486.4759	0.9147	+ 80	(2)	+ 4	----		---
SAA01/253	46486.4856	0.9215	+ 63	(3)	- 7	----		---
SAA01/255	46486.4952	0.9284	+ 62	(2)	- 1	----		---
SAA01/257	46486.5044	0.9348	+ 51	(3)	- 6	----		---
SAA02/017	46529.4585	0.2330	-187	(5)	- 7	+272	(3)	- 6
SAA02/019	46529.4941	0.2582	-198	(3)	-15	+275	(4)	- 7
SAA02/021	46529.5078	0.2678	-174	(4)	+ 9	+276	(4)	- 5
SAA02/250	46533.6084	0.1602	-153	(4)	+ 4	+229	(3)	-10
SAA02/252	46533.6133	0.1637	-155	(5)	+ 4	+253	(4)	- 9
SAA02/254	46533.6187	0.1674	-161	(3)	- 1	+251	(4)	- 6

The columns headed n indicate the number of lines measured for the mean velocity tabulated.

Table 2 : Orbital elements for AI Cru.

		Measured	Corrected
K_1 (kms ⁻¹)	=	172 ± 2	181 ± 3
K_2 (kms ⁻¹)	=	282 ± 3	296 ± 3
V_o (kms ⁻¹)	=	-12 ± 2	--
σ_1 (kms ⁻¹) *	=	7	--
σ_2 (kms ⁻¹) *	=	9	--
q (m_2/m_1)	=	0.61 ± 0.01	0.61 ± 0.01
e	=	0 (adopted)	0 (adopted)
$a_1 \sin i$ (R)	=	4.83 ± 0.07	5.07 ± 0.07
$a_1 \sin i$ (R ^o)	=	7.90 ± 0.09	8.30 ± 0.09
$a \sin i$ (R ^o)	=	12.73 ± 0.11	13.37 ± 0.12
$m_1 \sin^3 i$ (M)	=	8.6 ± 0.2	9.9 ± 0.2
$m_2 \sin^3 i$ (M ^o)	=	5.2 ± 0.1	6.1 ± 0.1

* - r.m.s. scatter of a single observation.

Table 3 : uvby observations.

1985 Feb 14/15		Differential Magnitude (v-c)			
H.J.D.	Phase	V	b-y	v-b	u-b
2446111.35093	0.3157	-0.302	-0.004	-0.022	-0.181
2446111.35524	0.3188	-0.303	-0.007	-0.021	-0.180
2446111.35875	0.3212	-0.303	-0.007	-0.020	-0.180
2446111.36211	0.3236	-0.301	-0.006	-0.021	-0.167
2446111.38252	0.3380	-0.302	-0.002	-0.012	-0.172
2446111.38615	0.3406	-0.292	-0.003	-0.024	-0.176
2446111.38951	0.3429	-0.287	-0.012	-0.013	-0.178
2446111.39377	0.3459	-0.290	-0.011	-0.010	-0.166
2446111.41587	0.3615	-0.278	-0.006	-0.010	-0.183
2446111.41910	0.3638	-0.273	-0.013	-0.014	-0.174
2446111.42236	0.3661	-0.274	-0.006	-0.018	-0.177
2446111.42622	0.3688	-0.272	-0.016	-0.014	-0.183
2446111.44205	0.3800	-0.267	0.000	-0.020	-0.194
2446111.44554	0.3825	-0.259	-0.009	-0.026	-0.187
2446111.44882	0.3848	-0.252	-0.017	-0.018	-0.185
2446111.45208	0.3871	-0.251	-0.012	-0.021	-0.186
2446111.47528	0.4034	-0.234	-0.014	-0.014	-0.174
2446111.47839	0.4056	-0.222	-0.021	-0.006	-0.170
2446111.48145	0.4078	-0.224	0.000	-0.014	-0.178
2446111.48464	0.4100	-0.214	-0.012	-0.019	-0.180
2446111.49978	0.4207	-0.183	-0.005	-0.028	-0.187
2446111.50292	0.4229	-0.178	-0.004	-0.024	-0.192
2446111.50657	0.4255	-0.174	-0.005	-0.023	-0.188
2446111.50985	0.4278	-0.167	-0.002	-0.026	-0.192
2446111.53231	0.4437	-0.083	-0.023	-0.021	-0.203
2446111.53573	0.4461	-0.076	-0.017	-0.025	-0.206
2446111.53883	0.4483	-0.071	-0.008	-0.031	-0.202
2446111.54201	0.4505	-0.055	-0.018	-0.029	-0.204
2446111.55692	0.4610	-0.023	-0.005	-0.028	-0.203
2446111.55985	0.4631	-0.008	-0.021	-0.022	-0.189
2446111.56278	0.4652	-0.005	-0.015	-0.022	-0.181
2446111.56596	0.4674	0.002	-0.012	-0.021	-0.198
2446111.58680	0.4821	0.059	-0.017	-0.019	-0.204
2446111.58977	0.4842	0.069	-0.015	-0.021	-0.206
2446111.59311	0.4865	0.079	-0.016	-0.026	-0.217
2446111.59637	0.4888	0.083	-0.018	-0.024	-0.214
2446111.60348	0.4939	0.090	-0.019	-0.014	-0.211
2446111.60649	0.4960	0.093	-0.014	-0.021	-0.219

1985 Feb 15/16		Differential Magnitude (v-c)			
H.J.D.	Phase	V	b-y	v-b	u-b
2446112.33373	0.0090	0.436	0.001	-0.019	-0.094
2446112.33849	0.0123	0.428	-0.008	-0.017	-0.098
2446112.34328	0.0157	0.396	-0.006	-0.012	-0.099

continued....

2446112.34842	0.0193	0.378	-0.014	-0.014	-0.109
2446112.36325	0.0298	0.277	-0.009	-0.005	-0.124
2446112.36751	0.0328	0.255	-0.016	-0.012	-0.130
2446112.37185	0.0358	0.227	-0.011	-0.012	-0.131
2446112.37613	0.0389	0.204	-0.012	-0.021	-0.143
2446112.39967	0.0555	0.075	-0.020	-0.023	-0.140
2446112.40290	0.0577	0.053	-0.014	-0.021	-0.149
2446112.40631	0.0602	0.036	-0.014	-0.017	-0.154
2446112.40976	0.0626	0.011	-0.013	-0.027	-0.154
2446112.42828	0.0756	-0.073	-0.018	-0.020	-0.158
2446112.43195	0.0782	-0.095	-0.009	-0.011	-0.153
2446112.43520	0.0805	-0.103	-0.013	-0.017	-0.158
2446112.43856	0.0829	-0.119	-0.014	-0.009	-0.152
2446112.45942	0.0976	-0.173	-0.020	-0.010	-0.155
2446112.46295	0.1001	-0.178	-0.022	-0.016	-0.146
2446112.46619	0.1024	-0.190	-0.017	-0.008	-0.164
2446112.46966	0.1048	-0.195	-0.022	-0.010	-0.149
2446112.48280	0.1141	-0.221	-0.009	-0.020	-0.166
2446112.48600	0.1164	-0.220	-0.013	-0.016	-0.173
2446112.48946	0.1188	-0.226	-0.010	-0.021	-0.162
2446112.49297	0.1213	-0.221	-0.021	-0.016	-0.161
2446112.51203	0.1347	-0.243	-0.012	-0.016	-0.157
2446112.51536	0.1371	-0.242	-0.022	-0.019	-0.145
2446112.51851	0.1393	-0.244	-0.017	-0.018	-0.155
2446112.52155	0.1414	-0.248	-0.010	-0.017	-0.165
2446112.53467	0.1507	-0.244	-0.021	-0.016	-0.153
2446112.53764	0.1528	-0.256	-0.006	-0.007	-0.153
2446112.54078	0.1550	-0.250	-0.024	0.001	-0.152
2446112.54404	0.1573	-0.255	-0.010	-0.003	-0.159
2446112.56329	0.1709	-0.266	-0.008	-0.026	-0.170
2446112.56635	0.1730	-0.266	-0.002	-0.028	-0.171
2446112.56955	0.1753	-0.271	-0.007	-0.022	-0.167
2446112.57283	0.1776	-0.271	-0.009	-0.021	-0.160
2446112.58538	0.1865	-0.271	-0.017	-0.017	-0.156
2446112.58835	0.1886	-0.274	-0.012	-0.019	-0.167
2446112.59132	0.1906	-0.274	-0.021	-0.011	-0.159
2446112.59438	0.1928	-0.270	-0.026	-0.013	-0.159
2446112.59734	0.1949	-0.278	-0.018	-0.018	-0.165
2446112.60029	0.1970	-0.284	-0.006	-0.023	-0.176

1985 Feb 16/17

Differential Magnitude (v-c)

H.J.D.	Phase	V	b-y	v-b	u-b
2446113.31859	0.7036	-0.318	-0.004	-0.009	-0.172
2446113.32173	0.7059	-0.313	-0.006	-0.018	-0.174
2446113.32498	0.7081	-0.317	-0.001	-0.021	-0.170
2446113.32816	0.7104	-0.316	-0.007	-0.022	-0.171
2446113.34343	0.7212	-0.316	-0.013	-0.016	-0.161
2446113.34645	0.7233	-0.313	-0.014	-0.014	-0.171
2446113.34948	0.7254	-0.315	-0.005	-0.015	-0.179
2446113.36779	0.7383	-0.304	-0.026	-0.014	-0.160

continued....

2446113.37093	0.7406	-0.312	-0.019	-0.008	-0.170
2446113.37427	0.7429	-0.310	-0.026	-0.006	-0.172
2446113.37805	0.7456	-0.319	-0.011	-0.016	-0.174
2446113.39019	0.7541	-0.321	-0.016	-0.020	-0.165
2446113.39314	0.7562	-0.312	-0.021	-0.018	-0.168
2446113.39612	0.7583	-0.317	-0.010	-0.018	-0.160
2446113.41712	0.7731	-0.308	-0.019	-0.012	-0.171
2446113.42828	0.7810	-0.298	-0.018	-0.017	-0.166
2446113.43467	0.7855	-0.295	-0.019	-0.013	-0.167
2446113.43788	0.7878	-0.293	-0.026	-0.006	-0.162
2446113.45202	0.7978	-0.296	-0.016	-0.014	-0.166
2446113.45512	0.7999	-0.295	-0.018	-0.008	-0.167
2446113.45802	0.8020	-0.296	-0.017	-0.013	-0.166
2446113.46120	0.8042	-0.291	-0.019	-0.009	-0.165
2446113.47974	0.8173	-0.285	-0.013	-0.006	-0.161
2446113.48272	0.8194	-0.285	-0.012	-0.007	-0.163
2446113.48568	0.8215	-0.284	-0.011	-0.009	-0.160
2446113.48872	0.8236	-0.283	-0.012	-0.008	-0.159
2446113.50089	0.8322	-0.280	-0.008	-0.011	-0.165
2446113.50394	0.8344	-0.272	-0.009	-0.009	-0.166
2446113.50690	0.8365	-0.271	-0.016	-0.005	-0.164
2446113.50991	0.8386	-0.265	-0.014	-0.005	-0.158
2446113.52886	0.8520	-0.249	-0.016	-0.016	-0.164
2446113.53189	0.8541	-0.256	-0.007	-0.023	-0.161
2446113.53477	0.8561	-0.251	-0.003	-0.025	-0.168
2446113.53780	0.8583	-0.244	-0.012	-0.015	-0.160
2446113.54948	0.8665	-0.239	-0.010	-0.012	-0.163
2446113.55240	0.8686	-0.235	-0.013	-0.011	-0.163
2446113.55531	0.8706	-0.228	-0.018	-0.008	-0.163
2446113.55828	0.8727	-0.225	-0.013	-0.027	-0.162
2446113.57507	0.8845	-0.222	-0.009	-0.014	-0.154
2446113.57795	0.8866	-0.216	-0.011	-0.018	-0.154
2446113.58100	0.8887	-0.208	-0.012	-0.016	-0.156
2446113.58398	0.8908	-0.205	-0.011	-0.018	-0.154
2446113.59545	0.8989	-0.190	-0.006	-0.017	-0.154
2446113.59835	0.9010	-0.186	-0.008	-0.015	-0.150
2446113.60129	0.9030	-0.180	-0.001	-0.009	-0.154
2446113.60425	0.9051	-0.169	-0.008	-0.012	-0.153

1985 Feb 17/18

Differential Magnitude (v-c)

H. J. D.	Phase	V	b-y	v-b	u-b
2446114.45170	0.5029	0.091	-0.015	-0.026	-0.220
2446114.45476	0.5050	0.094	-0.018	-0.020	-0.235
2446114.45785	0.5072	0.085	-0.012	-0.017	-0.225
2446114.46100	0.5095	0.095	-0.032	-0.011	-0.231
2446114.47329	0.5181	0.068	-0.026	-0.014	-0.229
2446114.47646	0.5204	0.055	-0.021	-0.020	-0.223
2446114.48020	0.5230	0.048	-0.013	-0.026	-0.235
2446114.48326	0.5252	0.032	-0.004	-0.032	-0.229
2446114.50101	0.5377	0.004	-0.020	-0.024	-0.212

continued....

2446114.50407	0.5398	-0.010	-0.015	-0.027	-0.217
2446114.50714	0.5420	-0.022	-0.012	-0.030	-0.216
2446114.51015	0.5441	-0.032	-0.011	-0.031	-0.220
2446114.52218	0.5526	-0.061	-0.022	-0.020	-0.201
2446114.52537	0.5549	-0.075	-0.024	-0.017	-0.195
2446114.52855	0.5571	-0.086	-0.022	-0.017	-0.203
2446114.53165	0.5593	-0.103	-0.010	-0.028	-0.207
2446114.54985	0.5721	-0.151	-0.014	-0.013	-0.192
2446114.55288	0.5743	-0.157	-0.012	-0.013	-0.198
2446114.55593	0.5764	-0.171	-0.005	-0.015	-0.197
2446114.55897	0.5786	-0.178	-0.004	-0.017	-0.190
2446114.57075	0.5869	-0.201	-0.002	-0.018	-0.190
2446114.57375	0.5890	-0.207	-0.003	-0.019	-0.200
2446114.57675	0.5911	-0.200	-0.014	-0.016	-0.195
2446114.57985	0.5933	-0.208	-0.011	-0.022	-0.197
2446114.60390	0.6102	-0.249	-0.009	-0.023	-0.186
2446114.60693	0.6124	-0.250	-0.020	-0.016	-0.178

1985 Feb 19/20

Differential Magnitude (v-c)

H.J.D.	Phase	V	b-y	v-b	u-b
2446116.33379	0.8304	-0.269	-0.021	0.000	-0.155
2446116.33695	0.8327	-0.267	-0.017	-0.012	-0.161
2446116.34033	0.8351	-0.272	-0.012	-0.006	-0.159
2446116.35517	0.8455	-0.263	-0.007	-0.013	-0.167
2446116.35835	0.8478	-0.268	-0.008	-0.015	-0.162
2446116.36625	0.8533	-0.270	0.001	-0.019	-0.168
2446116.36981	0.8559	-0.263	-0.003	-0.021	-0.169

1985 Feb 20/21

Differential Magnitude (v-c)

H.J.D.	Phase	V	b-y	v-b	u-b
2446117.36224	0.5559	-0.081	-0.017	-0.017	-0.195
2446117.36529	0.5580	-0.084	-0.016	-0.017	-0.206
2446117.36877	0.5605	-0.093	-0.026	-0.008	-0.193
2446117.45549	0.6217	-0.265	-0.002	-0.013	-0.183
2446117.45878	0.6240	-0.268	-0.010	-0.017	-0.182
2446117.46743	0.6301	-0.266	-0.006	-0.024	-0.194
2446117.47057	0.6323	-0.268	-0.009	-0.023	-0.189
2446117.47367	0.6345	-0.266	-0.015	-0.020	-0.181
2446117.47682	0.6367	-0.279	-0.004	-0.017	-0.183
2446117.48936	0.6455	-0.278	-0.007	-0.023	-0.183
2446117.49247	0.6477	-0.281	-0.008	-0.021	-0.187
2446117.49556	0.6499	-0.280	-0.011	-0.019	-0.187
2446117.49900	0.6523	-0.281	-0.012	-0.018	-0.183
2446117.51812	0.6658	-0.293	-0.002	-0.028	-0.186
2446117.52120	0.6680	-0.298	-0.004	-0.024	-0.181
2446117.52422	0.6701	-0.295	-0.008	-0.020	-0.175
2446117.52760	0.6725	-0.297	-0.007	-0.018	-0.180
2446117.54037	0.6815	-0.297	-0.009	-0.024	-0.178

continued....

2446117.54342	0.6837	-0.294	-0.013	-0.016	-0.178
2446117.54640	0.6858	-0.295	-0.014	-0.018	-0.178
2446117.54945	0.6879	-0.290	-0.014	-0.022	-0.184
2446117.56971	0.7022	-0.314	-0.008	-0.012	-0.179
2446117.57275	0.7044	-0.313	-0.008	-0.015	-0.176
2446117.57602	0.7067	-0.313	-0.015	-0.011	-0.165
2446117.57941	0.7091	-0.309	-0.014	-0.023	-0.177

1985 Feb 21/22

Differential Magnitude (v-c)

H.J.D.	Phase	V	b-y	v-b	u-b
2446118.32999	0.2385	-0.311	-0.014	-0.015	-0.156
2446118.33325	0.2408	-0.297	-0.019	-0.001	-0.174
2446118.33667	0.2432	-0.302	-0.023	-0.012	-0.171
2446118.33984	0.2454	-0.298	-0.029	-0.020	-0.173
2446118.38161	0.2749	-0.303	-0.003	-0.022	-0.174
2446118.38484	0.2772	-0.305	-0.018	-0.017	-0.178
2446118.38806	0.2795	-0.312	-0.014	-0.011	-0.165
2446118.39130	0.2817	-0.317	-0.015	-0.008	-0.161
2446118.40454	0.2911	-0.305	-0.017	-0.003	-0.170

1985 Feb 22/23

Differential Magnitude (v-c)

H.J.D.	Phase	V	b-y	v-b	u-b
2446119.31445	0.9329	-0.032	-0.003	-0.009	-0.141
2446119.31760	0.9351	-0.012	-0.009	-0.014	-0.138
2446119.32126	0.9377	0.008	-0.012	-0.005	-0.130
2446119.32455	0.9400	0.011	0.006	-0.016	-0.139
2446119.33632	0.9483	0.073	-0.002	-0.009	-0.115
2446119.33945	0.9505	0.099	-0.015	-0.004	-0.110
2446119.34267	0.9528	0.106	0.002	-0.017	-0.108
2446119.34593	0.9551	0.130	-0.003	0.002	-0.106
2446119.36404	0.9679	0.250	-0.004	-0.009	-0.099
2446119.36737	0.9702	0.269	-0.007	-0.004	-0.087
2446119.37090	0.9727	0.290	-0.007	-0.002	-0.086
2446119.37451	0.9753	0.310	0.001	-0.010	-0.078
2446119.38981	0.9860	0.404	-0.012	0.002	-0.078
2446119.39415	0.9891	0.435	-0.008	-0.009	-0.077

Table 4 : Data for AI Cru, CPD -60° 3727 and CPD -60° 3746.

	AI Cru	CPD -60° 3727	CPD -60° 3746
CoD no.	-60° 3971	-----	-60° 3984
SAO no.	-----	-----	SAO 251743
R.A. (1950)	$12^{\text{h}} 03^{\text{m}} 32^{\text{s}}$	$12^{\text{h}} 03^{\text{m}} 35^{\text{s}}$	$12^{\text{h}} 04^{\text{m}} 16^{\text{s}}$
Dec. (1950)	$-60^{\circ} 58' 42''$	$-60^{\circ} 58' 00''$	$-60^{\circ} 59' 32''$
Sp. type	B2IVe	B3	B0
V	$9^{\text{m}}.491 (0^{\text{p}}.25)$ $10^{\text{m}}.244 (0^{\text{p}}.00)$ $9^{\text{m}}.891 (0^{\text{p}}.50)$	$9^{\text{m}}.799 \pm 0^{\text{m}}.002$	$9^{\text{m}}.270 \pm 0^{\text{m}}.003$
(b-y)	$0^{\text{m}}.114 (0^{\text{p}}.25)$	$0^{\text{m}}.127 \pm 0^{\text{m}}.001$	$0^{\text{m}}.203 \pm 0^{\text{m}}.001$
m_1	$0^{\text{m}}.035 (0^{\text{p}}.25)$	$0^{\text{m}}.029 \pm 0^{\text{m}}.001$	$-0^{\text{m}}.035 \pm 0^{\text{m}}.002$
c_1	$0^{\text{m}}.105 (0^{\text{p}}.25)$	$0^{\text{m}}.247 \pm 0^{\text{m}}.002$	$-0^{\text{m}}.065 \pm 0^{\text{m}}.003$
(b-y) _o	$-0^{\text{m}}.110 (0^{\text{p}}.25)$	$-0^{\text{m}}.096$	$-0^{\text{m}}.129$
m_o	$0^{\text{m}}.107 (0^{\text{p}}.25)$	$0^{\text{m}}.100$	$0^{\text{m}}.071$
c_o	$-0^{\text{m}}.060 (0^{\text{p}}.25)$	$0^{\text{m}}.202$	$-0^{\text{m}}.131$
$E_{(b-y)}$	$0^{\text{m}}.224$	$0^{\text{m}}.223$	$0^{\text{m}}.332$

Table 5 : Photoelectric times of minima.

H.J.D. -2400000	Error (days)	Epoch (cycles)	Source reference
33466.3358	± 0.0002	0.0	Ollongren, 1956
40676.813	± 0.001	5086.0	Landolt, 1970.
46224.3175	± 0.0003	8999.0	This paper.
46557.4796	± 0.0002	9234.0	This paper.
46567.4063	± 0.0001	9241.0	This paper.

Table 6 : Light-curve solutions.

Adopted primary temperature 24200K

Colour	u	v	b	y
i (degrees)	80.7 ±2	80.84 ±6	81.1 ±1	81.0 ±1
T ₂ K (polar)	16830 ±120	17830 ±50	17620 ±70	17530 ±60
r ₁ (polar)	0.344 ±4	0.352 ±1	0.354 ±2	0.349 ±2
r ₁ (mean)	0.357 ±4	0.367 ±1	0.369 ±2	0.362 ±2
r ₂ (polar)	0.315 ±2	0.307 ±1	0.308 ±2	0.312 ±1
r ₂ (mean)	0.336 ±2	0.325 ±1	0.326 ±2	0.331 ±1
χ^2 (mmag.) ²	120.8	51.60	45.75	74.09
L ₂ /L ₁	0.376	0.435	0.429	0.478
r.m.s. error (mmag.)	9.1	6.3	5.9	7.5

Table 7 : Adopted light-curve solution using vby data only.

T_1 K (polar)	24200
q (spectroscopic)	0.61
Escat ₁ (adopted)	0.36
Escat ₂ (adopted)	0.22
β_1 (adopted)	0.25
β_2 (adopted)	0.25
i (degrees)	81.0 ± 1
T_2 K (polar)	17660 ± 150
r_1 (polar)	0.352 ± 3
r_1 (mean)	0.366 ± 3
r_2 (polar)	0.309 ± 3
r_2 (mean)	0.327 ± 3

Table 8 : Astrophysical data for AI Cru.

Uncorrected data

Absolute dimensions:	Primary	Secondary
M/M	8.9 ± 0.2	5.4 ± 0.1
R/R $_{\odot}$	4.72 ± 0.06	4.22 ± 0.05
log $^{\circ}$ g (cgs)	4.04 ± 0.01	3.92 ± 0.02

Photometric data:

T $_{\text{eff}}$ (K)	24200 ± 500	17700 ± 500
M $_{\text{bol}}$	$-4.^{\text{m}}90 \pm 0.^{\text{m}}09$	$-3.^{\text{m}}29 \pm 0.^{\text{m}}13$
log (L/L $_{\odot}$)	3.82 ± 0.04	3.19 ± 0.05
B.C.	$-2.^{\text{m}}43$	$-1.^{\text{m}}75$
M $_{\text{V}}$	$-2.^{\text{m}}47 \pm 0.^{\text{m}}09$	$-1.^{\text{m}}54 \pm 0.^{\text{m}}13$
E $_{(b-y)}$	$0.^{\text{m}}22$	
Distance (pc)	1880 ± 170	

Corrected data

Absolute dimensions:	Primary	Secondary
M/M	10.3 ± 0.2	6.3 ± 0.1
R/R $_{\odot}$	4.95 ± 0.06	4.43 ± 0.06
log $^{\circ}$ g (cgs)	4.06 ± 0.01	3.95 ± 0.02

Photometric data:

T $_{\text{eff}}$ (K)	24200 ± 500	17700 ± 500
M $_{\text{bol}}$	$-5.^{\text{m}}00 \pm 0.^{\text{m}}09$	$-3.^{\text{m}}40 \pm 0.^{\text{m}}13$
log (L/L $_{\odot}$)	3.88 ± 0.04	3.24 ± 0.05
B.C.	$-2.^{\text{m}}43$	$-1.^{\text{m}}75$
M $_{\text{V}}$	$-2.^{\text{m}}57 \pm 0.^{\text{m}}09$	$-1.^{\text{m}}65 \pm 0.^{\text{m}}13$
E $_{(b-y)}$	$0.^{\text{m}}22$	
Distance (pc)	1980 ± 180	

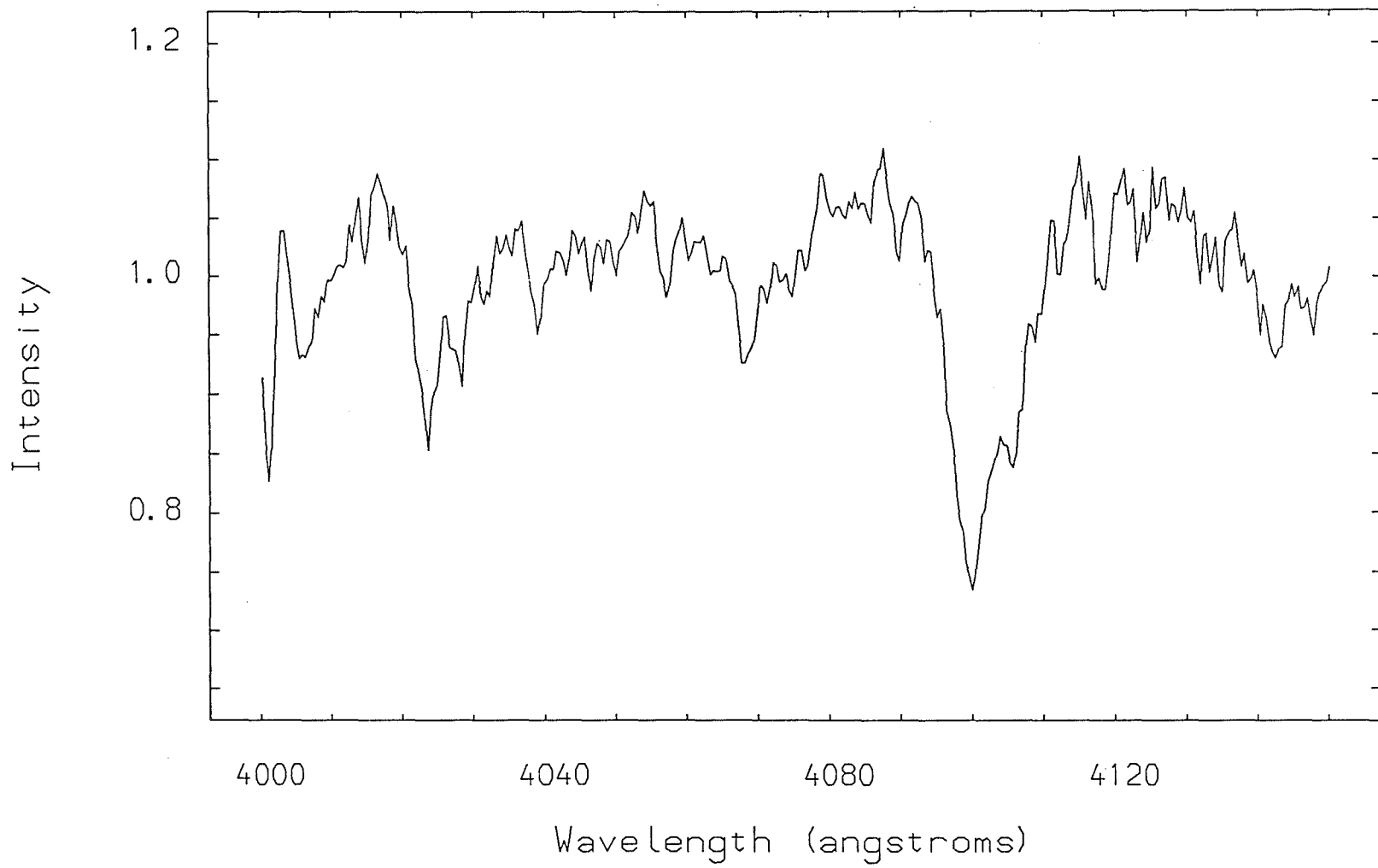
Table 9 : Comparison of the absolute dimensions of AI Cru with the stationary models of Horn et al. (1970).

Initial parameters:-

Model total mass (M_{\odot})	15.75 (constant)		
Model M_{pri} (M_{\odot})	9.0		
Model mass ratio	0.75		
Model Age ($\times 10^7$ yrs)	11.9	<u>AI Cru</u>	6.3
M_{pri} (M_{\odot})	5.5	6.3	6.7
R_{pri} (R_{\odot})	5.22	4.43	3.97
M_{sec} (M_{\odot})	10.2	10.3	9.1
$\log T_{\text{pri}}$	4.237	4.248	4.312
$\log T_{\text{sec}}$	4.423	4.384	4.396
Period (days)	1.861	1.418	1.103
Separation (R_{\odot})	15.96	13.54	11.25
Mass ratio	0.54	0.61	0.73

The subscripts pri and sec refer to the primary and secondary components respectively before the reversal of the mass ratio.

Figure 1.



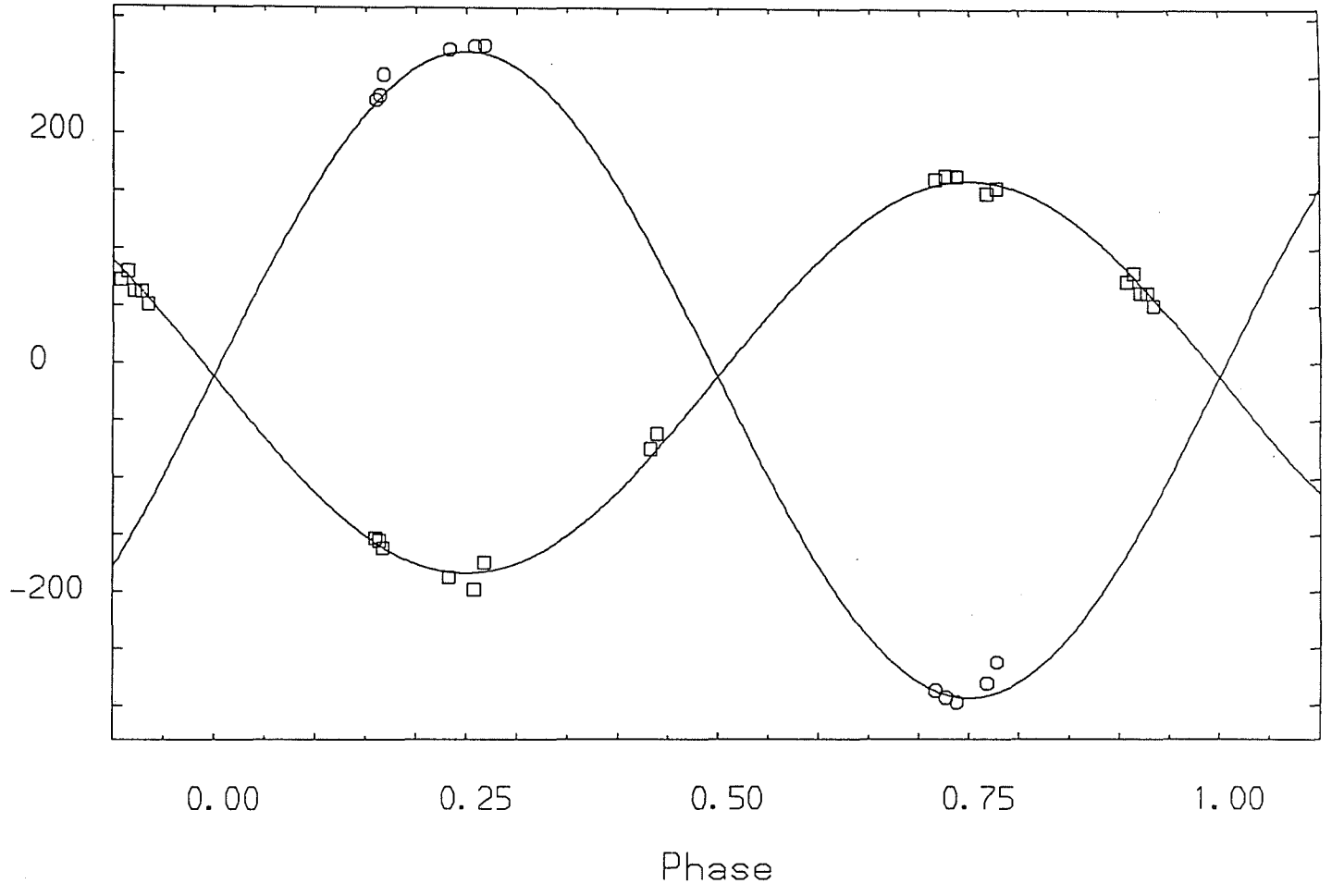


Figure 2.

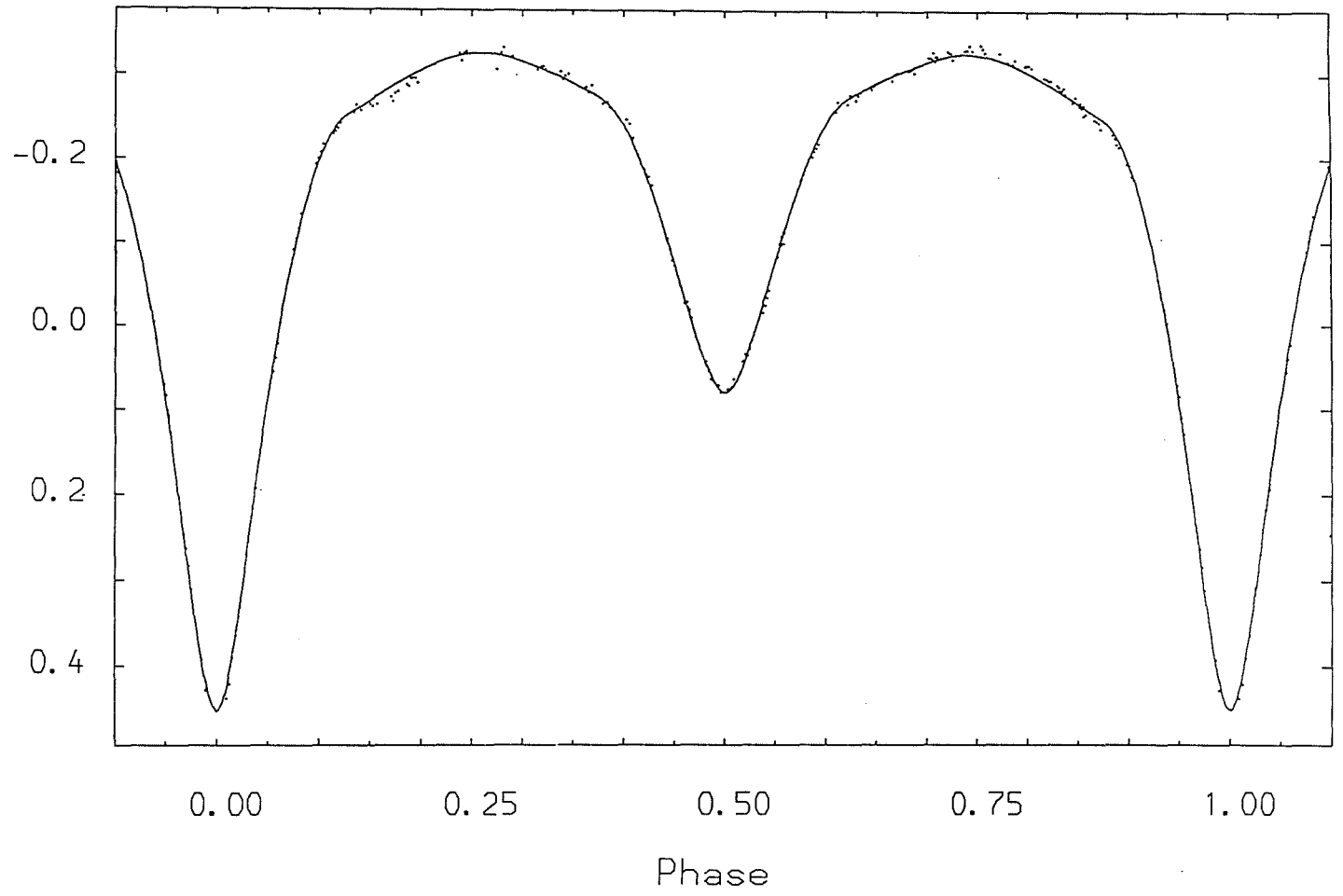


Figure 3.

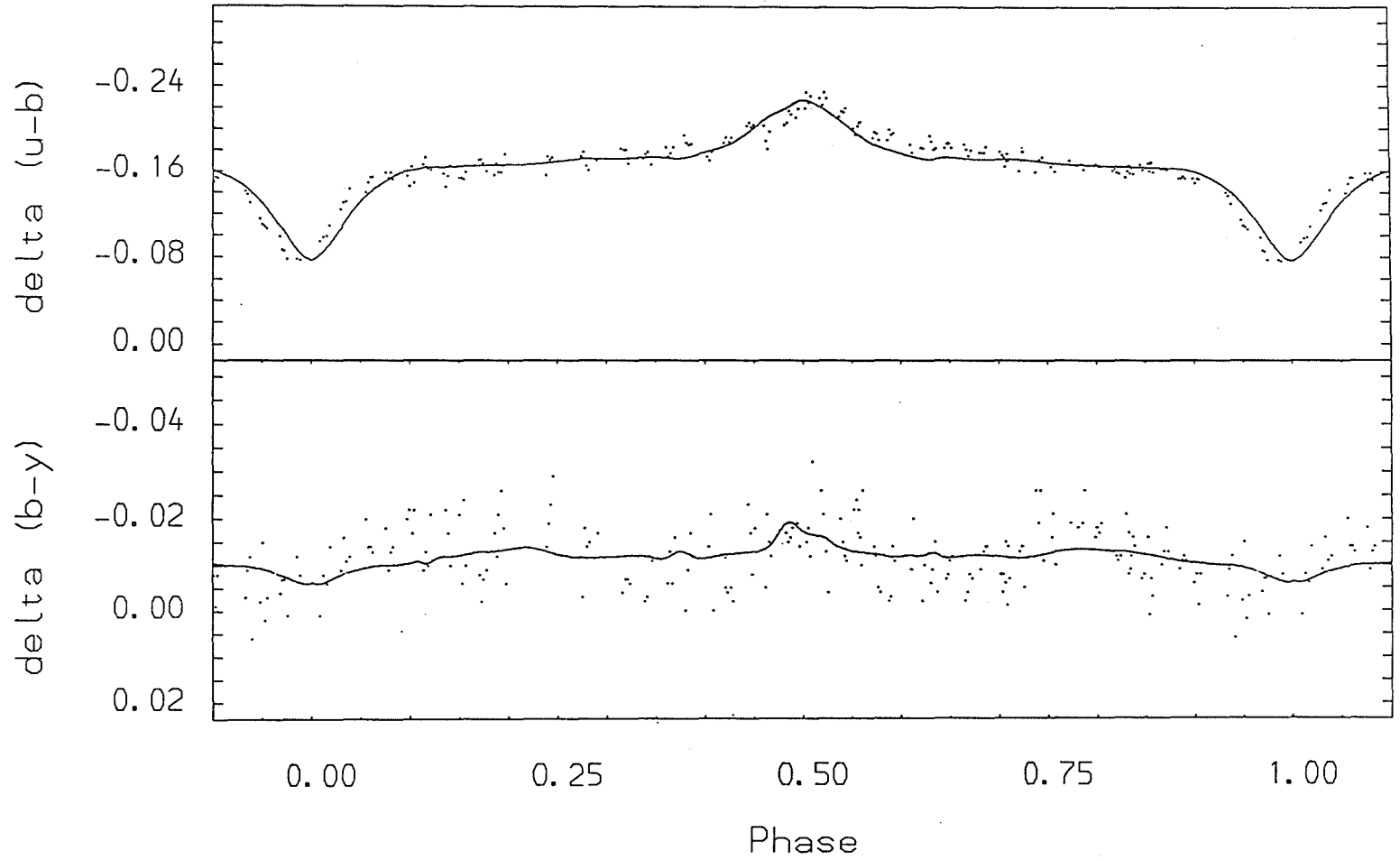
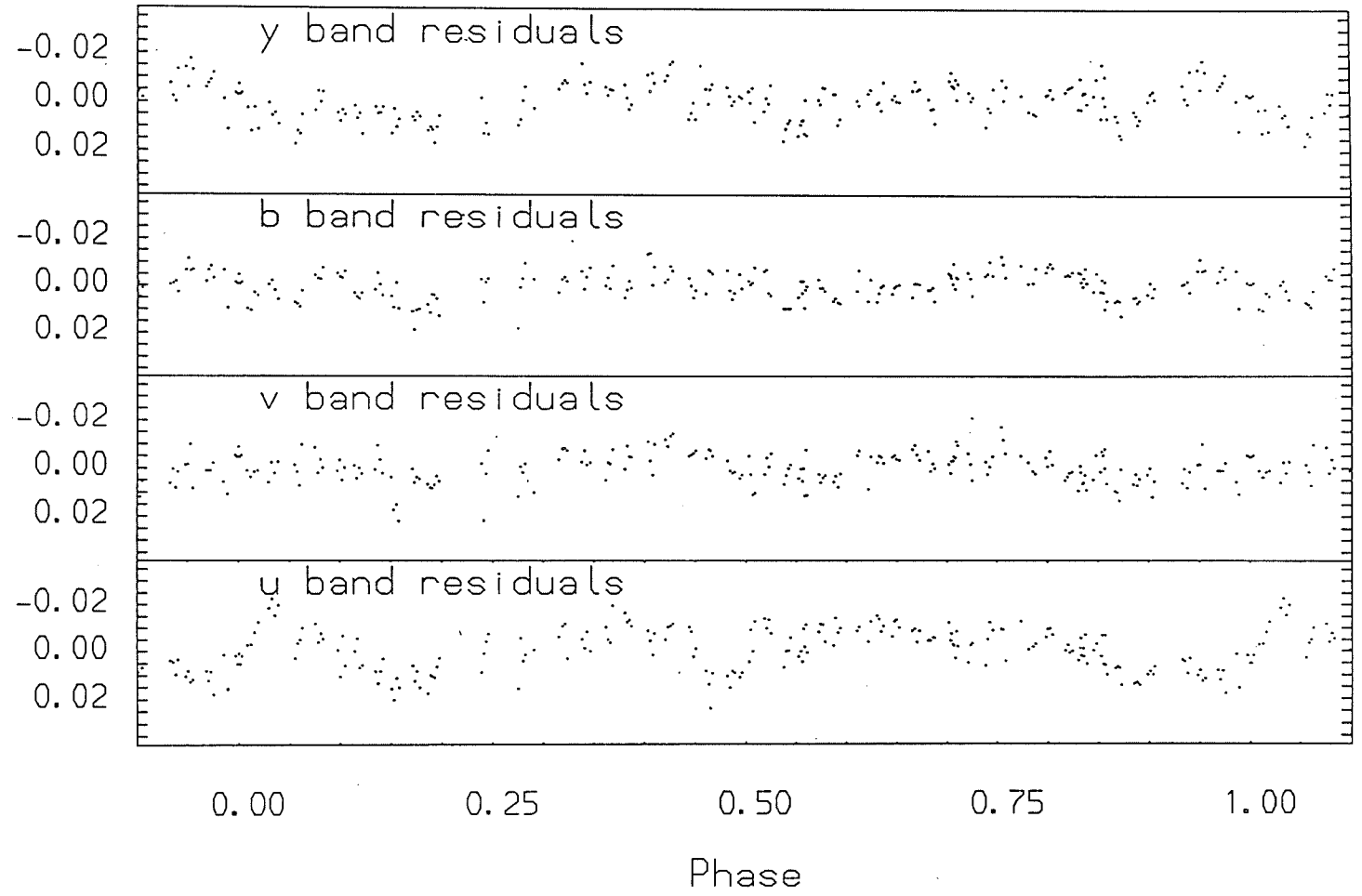


Figure 4.

Figure 5.



CHAPTER 8

A photometric and spectroscopic study of the early-type binary

V701 Scorpii.

A photometric and spectroscopic study of the early-type binary

V701 Scorpii.

S.A.Bell, University Observatory, Buchanan Gardens, St. Andrews,
Fife, KY16 9LZ, Scotland.

G.J.Malcolm, Boyden Observatory, Institute of Astronomy,
University of the Orange Free State, PO Box 339,
Bloemfontein 9300, South Africa.

Received _____

Correspondence to :-

S.A.Bell,
University Observatory,
Buchanan Gardens,
St. Andrews, Fife,
KY16 9LZ,
Scotland.

Summary

We present new UBV light curves and medium-dispersion spectroscopy of the early-type contact binary V701 Sco. The masses, radii and temperatures of the two components are found to be almost identical. A large period change thought to be caused by mass transfer cannot be supported by the observations presented here and it seems likely that the system is in a temporary equilibrium state after the rapid phase of case A mass transfer.

1) Introduction

The early-type binary V701 Sco was found to be variable by Plaut (1948) using data derived from 301 photographic plates. He showed the system to be an eclipsing binary of the W UMa type with a period of $0.^d761875$. The first photoelectric light curves of this object were obtained by Leung (1974) with Johnson B and V filters, and these data confirmed the sinusoidal shape of the light curve. Leung also noted that the secondary minimum of the B curve was slightly deeper than that of the primary and that there were some signs of asymmetry at the bottom of primary minimum in the V curve.

The low inclination of V701 Sco in conjunction with the contact configuration of the system made the rectification procedure employed by Leung unsuitable for this type of analysis since the procedure relies heavily on the shape and depth of the resulting eclipses. A more recent analysis has been made by Wilson and Leung (1977) using the Wilson and Devinney (1971) model. They found the surface of the common envelope to lie about half-way between the inner and outer contact surfaces. They also found that the solution was only weakly dependent on the mass ratio but that slightly better fits to the data were obtained adopting a mass ratio of unity.

The only radial velocity data available prior to this study were presented by Andersen et al. (1980; hereafter ANW) who made six radial velocity determinations for both components of V701 Sco. Their preliminary analysis showed the mass ratio to be 0.98 ± 0.04 and that the secondary component was slightly more luminous than the primary. They also presented Stromgren colours for the system and a further time of minimum. Using the available times of minima, they suggested that the system may be undergoing mass transfer of the

order of $10^{-5} M_{\odot} \text{yr}^{-1}$.

Eggen (1961) suggested that this system was a member of the open cluster NGC 6383. Sahade and Cavila (1963) and Lloyd Evans (1978) confirmed its membership and placed an upper age limit on the cluster of $4-5 \times 10^6$ yrs. The age determination for this cluster provides the opportunity to place more rigorous constraints on theoretical models with which this system may be compared.

In order to evaluate the evolutionary status of this system, it was decided to include V701 Sco in our study of early-type binaries with periods of less than 1.8^d and spectral types earlier than B5. Further spectroscopic data would provide a more reliable value for the mass ratio and further times of minima would improve the estimate of the mass transfer rate. It would then be possible to show whether V701 Sco is in an equilibrium state or if the system is passing through the rapid phase of case A mass exchange.

2) Spectroscopy

2.1) Observations

The spectroscopic data for V701 Sco were obtained using the 1.9m telescope at SAAO, Sutherland in conjunction with the Image Tube Spectrograph and Reticon Photon Counting System (RPCS). A total of 9 double-lined spectra was obtained by SAB during the period 1986 February 19-24 at a dispersion of 30\AA mm^{-1} . The observational procedure has been described in detail elsewhere (Bell et al., 1986a) and will not be discussed further here. The number of spectra obtained was limited by the fact that V701 Sco reached a position in the sky accessible by the telescope just before the end

of astronomical twilight leaving only a short period to make the exposures before dawn.

The spectrograms show two early B-type spectra which are almost identical in intensity but not quite completely resolved. The duration of each exposure was 600s ensuring that the diffuse spectral features were not degraded further by poor time resolution. In common with the study made by ANW, we find no evidence for circumstellar or circumbinary matter.

2.2) Reduction and Analysis

The spectroscopic data were processed on the University of St. Andrews VAX computers in the manner described by Bell et al. (1986a) using the STARLINK package FIGARO and the spectroscopic image-processing package REDUCE (Hill et al., 1982a).

Cross-correlation analysis using VCROSS (Hill, 1982) was attempted with the spectrum of the B4V star SAO 235690 adopted as a template. This method proved to be too susceptible to the inherent noise in the data and the mis-matching of the sharp standard-star lines compared with the extremely-rotationally broadened features of V701 Sco. The amplitude of the noise was approximately 6% of the continuum height, whereas the depths of the primary and secondary features were of the order of 15% of the continuum height.

Measurements of the radial velocity for both components by fitting double-gaussian profiles to several of the combined HeI features were attempted using VLINE (Hill et al., 1982b) but the technique was found to be extremely susceptible to noise spikes within the profiles. Very few features could be measured

successfully with this technique and its use was restricted to the determination of the projected rotational velocities of the two components. It was therefore necessary to measure the radial velocities of the two components using VELMEAS (Hill et al., 1982c) by fitting parabolae to those features which could be visually resolved and were not badly affected by noise spikes. Those features which could not be measured by parabola-fitting were measured by visual inspection of the line centres. The errors on the primary and secondary component radial velocities are estimated to be approximately 15kms^{-1} for this method.

The principal spectral features showing splitting were the HeI lines at $\lambda\lambda 4009, 4026, 4144, 4388$ and 4471 . The rest wavelengths adopted for this analysis have been taken from the list by Petrie (1953). The measurement of these lines for radial velocity proved to be consistent to better than 10kms^{-1} for each exposure. The Balmer lines, however, were omitted from the analysis due to their extremely Stark-broadened and rotationally-broadened profiles. The final radial velocities for both components of V701 Sco are listed in Table 1 and the radial velocity curves are shown in Figure 1. The six double-lined observations made by ANW have also been tabulated in Table 1. As the interstellar K line appeared at the blue end of the wavelength region being observed, no reliable measurements of the radial velocity of this feature could be made due to uncertainties in the wavelength calibration.

Examination of the U, B and V light curves of V701 Sco shows no clear evidence for any eccentricity in the orbit despite some distortions in the minima of the light curves. We have therefore assumed a circular orbit for the subsequent analysis using the radial velocity data obtained by ANW and those radial velocities

determined for this study. The radial velocity measurements of ANW have been phased using the time of minimum given by ANW and the period derived in this paper (see Section 3.3). Adopting the procedures of Popper (1974), the circular orbital elements of V701 Sco were computed by separate least-squares analyses of the radial velocities for each component to determine a velocity semi-amplitude and systemic velocity. The velocity semi-amplitude of the primary and the secondary K_1 and K_2 respectively, the mean systemic velocity V_0 , the derived mass functions and projected semi-major axes of the orbits of the two components, together with their standard errors, are given in Table 2.

By means of the measurement of the half-widths of both components of the HeI $\lambda 4471$ feature using VLINE, we have estimated the projected rotational velocities for both stars using the calibration of Slettebak et al. (1975). The exposure showing the most satisfactorily-resolved feature was SAA01/086, and from this spectrum we have estimated the projected rotational velocities of both the primary and secondary components to be $250 \pm 30 \text{ km s}^{-1}$. If synchronous rotation is adopted together with the final mean radii of the two stars derived from the corrected velocity semi-amplitudes (see Table 7), then theoretical projected rotational velocities of 258 km s^{-1} would be expected for both components. Measurements of the equivalent widths for the two components of the $\lambda 4471$ feature would imply a luminosity ratio of the secondary to the primary of 1.0 with an estimated error of approximately 10%. These determinations compare quite favourably with the analysis of ANW whose data were obtained at a somewhat higher dispersion.

3) Photometry

3.1) Observations

The photoelectric photometry for V701 Sco was obtained by GJM and SAB during the period 1985 May 13-16 and on 1985 July 9/10 by means of a 0.41m telescope at Boyden Observatory. Observations in the Johnson B band were obtained on 1986 May 18/19 and June 16/17 to determine further times of minima. The photometer and data acquisition programme have already been described in detail elsewhere (Malcolm and Bell, 1986). A 30 arcsecond diaphragm was used throughout the observations and the integration times were set at 30s for the monitoring sequence. Complete light curves for V701 Sco were obtained employing UBV filters and observations were made of several E-region standard stars (Cousins, 1983) during each night to allow the data to be transformed to the standard system.

The comparison star used for these observations was HD 317845 (Sp. type B1III-IV) and the check star was HD 317858 (Sp. type B2); data for the variable and comparison stars are given in Table 4. These two stars were also used by Leung (1974) in his photoelectric study of V701 Sco. Despite being noted as a possible spectroscopic binary by Lloyd Evans (1978) and listed as a suspected variable star with an amplitude of $\sim 0.^m.4$ by Kukarkin et al. (1982), no clear evidence of photometric variability has been found in HD 317845. The photographic observations made by Plaut (1948) over an interval of 4 years show no evidence for variability in HD 317845 which was used as the comparison star for V701 Sco. Similarly, the star HD 317858 was found to be constant in brightness to better than $0.^m.01$.

3.2) Reductions

The observations were reduced using the methods outlined by Bell et al. (1986b). Differential magnitudes were formed with respect to the comparison star using a spline-fitting program written by SAB. These data were then transformed to the standard system and phased according to the ephemeris given in Section 3.3. The differential V magnitudes, (B-V) and (U-B) colour index differences and corresponding mean times of observation are given in Table 3. The errors on a single observation in a single band are estimated to be less than 0.01^m . A total of 254 observations were made in each colour and the resulting B band light curve and colour changes are given in Figures 2 and 3 respectively.

3.3) Ephemeris

Plaut (1948) obtained 16 primary minima and 13 secondary minima for V701 Sco from which he obtained a period of 0.761875 ± 0.000009^d with a typical error on each minimum of $\sim 0.03^d$. Leung (1974) obtained the following ephemeris based on a weighted least-squares analysis of his own photoelectric minima and the photographic data of Plaut.

$$\text{Pri. Min.} = \text{H.J.D. } 2439329.6657 + 0.76187133 \text{ E}$$

+34

+34

A further time of minimum was obtained by ANW who revised the ephemeris using the available photoelectric times of minimum. This ephemeris is given below. The period determined by ANW is longer than that found by Leung but remarkably close to the value calculated by Plaut.

$$\text{Pri. Min.} = \text{H.J.D. } 2443574.8358 + 0.76187547 \text{ E}$$

± 2

± 27

Four mean times of minima for V701 Sco have been determined from the UBV data obtained during 1985/86 using the method of Kwee and van Woerden (1956). The quoted error has been derived from the interagreement of the three individual measurements for each passband. All the published photoelectric times of minimum are summarised in Table 5. A least-squares determination of the period using the available photoelectric data with the exception of that published by Bruton and Chambliss (1985) has been made. The derived ephemeris given below has been used to phase both the spectroscopic and photometric data with the exception of the radial velocity data of ANW.

$$\text{Pri. Min.} = \text{H.J.D. } 2446199.5059 + 0.76187645 \text{ E}$$

± 3

± 19

The maximum residual of the photoelectric data used for this period determination is ~ 8 minutes although the majority of the residuals are very much smaller. The observation of Bruton and Chambliss is somewhat discordant with this ephemeris, having a residual of 26 minutes. This determination was omitted from the analysis as a large short-term deviation in the period would be required for which there is no other observational evidence. The residuals of all the photographic and photoelectric times of minima relative to the ephemeris presented in this paper are given in Figure 4.

The photographic minima in the 30 year interval before the first photoelectric determinations show large positive residuals from the adopted ephemeris. These residuals are indicative of a change in the period. However, the errors on the photographic

minima are such that an accurate determination of the period change would be extremely difficult to evaluate. If the period was changing at the rate found by ANW, then the time of minimum determinations made for this study would have provided the necessary supportive evidence; this is not the case. It would appear that the period of V701 Sco has remained virtually constant over the last 20 years although there is some evidence for small-scale period changes within this interval. There is clear evidence for a smaller period change in the last 50 years but it seems unlikely that the mass transfer rate is as high as $10^{-5} M_{\odot} \text{yr}^{-1}$. More time of minimum determinations are required to clarify this point.

3.4) Colour indices

The observed and de-reddened colour indices for V701 Sco are given in Table 4. There appears to be little change in the (B-V) and (U-B) colour indices during the orbital cycle implying that both stars have similar temperatures. Reddening of $\sim 0.^m02$ can be seen at primary and secondary minima (see Figure 3) resulting from the cooler hemisphere of the occulting component facing the observer at each eclipse.

The colour excess in (B-V) for the variable and comparison stars were found to be consistent with each other and in excellent agreement with the value of $E(B-V) = 0.^m35$ obtained by Lloyd Evans (1978) for NGC 6383. ANW obtained Strömgren colour indices of V701 Sco from which they derived a colour excess in (b-y) of $0.^m26$. This gives good agreement with the determination of $E(B-V)$ employing the relationship $E(b-y) = 0.74 E(B-V)$.

3.5) Analysis

The light curves of V701 Sco show behaviour characteristic of a system of the WUMa type with approximately equal minima of depth $0^m.42$. Secondary minimum appears to be a little deeper than primary minimum although the scatter in the data at secondary minimum is slightly more pronounced. There are some signs of asymmetry in the bottom of primary minimum where egress is somewhat more shallow than ingress. This can be seen most clearly in the U and B light curves. There also appears to be a $0^m.03$ "dip" in the V light curve shortly after second quadrature which appears to a lesser degree in the other light curves. These effects are displayed in the residuals of the individual observations from the adopted theoretical curves for each passband in Figure 5.

As the observations were made on a single channel photometer, corrections have been applied to the phasing of each light curve corresponding to the difference between the mean time of observation and the actual time of observation for an individual passband. This correction amounts to less than $0^d.001$ and could have been ignored without affecting the analysis of the light curves.

The reference temperature for the system was adopted as 23500K using the Strömgren colour indices of ANW and the (c_o, T_{eff}) calibration of Davis and Shobbrook (1977). This is in good agreement with the $(B-V, T_{eff})$ calibration of Böhm-Vitense (1981) in which an intrinsic $(B-V)$ of $-0^m.25$ corresponds to a temperature of 23200K. The probable error on this estimate of the temperature is of the order of 1000K. This would imply that the system is composed of two stars of spectral type B1-B1.5.

As the light curves appear to be slightly asymmetric, each half of each of the light curves was analysed separately. During the course of the analysis, it became clear that the difference between the solutions for each half of a given light curve was negligible and that a solution could be made using the average light curve formed by folding the data about $0^{\text{P}}.5$. The results of the analysis presented here represent solutions to these averaged light curves.

Cubic spline fits were made to both halves of the light curves and were used to generate intensities normalised to the intensity at either $0^{\text{P}}.25$ or $0^{\text{P}}.75$ at intervals of $0^{\text{P}}.01$. The bolometric albedoes for the primary and secondary components α_1 and α_2 respectively were fixed at unity. Model atmosphere fluxes, corrected for line blanketing and covering a range of 3000K either side of the reference temperature, were taken from the model atmospheres of Kurucz (1979). The limb-darkening coefficients were taken from the tabulation of Wade and Rucinski (1985). The gravity darkening exponents β_1 and β_2 for the primary and secondary components respectively were fixed at 0.25 (von Zeipel, 1924). All of these parameters were not changed during the course of the analysis.

The remaining parameters to be determined from the analysis were the fractional temperature difference $x = (T_2 - T_1)/T_1$ in terms of the reference (primary component) temperature T_1 and the secondary component temperature T_2 , the "fill-out" factor f as defined by Rucinski (1973) and the orbital inclination i . The mass ratio q was fixed at the spectroscopically-determined value of 0.99.

The light-curve synthesis program WUMA5 (Rucinski, 1976a,b,c) has been employed throughout this analysis. For each colour, an initial light curve was generated using the spectroscopic mass ratio

and the geometric elements determined by Wilson and Leung (1977). Partial derivatives, $\delta l / \delta p_i$, which express the dependence of the total light of the system (l) on the variation in the values of the individual parameters (p_i) were then computed for each of the three parameters (x,f,i) using Rucinski's program. These partial derivatives, the normalised light curve and the theoretical light curve for the initial parameters were then entered into a least-squares solution of the 51 equations of condition which are of the form

$$\sum_{i=1}^n (\delta l / \delta p_i) \Delta p_i = l_{\text{observed}} - l_{\text{theoretical}} \quad n = 3.$$

Each solution was iterated numerous times with the input theoretical curve being modified each time. If the solution moved outside the range of the partial derivatives, then these were re-evaluated. The results of this procedure and the formal errors of the least-squares solution for the U, B and V light curves are given in Table 6. The volume radii of the primary component r_1 and the secondary component r_2 have been evaluated using the tabulation of Mochnacki (1984). The corresponding errors in the volume radii have been estimated using the errors in the determinations of the mass ratio and the mean value of the fill-out factor.

The solutions to the three light curves appear to be consistent within the formal errors of the solutions. In an attempt to assess the sensitivity of the solution on T_1 and q , small changes were made to these parameters corresponding to the errors in these quantities. The solutions showed only a very weak dependence on small changes in q and no dependence at all on T_1 . The adopted photometric solution

for V701 Sco is given in Table 7.

4) Discussion

4.1) Spectroscopy and Photometry

The velocity separation of approximately 550kms^{-1} for the two components of V701 Sco would probably be large enough for the effects of blending of the diffuse HeI lines to be ignored had the system been detached or even semi-detached. The large rotational velocities of the two components degrade the features to such an extent that the lines are never completely resolved and measurement of the radial velocities of the components will always be underestimated. The effects of reflection will systematically reduce the velocity semi-amplitudes of the two components in a close binary whose components are of significantly different temperatures. However, in the case of V701 Sco where the difference in the temperatures of the primary and secondary is very small, the effects of reflection are negligible. We have estimated the blending correction to the velocity semi-amplitudes to be of the order of 5%. This is at best a rough estimate and is based on experience with other early-type close binary systems and should be treated with caution. The orbital parameters derived from these corrected velocity semi-amplitudes are given in Table 2.

The photoelectric analysis presented here suggests that V701 Sco exhibits a larger degree of overcontact than that found by Wilson and Leung (1977). The mean radii of the two components are approximately 5% larger than their study while the orbital inclination is found to be lower by 1.0° . The explanation of these discrepancies is unclear. However, they may be connected with the

asymmetries present in all the photoelectric light curves obtained for this system.

Astrophysical data for this system are given in Table 8. Data based on both the observed and corrected velocity semi-amplitudes are tabulated. The bolometric corrections quoted in Table 8 are taken from the calibration of Davis and Shobbrook (1977). Since the errors quoted in Table 8 are formal errors which have been derived from the spectroscopic and photometric analyses, they are likely to be underestimated. The distribution of radial velocity data may well provide somewhat optimistic formal errors for the velocity semi-amplitudes and the blending corrections can only be rough estimates and consequently the real errors in the masses, radii and luminosities should take these uncertainties into account. It is probably more realistic to increase the formal error estimates by a factor of two for the radii and luminosities and by three for the masses.

4.2) Membership of NGC 6383

Lloyd Evans (1978) calculated a mean colour excess in (B-V) of $0.^m35 \pm 0.^m02$ for NGC 6383 and a distance of 1350pc. We find a comparable colour excess in (B-V) for V701 Sco and the two comparison stars (see Table 8) and determine a distance for V701 Sco of 1240 ± 190 pc using the corrected radial velocity data. The systemic velocity of V701 Sco is in reasonable agreement with the mean velocity of the cluster of 0 ± 2 kms⁻¹. It seems that there is little doubt that the variable and comparison stars are all members of NGC 6383. This conclusion is in agreement with the discussion of ANW.

4.3) Evolutionary state

Adopting the corrected masses for the two components, comparisons with the evolutionary tracks for single stars published by Hejlesen (1980) show that a chemical composition of ($X = 0.70$, $Z = 0.02$) provides good agreement with the locations of the primary and secondary components. The age determination using the temperature and surface gravity of the two stars lies very close to the 4×10^6 yrs isochrone. Lloyd Evans established an age of $4-5 \times 10^6$ yrs for NGC 6383 which is in good agreement with our estimate of the age of V701 Sco. Using the uncorrected masses increases the age estimate for the system by approximately 15%.

Comparing the mass and radius of the two components with the zero-age main sequence relation derived from the models of Hejlesen, it is clear that both stars are little evolved. The zero-age radius of a $10M_{\odot}$ star is $4.2R_{\odot}$ so it would appear that the radii of both the components of the system are about 2-3% larger than this.

Assuming that any period change could be attributed to mass transfer, ANW suggested three evolutionary scenarios for V701 Sco. The first possibility was that the system was in an equilibrium state fitting the trivial exception allowed under Kuiper's (1941) paradox for equal-mass components. The second option was a system with an increasing period in the rapid phase of mass transfer after mass-ratio reversal. The third model postulated for V701 Sco involves the re-adjustment of the binary to an equilibrium state after its formation by fission.

As ANW point out, it seems less likely that the increasing period could be attributed to the system overshooting the equal-mass configuration assuming that a fission process could produce a binary of mass ratio unity. The large mass transfer rate required by the second scenario is not supported by our observations. The evidence presented in this paper favours the first option although there is some evidence for a slowly-increasing period implying that the system has reached a temporary equilibrium state after the rapid phase of mass transfer. The existence for short-lived equilibrium states during case A mass transfer has been suggested by Hilditch (1984) in his study of υ Her. A further possible explanation for the observed period variations is the existence of a third body. However, no other evidence has been found to support this suggestion. In conclusion, it seems quite likely that the original configuration for V701 Sco was close to contact with a mass ratio close to unity and that the amount of mass transfer required to reverse the mass ratio was small.

5) Conclusion

We have presented new UBV photometry and medium-resolution spectroscopy of V701 Sco. A more reliable determination of the absolute dimensions of the components of the system has been made, and we have confirmed that the system contains two almost identical stars in an over-contact configuration. The mass ratio appears to be unity and there is no appreciable temperature difference between the two components. The large period change and correspondingly large mass-transfer rate suggested by previous studies cannot be supported by our observations though the system may be in a temporary equilibrium state during the case A mass transfer phase.

There are insufficient observational data of a high enough quality to make an accurate determination of any period change. However, there is some photometric evidence of photospheric activity which may be caused by mass flow in the system. It would be of considerable value to obtain more times of minima at regular intervals in the future in order to evaluate any period change which could then be attributed to mass transfer.

Acknowledgements

SAB would like to express his thanks for the hospitality and assistance extended to him by the staffs of the Institute of Astronomy of the University of the Orange Free State and the South African Astronomical Observatory and during the observing runs. PATT is acknowledged for the allocation of observing time at SAAO, and likewise the SERC for financial support in the form of a Research Studentship for one of us (SAB). SAB gratefully acknowledges a Visiting Fellowship from the University of the Orange Free State and financial assistance made available by the University of St. Andrews. The authors also wish to express their gratitude to Prof. A.H. Jarrett and Prof. D.W.N. Stibbs for the use of the facilities of the Boyden Observatory and the University Observatory, St. Andrews, respectively and to Dr. R.W. Hilditch for his constructive criticism and useful suggestions during the course of this investigation. We would also like to express our thanks to Dr. J. Andersen for his constructive criticism of this study.

References

- Andersen, J., Nordstrom, B. & Wilson, R.E., 1980. *Astron. Astrophys.*, 82, 225.
- Bell, S.A., Kilkenny, D. & Malcolm, G.J., 1986a. Submitted to *Mon. Not. R. astr. Soc.*
- Bell, S.A., Hilditch, R.W. & Adamson, A.J., 1986b. *Mon. Not. R. astr. Soc.*, 223, 513.
- Böhm-Vitense, E., 1981. *Ann. Rev. Astron. Astrophys.*, 19, 295.
- Bruton, J.R. & Chambliss, C.R., 1985. *Inf. Bull. Var. Stars*, No. 2805.
- Cousins, A.W.J., 1983. *S.A.A.O. Circ.*, 7, 36.
- Davis, J. & Shobbrook, R.R., 1977. *Mon. Not. R. astr. Soc.*, 178, 651.
- Eggen, O.J., 1961. *R. Obs. Bull.*, No. 27.
- Hejlesen, P.M., 1980. *Astron. Astrophys. Suppl. Ser.*, 39, 347.
- Hilditch, R.W., 1984. *Mon. Not. R. astr. Soc.*, 211, 943.
- Hill, G., 1982. *Publ. Dom. Astrophys. Obs.*, 16, 59.
- Hill, G., Fisher, W.A. & Poeckert, R., 1982a. *Publ. Dom. Astrophys. Obs.*, 16, 43.
- Hill, G., Fisher, W.A. & Poeckert, R., 1982b. *Publ. Dom. Astrophys. Obs.*, 16, 27.
- Hill, G., Ramsden, D., Fisher, W.A. & Morris, S.C., 1982c. *Publ. Dom.*

- Astrophys. Obs., 16, 11.
- Kuiper, G.P., 1941. Astrophys. J., 93, 133.
- Kukarkin, B.V., Kholopov, P.N., Artiukhina, N.M., Fedorovich, V.P.,
Frolov, M.S., Goranskij, V.P., Gorynya, N.A., Karitskaya, E.A.,
Kireeva, N.N., Kukarkina, N.P., Kurochkin, N.E., Medvedeva, G.I.,
Perova, N.B., Ponomareva, G.A., Samus, N.N., Shugarov, S.Yu., 1982. New
Catalogue of Suspected Variable Stars, ed. Kholopov, P.N. ("Nauka"
press, Moscow).
- Kurucz, R.L., 1979. Astrophys. J. Suppl. Ser., 40, 1.
- Kwee, K.K. & van Woerden, H., 1956. Bull. astr. Inst.
Netherlands, 12, 327.
- Leung, K.C., 1974. Astron. Astrophys. Suppl. Ser., 13, 315.
- Lloyd Evans, T., 1978. Mon. Not. R. astr. Soc., 184, 661.
- Malcolm, G.J. & Bell, S.A., 1986. Mon. Not. astr. Soc. South
Africa, 45, No. 1 & 2.
- Mochnaeki, S.W., 1984. Astrophys. J. Suppl. Ser., 55, 551.
- Petrie, R.M., 1953. Publ. Dom. Astrophys. Obs., 9, 297.
- Plaut, L., 1948. Leiden Ann., 20, 1.
- Popper, D.M., 1974. Astron. J., 79, 1307.
- Rucinski, S.M., 1973. Acta astr., 24, 119.
- Rucinski, S.M., 1976a. Pubs. astr. Soc. Pacific, 88, 244.
- Rucinski, S.M., 1976b. Acta astr., 26, 227.

Rucinski, S.M., 1976c. *Publs. astr. Soc. Pacific*, 88, 777.

Sahade, J. & Davila, F.B., 1963. *Ann. Astrophys.*, 26, 153.

Slettebak, A., Collins, G.W., Boyce, P.B., White, N.M. &
Parkinson, T.D., 1975. *Astrophys. J. Suppl. Ser.*, 29, 137.

Wade, R.A. & Rucinski, S.M., 1985. *Astron. Astrophys. Suppl. Ser.*, 60, 471.

Wilson, R.E. & Devinney, E.J., 1971. *Astrophys. J.*, 166, 605.

Wilson, R.E. & Leung, K.C., 1977. *Astron. Astrophys.*, 61, 137.

von Zeipel, H., 1924. *Mon. Not. R. astr. Soc.*, 84, 665.

Figure captions

Figure 1: Observed radial velocities and computed orbits for V701 Sco. The data obtained by Andersen et al. (1980) are represented by the squares and the SAAO data by diamonds.

Figure 2: B-magnitude differences in the sense variable minus comparison between V701 Sco and HD 317845 together with the final theoretical curve.

Figure 3: (B-V) and (U-B) colour-index differences in the sense variable minus comparison between V701 Sco and HD 317845 together with the final theoretical curves.

Figure 4: Observed minus calculated times of minima in fractions of a day based on the ephemeris computed in this paper. Crosses represent photographic times of minima and circles those obtained photoelectrically. The filled square represents the discrepant time of minimum obtained by Bruton and Chambliss (1985).

Figure 5: Residuals of the individual UBV observations from the final theoretical curves.

Table 1 : Radial-velocity data for V701 Sco.

SAAO data.

Tape/Run	H.J.D.	Phase	V_1	n	O-C	V_2	n	O-C
No.	-2400000		kms^{-1}		kms^{-1}	kms^{-1}		kms^{-1}
SAA01/086	46481.6077	0.2723	-268	(5)	-7	+297	(5)	+20
SAA01/088	46481.6181	0.2860	-284	(5)	-27	+284	(4)	+12
SAA01/176	46484.6116	0.2151	-240	(4)	+17	+255	(4)	-18
SAA01/178	46484.6195	0.2254	-244	(6)	+16	+264	(4)	-12
SAA01/180	46484.6277	0.2362	-261	(4)	+2	+279	(3)	+1
SAA01/272	46486.5728	0.7892	+277	(4)	0	-270	(4)	-5
SAA01/274	46486.5806	0.7995	+264	(5)	-8	-281	(4)	-21
SAA01/276	46486.5888	0.8103	+272	(3)	+6	-244	(4)	+9
SAA01/278	46486.5967	0.8206	+265	(4)	+7	-238	(3)	+8

The data of Andersen et al. (1980).

Tape/Run	H.J.D.	Phase	V_1	n	O-C	V_2	n	O-C
No.	-2400000		kms^{-1}		kms^{-1}	kms^{-1}		kms^{-1}
F 6100	43580.7925	0.8185	+265	(4)	+5	-262	(4)	-14
F 6103	43581.8378	0.1905	-242	(6)	+3	+256	(6)	-4
F 6104	43581.8958	0.2666	-248	(6)	+15	+275	(5)	-3
F 6120	43583.7991	0.7648	+274	(5)	-10	-264	(6)	+8
F 6136	43584.8915	0.1986	-271	(6)	-21	+269	(6)	+4
F 6158	43586.8025	0.7069	+275	(6)	0	-247	(6)	+16

The columns headed n indicate the number of lines measured for the mean velocity tabulated.

Table 2 : Orbital elements for V701 Sco.

		Measured	Corrected
K_1 (kms ⁻¹)	=	275 ± 4	288 ± 4
K_2 (kms ⁻¹)	=	276 ± 4	290 ± 4
V_{o1} (kms ⁻¹)	=	11 ± 3	--
V_{o1}° (kms ⁻¹)	=	3 ± 3	--
V_{o2} (kms ⁻¹)	=	7 ± 3	--
σ_1 (kms ⁻¹) *	=	12	--
σ_2 (kms ⁻¹) *	=	12	--
q (m_2/m_1)	=	0.99 ± 0.02	0.99 ± 0.02
e	=	0 (adopted)	0 (adopted)
$a_1 \sin i$ (R)	=	4.13 ± 0.05	4.34 ± 0.06
$a_1^{\circ} \sin i$ (R [⊙])	=	4.16 ± 0.05	4.36 ± 0.06
$a_2 \sin i$ (R _⊙)	=	8.29 ± 0.08	8.70 ± 0.08
$m_1 \sin^3 i$ (M)	=	6.6 ± 0.1	7.7 ± 0.2
$m_2 \sin^3 i$ (M _⊙)	=	6.6 ± 0.1	7.6 ± 0.2

* denotes the r.m.s. scatter of a single observation.

Table 3 : UBV observations.

1985 May 13/14		Differential Magnitude (v-c)		
H.J.D.	Phase	V	B-V	U-B
2446199.40147	0.8629	-0.225	0.018	0.020
2446199.40295	0.8649	-0.223	0.009	0.033
2446199.40612	0.8690	-0.224	0.029	0.004
2446199.41270	0.8777	-0.192	0.017	0.017
2446199.41441	0.8799	-0.200	0.021	0.021
2446199.41756	0.8840	-0.185	0.027	0.015
2446199.41924	0.8862	-0.178	0.017	0.044
2446199.42262	0.8907	-0.158	0.006	0.033
2446199.42410	0.8926	-0.172	0.022	0.040
2446199.44267	0.9170	-0.107	0.017	0.043
2446199.44393	0.9186	-0.106	0.024	0.029
2446199.44711	0.9228	-0.098	0.027	0.040
2446199.44938	0.9258	-0.105	0.044	0.055
2446199.45288	0.9304	-0.072	0.025	0.050
2446199.45768	0.9367	-0.054	0.023	0.034
2446199.46081	0.9408	-0.033	0.001	0.051
2446199.46220	0.9426	-0.038	0.020	0.038
2446199.46546	0.9469	-0.031	0.014	0.052
2446199.46828	0.9506	-0.021	0.013	0.043
2446199.47922	0.9650	0.022	0.014	0.038
2446199.48051	0.9667	0.020	0.023	0.039
2446199.48402	0.9713	0.015	0.038	0.033
2446199.49198	0.9817	0.047	0.022	0.029
2446199.49446	0.9850	0.043	0.027	0.043
2446199.49764	0.9891	0.049	0.030	0.040
2446199.49922	0.9912	0.049	0.035	0.024
2446199.50184	0.9947	0.064	0.020	0.021
2446199.50498	0.9988	0.053	0.025	0.034
2446199.50647	0.0007	0.061	0.018	0.028
2446199.51189	0.0079	0.053	0.018	0.026
2446199.51348	0.0099	0.061	0.006	0.021
2446199.51695	0.0145	0.050	0.021	0.023
2446199.51873	0.0168	0.052	0.008	0.034
2446199.52827	0.0293	0.023	0.014	0.045
2446199.52985	0.0314	0.032	0.008	0.041
2446199.53341	0.0361	0.013	0.013	0.049
2446199.53498	0.0382	0.005	0.021	0.035
2446199.53817	0.0423	0.005	0.000	0.048
2446199.54013	0.0449	0.003	0.006	0.041
2446199.54397	0.0500	-0.016	0.008	0.044
2446199.54552	0.0520	-0.013	-0.001	0.048
2446199.54999	0.0579	-0.035	0.005	0.032
2446199.55161	0.0600	-0.041	0.013	0.027
2446199.55633	0.0662	-0.067	0.018	0.042
2446199.55801	0.0684	-0.062	0.002	0.042
2446199.56126	0.0727	-0.073	0.007	0.038

continued

2446199.56293	0.0748	-0.067	-0.008	0.040
2446199.57332	0.0885	-0.111	0.014	0.045
2446199.57487	0.0905	-0.112	0.008	0.045
2446199.57818	0.0949	-0.138	0.017	0.035
2446199.57976	0.0969	-0.130	0.010	0.030
2446199.59347	0.1149	-0.173	0.008	0.044
2446199.59500	0.1169	-0.173	0.003	0.038
2446199.59799	0.1209	-0.176	-0.008	0.042
2446199.59971	0.1231	-0.183	0.000	0.037
2446199.60242	0.1267	-0.201	-0.002	0.038
2446199.60399	0.1287	-0.213	0.021	0.033
2446199.60719	0.1329	-0.222	0.006	0.040
2446199.60887	0.1351	-0.222	0.017	0.031

1985 May 14/15

Differential Magnitude (v-c)

H.J.D.	Phase	V	B-V	U-B
2446200.38729	0.1568	-0.272	0.014	0.042
2446200.38912	0.1593	-0.265	0.014	0.036
2446200.39395	0.1656	-0.273	0.005	0.026
2446200.39880	0.1720	-0.292	0.009	0.035
2446200.40182	0.1759	-0.302	0.010	0.045
2446200.40381	0.1785	-0.304	0.016	0.029
2446200.40700	0.1827	-0.298	-0.006	0.030
2446200.40977	0.1864	-0.311	0.002	0.022
2446200.43509	0.2196	-0.358	0.017	0.027
2446200.43675	0.2218	-0.355	0.006	0.031
2446200.44128	0.2277	-0.341	-0.013	0.026
2446200.44402	0.2313	-0.349	0.000	0.015
2446200.44750	0.2359	-0.348	-0.007	0.022
2446200.44935	0.2383	-0.344	-0.018	0.033
2446200.45329	0.2435	-0.359	-0.001	0.026
2446200.45565	0.2466	-0.359	0.003	0.028
2446200.45901	0.2510	-0.353	-0.008	0.021
2446200.46113	0.2538	-0.346	-0.007	0.016
2446200.48144	0.2804	-0.352	0.017	0.011
2446200.48589	0.2863	-0.340	0.000	0.014
2446200.48778	0.2887	-0.334	0.002	0.024
2446200.49117	0.2932	-0.345	0.013	0.015
2446200.49327	0.2960	-0.338	0.014	0.020
2446200.49667	0.3004	-0.330	0.007	0.022
2446200.49846	0.3028	-0.337	0.015	0.032
2446200.50347	0.3093	-0.330	0.020	0.012
2446200.50550	0.3120	-0.326	0.022	0.030
2446200.50951	0.3173	-0.307	0.010	0.021
2446200.51177	0.3202	-0.321	0.028	0.037
2446200.52802	0.3416	-0.276	-0.001	0.026
2446200.53431	0.3498	-0.250	0.005	0.022
2446200.53651	0.3527	-0.257	0.003	0.036
2446200.55241	0.3736	-0.211	0.000	0.025
2446200.55471	0.3766	-0.208	0.005	0.037

continued

2446200.55910	0.3824	-0.183	0.001	0.022
2446200.56110	0.3850	-0.175	0.001	0.035
2446200.56587	0.3912	-0.155	0.003	0.038
2446200.56878	0.3951	-0.157	0.018	0.007
2446200.58934	0.4221	-0.081	0.013	0.025
2446200.59131	0.4246	-0.076	0.009	0.027
2446200.59486	0.4293	-0.048	-0.005	0.022
2446200.59666	0.4317	-0.048	-0.002	0.017
2446200.60005	0.4361	-0.032	0.002	0.015
2446200.60231	0.4391	-0.027	0.000	0.032
2446200.60632	0.4443	-0.006	-0.008	0.022
2446200.60838	0.4471	-0.020	0.014	0.032

1985 May 15/16

Differential Magnitude (v-c)

H.J.D.	Phase	V	B-V	U-B
2446201.34906	0.4192	-0.090	0.015	0.013
2446201.35167	0.4226	-0.094	0.024	0.031
2446201.36237	0.4367	-0.048	0.017	0.023
2446201.36460	0.4396	-0.058	0.040	0.033
2446201.36980	0.4465	-0.021	0.014	0.038
2446201.37228	0.4497	-0.023	0.032	0.035
2446201.38153	0.4618	0.011	0.015	0.049
2446201.38315	0.4640	0.014	0.021	0.030
2446201.38728	0.4694	0.019	0.025	0.037
2446201.38881	0.4714	0.014	0.029	0.057
2446201.39168	0.4752	0.028	0.020	0.034
2446201.39328	0.4773	0.025	0.030	0.032
2446201.39602	0.4809	0.043	0.010	0.039
2446201.39796	0.4834	0.045	0.018	0.043
2446201.40058	0.4868	0.054	0.008	0.045
2446201.40203	0.4888	0.042	0.022	0.055
2446201.40510	0.4928	0.050	0.021	0.046
2446201.40692	0.4952	0.054	0.025	0.035
2446201.41599	0.5071	0.061	0.015	0.041
2446201.41777	0.5094	0.068	0.006	0.039
2446201.42212	0.5151	0.062	0.005	0.041
2446201.42388	0.5174	0.051	0.009	0.051
2446201.42816	0.5230	0.024	0.017	0.054
2446201.42985	0.5253	0.024	0.024	0.039
2446201.43281	0.5292	0.023	0.015	0.043
2446201.43450	0.5314	0.030	0.005	0.045
2446201.43956	0.5380	-0.006	0.027	0.047
2446201.44221	0.5415	0.004	0.016	0.045
2446201.44866	0.5500	-0.026	0.018	0.040
2446201.45047	0.5523	-0.021	0.014	0.036
2446201.45480	0.5580	-0.040	0.014	0.052
2446201.45651	0.5603	-0.038	0.007	0.043
2446201.46202	0.5675	-0.053	0.009	0.039
2446201.47811	0.5886	-0.129	0.020	0.048
2446201.47970	0.5907	-0.127	0.013	0.038

continued

2446201.48401	0.5963	-0.138	0.010	0.053
2446201.48569	0.5986	-0.145	0.008	0.050
2446201.48913	0.6031	-0.148	0.009	0.051
2446201.49084	0.6053	-0.160	0.010	0.054
2446201.49373	0.6091	-0.159	0.003	0.049
2446201.49546	0.6114	-0.163	0.007	0.043
2446201.49928	0.6164	-0.181	0.002	0.048
2446201.50109	0.6188	-0.192	0.010	0.035
2446201.50521	0.6242	-0.201	0.003	0.032
2446201.50718	0.6268	-0.207	0.003	0.043
2446201.51051	0.6311	-0.223	0.008	0.044
2446201.51222	0.6334	-0.223	0.000	0.033
2446201.53449	0.6626	-0.283	0.002	0.043
2446201.53624	0.6649	-0.275	-0.007	0.023
2446201.54008	0.6699	-0.290	0.003	0.034
2446201.54185	0.6723	-0.291	-0.002	0.035
2446201.54529	0.6768	-0.303	0.000	0.040
2446201.54702	0.6791	-0.312	0.013	0.029
2446201.55011	0.6831	-0.315	0.000	0.033
2446201.55200	0.6856	-0.315	0.005	0.026
2446201.55514	0.6897	-0.320	-0.001	0.020
2446201.55707	0.6922	-0.322	-0.001	0.036
2446201.56054	0.6968	-0.316	-0.015	0.030
2446201.56270	0.6996	-0.329	0.002	0.023
2446201.56755	0.7060	-0.349	0.009	0.031
2446201.56938	0.7084	-0.341	-0.001	0.027
2446201.57290	0.7130	-0.350	0.007	0.034
2446201.57470	0.7154	-0.358	0.015	0.026
2446201.57833	0.7202	-0.362	0.014	0.027
2446201.58019	0.7226	-0.361	0.010	0.036
2446201.58452	0.7283	-0.362	0.015	0.029
2446201.58645	0.7308	-0.360	0.010	0.021
2446201.59036	0.7359	-0.359	0.006	0.031
2446201.59221	0.7384	-0.352	-0.005	0.031
2446201.60497	0.7551	-0.367	0.008	0.016
2446201.60713	0.7580	-0.361	0.006	0.020
2446201.61019	0.7620	-0.358	-0.001	0.011
2446201.61199	0.7643	-0.365	0.007	0.016

1985 May 16/17

Differential Magnitude (v-c)

H.J.D.	Phase	V	B-V	U-B
2446202.35420	0.7385	-0.364	0.005	0.035
2446202.35582	0.7406	-0.369	0.014	0.027
2446202.35962	0.7456	-0.353	-0.005	0.028
2446202.36138	0.7479	-0.362	0.009	0.016
2446202.36453	0.7521	-0.359	-0.001	0.040
2446202.36617	0.7542	-0.359	-0.001	0.030
2446202.36924	0.7583	-0.366	0.010	0.014
2446202.37070	0.7602	-0.359	0.000	0.031
2446202.37366	0.7641	-0.358	0.000	0.020

continued

2446202.37531	0.7662	-0.350	-0.003	0.017
2446202.37817	0.7700	-0.344	-0.005	0.016
2446202.37972	0.7720	-0.342	-0.015	0.023
2446202.38953	0.7849	-0.329	0.005	0.040
2446202.39132	0.7872	-0.331	0.006	0.038
2446202.39436	0.7912	-0.322	-0.007	0.034
2446202.39600	0.7934	-0.319	-0.006	0.038
2446202.39910	0.7975	-0.307	-0.015	0.034
2446202.40086	0.7998	-0.313	-0.006	0.043
2446202.40378	0.8036	-0.313	-0.005	0.045
2446202.40541	0.8057	-0.318	0.010	0.035
2446202.40929	0.8108	-0.302	-0.014	0.039
2446202.41095	0.8130	-0.307	0.000	0.030
2446202.41415	0.8172	-0.302	-0.005	0.036
2446202.41587	0.8195	-0.303	-0.003	0.030
2446202.42112	0.8264	-0.280	-0.006	0.026
2446202.44192	0.8537	-0.252	0.018	0.033
2446202.44356	0.8558	-0.259	0.024	0.043
2446202.44664	0.8598	-0.247	0.023	0.025
2446202.44831	0.8620	-0.233	0.009	0.032
2446202.45096	0.8655	-0.234	0.020	0.037
2446202.45256	0.8676	-0.236	0.035	0.019
2446202.45569	0.8717	-0.221	0.024	0.034
2446202.45745	0.8740	-0.219	0.018	0.028
2446202.46055	0.8781	-0.200	0.010	0.016
2446202.46213	0.8802	-0.192	0.007	0.037

1985 Jul 09/10

Differential Magnitude (v-c)

H.J.D.	Phase	V	B-V	U-B
2446256.25712	0.4887	0.058	0.017	0.037
2446256.25912	0.4914	0.056	0.018	0.045
2446256.26178	0.4948	0.063	0.017	0.040
2446256.26351	0.4971	0.072	0.006	0.044
2446256.26611	0.5005	0.054	0.029	0.029
2446256.26800	0.5030	0.066	0.018	0.027
2446256.27072	0.5066	0.059	0.023	0.039
2446256.27270	0.5092	0.055	0.018	0.036
2446256.28437	0.5245	0.031	0.025	0.035
2446256.28641	0.5272	0.042	-0.002	0.048
2446256.28903	0.5306	0.030	0.009	0.042
2446256.29097	0.5332	0.020	0.014	0.046
2446256.29379	0.5369	0.021	0.001	0.037
2446256.29580	0.5395	0.003	0.023	0.030
2446256.30560	0.5524	-0.044	0.036	0.042
2446256.30746	0.5548	-0.035	0.016	0.059
2446256.30868	0.5564	-0.036	0.010	0.067
2446256.31144	0.5600	-0.033	0.003	0.051
2446256.31270	0.5617	-0.044	0.014	0.039
2446256.31548	0.5653	-0.058	0.010	0.049
2446256.32547	0.5784	-0.097	0.016	0.048

continued

2446256.32763	0.5813	-0.100	0.014	0.038
2446256.32928	0.5834	-0.120	0.030	0.043
2446256.33141	0.5862	-0.114	0.018	0.035
2446256.33335	0.5888	-0.133	0.027	0.038
2446256.33558	0.5917	-0.137	0.024	0.028
2446256.33724	0.5939	-0.145	0.027	0.024
2446256.33993	0.5974	-0.144	0.013	0.043
2446256.34147	0.5994	-0.166	0.031	0.038
2446256.34349	0.6021	-0.166	0.022	0.026
2446256.34515	0.6043	-0.175	0.025	0.027

Table 4 : Data for V701 Sco, HD 317845 and HD 317858.

	V701 Sco	HD 317845	HD 317858
CPD no.	-32° 4606	-32° 4603	-32° 4602
R.A. (1950)	17 ^h 31 ^m 08 ^s	17 ^h 31 ^m 07 ^s	17 ^h 31 ^m 00 ^s
Dec. (1950)	-32° 28' 16"	-32° 31' 50"	-32° 34' 45"
Sp. type	B2:nn	B1III-IV	B2V
V	8 ^m .66 (0 ^p .25) 9 ^m .07 (0 ^p .00) 9 ^m .08 (0 ^p .50)	9 ^m .02 ± 0 ^m .01	9 ^m .55 ± 0 ^m .01
(B-V)	0 ^m .10 (0 ^p .25)	0 ^m .10 ± 0 ^m .01	0 ^m .15 ± 0 ^m .01
(U-B)	-0 ^m .70 (0 ^p .25)	-0 ^m .72 ± 0 ^m .01	-0 ^m .53 ± 0 ^m .01
(B-V) _o	-0 ^m .26 (0 ^p .25)	-0 ^m .26	-0 ^m .21
(U-B) _o	-0 ^m .96 (0 ^p .25)	-0 ^m .98	-0 ^m .79
E(B-V)	0 ^m .36	0 ^m .36	0 ^m .36
E(U-B)	0 ^m .26	0 ^m .26	0 ^m .26

Table 5 : Photoelectric times of minima.

H.J.D.	Error (days)	Epoch (cycles)	O-C (days)	Source reference
-2400000				
39330.0455		-9016.5	-0.0014	Leung, 1974
39331.9516		-9014.5	-0.0000	Leung, 1974
39341.8572		-9001.0	0.0012	Leung, 1974
43574.8358	± 0.0002	-3445.0	-0.0057	Andersen et al., 1980
45918.0107		-369.5	0.0181	Bruton & Chambliss, 1985 *
46199.5059	± 0.0003	0.0	0.0000	This paper.
46201.4110	± 0.0005	2.5	0.0004	This paper.
46569.3960	± 0.0003	485.5	-0.0009	This paper.
46598.3489	± 0.0003	523.5	0.0006	This paper.

* omitted from the analysis (see Section 3.3).

Table 6 : Light-curve solutions.

Adopted primary temperature 23500K

Colour	U	B	V
i (degrees)	64.8 ±2	65.2 ±2	65.1 ±2
f	0.36 ±2	0.37 ±2	0.38 ±2
x	-0.006 ±8	-0.009 ±8	-0.012 ±9
$\Sigma(o-c)^2 \times 10^3$	1.05	0.82	0.74
Std. devn. (mmag.)	4.5	4.2	3.7

Table 7 : Adopted light-curve solution.

T_1 K (polar)	23500
q (spectroscopic)	0.99
α_1 (adopted)	1.00
α_2 (adopted)	1.00
β_1 (adopted)	0.25
β_2 (adopted)	0.25
i (degrees)	65.0 ± 2
x	-0.009 ± 0.008
T_2 K (polar)	23300 ± 200
r_1 (mean)	0.448 ± 2
r_2 (mean)	0.446 ± 2

Table 8 : Astrophysical data for V701 Sco.

Uncorrected data

Absolute dimensions:	Primary	Secondary
M/M _☉	8.9 ± 0.2	8.8 ± 0.2
R/R _☉	4.10 ± 0.04	4.08 ± 0.04
log [☉] g (cgs)	4.16 ± 0.01	4.16 ± 0.01

Photometric data:

T _{eff} (K)	23500 ± 1000	23300 ± 1000
M _{bol}	-4 ^m .5 ± 0 ^m .2	-4 ^m .4 ± 0 ^m .2
log (L/L _☉)	3.66 ± 0.07	3.64 ± 0.08
B.C.	-2 ^m .35	-2 ^m .33
M _V	-2 ^m .1 ± 0 ^m .2	-2 ^m .1 ± 0 ^m .2
E _(B-V)	0 ^m .36	
Distance (pc)	1180 ± 170	

Corrected data

Absolute dimensions:	Primary	Secondary
M/M _☉	10.3 ± 0.2	10.3 ± 0.2
R/R _☉	4.30 ± 0.04	4.28 ± 0.04
log [☉] g (cgs)	4.18 ± 0.01	4.18 ± 0.01

Photometric data:

T _{eff} (K)	23500 ± 1000	23300 ± 1000
M _{bol}	-4 ^m .6 ± 0 ^m .2	-4 ^m .5 ± 0 ^m .2
log (L/L _☉)	3.70 ± 0.07	3.69 ± 0.08
B.C.	-2 ^m .35	-2 ^m .33
M _V	-2 ^m .2 ± 0 ^m .2	-2 ^m .2 ± 0 ^m .2
E _(b-y)	0 ^m .36	
Distance (pc)	1240 ± 190	

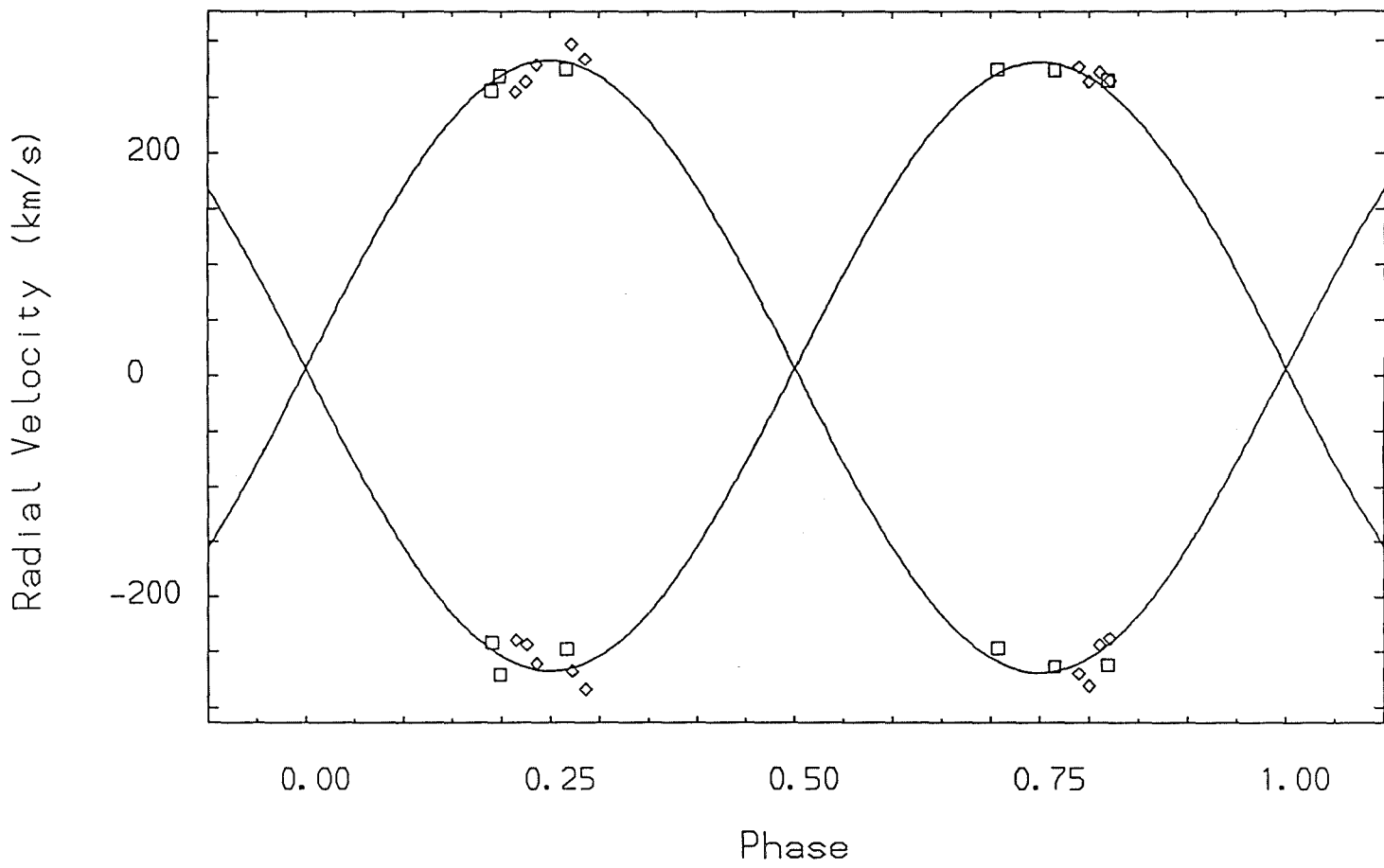


Figure 1.

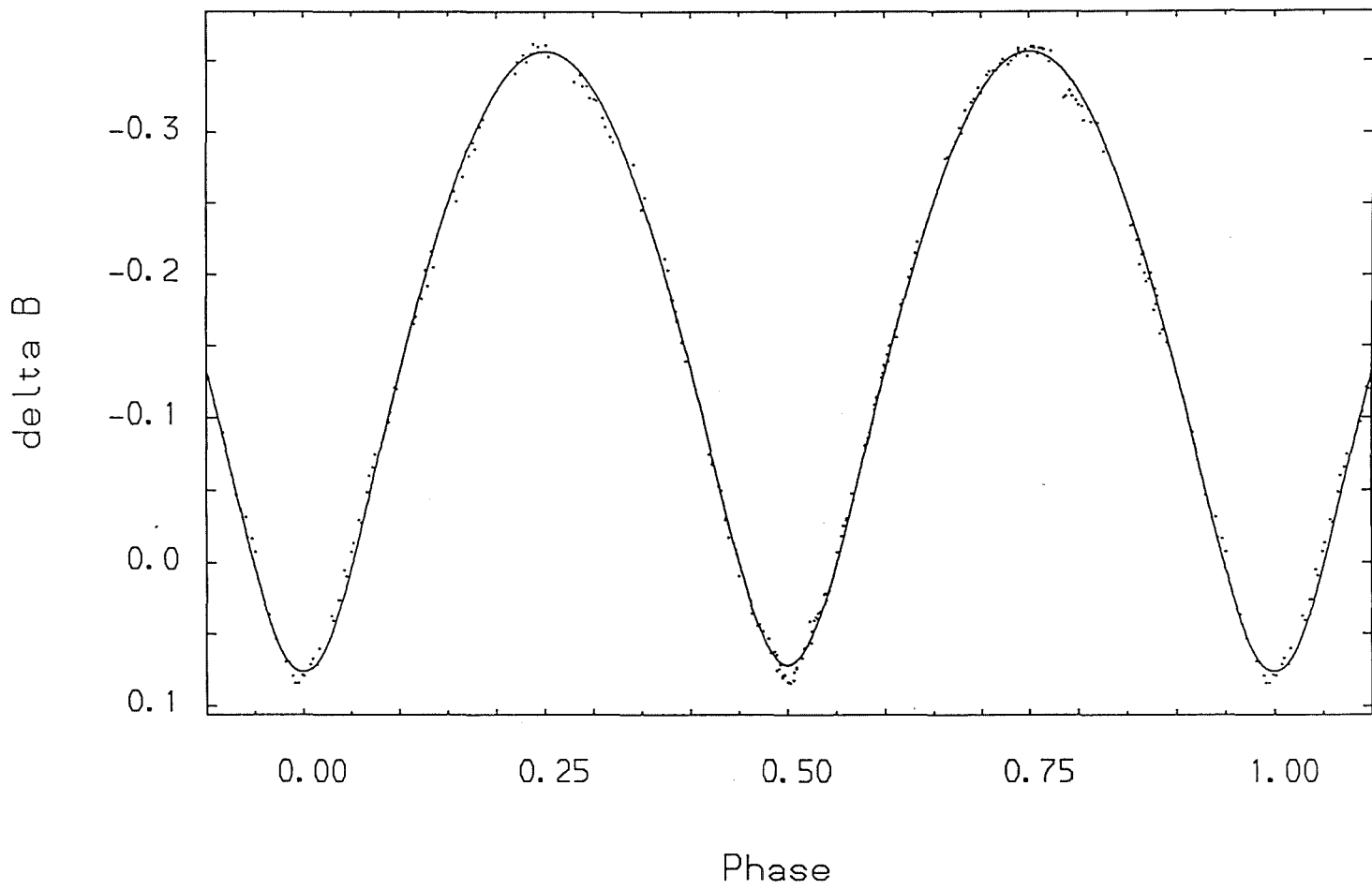


Figure 2.

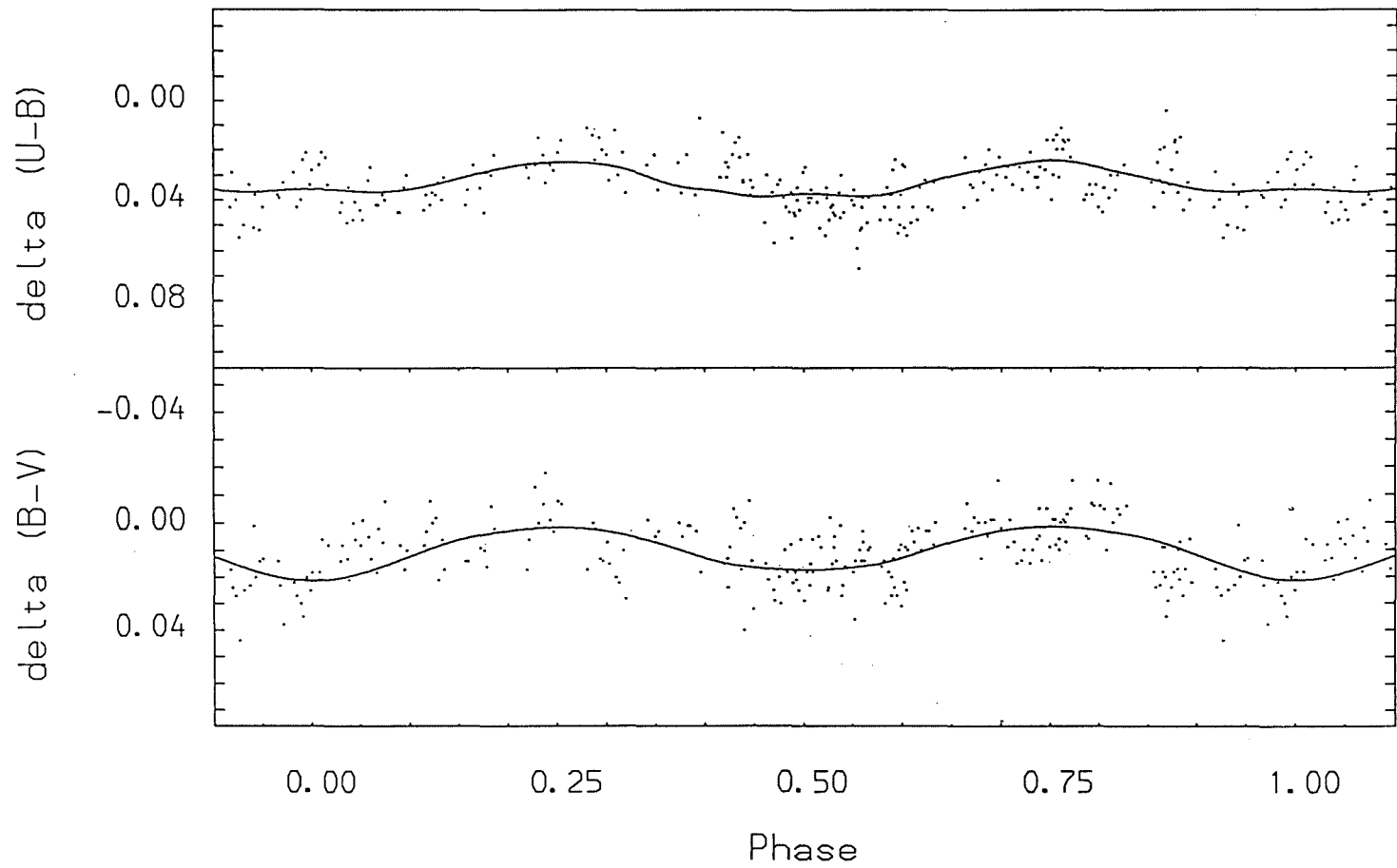
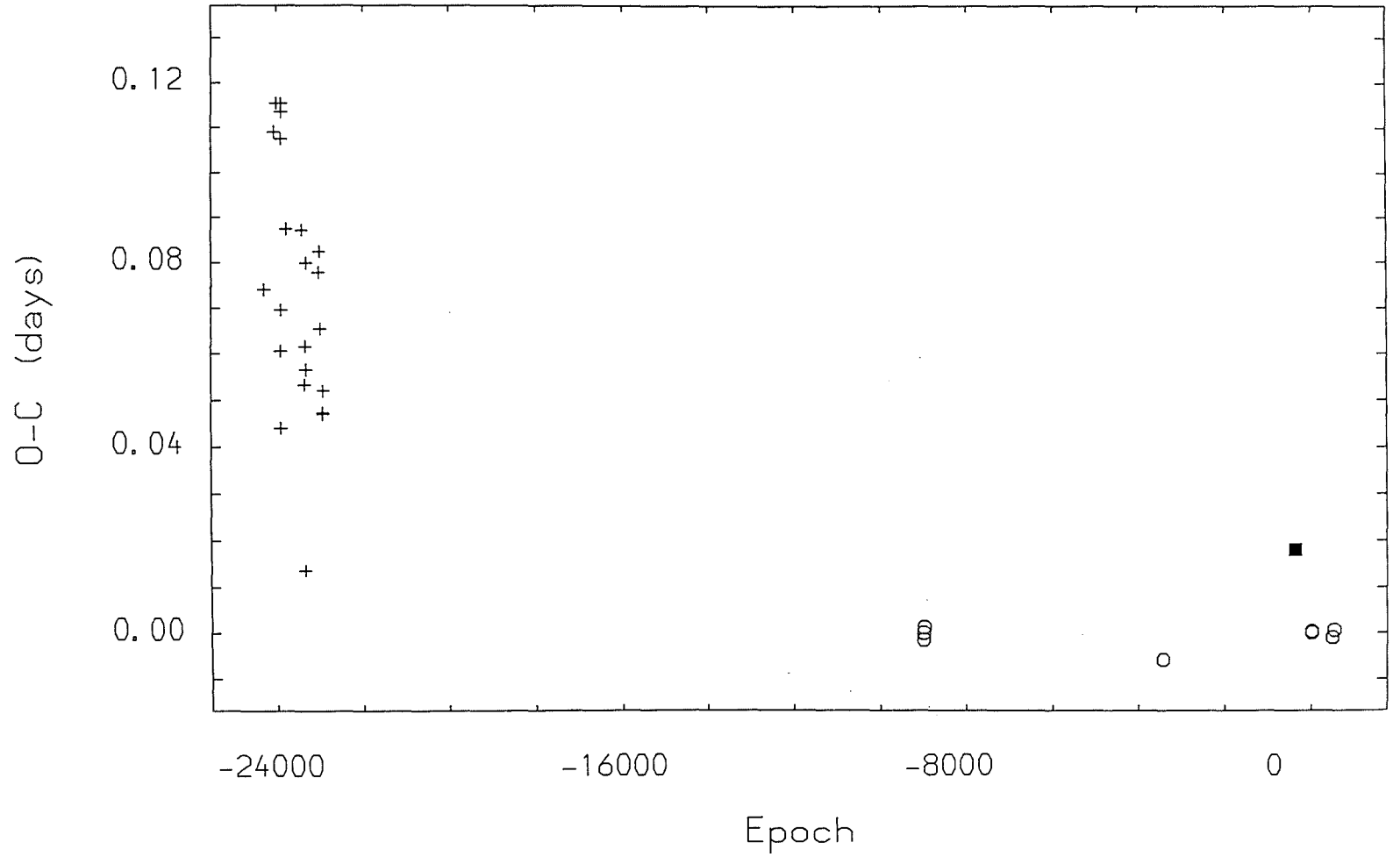


Figure 3.

Figure 4.



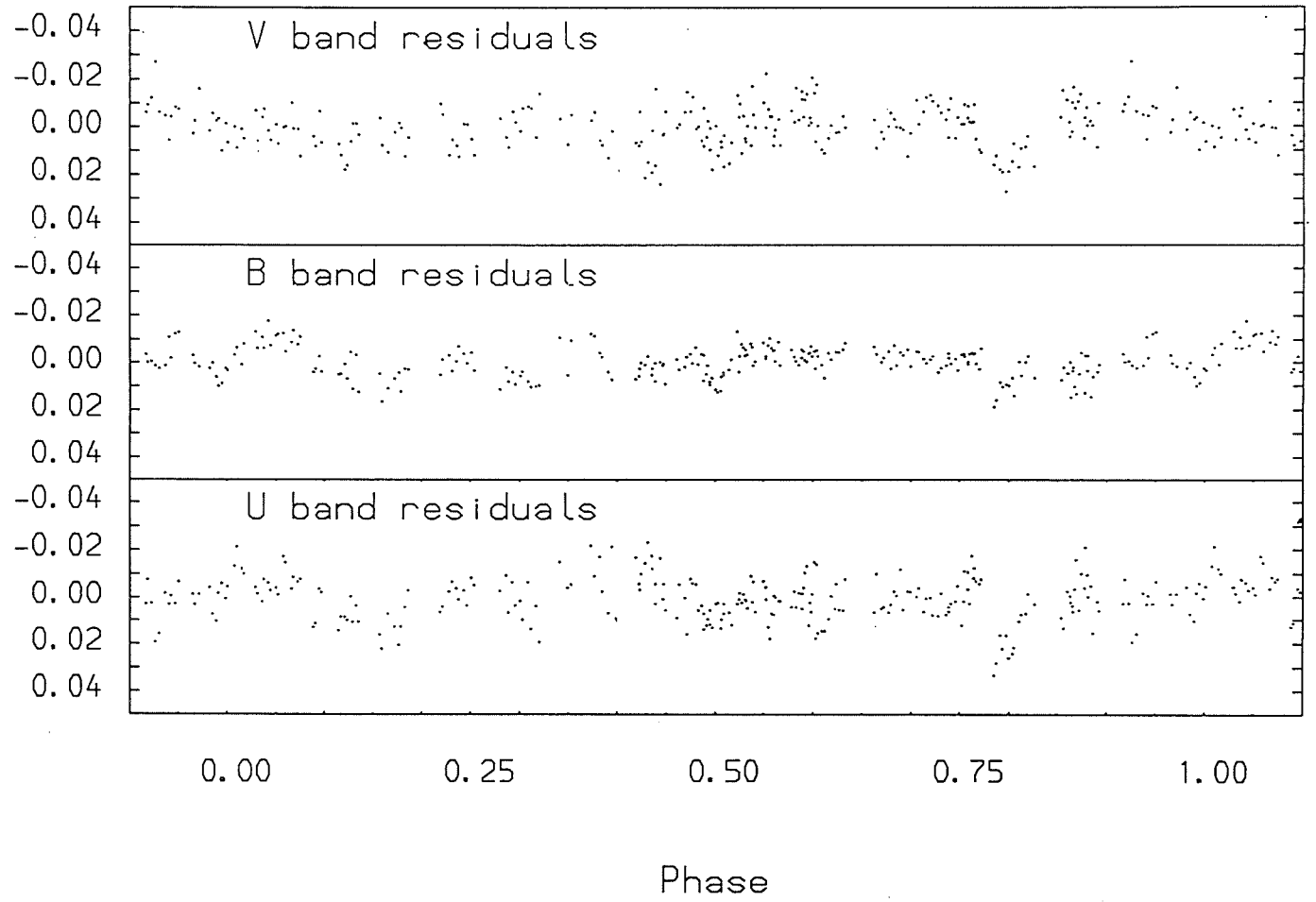


Figure 5.

CHAPTER 9

RZ Pyxidis : An early-type marginal contact binary.

RZ Pyxidis : An early-type marginal contact binary.

S.A.Bell, University Observatory, Buchanan Gardens, St. Andrews,
Fife, KY16 9LZ, Scotland.

G.J.Malcolm, Boyden Observatory, Institute of Astronomy,
University of the Orange Free State, PO Box 339,
Bloemfontein 9300, South Africa.

Received _____

Correspondence to :-

S.A.Bell,
University Observatory,
Buchanan Gardens,
St. Andrews, Fife,
KY16 9LZ,
Scotland.

Summary

The first modern photometric and spectroscopic study of the early-type binary RZ Pyx is presented. The analysis suggests that the system is in a marginal contact configuration with components on the zero-age main sequence. The masses and radii of the two components are found to be (5.3 ± 0.4) and (4.3 ± 0.2) solar masses and (2.61 ± 0.10) and (2.44 ± 0.06) solar radii respectively. The age estimate for the system is less than 2×10^6 yrs. The system may have evolved into contact within this period of time or have arrived on the main sequence in a contact configuration.

1) Introduction

The early-type binary RZ Pyx was found to be variable by Hoffmeister (1936). Subsequent visual observations were made by Kaho (1937) who concluded that the star was an RR Lyrae variable with a period of $0.^d4888$. Kinman (1960) obtained photoelectric data for RZ Pyx and found small colour changes during the cycle. He concluded from these data and the spectral classification of B7 assigned to RZ Pyx that the variable was not an RR Lyrae of Bailey type c, but an eclipsing binary with equal depth minima. The period of RZ Pyx was then revised to $0.^d65627$. Kinman also obtained a limited number of spectroscopic observations at 498mm^{-1} and performed a light-curve analysis by means of a rectification procedure. The resulting radial-velocity data were not of sufficiently high quality to enable a reliable determination of the velocity semi-amplitudes to be made, and the adopted photometric analysis was unsuitable for systems that display continuously variable light curves. Breger (1968) made a limited number of photoelectric observations of RZ Pyx and found small changes in the shape of one of the eclipses of the system although the nature of those differences was uncertain. Eggen (1977) and Wolf and Kern (1983) obtained Stromgren colour indices for the system which suggest that the spectral type of RZ Pyx is earlier than B7.

RZ Pyx is one of a small group of early-type close binaries with periods of less than one day which includes V701 Sco and BH Cen. No modern photoelectric or spectroscopic data have been published for this object and an analysis of RZ Pyx would provide valuable information on the evolutionary state of this short-period binary system. By means of well-determined absolute dimensions, it would then be possible to show whether or not this system is a

contact binary that has evolved into contact early in its main sequence life-time.

2) Spectroscopy

2.1) Observations

The spectroscopic data for RZ Pyx were obtained using the 1.9m telescope at SAAO, Sutherland in conjunction with the Image Tube Spectrograph and Reticon Photon Counting System. A total of 23 double-lined spectra was obtained by SAB during the period 1986 February 21-24, each observation consisting of a spectrogram centred on 4200\AA with a useful range of 500\AA at a dispersion of 30\AA mm^{-1} . The observational procedure has been described in detail elsewhere (Bell et al., 1986a) and will not be discussed further here. The spectrograms show two B-type spectra that are similar in appearance although not completely resolved. As the period of RZ Pyx is 0.656^d , the duration of each exposure was limited to 800s to ensure that the diffuse spectral features were not degraded further by poor time resolution.

2.2) Reduction and Analysis

The spectroscopic data were processed on the University of St. Andrews VAX computers in the manner described by Bell et al. (1986a) using the STARLINK package FIGARO and the spectroscopic image-processing package REDUCE (Hill et al., 1982a). Cross-correlation analyses using VCROSS (Hill, 1982) were attempted using the spectra of SAO 235690 (Sp. type B4V) and SAO 198315 (Sp. type B7V) as templates. This method proved to be too susceptible to

the inherent noise in the data and the mis-matching of the sharp standard-star lines with the rotationally-broadened features of RZ Pyx. The amplitude of the noise was approximately 8% of the continuum height, whereas the depths of the primary and secondary features were of the order of 20 and 15% of the continuum height respectively. For this reason, it was necessary to measure the radial velocities of the two components using VELMEAS (Hill et al., 1982b) by fitting parabolae to those features that could be visually resolved and were not badly affected by noise spikes. Those features which could not be measured by this technique were measured by visual inspection of the line centres. The errors on the primary and secondary radial velocities are estimated to be of the order of 20kms^{-1} .

The principal spectral features showing splitting were the HeI lines at $\lambda\lambda 4026$, 4388 and 4471 and the MgII line at $\lambda 4481$. The lines of HeI at $\lambda 4009$ and $\lambda 4120$ were also present as single features but these lines could not be measured with sufficient accuracy to warrant inclusion in the radial-velocity analysis. The presence of these lines would imply that the spectral type of the primary component is at least two sub-classes earlier than B7. These lines may also have been present in the secondary component but the signal-to-noise is not sufficiently high to remove any ambiguity. The blue-shifted component of the MgII $\lambda 4481$ feature and the red-shifted component of HeI $\lambda 4471$ feature were often strongly blended and proved to be impossible to measure for radial velocity. The rest wavelengths adopted for this analysis have been taken from the list by Petrie (1953). The Balmer lines, however, were omitted from the analysis due to their extremely Stark-broadened and rotationally-broadened profiles. The final

radial velocities for both components of RZ Pyx are listed in Table 1 and the radial velocity curves are shown in Figure 1. The interstellar H line of CaII was also measured and a mean velocity of $29 \pm 2 \text{ km s}^{-1}$ was determined. As this feature appeared at the blue end of the wavelength region observed and was often badly blended with H ϵ , only six spectra were found to be clearly measurable and sufficiently well calibrated to allow a reliable determination of the radial velocity of this feature.

Examination of the U, B and V light curves of RZ Pyx shows no clear evidence for any eccentricity in the orbit, despite some distortions in the minima of the light curves. We have therefore assumed a circular orbit for the subsequent analysis. Adopting the ephemeris of Breger (1968), it was found that the velocity of the more luminous (primary) component was negative at second quadrature. This would suggest that the existing ephemeris was in error by half a period. The most likely explanation for this discrepancy is that because of the similarity of their depths, the primary and secondary minima were confused in previous studies of RZ Pyx. The observations made by Kinman (1960) and Breger (1968) were not of sufficient quality to identify the deeper minimum (see Section 3.3). Using the ephemeris presented in Section 3.3 and adopting the procedures of Popper (1974), the circular orbital elements of RZ Pyx were computed by separate least-squares analyses of each component to determine the velocity semi-amplitude and systemic velocity. The velocity semi-amplitude of the primary and the secondary (K_1 and K_2 respectively), the mean systemic velocity V_0 , the derived mass functions and projected semi-major axes of the orbits of the two components, together with their standard errors, are given in Table 2.

By means of the measurement of the half-widths of both components of the HeI $\lambda 4026$ feature using VLINE (Hill et al., 1982c), we have estimated the projected rotational velocities for both stars in conjunction with the calibration of Olson (1984). The exposure showing the most satisfactorily-resolved feature was SAA01/243, and from this spectrum we have estimated the projected rotational velocities of the primary and secondary components to be $200 \pm 20 \text{ km s}^{-1}$ and $190 \pm 20 \text{ km s}^{-1}$ respectively. If synchronous rotation is adopted together with the final mean radii of the two stars (see Table 9), then theoretical velocities of 201 km s^{-1} and 188 km s^{-1} would be expected for the primary and secondary components based on the uncorrected velocity semi-amplitudes. If the corrected values of K_1 and K_2 are used, these theoretical values should be increased by 5%. The agreement between theoretical and observed projected rotational velocities is very good considering that the features are not completely resolved. Measurements of the equivalent widths for the two components of the HeI $\lambda 4026$ feature in SAA01/243 would imply a luminosity ratio of the secondary to the primary of 0.81 with an estimated error of approximately 10%. This determination compares very favourably with the photometric analysis.

3) Photometry

3.1) Observations

The photoelectric photometry for RZ Pyx was obtained by GJM during the period 1986 March 3-31 by means of a 0.41m telescope at Boyden Observatory. Further observations in the Johnson V band were obtained on 1986 April 1/2 and 2/3 to supplement the number of times

of minima for the system. The photometer and data acquisition programme have already been described in detail elsewhere (Malcolm and Bell, 1986) and will not be discussed further here. A 30 arcsecond diaphragm was used throughout the observations and integration times were fixed at 30s for the monitoring sequence. Complete differential light curves for RZ Pyx were obtained employing UBV filters and these data were transformed to the standard system using observations of the comparison stars and many E-region standard stars (Cousins, 1983) during the 1986 observing season.

Observations using a blue filter with a somewhat wider passband than the normal Johnson B filter were made by GJM and SAB during the period 1985 March 3-20. The 0.41m telescope referred to above was also used for these observations in conjunction with a CO₂ snow-cooled photometer and an EMI 6256 photomultiplier. SAO 176605 (Sp. type A5/A6V) was used as the comparison star and SAO 176536 (Sp. type B9.5IV) as the check star. Subsequent analysis showed that the comparison star was variable with an amplitude of approximately 0.^m06 over a time-scale of the order of a few days. However, no significant variation in the comparison star was observed over a single night and three reliable times of minima have been derived from these data.

The 1986 observations employed SAO 176697 (Sp. type A3IV) as the comparison star and SAO 176536 as the check star; data for RZ Pyx and the comparison stars used during the 1986 observations are given in Table 4. SAO 176697 (δ Pyx) was also used as the comparison star in the photoelectric studies by Kinman (1960) and Breger (1968). No evidence for variability in SAO 176697 was reported in either of these studies.

3.2) Reductions

The observations were reduced using the methods described by Bell et al. (1986b). Differential magnitudes were formed with respect to the comparison star using a spline-fitting program written by SAB. These data were then transformed to the standard system and phased according to the ephemeris adopted in Section 3.3. The differential V magnitudes, (B-V) and (U-B) colour index differences and corresponding mean times of observation are given in Table 3. A total of 299 observations were made in each colour and the resulting B-band light curve and (B-V) and (U-B) colour changes are given in Figures 2 and 3 respectively. The errors on a single observation in a single band are estimated to be less than 0.01^m , and no evidence of photometric variability exceeding this limit has been found in either the comparison or check star for the 1986 observations.

3.3) Ephemeris

Breger (1968) calculated the following ephemeris for RZ Pyx based on his own observations and those of Kinman (1960). The definition of primary minimum for these studies was selected arbitrarily as the depths of minima appeared to be the same. It has been referred to in the ephemeris given below as "minimum light".

$$\text{Minimum light} = \text{H.J.D. } 2438431.474 + 0.656273 E$$

+34

Nine new photoelectric times of minima are presented in Table 5 along with three times of minima evaluated from the data of Kinman and Breger as well as a determination by Wolf and Kern (1983). The calculation of the times of minima have been made using the method

irregular variations would appear to be the asymmetries in the B-band light curve close to secondary minimum. This will clearly affect any estimate of the primary temperature using these colour indices. Adopting the mean quadrature colours for the system would imply a colour excess $E(B-V)$ of 0.15. The observed and de-reddened colour indices of RZ Pyx and the comparison and check stars are given in Table 4.

In addition to the UBV light curves presented here, Strömgren photometry for RZ Pyx was obtained by SAB during 1985, February using the 0.5m telescope at SAAO. A section of the light curve around second quadrature was obtained in addition to several measurements of the comparison and check stars. The resulting observed and de-reddened colour indices for these stars have been given in Table 4. These observations would imply a colour excess $E(b-y)$ of 0.07^m for RZ Pyx which is clearly lower than that obtained from the UBV photometry using the relationship $E(b-y) = 0.74 E(B-V)$. Warren (1976) has suggested that the c_0 colour index appears to be affected by projected rotational velocities of greater than 250kms^{-1} in B stars. However, the projected rotational velocities for RZ Pyx are somewhat smaller than this limit and no correction has been made for this effect.

This discrepancy could be attributed to an error in the data-reduction procedure. This has been ruled out as the UBV observations of the comparison star are in excellent agreement with those obtained by Nicolet (1978) and the Q parameter (Johnson and Morgan, 1953) for the check star of -0.13 confirms the spectral classification of B9.5 made by Houk (1982). The Strömgren photometry for the comparison star is in excellent agreement with the colours obtained by Gronbech and Olsen (1976). However the c_1

colour index for RZ Pyx is 0.05^m brighter than that obtained by Wolf and Kern (1983). It seems likely that RZ Pyx displays irregular variations in its colour indices since the discrepancies described here are larger than the typical errors in the photometry. The agreement between the colours of the comparison star in both photometric systems and those of previous studies vindicates the reduction procedure.

3.5) Analysis

The light curves of RZ Pyx display behaviour characteristic of a system of the WUMa type with nearly equal minima of depth $\sim 0.85^m$. Primary minimum, as defined by the radial velocity data of the two components, is approximately 0.04^m deeper than secondary minimum. There are indications of distortions in all three light curves which are particularly noticeable in both eclipses. The most significant asymmetry ($\sim 0.04^m$) is in the ingress to secondary minimum in the B-band light curve (see Figure 2). Second quadrature also appears to be brighter than first quadrature by 0.01^m - 0.02^m . Other smaller-scale distortions can be seen at the bottom of both the minima for the U and V light curves. These effects are displayed in the residuals of the individual observations from the adopted theoretical curves for each band in Figure 4.

As the observations were made on a single-channel photometer, corrections have been applied to the phasing of each light curve corresponding to the difference between the mean time of observation and the actual time of observation for an individual band. This correction amounts to less than 0.001^P and could have been ignored without affecting the analysis of the light curves.

Assuming the components of the system have similar temperatures, the Strömgen colour indices in conjunction with the (c_o, T_{eff}) calibration of Davis and Shobbrook (1977) would suggest a primary component temperature of 16400K. However, the $((u-b)_o, T_{\text{eff}})$ calibration of Davis and Shobbrook favours a temperature 17400K. The former estimate is in better agreement with the $(B-V, T_{\text{eff}})$ calibration of Böhm-Vitense (1981) in which a $(B-V)_o$ of -0.19 at secondary minimum corresponds to a primary component temperature of 16800K. The tabulation of Popper (1980) would suggest a temperature of 17200K based on a spectral type for the primary component of B4. Considering the variation in the estimates for the temperature of both components, a primary component temperature of 17000K has been adopted with an estimated error of 1000K. This value represents a lower limit to the temperature of the primary component as the Strömgen colour indices represent the combined colour of the system and the $(B-V)_o$ has been derived from the distorted secondary minimum of the B-band light curve. It would appear that the spectral type of the primary component is in the range B3-B4. This is in good agreement with the spectroscopic observations (see Section 2.2).

The first attempt at a photometric solution was made using the light-curve synthesis program of Rucinski (1976a,b,c). In an attempt to overcome the small-scale asymmetries in the light curves, an average light curve was formed by folding the data about $0^{\text{P}}.5$. Cubic spline fits were made to these averaged light curves and were used to generate intensities normalised to the intensity at $0^{\text{P}}.25$ in steps of $0^{\text{P}}.01$. The method of analysis has been described in detail elsewhere for the system V701 Sco (Bell and Malcolm, 1986). The bolometric albedo α and the gravity darkening exponent β for both components of the system have been fixed at unity and 0.25

respectively. The limb-darkening coefficients were taken from the tabulation of Wade and Rucinski (1985). The remaining parameters to be determined from the analysis were the fractional temperature difference $x = (T_2 - T_1)/T_1$ in terms of the primary component temperature T_1 and the secondary component temperature T_2 , the "fill-out" factor f as defined by Rucinski (1973) and the orbital inclination i . The mass ratio q was fixed at the spectroscopically-determined value of 0.82 and the initial values of f and x were assumed to be unity and zero respectively.

The results of this procedure and the formal errors of the least-squares solution for the U, B and V light curves are given in Table 6. The standard deviation and sum of residuals quoted in this table were based on the 51 normal points generated from the cubic spline fit. The volume radii of the primary component r_1 and the secondary component r_2 have been evaluated using the tabulation of Mochnacki (1984). The corresponding errors in the volume radii have been estimated by combining the errors in the determinations of the mass ratio and the fill-out factor. It can be seen from Figure 2 that the dotted line representing this light-curve solution does not fit secondary minimum. The same situation was found to be true for both the U and V band observations. Large variations in the values of f for the different bands were found, two of which suggested the system was not in contact ($f > 1$). The B band solution suggested a marginal contact configuration with $f = 0.92$.

It was decided to use LIGHT (Hill, 1979) in an attempt to improve the solutions to the light curves. Although LIGHT is not well-suited to the analysis of over-contact systems, it has been used here to determine the proximity of the components of RZ Pyx to a contact configuration. LIGHT was used to make two solutions for

each light curve; one solution allowed the mass ratio to be treated as a free parameter and the other held the mass ratio fixed at the spectroscopically-determined value. The other free parameters for both solutions were the fractional primary-component radius r_1 , the secondary-component temperature T_2 and fractional radius r_2 , and the inclination of the system i . As a first approximation, the contact configuration was used and the primary component temperature was fixed at 17000K by the method described above. Tables 7 & 8 summarise the results of both analyses for the three light curves. The fit to secondary minimum of the B light curve is substantially better than Rucinski's method and is displayed in Figure 2 as the solid line. The rms errors quoted in Tables 7 & 8 were based on all the observed data in each band.

The following assumptions were made for each analysis using LIGHT. Black-body fluxes were adopted because experience with the analysis of other light curves of early-type systems has shown that the model atmospheres of Kurucz (1979) give inferior fits. Synchronous rotation was assumed since the projected rotational velocities computed from our final fit agreed quite well with the observed values (Section 2.2). Gravity-darkening exponents (β_1 and β_2) were set at 0.25 for both components, and electron scattering fractions (Escat_1 and Escat_2) were taken from the tabulation of Hutchings and Hill (1971). The limb-darkening coefficients were calculated automatically within LIGHT at each iteration of the solution using interpolation from the tabulation by Carbon and Gingerich (1969).

The small difference in brightness between first and second quadrature could induce errors in the B light-curve solution. Both halves of the light curve were analysed separately with q fixed at 0.82 to quantify these differences. The solutions proved to be almost identical to within the formal errors of the free parameters and it can be concluded that taking the solution for all the B-band data is valid.

Attempts were also made to evaluate the dependence of the solution on the adopted temperature and mass ratio. Further solutions were made of all three light curves adjusting T_1 by $\pm 1000\text{K}$ and q by ± 0.02 . The changes in the free parameters were of the order of the formal errors of those quantities. It is reasonable to assume that the solution is relatively insensitive to small changes in q and T_1 .

4) Discussion

4.1) Spectroscopy and Photometry

The velocity separation of approximately 520kms^{-1} for the two components of RZ Pyx would probably be large enough for the effects of blending of the diffuse HeI lines to be ignored if the system had been detached or even semi-detached. The rotational velocities of the two components are such that the features are never completely resolved and measurement of the radial velocities of the components will always be underestimated. The effects of reflection in the spectroscopic analysis can be ignored for RZ Pyx as the two components have very nearly identical temperatures. However, this effect has been included in the photometric analyses. We have estimated the blending correction to the velocity semi-amplitudes to

be of the order of 3%. This is at best a rough estimate and is based on experience with other early-type close binary systems. The orbital parameters derived from these corrected velocity semi-amplitudes are given in Table 2.

The LIGHT solutions with q fixed at 0.82 provide the most satisfactory fits to the observed data and have been adopted for the final analysis (see Table 9). The good agreement between the photometric mass ratio obtained using LIGHT and that determined spectroscopically is gratifying and confirms the marginal contact configuration of the LIGHT solution. However, the scatter in the residuals displayed in Figure 4 is larger than would have been expected. Observations of light curves for other systems using the same telescope and observational technique show a typical scatter of $0^m.01$ - $0^m.02$. The trends displayed in the (B-V) and (U-B) colour curves (see Figure 3) appear to be caused by the presence of asymmetries in the light curves of up to $0^m.04$ which detract from the quality of the light-curve solution.

Astrophysical data for this system are given in Table 10. Data based on both the observed and corrected velocity semi-amplitudes are tabulated. The bolometric corrections quoted in Table 10 are taken from the calibration of Davis and Shobbrook (1977) and the adopted colour excess $E(B-V)$ is that determined from the Strömgren photometry obtained for this study in conjunction with the relation $E(b-y) = 0.74 E(B-V)$. The determination of the colour excess for RZ Pyx was made using the Strömgren observations because the c_0 index is less sensitive to the effects of interstellar reddening.

The errors quoted in Table 10 are formal errors and are likely to be underestimates of the real errors in the physical parameters. The distribution of the radial velocity data favour somewhat smaller errors in the velocity semi-amplitudes than might otherwise be the case. The blending correction is a simple estimate and should also be included in the determination of the error in the velocity semi-amplitudes. The asymmetries in the light curves will also increase the error in the fractional radii of both components. It is probably more realistic to increase the error estimates by a factor of two for the masses, radii and luminosities of both components.

4.2) Evolutionary state

Adopting the uncorrected masses for the two components, comparisons with the evolutionary tracks for single stars published by Hejlesen (1980) show that a chemical composition of ($X = 0.70$, $Z = 0.02$) provides reasonable agreement with the locations of the primary and secondary components in the theoretical HR diagram. However, both components lie slightly below the mass track appropriate to their masses. Using the temperature and surface gravity g of the two components, an age determination for the system can be made using the $(\log g, \log T_{\text{eff}})$ diagrams given by Hejlesen. This would indicate the system is less than 2×10^6 yrs old and essentially unevolved. In this part of the $(\log g, \log T_{\text{eff}})$ diagram, the isochrones are closely packed and this estimate must be regarded as an upper limit to the age of the system. Adopting the corrected masses, the age estimate for the system is decreased by approximately 50%, although the discrepancy between the appropriate mass track and the observed luminosity and temperature becomes more

apparent.

Comparing the uncorrected masses and radii of the two components with the ZAMS mass-radius relation derived from the models of Hejlesen, it is clear that both stars are unevolved. The zero-age main sequence radii of stars of 5.3 and $4.3M_{\odot}$ are 2.58 and $2.30R_{\odot}$ respectively. However, if the masses corrected for blending effects of 5.8 and $4.7M_{\odot}$ are adopted, then the corresponding zero-age main-sequence radii are 2.72 and $2.43R_{\odot}$ respectively. In order to improve the agreement between the components of the system and the theoretical HR diagram of Hejlesen, the primary component temperature must be increased by approximately $1000K$ which is acceptable on the basis of the probable errors in the original estimate (see Section 3.5). The masses of both components must be marginally larger than the uncorrected masses, implying that the blending correction is smaller than the estimate made in Section 4.1.

If RZ Pyx is as young as it would appear, it is of considerable interest to know whether the system has recently evolved into contact via case A evolution or if it was already in contact at the beginning of its main-sequence lifetime. The absence of period changes would indicate that the system is not in the rapid phase of case A mass transfer. The possibility of a contact system in an equilibrium state after the phase of rapid mass transfer may exist, although one might expect a detached primary component. This is not clearly supported by the analysis presented here. The formation of RZ Pyx is of particular interest if the system has been in contact for the duration of its main-sequence lifetime.

4.3) Kinematics

RZ Pyx is situated in the local arm of the Galaxy at a distance of 900pc from the Sun and lies 170pc above the galactic plane. The age estimate for the system suggests that it should be associated with a region of recent star formation; this is not the case. The motion of RZ Pyx with respect to the local standard of rest should yield some information about the point of origin of the system. However, the large errors on the proper motions of this system preclude accurate determinations of the motion of RZ Pyx and it is not possible to establish whether the system is moving into or out of the plane. Consequently, more precise proper motions are required before any further investigation of the point of origin of RZ Pyx can be made.

5) Conclusion

UBV photometry and medium-resolution spectroscopy of RZ Pyx are presented. A reliable determination of the absolute dimensions of the components of the system has been made which shows that the two stars are of similar temperature and slightly differing masses. The blending correction for the velocity semi-amplitudes appears to be negligible and the uncorrected masses and radii have been adopted in the final analysis. It is suggested that the system is in a marginal contact configuration and that its age is less than 2×10^6 yrs. No evidence has been found for any period change but there is some photometric evidence for photospheric activity. The possibilities exist that this system may have arrived on the main sequence in a contact configuration or that it has evolved into contact within 2×10^6 yrs.

Acknowledgements

SAB would like to express his thanks for the hospitality and assistance extended to him by the staffs of the Institute of Astronomy of the University of the Orange Free State and the South African Astronomical Observatory and during the observing runs. PATT is acknowledged for the allocation of observing time at SAAO, and likewise the SERC for financial support in the form of a Research Studentship for one of us (SAB). SAB gratefully acknowledges a Visiting Fellowship from the University of the Orange Free State and financial assistance made available by the University of St. Andrews. The authors also wish to express their gratitude to Prof. A.H. Jarrett and Prof. D.W.N. Stibbs for the use of the facilities of the Boyden Observatory and the University Observatory, St. Andrews, respectively and to Dr. R.W. Hilditch for many useful discussions and constructive criticism throughout this investigation.

References

- Bell, S.A. & Malcolm, G.J., 1986. Submitted to Mon. Not. R. astr. Soc.
- Bell, S.A., Kilkenny, D. & Malcolm, G.J., 1986a. Submitted to Mon. Not. R. astr. Soc.
- Bell, S.A., Hilditch, R.W. & Adamson, A.J., 1986b. Mon. Not. R. astr. Soc. in print.
- Böhm-Vitense, E., 1981. Ann. Rev. Astron. Astrophys., 19, 295.
- Breger, M., 1968. Publ. astr. Soc. Pacific, 80, 417.
- Carbon, D.F. & Gingerich, O.J., 1969. Theory and Observations of Normal Stellar Atmospheres, ed. Gingerich, O.J. (M.I.T. press, Cambridge), 377.
- Cousins, A.W.J., 1983. S.A.A.O. Circ., 7, 36.
- Davis, J. & Shobbrook, R.R., 1977. Mon. Not. R. astr. Soc., 178, 651.
- Eggen, O.J., 1977. Astron. J., 83, 288.
- Gronbech, B. & Olsen, E.H., 1976. Astron. Astrophys. Suppl. Ser., 25, 213.
- Hejlesen, P.M., 1980. Astron. Astrophys. Suppl. Ser., 39, 347.
- Hill, G., 1979. Pub. Dom. Astrophys. Obs., 15, 297.
- Hill, G., 1982. Publ. Dom. Astrophys. Obs., 16, 59.
- Hill, G., Fisher, W.A. & Poekert, R., 1982a. Publ. Dom. Astrophys.

Obs., 16, 43.

Hill,G., Ramsden,D., Fisher,W.A. & Morris,S.C., 1982b. Publ. Dom. Astrophys. Obs., 16, 11.

Hill,G., Fisher,W.A. & Poeckert,R., 1982c. Publ. Dom. Astrophys. Obs., 16, 27.

Hoffmeister,C., 1936. Astron. Nachr., 258, 39.

Houk,N., 1982. Catalogue of two-dimensional spectral types for the HD stars -40 to -26 degrees, Ann Arbor, Dept. of Astronomy, Univ. of Michigan, vol. 3.

Hutchings,J.B. & Hill,G., 1971. Astrophys. J., 167, 137.

Johnson,H.L. & Morgan,W.W., 1953. Astrophys. J., 117, 313.

Kaho,S., 1937. Tokyo Astr. Bull., No. 209.

Kinman,T.D., 1960. Mon. Not. R. astr. Soc. South Africa, 19, 62.

Kurucz,R.L., 1979. Astrophys. J. Suppl. Ser., 40, 1.

Kwee,K.K. & van Woerden,H., 1956. Bull. astr. Inst. Netherlands, 12, 327.

Malcolm,G.J. & Bell,S.A., 1986. Mon. Not. astr. Soc. South Africa, 45, No. 1 & 2.

Mochnecki,S.W., 1984. Astrophys. J. Suppl. Ser., 55, 551.

Nicolet,B., 1978. Astron. Astrophys. Suppl. Ser., 34, 1.

Olson,E.C., 1984. Publ. astr. Soc. Pacific, 96, 376.

- Petrie, R.M., 1953. Publ. Dom. Astrophys. Obs., 9, 297.
- Popper, D.M., 1974. Astron. J., 79, 1307.
- Popper, D.M., 1980, Ann. Rev. Astron. Astrophys, 18, 115.
- Rucinski, S.M., 1973. Acta astr., 24, 119.
- Rucinski, S.M., 1976a. Pubs. astr. Soc. Pacific, 88, 244.
- Rucinski, S.M., 1976b. Acta astr., 26, 227.
- Rucinski, S.M., 1976c. Pubs. astr. Soc. Pacific, 88, 777.
- Wade, R.A. & Rucinski, S.M., 1985. Astron. Astrophys. Suppl. Ser., 60, 471.
- Warren, W.H., 1976. Mon. Not. R. astr. Soc., 174, 111.
- Wolf, G.W. & Kern, J.T., 1983. Astrophys. J. Suppl. Ser., 52, 429.

Figure captions

Figure 1: Observed radial velocities and computed orbits for RZ Pyx. The primary-component radial velocities are represented by the squares and the data for the secondary component by diamonds.

Figure 2: B-magnitude differences in the sense variable minus comparison between RZ Pyx and SAO 176697 together with the theoretical curves calculated using LIGHT (solid line) and Rucinski's method (dashed line).

Figure 3: (B-V) and (U-B) colour-index differences in the sense variable minus comparison between RZ Pyx and SAO 176697 together with the theoretical curves calculated using LIGHT.

Figure 4: Residuals of the individual UBV observations from the final theoretical curves using LIGHT.

Table 1 : Radial-velocity data for RZ Pyx.

Tape/Run	H.J.D.	Phase	V_1	n	O-C	V_2	n	O-C
No.	-2400000		kms^{-1}		kms^{-1}	kms^{-1}		kms^{-1}
SAA01/117	46483.4288	0.7096	+230	(2)	-24	-265	(2)	- 5
SAA01/119	46483.4457	0.7354	+242	(2)	-19	-263	(2)	+ 5
SAA01/121	46483.4584	0.7547	+252	(2)	-10	-246	(2)	+23
SAA01/158	46484.3708	0.1450	-152	(3)	+ 6	+248	(2)	+ 7
SAA01/160	46484.3801	0.1592	-155	(2)	+15	+259	(1)	+ 3
SAA01/162	46484.3896	0.1736	-160	(1)	21	+290	(1)	+21
SAA01/197	46485.3450	0.6294	+225	(1)	+28	-220	(2)	-27
SAA01/199	46485.3564	0.6468	+237	(3)	+23	-233	(3)	-21
SAA01/201	46485.3678	0.6642	+240	(2)	+12	-219	(1)	+10
SAA01/215	46486.3177	0.1116	-146	(1)	-22	+202	(1)	+ 2
SAA01/217	46486.3264	0.1248	-154	(3)	-16	+246	(2)	+29
SAA01/219	46486.3352	0.1383	-165	(3)	-13	+258	(2)	+24
SAA01/221	46486.3438	0.1513	-167	(3)	- 3	+265	(2)	+17
SAA01/223	46486.3531	0.1656	-151	(2)	+24	+280	(1)	+18
SAA01/225	46486.3626	0.1800	-187	(3)	- 2	+279	(2)	+ 5
SAA01/227	46486.3719	0.1942	-198	(2)	- 5	+276	(1)	- 8
SAA01/229	46486.3807	0.2075	-191	(2)	+ 8	+269	(2)	-22
SAA01/233	46486.3978	0.2339	-204	(3)	+ 2	+281	(3)	-19
SAA01/235	46486.4068	0.2473	-224	(2)	-17	+311	(1)	+10
SAA01/237	46486.4157	0.2609	-215	(2)	- 8	+290	(2)	-11
SAA01/239	46486.4243	0.2741	-208	(2)	- 4	+284	(2)	-14
SAA01/241	46486.4329	0.2871	-194	(3)	+ 7	+279	(1)	-15
SAA01/243	46486.4419	0.3008	-198	(3)	- 3	+256	(3)	-31

The columns headed n indicate the number of lines measured for the mean velocity tabulated.

Table 2 : Orbital elements for RZ Pyx.

		Measured	Corrected
K_1 (kms ⁻¹)	=	234 ± 4	241 ± 4
K_2 (kms ⁻¹)	=	285 ± 5	294 ± 5
V_{o1} (kms ⁻¹)	=	27 ± 4	--
V_{o1} (kms ⁻¹)	=	16 ± 4	--
V_{o2} (kms ⁻¹)	=	22 ± 3	--
σ_1 (kms ⁻¹) *	=	15	--
σ_2 (kms ⁻¹) *	=	17	--
q (m_2/m_1)	=	0.82 ± 0.02	0.82 ± 0.02
e	=	0 (adopted)	0 (adopted)
$a_1 \sin i$ (R _⊙)	=	3.04 ± 0.05	3.13 ± 0.06
$a_2 \sin i$ (R _⊙)	=	3.70 ± 0.06	3.81 ± 0.06
$a \sin i$ (R _⊙)	=	6.74 ± 0.08	6.94 ± 0.09
$m_1 \sin^3 i$ (M _⊙)	=	5.25 ± 0.16	5.74 ± 0.17
$m_2 \sin^3 i$ (M _⊙)	=	4.32 ± 0.13	4.71 ± 0.14

* denotes the r.m.s. scatter of a single observation.

Table 3 : UBV observations.

1986 Mar 03/04		Differential Magnitude (v-c)		
H.J.D.	Phase	V	B-V	U-B
2446493.41803	0.9308	4.422	-0.084	-0.809
2446493.41943	0.9329	4.418	-0.075	-0.809
2446493.42143	0.9359	4.423	-0.069	-0.797
2446493.42287	0.9382	4.454	-0.095	-0.788
2446493.42577	0.9426	4.467	-0.073	-0.790
2446493.42726	0.9448	4.500	-0.087	-0.811
2446493.42910	0.9476	4.502	-0.070	-0.801
2446493.43050	0.9498	4.546	-0.103	-0.813
2446493.43217	0.9523	4.547	-0.069	-0.800
2446493.43363	0.9545	4.588	-0.112	-0.794
2446493.43539	0.9572	4.595	-0.081	-0.793
2446493.43684	0.9594	4.636	-0.112	-0.792
2446493.44008	0.9644	4.645	-0.070	-0.783
2446493.44156	0.9666	4.691	-0.106	-0.800
2446493.444963	0.9789	4.780	-0.102	-0.742
2446493.45113	0.9812	4.819	-0.123	-0.750
2446493.45326	0.9845	4.821	-0.081	-0.756
2446493.45483	0.9868	4.860	-0.083	-0.794
2446493.45686	0.9899	4.889	-0.106	-0.745
2446493.45833	0.9922	4.922	-0.122	-0.753
2446493.46151	0.9970	4.940	-0.109	-0.741
2446493.46301	0.9993	4.959	-0.100	-0.772
2446493.46476	0.0020	4.946	-0.089	-0.757
2446493.46626	0.0043	4.942	-0.091	-0.776
2446493.46807	0.0070	4.938	-0.095	-0.754
2446493.46945	0.0091	4.905	-0.089	-0.747
2446493.47131	0.0120	4.911	-0.113	-0.761
2446493.47298	0.0145	4.876	-0.107	-0.760
2446493.48146	0.0274	4.755	-0.087	-0.775
2446493.48281	0.0295	4.741	-0.096	-0.770
2446493.48451	0.0321	4.709	-0.102	-0.783
2446493.48618	0.0346	4.677	-0.102	-0.749

1986 Mar 12/13		Differential Magnitude (v-c)		
H.J.D.	Phase	V	B-V	U-B
2446502.26356	0.4092	4.334	-0.117	-0.774
2446502.26509	0.4115	4.347	-0.127	-0.771
2446502.26944	0.4181	4.363	-0.120	-0.775
2446502.27039	0.4196	4.363	-0.105	-0.792
2446502.27312	0.4238	4.377	-0.106	-0.785
2446502.27410	0.4253	4.389	-0.098	-0.791
2446502.28260	0.4382	4.472	-0.089	-0.767
2446502.28650	0.4441	4.478	-0.078	-0.784
2446502.28983	0.4492	4.514	-0.083	-0.766

continued

2446502.29119	0.4513	4.525	-0.075	-0.781
2446502.29382	0.4553	4.564	-0.094	-0.772
2446502.29485	0.4569	4.573	-0.085	-0.776
2446502.30190	0.4676	4.675	-0.085	-0.759
2446502.30506	0.4724	4.680	-0.072	-0.779
2446502.30857	0.4778	4.718	-0.060	-0.761
2446502.30998	0.4799	4.757	-0.083	-0.770
2446502.31269	0.4841	4.799	-0.090	-0.770
2446502.31365	0.4855	4.801	-0.072	-0.767
2446502.32246	0.4989	4.896	-0.098	-0.775
2446502.32652	0.5051	4.921	-0.134	-0.773
2446502.33209	0.5136	4.816	-0.104	-0.758
2446502.33456	0.5174	4.801	-0.126	-0.763
2446502.33828	0.5230	4.781	-0.137	-0.780
2446502.33989	0.5255	4.733	-0.111	-0.763
2446502.34207	0.5288	4.715	-0.128	-0.789
2446502.34368	0.5313	4.692	-0.130	-0.776
2446502.35401	0.5470	4.565	-0.130	-0.799
2446502.35549	0.5493	4.539	-0.119	-0.795
2446502.35892	0.5545	4.515	-0.125	-0.812
2446502.36042	0.5568	4.489	-0.122	-0.803
2446502.36244	0.5599	4.487	-0.139	-0.802
2446502.36393	0.5621	4.466	-0.139	-0.791
2446502.37378	0.5771	4.366	-0.119	-0.808
2446502.37523	0.5794	4.354	-0.127	-0.796
2446502.37865	0.5846	4.334	-0.123	-0.811
2446502.38012	0.5868	4.320	-0.120	-0.796
2446502.38222	0.5900	4.326	-0.139	-0.811
2446502.38373	0.5923	4.300	-0.129	-0.794
2446502.38578	0.5954	4.291	-0.130	-0.805
2446502.38736	0.5978	4.286	-0.135	-0.795
2446502.40066	0.6181	4.216	-0.119	-0.797
2446502.40205	0.6202	4.202	-0.107	-0.796
2446502.40486	0.6245	4.200	-0.118	-0.798
2446502.40623	0.6266	4.201	-0.125	-0.783
2446502.40831	0.6298	4.184	-0.104	-0.800
2446502.40981	0.6320	4.181	-0.112	-0.794
2446502.42163	0.6501	4.169	-0.145	-0.787
2446502.42309	0.6523	4.158	-0.128	-0.785
2446502.42610	0.6569	4.137	-0.118	-0.787
2446502.42753	0.6590	4.140	-0.130	-0.773
2446502.42952	0.6621	4.145	-0.128	-0.789
2446502.43103	0.6644	4.143	-0.136	-0.782
2446502.43313	0.6676	4.125	-0.113	-0.796
2446502.43451	0.6697	4.131	-0.151	-0.763
2446502.44391	0.6840	4.113	-0.136	-0.770
2446502.44556	0.6865	4.122	-0.136	-0.781
2446502.44900	0.6918	4.106	-0.132	-0.778
2446502.45044	0.6940	4.105	-0.133	-0.781
2446502.45239	0.6969	4.116	-0.141	-0.780
2446502.45397	0.6993	4.110	-0.130	-0.778
2446502.45610	0.7026	4.102	-0.140	-0.766

continued

2446502.45810	0.7056	4.104	-0.130	-0.774
2446502.46774	0.7203	4.102	-0.155	-0.753
2446502.46919	0.7225	4.104	-0.162	-0.742
2446502.47216	0.7271	4.095	-0.149	-0.748
2446502.47368	0.7294	4.094	-0.151	-0.743
2446502.47559	0.7323	4.096	-0.150	-0.755
2446502.47716	0.7347	4.096	-0.156	-0.752
2446502.48671	0.7492	4.095	-0.156	-0.744
2446502.48818	0.7515	4.086	-0.140	-0.752

1986 Mar 13/14

Differential Magnitude (v-c)

H.J.D.	Phase	V	B-V	U-B
2446503.25137	0.9144	4.333	-0.125	-0.770
2446503.25306	0.9170	4.359	-0.135	-0.790
2446503.25626	0.9218	4.350	-0.109	-0.772
2446503.25779	0.9242	4.372	-0.119	-0.781
2446503.25969	0.9271	4.378	-0.097	-0.785
2446503.26136	0.9296	4.410	-0.115	-0.795
2446503.27192	0.9457	4.492	-0.091	-0.773
2446503.27361	0.9483	4.520	-0.109	-0.788
2446503.27732	0.9539	4.543	-0.080	-0.775
2446503.27888	0.9563	4.588	-0.114	-0.793
2446503.28082	0.9593	4.587	-0.088	-0.759
2446503.28251	0.9618	4.635	-0.117	-0.781
2446503.28470	0.9652	4.640	-0.082	-0.782
2446503.28641	0.9678	4.685	-0.107	-0.795
2446503.30182	0.9912	4.905	-0.080	-0.774
2446503.30305	0.9931	4.937	-0.095	-0.776
2446503.30588	0.9974	4.947	-0.091	-0.763
2446503.30736	0.9997	4.956	-0.091	-0.775
2446503.31059	0.0046	4.950	-0.100	-0.765
2446503.31210	0.0069	4.924	-0.083	-0.765
2446503.31419	0.0101	4.932	-0.113	-0.786
2446503.31585	0.0126	4.885	-0.090	-0.770
2446503.32571	0.0276	4.769	-0.127	-0.805
2446503.32728	0.0300	4.723	-0.097	-0.787
2446503.33036	0.0347	4.694	-0.119	-0.788
2446503.33277	0.0384	4.635	-0.094	-0.786
2446503.33462	0.0412	4.637	-0.119	-0.787
2446503.33613	0.0435	4.588	-0.096	-0.772
2446503.33817	0.0466	4.589	-0.110	-0.793
2446503.33965	0.0489	4.556	-0.111	-0.773
2446503.35076	0.0658	4.453	-0.110	-0.812
2446503.35222	0.0680	4.423	-0.094	-0.802
2446503.35533	0.0728	4.406	-0.118	-0.806
2446503.35692	0.0752	4.383	-0.114	-0.785
2446503.35886	0.0782	4.379	-0.129	-0.786
2446503.36042	0.0805	4.349	-0.111	-0.781
2446503.36290	0.0843	4.346	-0.118	-0.798
2446503.36451	0.0868	4.325	-0.107	-0.782

continued

2446503.37513	0.1030	4.260	-0.112	-0.809
2446503.37678	0.1055	4.251	-0.112	-0.797
2446503.38046	0.1111	4.235	-0.113	-0.797
2446503.38201	0.1134	4.223	-0.114	-0.782
2446503.38384	0.1162	4.227	-0.129	-0.792
2446503.38541	0.1186	4.215	-0.120	-0.803
2446503.40045	0.1415	4.175	-0.125	-0.778
2446503.40193	0.1438	4.179	-0.126	-0.773
2446503.40518	0.1487	4.169	-0.128	-0.780
2446503.40661	0.1509	4.170	-0.132	-0.769
2446503.40897	0.1545	4.167	-0.130	-0.783
2446503.41049	0.1568	4.150	-0.120	-0.768
2446503.42050	0.1721	4.131	-0.117	-0.771
2446503.42199	0.1744	4.138	-0.123	-0.777
2446503.42490	0.1788	4.127	-0.113	-0.766
2446503.42640	0.1811	4.132	-0.118	-0.764
2446503.42825	0.1839	4.126	-0.125	-0.758
2446503.42978	0.1862	4.119	-0.117	-0.761
2446503.44000	0.2018	4.129	-0.140	-0.758
2446503.44149	0.2041	4.117	-0.140	-0.755
2446503.44443	0.2086	4.107	-0.136	-0.752
2446503.44593	0.2108	4.118	-0.137	-0.768
2446503.44788	0.2138	4.118	-0.134	-0.768
2446503.44936	0.2161	4.115	-0.141	-0.762
2446503.45854	0.2300	4.092	-0.136	-0.756
2446503.45993	0.2322	4.110	-0.150	-0.754
2446503.46258	0.2362	4.099	-0.139	-0.758
2446503.46395	0.2383	4.108	-0.154	-0.756
2446503.46598	0.2414	4.096	-0.134	-0.775
2446503.46734	0.2435	4.105	-0.159	-0.754
2446503.46926	0.2464	4.106	-0.159	-0.755
2446503.47071	0.2486	4.098	-0.142	-0.765
2446503.48004	0.2628	4.102	-0.143	-0.769
2446503.48166	0.2653	4.098	-0.142	-0.766

1986 Mar 19/20

Differential Magnitude (v-c)

H.J.D.	Phase	V	B-V	U-B
2446509.34525	0.2000	4.123	-0.126	-0.786
2446509.34690	0.2025	4.128	-0.139	-0.773
2446509.35003	0.2072	4.114	-0.126	-0.775
2446509.35153	0.2095	4.117	-0.141	-0.766
2446509.35333	0.2123	4.107	-0.134	-0.767
2446509.35479	0.2145	4.112	-0.137	-0.763
2446509.35762	0.2188	4.112	-0.137	-0.770
2446509.35914	0.2211	4.115	-0.136	-0.781
2446509.36878	0.2358	4.089	-0.113	-0.781
2446509.37047	0.2384	4.089	-0.126	-0.769
2446509.37375	0.2434	4.086	-0.120	-0.769
2446509.37532	0.2458	4.091	-0.136	-0.763
2446509.37709	0.2485	4.092	-0.132	-0.769

continued

2446509.37861	0.2508	4.090	-0.125	-0.770
2446509.38071	0.2540	4.085	-0.125	-0.769
2446509.38217	0.2562	4.084	-0.128	-0.760
2446509.38543	0.2612	4.087	-0.130	-0.768
2446509.38689	0.2634	4.094	-0.142	-0.764
2446509.39847	0.2811	4.091	-0.149	-0.745
2446509.39992	0.2833	4.095	-0.154	-0.739
2446509.40484	0.2908	4.098	-0.134	-0.757
2446509.40630	0.2930	4.108	-0.157	-0.746
2446509.40824	0.2959	4.103	-0.141	-0.752
2446509.40987	0.2984	4.116	-0.154	-0.754

1986 Mar 20/21

Differential Magnitude (v-c)

H.J.D.	Phase	V	B-V	U-B
2446510.35419	0.7373	4.101	-0.141	-0.766
2446510.35566	0.7396	4.090	-0.127	-0.759
2446510.35882	0.7444	4.076	-0.111	-0.769
2446510.36029	0.7466	4.083	-0.129	-0.766
2446510.36209	0.7494	4.083	-0.130	-0.767
2446510.36358	0.7516	4.082	-0.141	-0.746
2446510.36548	0.7545	4.078	-0.127	-0.764
2446510.36699	0.7568	4.086	-0.129	-0.754
2446510.37011	0.7616	4.090	-0.139	-0.762
2446510.37155	0.7638	4.085	-0.141	-0.749
2446510.37333	0.7665	4.089	-0.141	-0.756
2446510.37482	0.7688	4.096	-0.152	-0.752
2446510.38697	0.7873	4.115	-0.151	-0.748
2446510.38843	0.7895	4.118	-0.148	-0.749
2446510.39134	0.7939	4.120	-0.143	-0.742
2446510.39282	0.7962	4.135	-0.162	-0.742
2446510.39473	0.7991	4.131	-0.147	-0.754
2446510.39655	0.8019	4.128	-0.147	-0.745
2446510.39837	0.8047	4.137	-0.156	-0.758
2446510.39981	0.8068	4.137	-0.159	-0.758
2446510.40252	0.8110	4.125	-0.129	-0.742
2446510.40394	0.8131	4.132	-0.141	-0.748
2446510.41254	0.8263	4.129	-0.136	-0.759
2446510.41391	0.8283	4.151	-0.148	-0.764
2446510.41686	0.8328	4.137	-0.142	-0.746
2446510.41837	0.8351	4.147	-0.143	-0.752
2446510.42029	0.8381	4.154	-0.150	-0.749
2446510.42177	0.8403	4.142	-0.132	-0.759
2446510.43204	0.8560	4.179	-0.152	-0.764
2446510.43347	0.8581	4.174	-0.142	-0.754
2446510.43627	0.8624	4.187	-0.140	-0.738
2446510.43780	0.8647	4.192	-0.129	-0.754
2446510.44016	0.8683	4.203	-0.140	-0.755
2446510.44207	0.8712	4.206	-0.152	-0.745
2446510.45085	0.8846	4.238	-0.161	-0.728
2446510.45229	0.8868	4.252	-0.167	-0.743

continued

2446510.45509	0.8911	4.252	-0.147	-0.741
2446510.45652	0.8933	4.278	-0.165	-0.739
2446510.45837	0.8961	4.274	-0.140	-0.748
2446510.45993	0.8985	4.270	-0.139	-0.739
2446510.46912	0.9125	4.330	-0.141	-0.732
2446510.47063	0.9148	4.340	-0.150	-0.725
2446510.47315	0.9186	4.358	-0.155	-0.718
2446510.47452	0.9207	4.375	-0.154	-0.726
2446510.47616	0.9232	4.385	-0.151	-0.736
2446510.47753	0.9253	4.383	-0.149	-0.723

1986 Mar 31/Apr 01

Differential Magnitude (v-c)

H.J.D.	Phase	V	B-V	U-B
2446521.24199	0.3277	4.145	-0.125	-0.776
2446521.24532	0.3328	4.134	-0.109	-0.792
2446521.24693	0.3352	4.131	-0.097	-0.801
2446521.25027	0.3403	4.134	-0.105	-0.787
2446521.25193	0.3428	4.143	-0.112	-0.801
2446521.25409	0.3461	4.142	-0.094	-0.802
2446521.25576	0.3487	4.158	-0.113	-0.803
2446521.25772	0.3516	4.145	-0.090	-0.815
2446521.25926	0.3540	4.170	-0.119	-0.805
2446521.26949	0.3696	4.182	-0.089	-0.815
2446521.27100	0.3719	4.188	-0.081	-0.827
2446521.27408	0.3766	4.197	-0.088	-0.806
2446521.27559	0.3789	4.203	-0.091	-0.814
2446521.27744	0.3817	4.204	-0.078	-0.818
2446521.27896	0.3840	4.218	-0.084	-0.824
2446521.28099	0.3871	4.224	-0.074	-0.824
2446521.28256	0.3895	4.238	-0.088	-0.831
2446521.28464	0.3927	4.240	-0.075	-0.809
2446521.28625	0.3951	4.253	-0.088	-0.809
2446521.28827	0.3982	4.251	-0.074	-0.812
2446521.28970	0.4004	4.269	-0.088	-0.813
2446521.30566	0.4247	4.361	-0.076	-0.817
2446521.30711	0.4269	4.389	-0.081	-0.821
2446521.31061	0.4322	4.403	-0.075	-0.814
2446521.31213	0.4345	4.430	-0.091	-0.821
2446521.31419	0.4377	4.425	-0.063	-0.802
2446521.31588	0.4403	4.464	-0.097	-0.805
2446521.31785	0.4433	4.482	-0.083	-0.807
2446521.31945	0.4457	4.508	-0.090	-0.812
2446521.32145	0.4488	4.500	-0.066	-0.807
2446521.32307	0.4512	4.539	-0.096	-0.814
2446521.32515	0.4544	4.543	-0.065	-0.814
2446521.32670	0.4568	4.579	-0.097	-0.811
2446521.34034	0.4775	4.748	-0.082	-0.773
2446521.34200	0.4801	4.791	-0.100	-0.799
2446521.34534	0.4852	4.826	-0.096	-0.768
2446521.34675	0.4873	4.857	-0.120	-0.762

continued

2446521.35360	0.4977	4.919	-0.126	-0.754
2446521.35498	0.4999	4.921	-0.125	-0.761
2446521.35761	0.5039	4.916	-0.137	-0.756
2446521.35933	0.5065	4.895	-0.128	-0.758
2446521.36121	0.5093	4.877	-0.123	-0.778
2446521.36262	0.5115	4.844	-0.114	-0.748
2446521.36524	0.5155	4.820	-0.136	-0.761
2446521.36673	0.5178	4.789	-0.132	-0.736
2446521.36859	0.5206	4.777	-0.137	-0.757
2446521.37018	0.5230	4.739	-0.127	-0.739
2446521.37295	0.5272	4.714	-0.136	-0.755
2446521.37446	0.5295	4.689	-0.135	-0.731
2446521.37624	0.5322	4.672	-0.141	-0.753
2446521.37765	0.5344	4.642	-0.123	-0.747
2446521.38725	0.5490	4.523	-0.122	-0.760
2446521.38890	0.5515	4.500	-0.120	-0.749
2446521.39195	0.5562	4.470	-0.128	-0.751
2446521.39360	0.5587	4.462	-0.129	-0.755

Table 4 : Data for RZ Pyx, SAO 176697 and SAO 176536.

	RZ Pyx	SAO 176697	SAO 176536
HD no.	HD 75920	HD 76483	HD 75547
CPD no.	-27° 3452	-27° 3497	-27° 3432
R.A. (1950)	8 ^h 49 ^m 56 ^s	8 ^h 53 ^m 23 ^s	8 ^h 47 ^m 35 ^s
Dec. (1950)	-27° 17' 42"	-27° 29' 19"	-28° 04' 10"
Sp. type	B7	A3IV	B9.5IV

Johnson Photometry

V	8 ^m .98 (0 ^p .25) 9 ^m .84 (0 ^p .00) 9 ^m .80 (0 ^p .50)	4 ^m .88 ± 0 ^m .01	7 ^m .46 ± 0 ^m .01
(B-V)	-0 ^m .04 *	0 ^m .11 ± 0 ^m .01	0 ^m .04 ± 0 ^m .01
(U-B)	-0 ^m .61 *	0 ^m .14 ± 0 ^m .01	-0 ^m .10 ± 0 ^m .01
(B-V) _o	-0 ^m .19 *	0 ^m .02	-0 ^m .00
(U-B) _o	-0 ^m .72 *	0 ^m .08	-0 ^m .13
E(B-V)	0 ^m .15	0 ^m .09	0 ^m .04
E(U-B)	0 ^m .11	0 ^m .06	0 ^m .03

* denotes the mean quadrature colour.

Strömgren Photometry

V	8 ^m .98 (0 ^p .75)	4 ^m .878 ± 0 ^m .003	7 ^m .451 ± 0 ^m .004
(b-y)	-0 ^m .010 (0 ^p .75)	0 ^m .053 ± 0 ^m .003	0 ^m .007 ± 0 ^m .002
m ₁	0 ^m .098 (0 ^p .75)	0 ^m .210 ± 0 ^m .003	0 ^m .156 ± 0 ^m .003
c ₁	0 ^m .371 (0 ^p .75)	1 ^m .096 ± 0 ^m .005	1 ^m .035 ± 0 ^m .006
(b-y) _o	-0 ^m .080	-0 ^m .010	-0 ^m .016
m _o	0 ^m .120	0 ^m .230	0 ^m .163
c _o	0 ^m .357	1 ^m .083	1 ^m .030
E(b-y)	0 ^m .070	0 ^m .053	0 ^m .023

Table 5 : Photoelectric times of minima.

H.J.D. -2400000	Error (days)	Epoch (cycles)	Source reference
37006.3757	± 0.0005	-14500.0	Kinman, 1960. *
37028.3618	± 0.0004	-14466.5	Kinman, 1960. *
38431.4730	± 0.0009	-12328.5	Breger, 1968. *
44245.7195		-3469.0	Wolf and Kern, 1983.
46141.37207	± 0.00008	-580.5	This paper.
46142.35512	± 0.00012	-579.0	This paper.
46144.32599	± 0.00008	-576.0	This paper.
46493.46457	± 0.00012	-44.0	This paper.
46502.32279	± 0.00022	-30.5	This paper.
46503.30816	± 0.00010	-29.0	This paper.
46521.35498	± 0.00011	-1.5	This paper.
46522.33949	± 0.00006	0.0	This paper.
46523.32413	± 0.00008	1.5	This paper.

* denotes the original data were re-analysed in this study.

Table 6 : Light-curve solutions using Rucinski's method.

Adopted primary temperature 17000K

Colour	U	B	V
α_1 & α_2	1.00	1.00	1.00
β_1 & β_2	0.25	0.25	0.25
i (degrees)	89.5 ± 8	88.4 ± 5	88.6 ± 5
f	1.110 ± 11	0.922 ± 7	1.020 ± 7
r_1 (volume)	0.333 ± 6	0.404 ± 2	0.385 ± 5
r_2 (volume)	0.299 ± 6	0.369 ± 2	0.350 ± 5
x	-0.028 ± 5	-0.033 ± 2	-0.029 ± 5
$\Sigma(o-c)^2 \times 10^3$	3.0	1.7	1.3
Std. devn. (mmag.)	8.1	6.6	5.6

Table 7 : Light-curve solutions using LIGHT.

Adopted primary temperature 17000K and q fixed at 0.82.

Colour	U	B	V
i (degrees)	88.11 ±1	87.13 ±7	87.06 ±21
T ₂ K (polar)	16760 ±40	16720 ±50	16810 ±50
r ₁ (polar)	0.365 ±1	0.370 ±1	0.361 ±2
r ₁ (mean)	0.386 ±1	0.393 ±1	0.381 ±2
r ₂ (polar)	0.339 ±1	0.340 ±1	0.340 ±1
r ₂ (mean)	0.360 ±1	0.361 ±1	0.361 ±1
χ^2 (mmag.) ²	395.4	493.9	306.0
L ₂ /L ₁	0.846	0.823	0.885
r.m.s. error (mmag.)	15.5	16.8	12.7

Table 8 : Light-curve solutions using LIGHT.

Adopted primary temperature 17000K and solving for q.

Colour	U	B	V
i (degrees)	88.43 ±1	87.13 ±31	87.14 ±19
q	0.803 ±55	0.820 ±2	0.853 ±2
T ₂ K (polar)	16760 ±200	16730 ±80	16650 ±40
r ₁ (polar)	0.365 ±1	0.370 ±3	0.362 ±2
r ₁ (mean)	0.386 ±1	0.393 ±3	0.383 ±2
r ₂ (polar)	0.336 ±1	0.340 ±3	0.339 ±1
r ₂ (mean)	0.357 ±1	0.361 ±3	0.360 ±1
χ^2 (mmag.) ²	387.2	552.5	387.2
L ₂ /L ₁	0.831	0.824	0.851
r.m.s. error (mmag.)	15.3	16.8	12.7

Table 9 : Adopted light-curve solution using LIGHT.

T_1 K (polar)	17000
q (spectroscopic)	0.82
Escat ₁ (adopted)	0.20
Escat ₂ (adopted)	0.20
β_1 (adopted)	0.25
β_2 (adopted)	0.25
i (degrees)	87.4 ±6
T_2 K (polar)	16760 ±50
r_1 (polar)	0.365 ±5
r_1 (mean)	0.387 ±6
r_2 (polar)	0.340 ±1
r_2 (mean)	0.361 ±1

Table 10 : Astrophysical data for RZ Pyx.

Uncorrected data

Absolute dimensions:	Primary	Secondary
M/M	5.27 ± 0.16	4.33 ± 0.13
R/R $_{\odot}$	2.61 ± 0.05	2.44 ± 0.03
log $^{\circ}g$ (cgs)	4.33 ± 0.02	4.30 ± 0.02
Photometric data:		
T $_{\text{eff}}$ (K)	17000 ± 1000	16800 ± 1000
M $_{\text{bol}}$	$-2.^{\text{m}}08 \pm 0.^{\text{m}}26$	$-1.^{\text{m}}88 \pm 0.^{\text{m}}26$
log (L/L $_{\odot}$)	2.71 ± 0.10	2.63 ± 0.10
B.C.	$-1.^{\text{m}}66$	$-1.^{\text{m}}63$
M $_{\text{V}}$	$-0.^{\text{m}}42 \pm 0.^{\text{m}}26$	$-0.^{\text{m}}25 \pm 0.^{\text{m}}26$
E $_{\text{(B-V)}}$	$0.^{\text{m}}10$	
Distance (pc)	890 ± 180	

Corrected data

Absolute dimensions:	Primary	Secondary
M/M	5.76 ± 0.17	4.73 ± 0.14
R/R $_{\odot}$	2.69 ± 0.05	2.51 ± 0.03
log $^{\circ}g$ (cgs)	4.34 ± 0.02	4.31 ± 0.02
Photometric data:		
T $_{\text{eff}}$ (K)	17000 ± 1000	16800 ± 1000
M $_{\text{bol}}$	$-2.^{\text{m}}14 \pm 0.^{\text{m}}26$	$-1.^{\text{m}}94 \pm 0.^{\text{m}}26$
log (L/L $_{\odot}$)	2.73 ± 0.10	2.65 ± 0.10
B.C.	$-1.^{\text{m}}66$	$-1.^{\text{m}}63$
M $_{\text{V}}$	$-0.^{\text{m}}48 \pm 0.^{\text{m}}26$	$-0.^{\text{m}}31 \pm 0.^{\text{m}}26$
E $_{\text{(B-V)}}$	$0.^{\text{m}}10$	
Distance (pc)	920 ± 190	

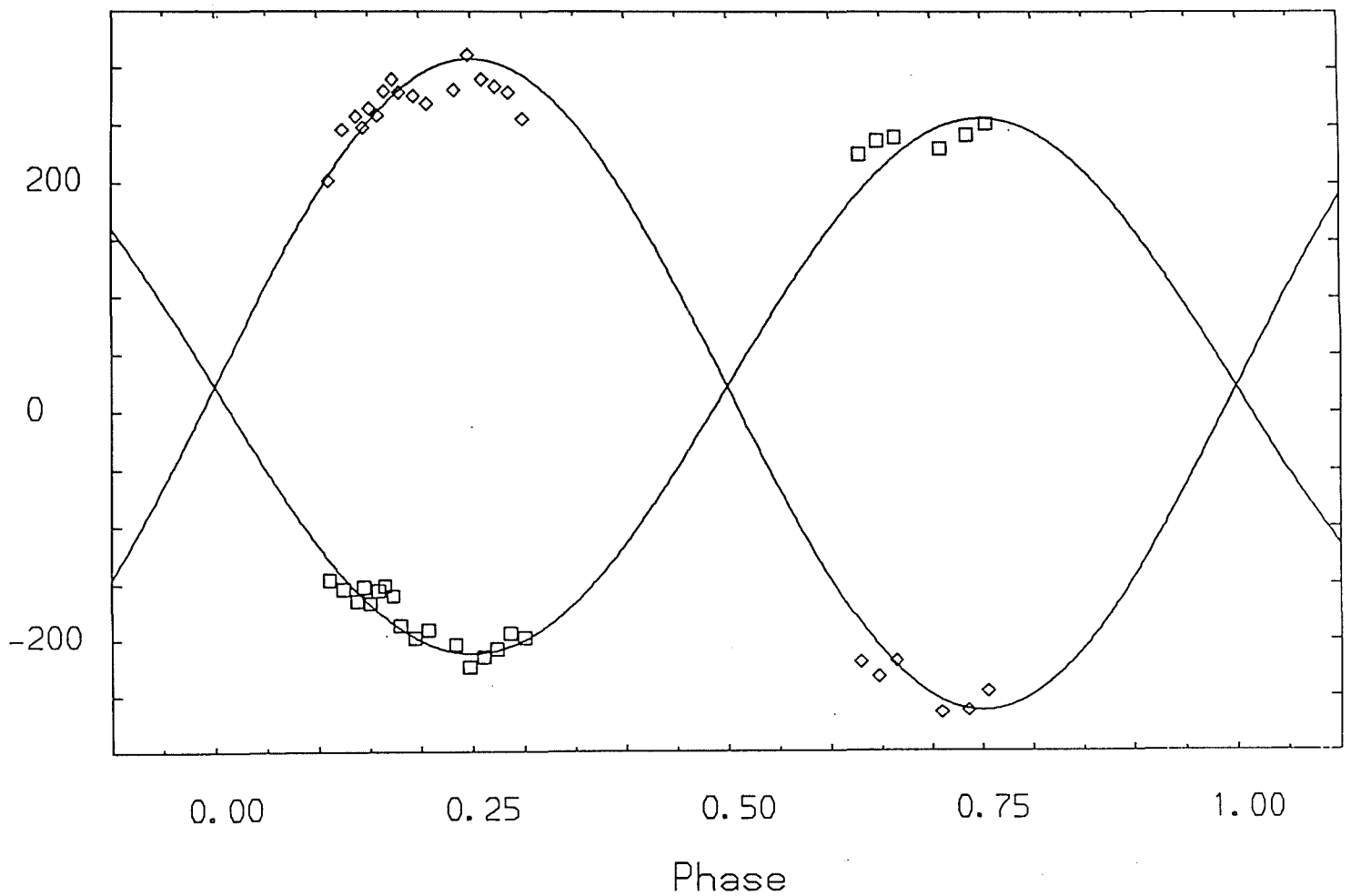


Figure 1.

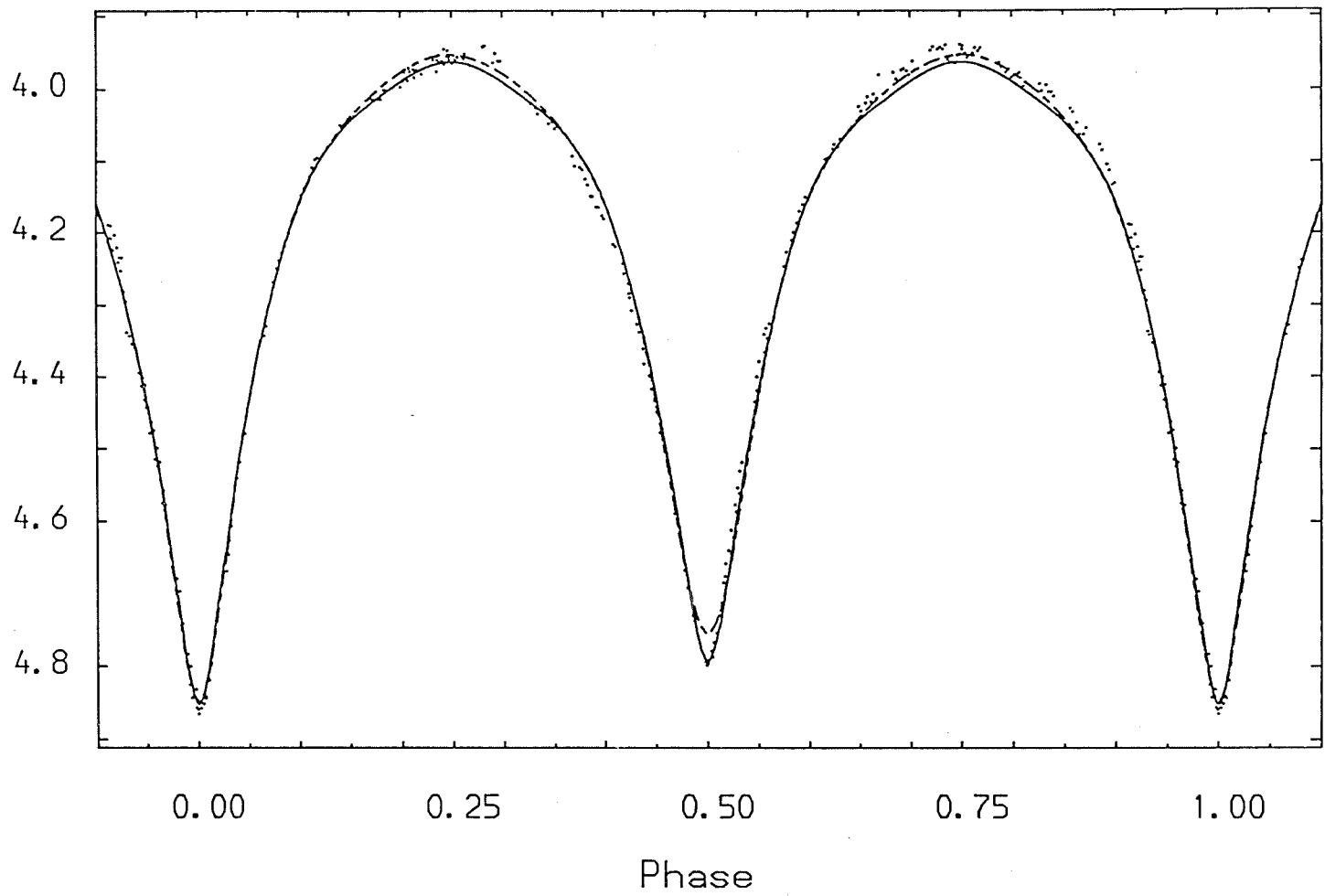


Figure 2.

Figure 3.

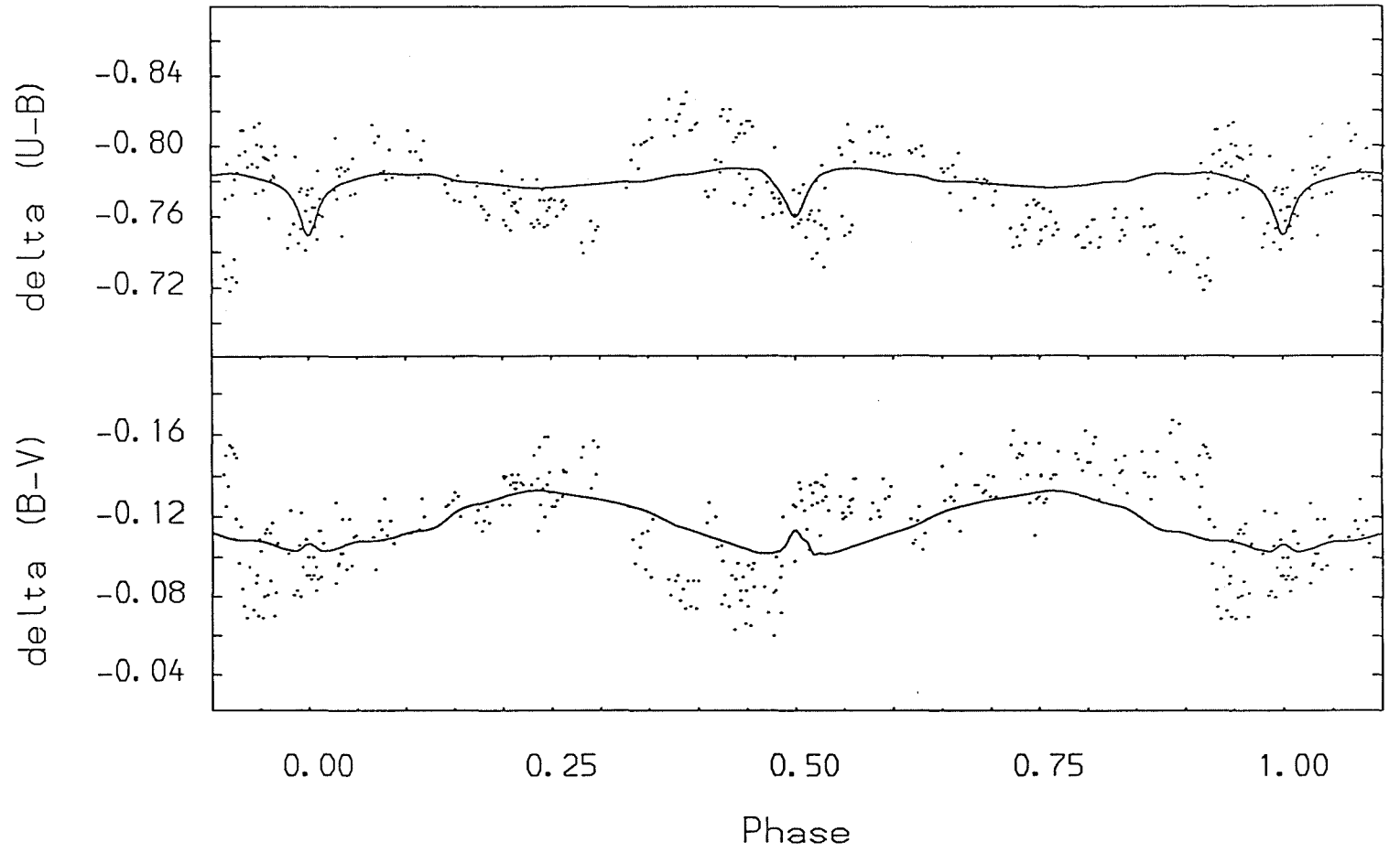
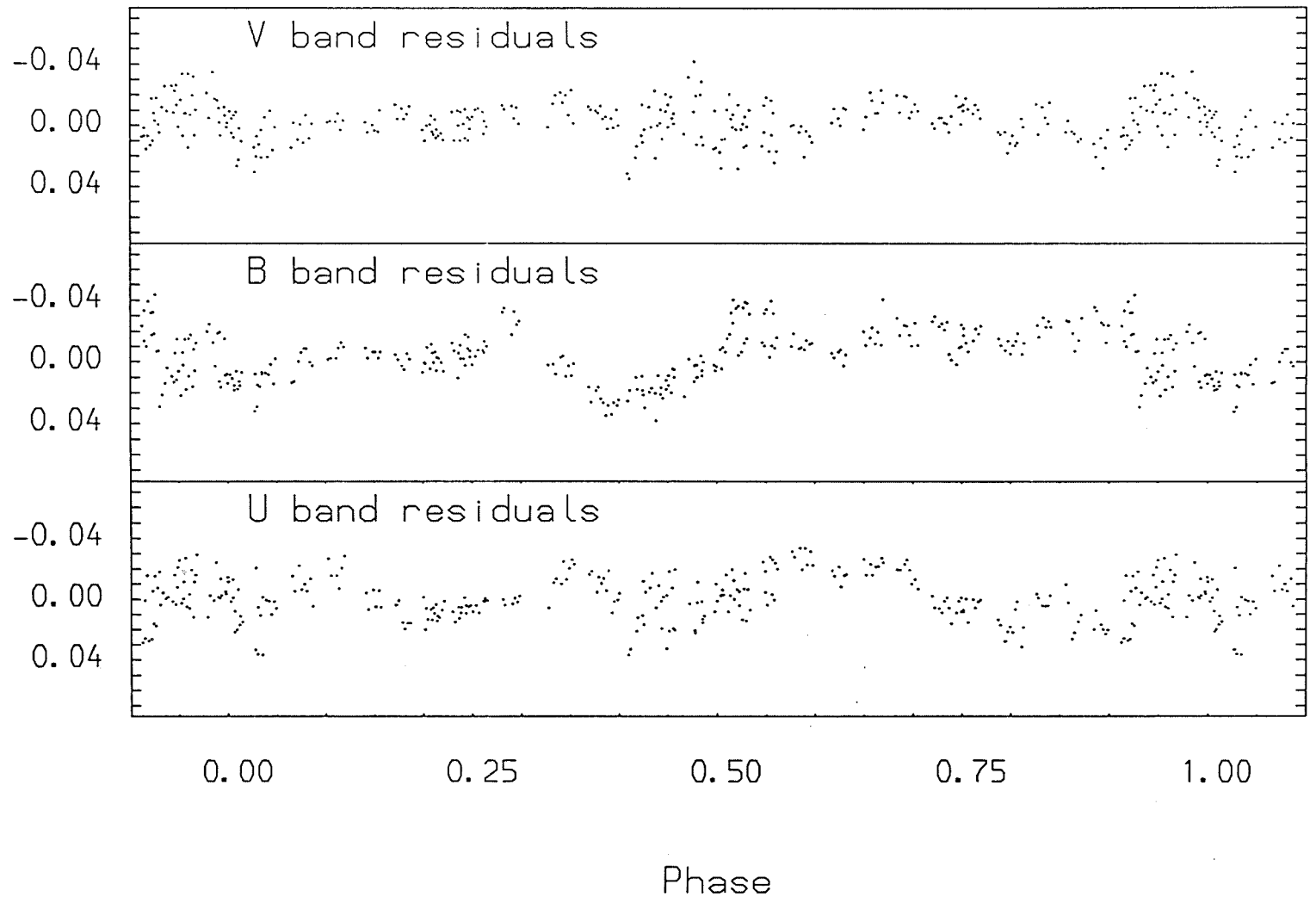


Figure 4.



CHAPTER 10

Conclusion

1) Resume of analyses

1.1) Detached systems

Two detached systems have been observed and analysed for this study. Both systems contain O- and very early B-type stars and have periods at the upper limit of the range considered here. AH Cephei contains two similar components whereas V1182 Aql is made up of two stars of very different masses.

Since the paper on AH Cephei was presented, Sybesma (1986) published evolutionary sequences for massive binary systems including mass loss and convective overshooting. He studied case A mass transfer for systems with an initial primary component mass of $20M_{\odot}$ and initial mass ratios of 0.8 and 0.9. Initial periods of between 1.4 and 10 days were adopted and calculations of the simultaneous evolution of both components were carried out. These models have been discussed in Chapter 1 and they provide an excellent opportunity to compare the observed quantities for AH Cephei with those of the model with the most appropriate period. The uncertainties in the determination of the primary temperature make the comparison more difficult, but cannot refute the high probability that this system will evolve via case A mass transfer.

On the basis of traditional single star models, the suggestion was made in Chapter 4 that the presence of a substantial stellar wind from one or both of the components of AH Cephei would prevent case A evolution. The models produced by Sybesma have shown that the period would have to increase to such an extent that prevention of case A evolution is not tenable. Assuming that the age estimate of 6×10^6 yrs for AH Cephei is correct, it now seems likely that the system will pass through a phase of rapid mass transfer within $\sim 2 \times 10^6$ yrs transferring around 30% of the primary component mass to the secondary component. This would be followed by a phase of slow mass transfer lasting approximately 3×10^6 yrs. At this point, AH Cephei may form a very short-lived contact binary. This unstable contact phase may be repeated several times during the main-sequence lifetime of the primary component.

A different explanation for the period changes in AH Cephei has been proposed by Mayer and Wolf (1986). Their analysis of the published times of minima suggested that the system may contain a third or even a fourth body each of approximately $7-8M_{\odot}$. Mayer and Wolf noted that this conclusion was based on a small number of well-determined times of minima. However, the times of minima obtained for the study presented here were not available for their analysis. No photometric or spectroscopic evidence for a third or fourth body has been found in the course of the study of AH Cephei.

Doom (1984) established a limit on the initial mass of the primary component of a binary system beyond which either case A mass transfer occurs or the two components evolve separately. The primary component of V1182 Aquilae has a mass of $38M_{\odot}$ which lies well beyond this limit, however both components are reasonably close to their respective Roche lobes. The mass ratio of 0.36 is more

extreme than that of AH Cephei for which models are available. It is difficult to speculate upon the post case A evolution of this object but on the basis of Sybesma's models, it seems unlikely that this system will form a short-lived contact configuration and would probably pass through case B mass transfer at the end of the hydrogen-core burning stage of the primary component.

1.2) Semi-detached systems

Three semi-detached systems have been observed; TT Aurigae, SX Aurigae and AI Crucis. All these systems have similar periods and component masses, although SX Aurigae is probably somewhat more evolved than either TT Aurigae or AI Crucis. These systems join the existing group of semi-detached systems with properties significantly different from classical Algol systems using traditional modelling. Other members of this group are V Puppis, u Herculis, V356 Sagittarii, IU Aurigae and Z Vulpeculae. An upper limit to the age of 25×10^6 yrs for AI Crucis can be established because of its membership of the open cluster NGC 4103. It is very likely that all these systems have passed through the rapid phase of case A mass transfer and mass ratio reversal.

All the systems in this group have periods of less than 2.5 days except V356 Sagittarii whose primary component is clearly underluminous for its mass (1.5^m less than a $12M_{\odot}$ star on the zero-age main sequence) and whose secondary component has evolved beyond the terminal-age main sequence. On the mass-luminosity diagram, all the secondary components are clearly overluminous compared with the zero- and terminal-age main sequences of Bressan et al. (1981) and Bertelli et al. (1986). Likewise, the

mass-radius diagram shows the secondary components to be larger than expected.

1.3) Contact systems

The contact systems V701 Sco and RZ Pyx have been observed and analysed during this study. These systems are both young; V701 Sco is estimated to be $\sim 4 \times 10^6$ yrs old whilst RZ Pyx is probably less than 2×10^6 yrs old. V701 Sco is a member of the open cluster NGC 6383 whereas RZ Pyx cannot be associated with any region of recent star formation. Both systems may have evolved into contact via case A evolution.

It has been suggested that V701 Sco exhibits a large mass transfer rate indicative of the rapid phase of case A evolution. The data presented in this study does not support this conclusion. The possible evolutionary scenarios have been discussed in Chapter 8 but it seems likely that the original system was close to a contact configuration before case A mass transfer occurred. The possibility exists that the system could be in a temporary equilibrium state. However, the depth of contact is probably too large for the system to be in one of the unstable contact configurations described by Sybesma (1986).

It is surprising that a very young system such as RZ Pyx cannot be associated with a region of recent star formation. The motion of RZ Pyx cannot be established with any accuracy because of the poorly-determined proper motions of the system. The marginal contact configuration suggests that it has evolved into contact via case A evolution in less than 2×10^6 yrs or that it arrived on the zero-age main sequence as a contact system.

2) Comparison with evolutionary models

Popper (1980) compiled tables of well-determined physical parameters for a number of stars including visual and eclipsing binaries. For systems of spectral type B5 and earlier he tabulated 13 detached systems, 4 semi-detached systems and 3 contact systems. In this sample, ten individual components define the 0 star main sequence of which six are members of contact binaries. The majority of the stars are around spectral type B3-B4. The conditions for systems being included in these tabulations have been considered to be too stringent by some, but theoretical modelling of the evolution of stars can only be defined by those systems which have accurately-known physical parameters.

The logarithmic masses, radii, temperatures and luminosities for the components of 34 binary systems and their associated errors are presented in Table 1. This Table has been compiled from published data for binaries with a primary component of spectral type B5 or earlier and which are of a similar standard to those compiled by Popper including the analyses of the systems in this study. These data have been plotted in a HR, mass-luminosity (ML) and mass-radius (MR) diagram in Figures 1-3 respectively. The components of each binary system are joined by a solid line. The size of the cross represents the error in each quantity in all three diagrams.

The combined models of Stothers (1972) and Hejlesen (1980) have been plotted in Figures 4-6 to provide zero-age and terminal-age main sequences for comparison with the individual components of the binary systems. Two sets of sequences have been plotted for compositions of ($X = 0.70, Z = 0.02$) and ($X = 0.70, Z = 0.04$). It

can be seen that an intermediate value of ($Z = 0.03$) would give better agreement with the lower envelope of the observed data.

A third sequence by Bressan et al. (1981) has been plotted which has a composition of ($X = 0.70, Z = 0.02$) and which includes the effect of mass loss calculated via the relationship given by Castor et al. (1975). All of the models use the classical mixing-length theory for convection. It is clear from the HR, ML and MR diagrams in Figures 4-6 respectively that these models do not provide a sufficiently-wide main sequence for the observed systems.

The inclusion of convective overshooting in the modelling of stars can be seen clearly in the HR, ML and MR diagrams in Figures 7-9 respectively. The zero-age and terminal-age main sequences using a combination of sequences produced by Bressan et al. (1981) and Bertelli et al. (1986) for a composition of ($X = 0.70, Z = 0.02$) have been plotted. The main-sequence band is twice as wide as that found using classical convection. For comparison, the terminal-age main sequence of the combined Stothers (1972) and Hejlesen (1980) models for the same composition has been plotted.

The widening of the main sequence becomes very large at high luminosities extending over a very large range in temperature. This feature can be replaced by a narrowing of the main-sequence band if mass loss is introduced. The high mass models ($20-100M_{\odot}$) of Bressan et al. (1981) including mass loss calculated from the relationship by Castor et al. have also been plotted to show this effect. Nearly all the components of the binary systems in Table 1 lie within the bounds of the main-sequence band which includes convective overshooting and mass loss in Figure 7. However, no stars have been observed which lie within the low temperature

extension of the main sequence at high luminosities. The components of V356 Sagittarii still lie outside the main sequence bands of Figures 7-9. The inclusion of mass loss in models of lower mass should make the main-sequence band in Figures 8 and 9 wide enough to accommodate practically all the components.

The variation in the amount of convective overshooting is illustrated in Figures 10-12 for the HR, ML and MR diagrams. The zero-age and terminal-age main sequences of Doom (1982a,b) for a composition of ($X = 0.70$, $Z = 0.03$) have been plotted as well as those of Bressan et al. (1981) and Bertelli et al. (1986). The mass loss sequence of Bressan et al. has been included for comparison. Some components lie within the bulge in the main-sequence band in Figure 11 but this is not the case for Figure 10.

3) Summary

It is clear from this study that case A mass transfer will play and has played an important role in the evolution of five out of the seven systems. It is debatable whether or not the contact systems have passed through a mass transfer phase, particularly RZ Pyx. The parameters of 14 stars have been found, including four O stars in detached systems. Therefore the number of stars with well-determined masses of greater than $30M_{\odot}$ has been increased by 25%! The evolutionary history of RZ Pyx is of particular interest, especially if this binary was in a marginal contact configuration on its arrival on the main sequence.

Attempts have been made to look for intrinsic variability in these systems but no periodic variation has been found in any of the systems. If such a phenomenon exists in one of the components of the binaries in the sample then it must have an amplitude of less than 0.01^m .

The comparison of the parameters of 67 stars with theoretical zero-age and terminal-age main sequences shows that traditional modelling of semi-convection without mass loss is not adequate. Convective overshooting and mass loss play an important part of the evolution of massive close binary systems of short period. More models including these properties are required to make a more complete comparison with the observed data. More theoretical modelling of the type made by Sybesma (1986) is required to compare the observed systems with primary component masses of the order of $10M_{\odot}$ and mass ratios of the order of 0.5-0.6.

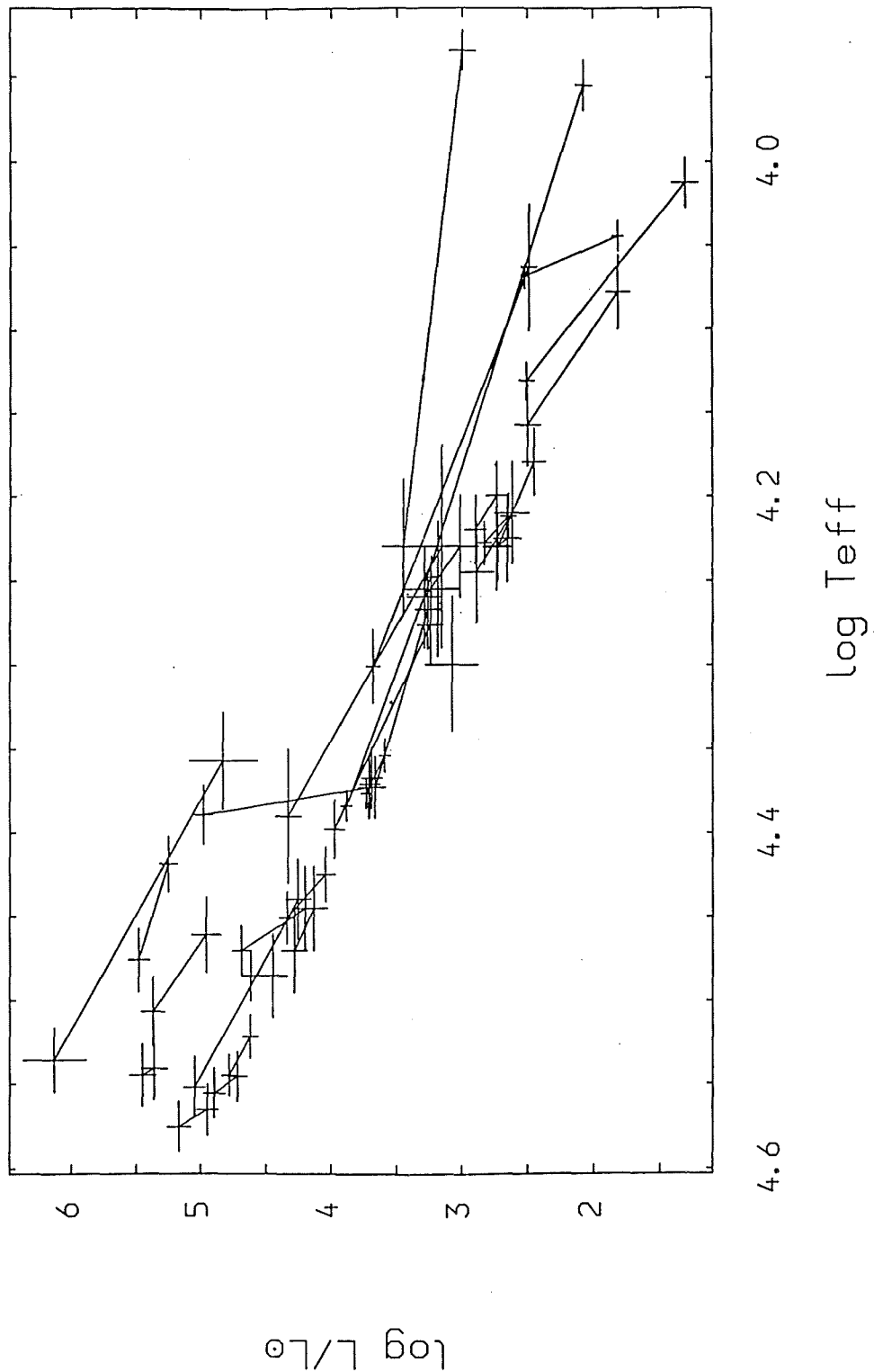


Figure 1. The HR diagram for the components of 34 binary systems for which accurately-determined parameters have been obtained. Each component is represented by a cross whose size is indicative of the errors in the temperature and luminosity of the star. The two components of each system are joined by a solid line.

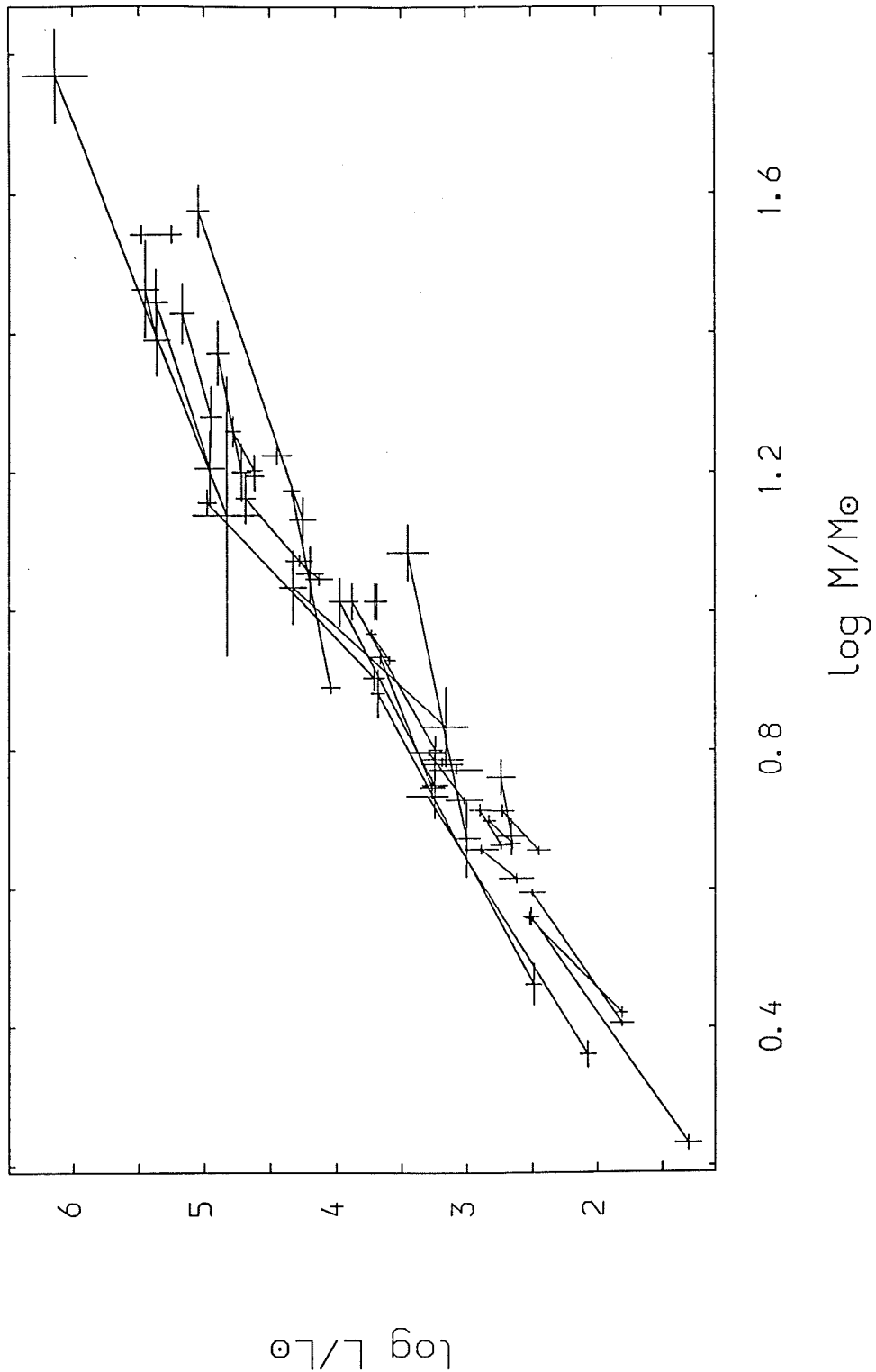


Figure 2. The Mass-Luminosity diagram for those objects plotted in Figure 1. The size of the cross for each component is indicative of the errors in the mass and luminosity for that star. The two components of each system are joined by a solid line.

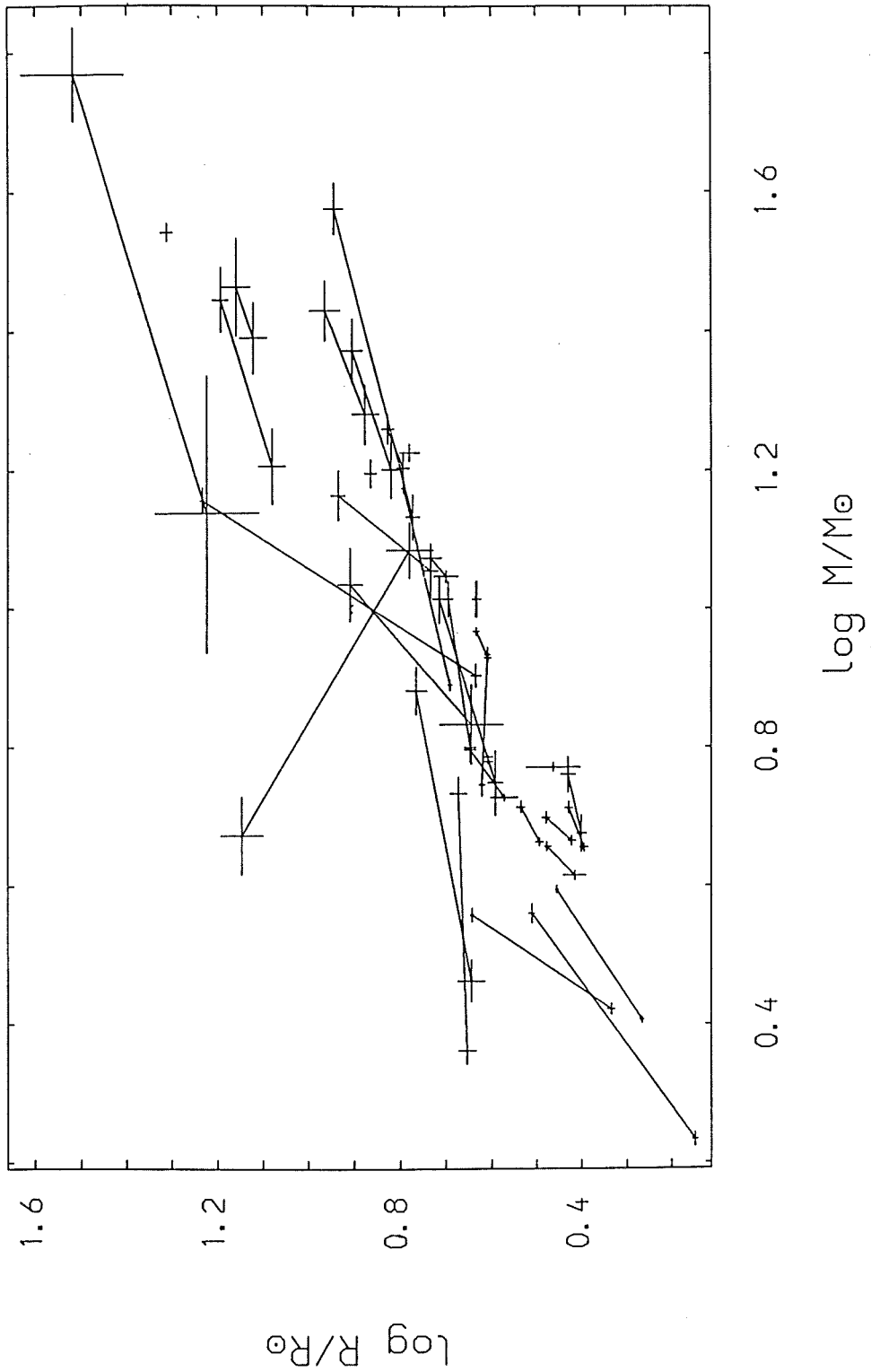


Figure 3. The Mass-Radius diagram for those objects plotted in Figure 1. The size of the cross for each component is indicative of the errors in the mass and radius for that star. The two components of each system are joined by a solid line.

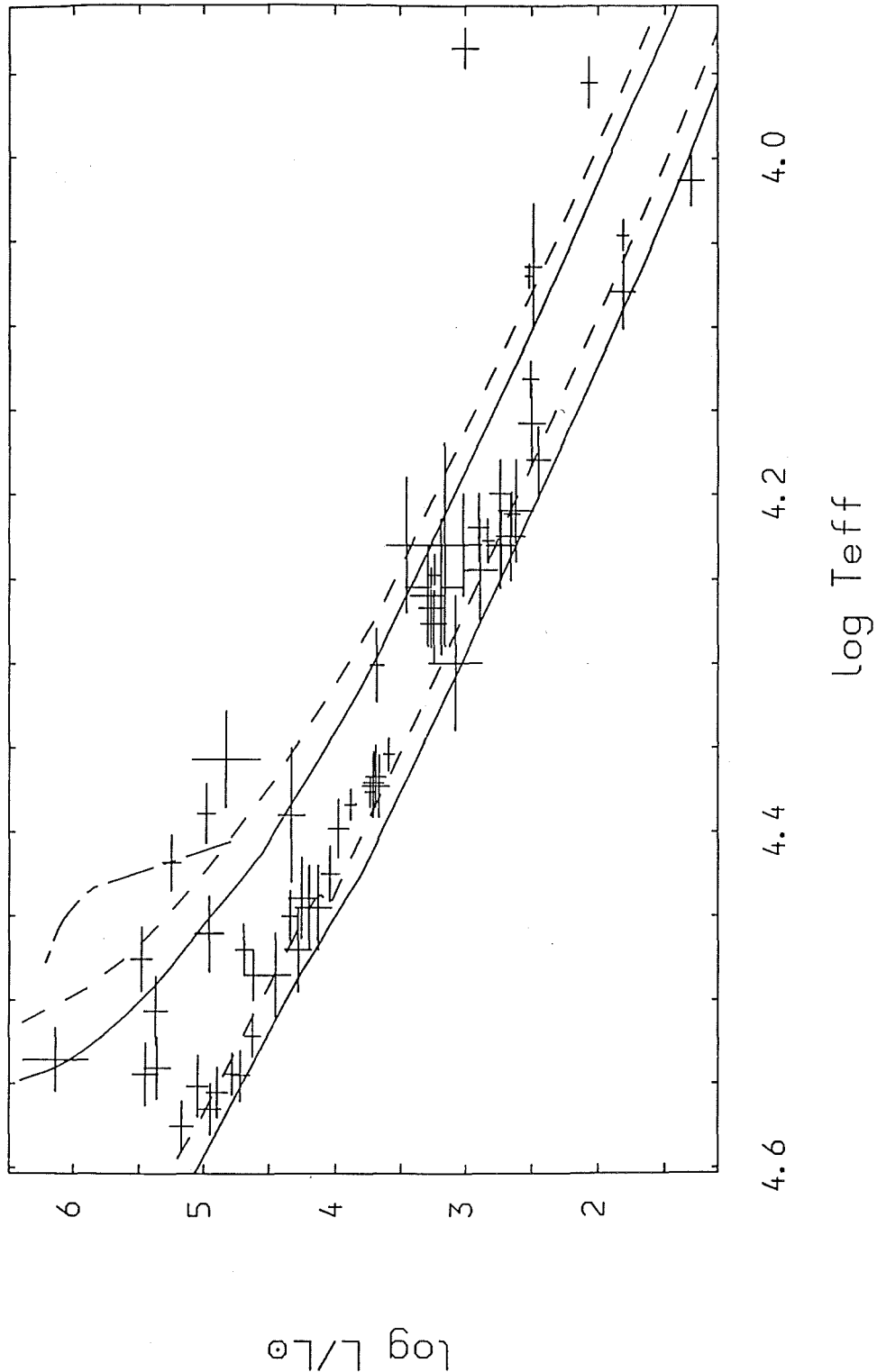


Figure 4. The HR diagram for those objects plotted in Figure 1. The lower and upper solid lines represent the zero-age and terminal age main sequences for the combined models of Stothers (1972) and Hejlesen (1980) for a composition with ($X = 0.70$, $Z = 0.02$). Similarly the dashed lines represent the same combination for a composition ($X = 0.70$, $Z = 0.04$). The dot-dashed line represents the model of Bressan et al. (1981) with a composition ($X = 0.70$, $Z = 0.02$) including mass loss.

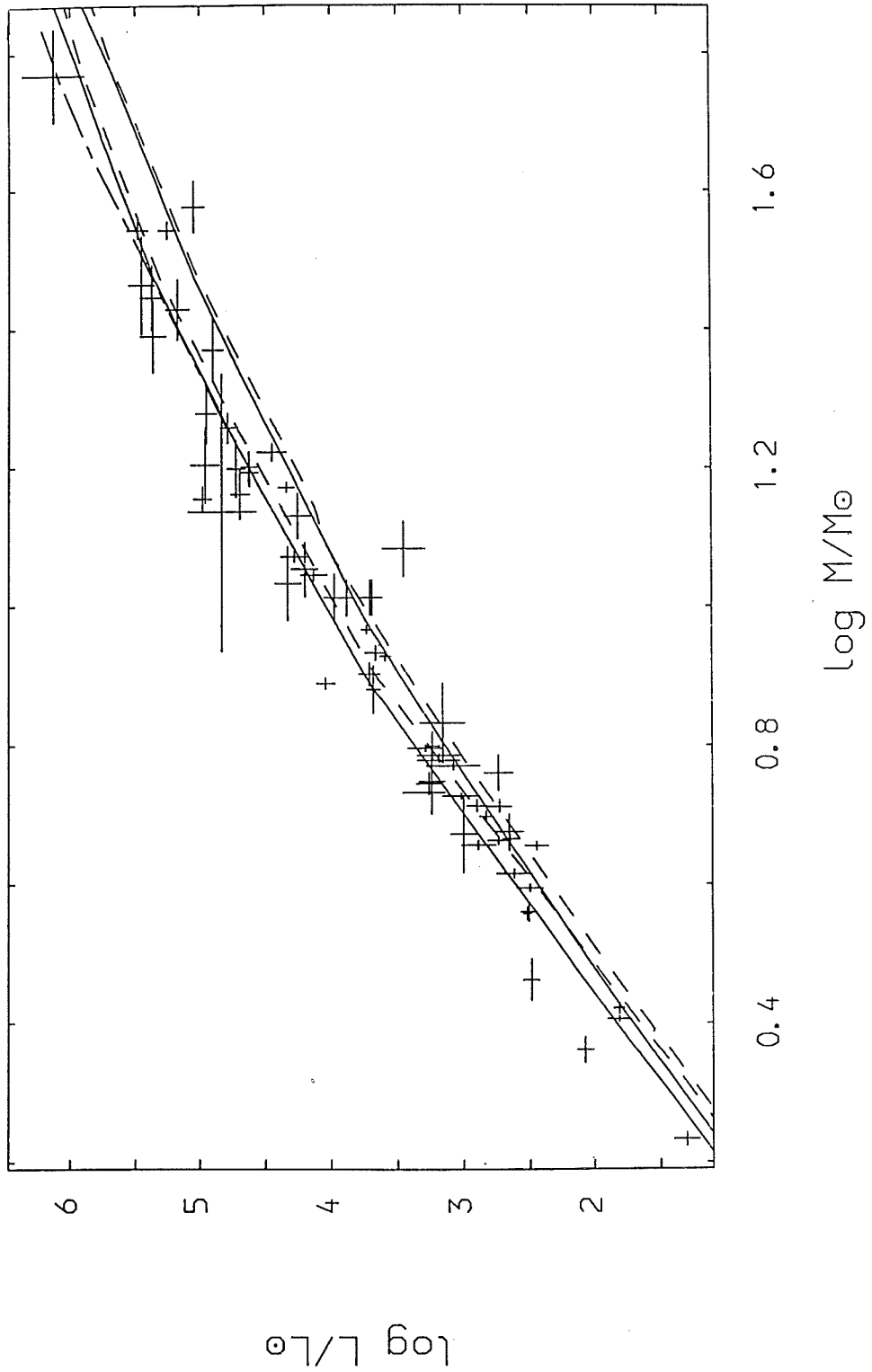


Figure 5. The Mass-Luminosity diagram for those objects plotted in Figure 1. The lines have the same meaning as those in Figure 4.

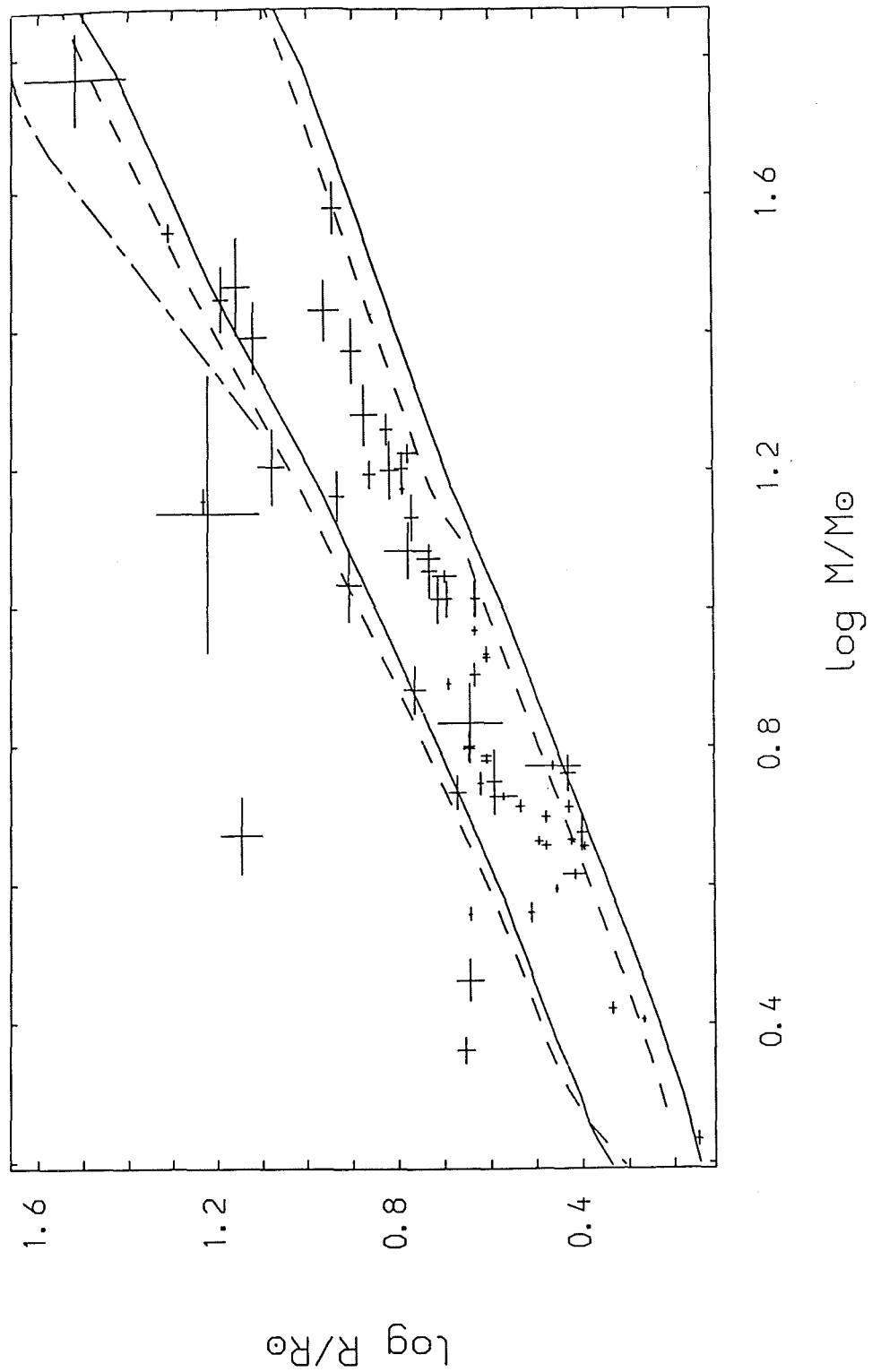
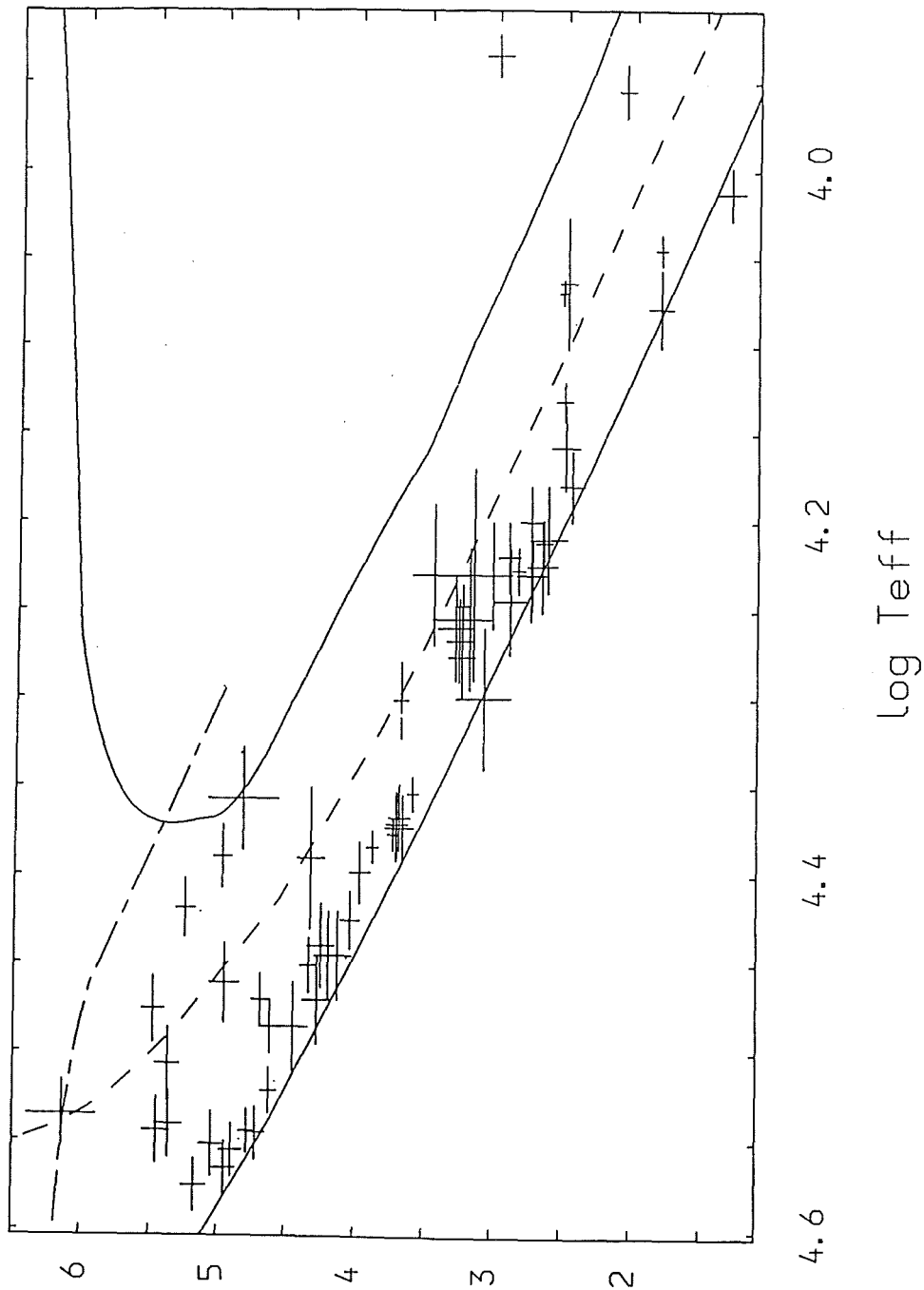


Figure 6. The Mass-Radius diagram for those objects plotted in Figure 1. The lines have the same meaning as those in Figure 4.



$\log L/L_{\odot}$

Figure 7. The HR diagram for those objects plotted in Figure 1. The lower and upper solid lines represent the combined zero-age and terminal-age main sequences of Bressan et al. (1981) and Bertelli et al. (1986). Convective overshooting is included in these sequences without the effects of mass loss. The dashed line represents the combined terminal-age main sequence of Stothers (1972) and Hejlesen (1980) adopting the traditional mixing-length theory of convection. The dot-dashed line represents the terminal-age main sequence of Bressan et al. (1981) including convective overshooting and mass loss. All models have a composition of ($X = 0.70$, $Z = 0.02$).

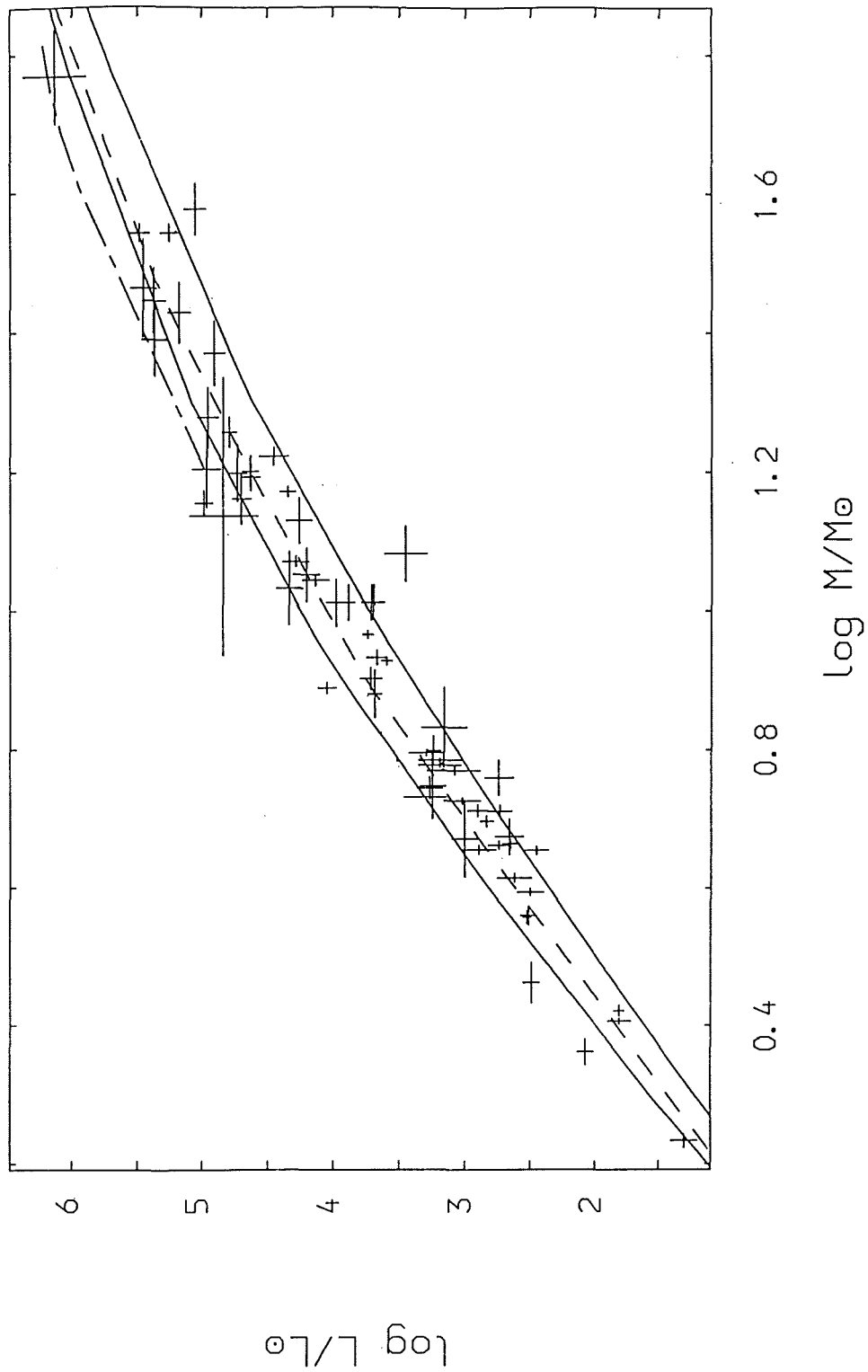


Figure 8. The Mass-Luminosity diagram for those objects plotted in Figure 1. The lines have the same meaning as those in Figure 7.

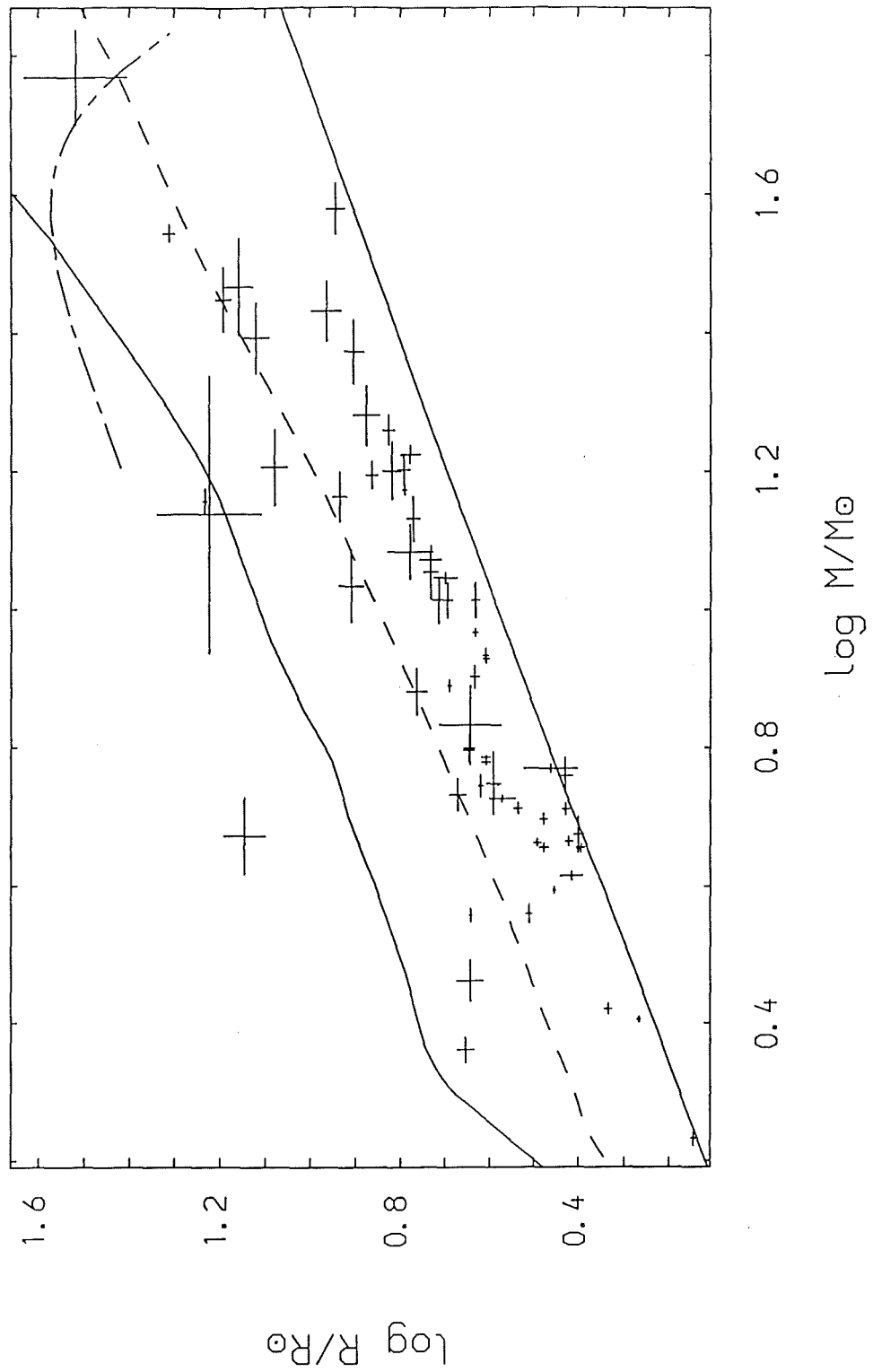
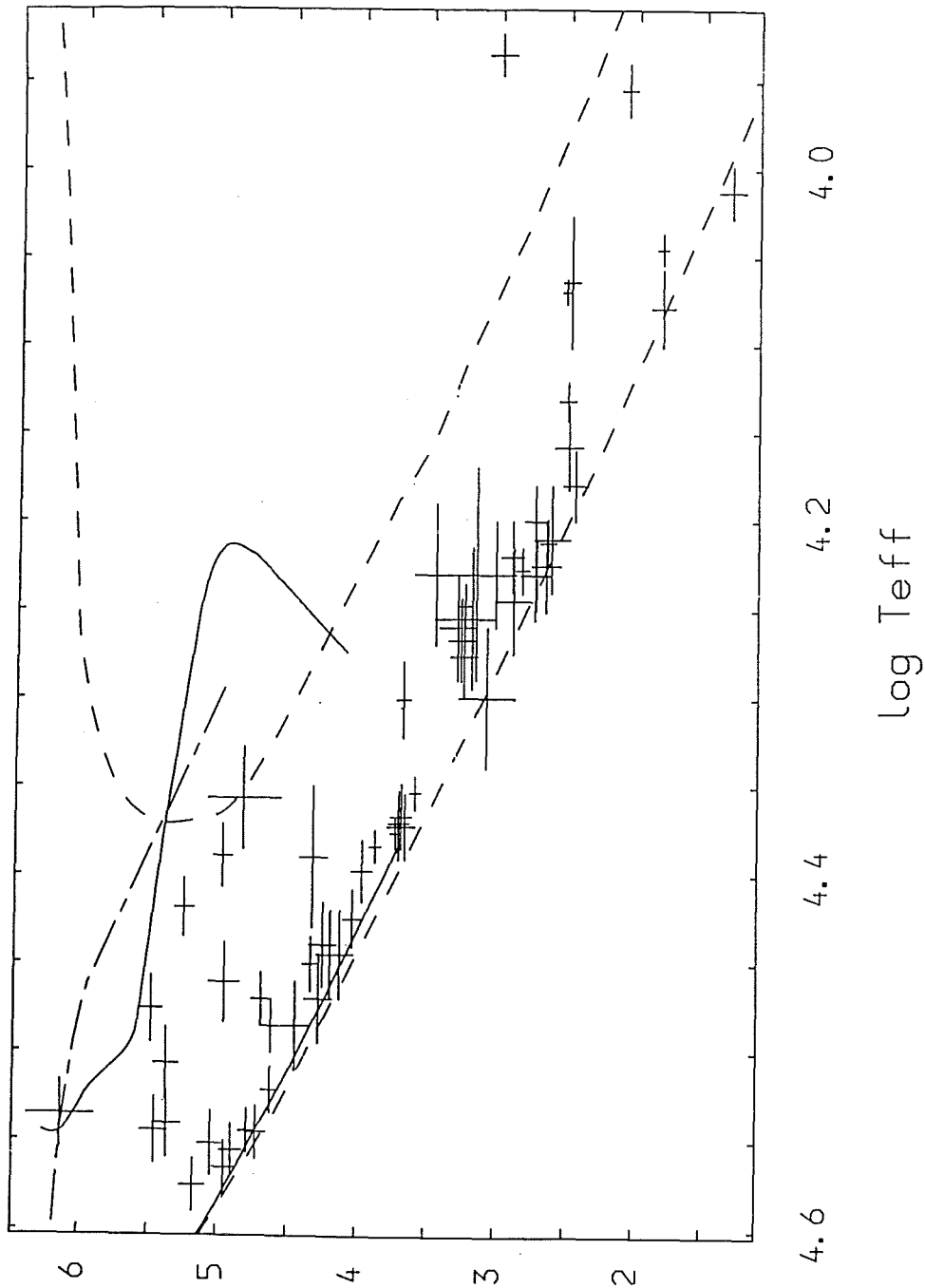


Figure 9. The Mass-Radius diagram for those objects plotted in Figure 1. The lines have the same meaning as those in Figure 7.



$\log L/L_{\odot}$

Figure 10. The HR diagram for those objects plotted in Figure 1. The lower and upper solid lines represent the zero-age and terminal-age main sequences of Doom (1982a,b). These sequences include mass loss with differing amounts of convective overshooting. The lower and upper dashed lines represent the combined zero-age and terminal-age main sequences of Bressan et al. (1981) and Bertelli et al. (1986). These models do not include mass loss but are otherwise similar. The dot-dashed line represents the terminal-age main sequence of Bressan et al. (1981) including convective overshooting and mass loss. All models have a composition of ($X = 0.70$, $Z = 0.02$) except those of Doom where $Z = 0.03$.

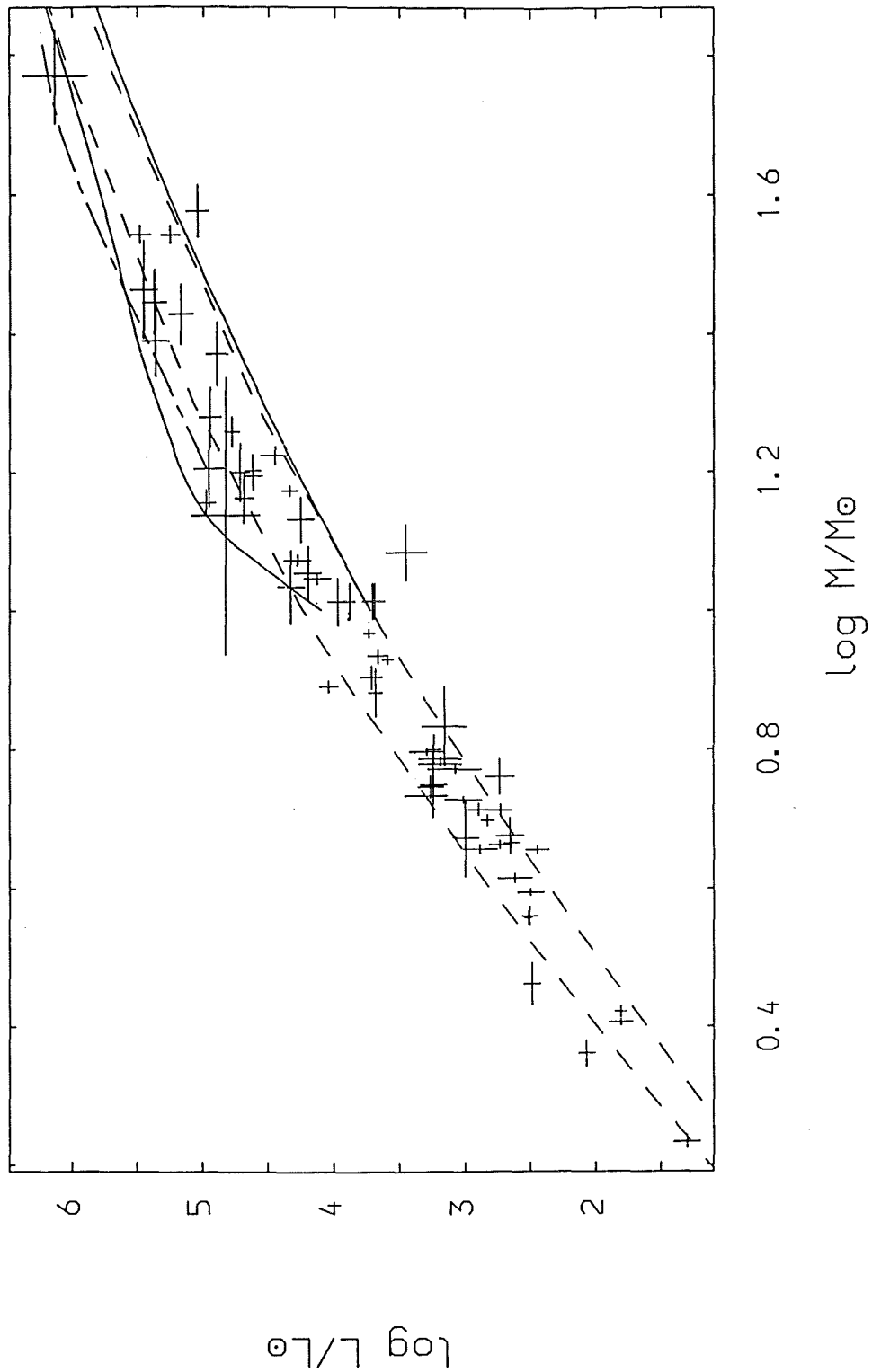


Figure 11. The Mass-Luminosity diagram for those objects plotted in Figure 1. The lines have the same meaning as those in Figure 10.

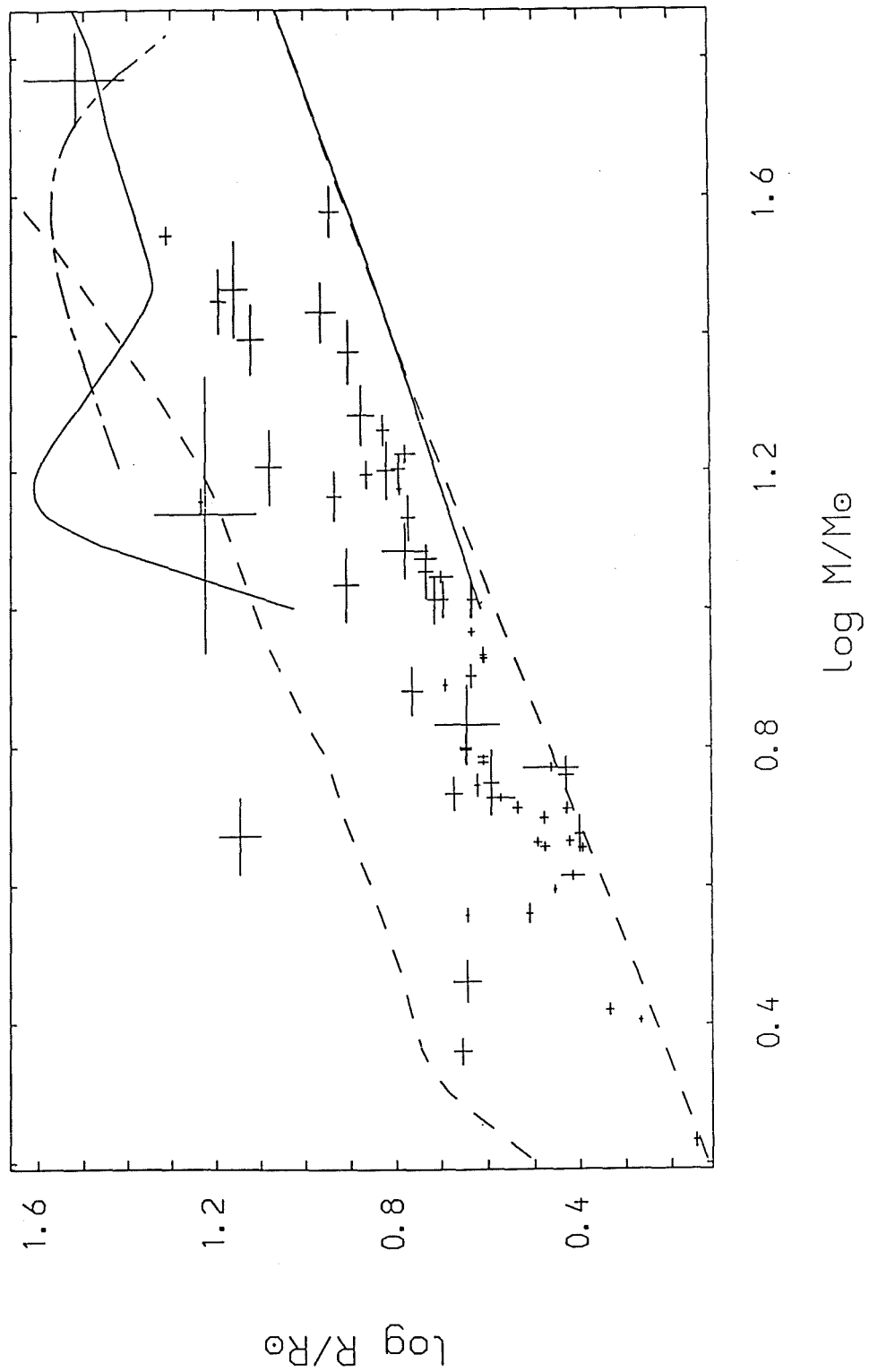


Figure 12. The Mass-Radius diagram for those objects plotted in Figure 1. The lines have the same meaning as those in Figure 10.

Table 1 : Data for 34 binary systems.

Name/comp.	Per.	log M error	log R error	log T error	log L error
V729 Cyg	A 6. ^d 598	1.769±0.067	1.518±0.113	4.535±0.019	6.130±0.240
	B	1.137±0.200	1.223±0.114	4.357±0.029	4.830±0.260
V1182 Aql	A 1. ^d 622	1.577±0.037	0.945±0.020	4.551±0.018	5.050±0.083
	B	1.130±0.032	0.771±0.015	4.439±0.024	4.254±0.099
V348 Car	A 5. ^d 562	1.544±0.012	1.312±0.013	4.476±0.019	5.480±0.080
	B	1.544±0.012	1.312±0.013	4.418±0.017	5.250±0.070
LY Aur	A 4. ^d 025	1.447±0.047	1.193±0.017	4.506±0.020	5.370±0.090
	B	1.204±0.054	1.079±0.029	4.461±0.023	4.960±0.110
V382 Cyg	A 1. ^d 886	1.430±0.044	0.964±0.033	4.575±0.015	5.170±0.090
	B	1.279±0.043	0.875±0.029	4.565±0.015	4.950±0.080
AO Cas	A 3. ^d 523	1.391±0.051	1.121±0.030	4.540±0.019	5.360±0.100
	B	1.465±0.070	1.158±0.030	4.544±0.019	5.450±0.100
TU Mus	A 1. ^d 387	1.371±0.046	0.903±0.022	4.555±0.015	4.900±0.080
	B	1.199±0.041	0.820±0.020	4.545±0.015	4.720±0.070
AH Cep	A 1. ^d 775	1.258±0.022	0.826±0.013	4.544±0.012	4.784±0.056
	B	1.201±0.022	0.792±0.014	4.521±0.013	4.625±0.059
Y Cyg	A 2. ^d 996	1.223±0.013	0.778±0.022	4.485±0.025	4.450±0.110
	B	1.223±0.013	0.778±0.022	4.485±0.025	4.450±0.110
V478 Cyg	A 2. ^d 881	1.193±0.020	0.863±0.012	4.485±0.015	4.620±0.070
	B	1.193±0.020	0.863±0.012	4.485±0.015	4.620±0.070
V Pup	A 1. ^d 455	1.172±0.007	0.791±0.005	4.450±0.015	4.340±0.060
	B	0.890±0.008	0.690±0.004	4.425±0.016	4.040±0.070
V453 Cyg	A 3. ^d 890	1.161±0.036	0.934±0.015	4.470±0.015	4.690±0.070
	B	1.053±0.038	0.732±0.016	4.445±0.025	4.200±0.100
V380 Cyg	A 12. ^d 426	1.155±0.018	1.233±0.005	4.389±0.018	4.980±0.070
	B	0.903±0.016	0.633±0.010	4.373±0.018	3.710±0.080
V356 Sgr	A 8. ^d 896	1.083±0.040	0.778±0.051	4.230±0.040	3.450±0.160
	B	0.672±0.055	1.146±0.047	3.935±0.012	3.000±0.100
CW Cep	A 2. ^d 729	1.072±0.007	0.732±0.024	4.470±0.025	4.280±0.100
	B	1.045±0.008	0.699±0.026	4.445±0.025	4.130±0.100
Alpha Vir	A 4. ^d 014	1.033±0.052	0.909±0.027	4.390±0.040	4.330±0.100
	B	0.832±0.058	0.643±0.069	4.230±0.060	3.160±0.170
SX Aur	A 1. ^d 210	1.013±0.034	0.714±0.015	4.398±0.017	3.974±0.076
	B	0.748±0.047	0.591±0.016	4.277±0.023	3.243±0.097
AI Cru	A 1. ^d 418	1.013±0.025	0.695±0.010	4.384±0.009	3.880±0.042
	B	0.799±0.021	0.646±0.012	4.248±0.012	3.240±0.054

Table 1 (continued)

Name/comp.	Per.	log M error	log R error	log T error	log L error	
V701 Sco	A	0. ^d 762	1.013±0.025	0.633±0.008	4.371±0.019	3.707±0.076
	B		1.013±0.025	0.631±0.008	4.367±0.019	3.688±0.076
QX Car	A	4. ^d 478	0.967±0.006	0.632±0.006	4.377±0.009	3.730±0.040
	B		0.928±0.006	0.608±0.006	4.354±0.010	3.590±0.040
TT Aur	A	1. ^d 333	0.933±0.010	0.609±0.006	4.373±0.018	3.664±0.075
	B		0.745±0.016	0.620±0.006	4.267±0.023	3.264±0.095
u Her	A	2. ^d 051	0.881±0.034	0.763±0.023	4.301±0.022	3.680±0.050
	B		0.462±0.030	0.643±0.030	4.064±0.037	2.490±0.060
V539 Ara	A	3. ^d 169	0.796±0.005	0.646±0.012	4.260±0.030	3.290±0.130
	B		0.727±0.005	0.572±0.029	4.230±0.030	3.020±0.140
CV Vel	A	6. ^d 892	0.785±0.003	0.608±0.011	4.255±0.040	3.190±0.160
	B		0.778±0.003	0.608±0.011	4.255±0.040	3.190±0.160
BM Ori	A	6. ^d 471	0.771±0.006	0.462±0.060	4.300±0.040	3.080±0.200
RZ Pyx	A	0. ^d 656	0.760±0.026	0.430±0.016	4.230±0.025	2.737±0.107
	B		0.675±0.026	0.400±0.010	4.225±0.026	2.656±0.106
Z Vul	A	2. ^d 455	0.732±0.024	0.672±0.019	4.255±0.040	3.300±0.160
	B		0.362±0.019	0.653±0.019	3.955±0.015	2.070±0.060
U Oph	A	1. ^d 677	0.713±0.008	0.535±0.009	4.220±0.020	2.900±0.080
	B		0.663±0.006	0.493±0.008	4.200±0.020	2.740±0.080
DI Her	A	10. ^d 550	0.712±0.008	0.428±0.008	4.230±0.020	2.730±0.090
	B		0.655±0.006	0.394±0.009	4.180±0.020	2.450±0.090
V760 Sco	A	1. ^d 731	0.697±0.008	0.479±0.009	4.228±0.013	2.830±0.050
	B		0.665±0.007	0.422±0.008	4.212±0.013	2.650±0.060
AG Per	A	2. ^d 029	0.656±0.007	0.477±0.010	4.245±0.030	2.890±0.130
	B		0.615±0.006	0.415±0.025	4.210±0.030	2.620±0.130
Zeta Phe	A	1. ^d 670	0.594±0.005	0.455±0.003	4.158±0.024	2.500±0.100
	B		0.407±0.004	0.267±0.005	4.079±0.022	1.810±0.090
AL Scl	A	2. ^d 445	0.560±0.013	0.511±0.007	4.132±0.011	2.510±0.060
	B		0.233±0.010	0.146±0.006	4.013±0.015	1.300±0.100
Chi ² Hya	A	2. ^d 268	0.558±0.010	0.642±0.004	4.070±0.007	2.520±0.030
	B		0.422±0.008	0.335±0.008	4.045±0.009	1.810±0.040

References:

V382 Cyg, Y Cyg, V478 Cyg, V453 Cyg, V356 Sgr, CW Cep, Alpha Vir, CV Vel, BM Ori, Z Vul, U Oph & AG Per (Popper, 1980 and references therein); V729 Cyg (Leung & Schneider, 1978); V1182 Aql (Bell et

al., 1987b); V348 Car (Hilditch & Lloyd Evans, 1984); LY Aur (Li & Leung, 1985); AO Cas (Schneider & Leung, 1978); TU Mus (Andersen & Gronbech, 1975); AH Cep (Bell et al., 1986); V Pup (Andersen et al., 1983a); V380 Cyg (Hill & Batten, 1984); SX Aur (Bell et al., 1987a); AI Cru (Bell et al., 1987c); V701 Sco (Bell & Malcolm, 1987a); QX Car (Andersen et al., 1983b); TT Aur (Bell et al., 1987a); u Her (Hilditch, 1984); V539 Ara (Andersen, 1983); RZ Pyx (Bell & Malcolm, 1987b); DI Her (Popper, 1982); V760 Sco (Andersen et al., 1985); Zeta Phe (Clausen et al., 1975); AL Scl (Skillen, 1985) and Chi² Hya (Clausen & Nordstrom, 1977).

References

- Andersen, J., 1983. *Astron. Astrophys.*, 118, 255.
- Andersen, J. & Gronbech, B., 1975. *Astron. Astrophys.*, 45, 107.
- Andersen, J., Clausen, J.V., Nordstrom, B. & Reipurth, B., 1983. *Astron. Astrophys.*, 121, 271.
- Andersen, J., Clausen, J.V., Gimenez, A. & Nordstrom, B., 1983. *Astron. Astrophys.*, 128, 17.
- Andersen, J., Clausen, J.V., Nordstrom, B. & Popper, D.M., 1985. *Astron. Astrophys.*, 151, 329.
- Bell, S.A. & Malcolm, G.J., 1987a. *Mon. Not. R. astr. Soc.*, in press.
- Bell, S.A. & Malcolm, G.J., 1987b. Submitted to *Mon. Not. R. astr. Soc.*
- Bell, S.A., Hilditch, R.W. & Adamson, A.J., 1986a. *Mon. Not. R. astr. Soc.*, 223, 513.
- Bell, S.A., Adamson, A.J. & Hilditch, R.W., 1987a. *Mon. Not. R. astr. Soc.*, 224, 649.
- Bell, S.A., Hilditch, R.W. & Adamson, A.J., 1987b. *Mon. Not. R. astr. Soc.*, in press.
- Bell, S.A., Malcolm, G.J. & Kilkenny, D., 1987c. *Mon. Not. R. astr. Soc.*, in press.
- Bertelli, G., Bressan, A., Chiosi, C. & Angerer, K., *Astron. Astrophys. Suppl. Ser.*, 66, 191.

- Bressan, A., Bertelli, G. & Chiosi, C., 1981. *Astron. Astrophys.*, 102, 25.
- Castor, J.I., Abbott, D.C. & Klein, R.I., 1975. *Astrophys. J.*, 195, 157.
- Clausen, J.V. & Gyldenkerne, K., 1975. *Astron. Astrophys.*, 46, 205.
- Clausen, J.V. & Nordstrom, B., 1977. *Astron. Astrophys.*, 67, 15.
- Doom, C., 1982a. *Astron. Astrophys.*, 116, 303.
- Doom, C., 1982b. *Astron. Astrophys.*, 116, 308.
- Doom, C., 1984. *Astron. Astrophys.*, 138, 101.
- Hejlesen, P.M., 1980. *Astron. Astrophys. Suppl. Ser.*, 39, 347.
- Hilditch, R.W., 1984. *Mon. Not. R. astr. Soc.*, 211, 943.
- Hilditch, R.W. & Lloyd Evans, T.L., 1984. *Mon. Not. R. astr. Soc.*, 213, 75.
- Hill, G. & Batten, A.H., 1984. *Astron. Astrophys.*, 141, 39.
- Lamers, H.J.G.L.M., 1981. *Astrophys. J.*, 245, 593.
- Leung, K.-C. & Schneider, D.P., 1978. *Astrophys. J.*, 224, 565.
- Li, Y.-F., & Leung, K.-C., 1985. *Astrophys. J.*, 298, 345.
- Mayer, P. & Wolf, M., 1986. *Inf. Bull. Var. Stars*, No. 2886.
- Popper, D.M., 1980. *Ann. Rev. Astron. Astrophys.*, 18, 115.
- Popper, D.M., 1982. *Astrophys. J.*, 254, 203.
- Schneider, D.P. & Leung, K.-C., 1978. *Astrophys. J.*, 223, 202.

Skillen, W.J., 1985. Ph.D. thesis, University of St. Andrews.

Stothers, R., 1972. *Astrophys. J.*, 175, 431.

Sybesma, C.H.B., 1986. *Astron. Astrophys.*, 159, 108.